On moduli spaces of Riemann surfaces: new generators in their unstable homology and the homotopy type of their harmonic compactification

Dissertation

zur
Erlangung des Doktorgrades (Dr. rer. nat.)
der
Mathematisch-Naturwissenschaftlichen Fakultät
der
Rheinischen Friedrich-Wilhelms-Universität Bonn

vorgelegt von

Felix Jonathan Boes
aus
Solingen, Germany

Bonn, 15. März 2018

Angefertigt mit Genehmigung der Mathematisch-Naturwissenschaftlichen Fakultät
der Rheinischen Friedrich-Wilhelms-Universität Bonn

1. Gutachter: Prof. Dr. Carl-Friedrich Bödigheimer

2. Gutachter: Prof. Dr. Nathalie Wahl

Tag der Promotion: 05. Juni 2018

Erscheinungsjahr: 2018

Summary

By $\mathfrak{M}_g^\bullet(m,n)$ we denote the moduli space of conformal structures on an oriented compact cobordism $S_g(m,n)$ of genus $g \geq 0$ and with $m+n \geq 0$ enumerated, parametrized boundary components of which n are "incoming" and m are "outgoing". The study of these spaces reflects a strong relationship between geometry, topology and mathematical physics. In this thesis, we study (1) the homotopy type of Bödigheimer's harmonic compactification of these moduli spaces (and of variations of these) and (2) the unstable homology of these moduli spaces (and of variations of these). Some of our results are from a joint-project with Daniela Egas-Santander, see [BE17].

On the homotopy type of the harmonic compactifications

The free loop space of a simply connected, closed manifold M is denoted by LM. Its homology is an algebra over the homology of the operad of framed discs $H_*(\mathcal{D}_2)$. As an algebra over this operad, it is isomorphic to the Hochschild cohomology of the cochains $C^\bullet(M)$, see [CJ02]. There are numerous extensions of the action of $H_*(\mathcal{D}_2)$ on the loop homology and on the Hochschild cohomology of an A_∞-algebra to an action of the homology of the moduli spaces $\mathfrak{M}_g^\bullet(m,n)$ and their harmonic compactifications $\overline{\mathfrak{M}}_g^\bullet(m,n)$, see e.g. [CG04, TZ06, Cos07a, Cos07b, Kau07, Kau08a, KS09, Kau10, PR11, Ega14a, WW16]. Our main result is the following:

Theorem 6.1 (B.)**.** *The harmonic compactification $\overline{\mathfrak{M}}_g^\bullet(m,1)$ is $(g+m-2)$-connected for every $g \geq 2$ and $m \geq 1$ or $g \geq 0$ and $m \geq 3$.*

As usual, the $n+m$ enumerated parametrized boundary curves of the cobordism $S_g(m,n)$ are partitioned into n "incoming boundaries" and m "outgoing boundaries". Note that the m-dimensional torus acts on $\mathfrak{M}_g^\bullet(m,n)$ by reparametrization of the m outgoing boundary components. The orbit space is denoted by $\mathfrak{M}_g^\circ(m,n)$.

Theorem 4.4.1 (B., Egas)**.** *Let $g \geq 0$, $m \geq 1$ and $\star \in \{\bullet, \circ\}$. The stabilization maps of the moduli spaces $\varphi_g \colon \mathfrak{M}_g^\star(m,1) \to \mathfrak{M}_{g+1}^\star(m,1)$ extend to the harmonic compactification, i.e., there is a map $\varphi_g \colon \overline{\mathfrak{M}}_g^\star(m,1) \to \overline{\mathfrak{M}}_{g+1}^\star(m,1)$ making the following diagram commutative.*

$$\begin{array}{ccc} \mathfrak{M}_g^\star(m,1) & \xrightarrow{\varphi_g} & \mathfrak{M}_{g+1}^\star(m,1) \\ \downarrow & & \downarrow \\ \overline{\mathfrak{M}}_g^\star(m,1) & \xrightarrow{\overline{\varphi}_g} & \overline{\mathfrak{M}}_{g+1}^\star(m,1) \end{array}$$

The stabilization map $\overline{\varphi}_g$ induces an isomorphism in homology in degrees $* \leq g+m-2$. Moreover, if $\star = \bullet$ or if $m > 2$, the stabilization map $\overline{\varphi}_g$ is $(g+m-2)$-connected.

The orbit projection $\mathfrak{M}_g^\bullet(m,n) \to \mathfrak{M}_g^\circ(m,n)$ is an m-dimensional torus bundle. Unfortunately, the extension of this map to the harmonic compactification is not even a fibration. In this thesis, we study the following retract of the moduli spaces $\mathfrak{M}_g^\star(m,n)$. By $N\mathfrak{M}_g^\star(m,n)$ we denote the subspace of $\mathfrak{M}_g^\star(m,n)$ where all outgoing boundary curves have a fixed circumference, say 1; Its harmonic compactification $\overline{N\mathfrak{M}}_g^\star(m,n)$ is a closed subspace of $\overline{\mathfrak{M}}_g^\star(m,n)$.

Theorem 5.2.11 (B.)**.** *Let $m \geq 1$, $g \geq 0$. Forgetting the parametrization of the outgoing boundaries defines m-dimensional torus fibrations.*

$$\begin{array}{ccc} N\mathfrak{M}_g^\bullet(m,1) & \longhookrightarrow & \overline{N\mathfrak{M}}_g^\bullet(m,1) \\ \downarrow & & \downarrow \\ N\mathfrak{M}_g^\circ(m,1) & \longhookrightarrow & \overline{N\mathfrak{M}}_g^\circ(m,1) \end{array}$$

The forgetful maps are compatible with the stabilization maps φ_g and $\overline{\varphi}_g$. The stabilization maps $\overline{\varphi}_g$ and the classifying map $\overline{N\mathfrak{M}}_g^\circ(m,1) \to BU(1)^m \simeq (\mathbb{C}P^\infty)^m$ are $(g-1)$-connected. In particular, $\overline{N\mathfrak{M}}_g^\bullet(m,1)$ is $(g-1)$-connected.

Moreover, the homology of the harmonic compactifications $\overline{\mathfrak{M}}_g^\star(m,n)$ and $\overline{N\mathfrak{M}}_g^\star(m,n)$ is related by our desuspension Theorem 5.1.22. Finally, we construct infinite families of (unstable) homology classes of infinite order in the harmonic compactification $\overline{\mathfrak{M}}_g^\bullet(m,1)$. All of these classes correspond to non-trivial higher string operations.

On the unstable homology of the moduli spaces

The homology of the moduli spaces of surfaces is independent of the genus in a range of homological degrees and, in this range, it is known for coefficients in the rationals or in finite fields. Below this range and with coefficients in the integers, the homology of the moduli spaces is almost unknown besides computations for small genera or in low homological degrees. In this thesis, we detect three non-trivial generators, called f, s and w_3. They live in the homology of the moduli spaces $\mathfrak{M}_{g,1}^m$ of surfaces of genus g, with 1 parametrized boundary curve and with m permutable punctures.

Theorem 7.0.1 (B., Bödigheimer, Ehrenfried, Mehner)**.** *The integral homology of the moduli space $\mathfrak{M}_{2,1}$ and $\mathfrak{M}_{1,1}^2$ is as follows.*

$$H_*(\mathfrak{M}_{2,1};\mathbb{Z}) = \begin{cases} \mathbb{Z}\langle c^2\rangle & *=0 \\ \mathbb{Z}_{10}\langle cd\rangle & *=1 \\ \mathbb{Z}_2\langle d^2\rangle & *=2 \\ \mathbb{Z}\langle \lambda s\rangle \oplus \mathbb{Z}_2\langle T(e)\rangle & *=3 \\ \mathbb{Z}_2\langle ?\rangle \oplus \mathbb{Z}_3\langle w_3\rangle & *=4 \\ 0 & *\geq 5 \end{cases} \qquad H_*(\mathfrak{M}_{1,1}^2;\mathbb{Z}) = \begin{cases} \mathbb{Z}\langle a^2c\rangle & *=0 \\ \mathbb{Z}\langle a^2d\rangle \oplus \mathbb{Z}_2\langle bc\rangle & *=1 \\ \mathbb{Z}_2\langle a^2e\rangle \oplus \mathbb{Z}_2\langle bd\rangle & *=2 \\ \mathbb{Z}_2\langle f\rangle & *=3 \\ 0 & *\geq 4 \end{cases}$$

Here, the known generators a,b,c,d,e,t and their products have been described in [Meh11, Kapitel 1], see also [BB18a]. The only generator remaining unkown is denoted by ?.

The non-trivial generator $f \in H_3(\mathfrak{M}^2_{1,1};\mathbb{Z})$ is an embedded 3-dimensional torus. The non-trivial generator $s \in H_3(\mathfrak{M}^1_{2,1};\mathbb{Q})$ is the image of the (rational) fundamental class $[U]$ of the fibration $U \hookrightarrow \mathfrak{M}_{2,1} \to \mathfrak{M}_{2,0}$, where U is the unit tangent bundle of the closed oriented surface of genus two. In [ST07, ST08], Song–Tillmann and Segal–Tillman construct geometric maps from the braid groups to mapping class groups. More precisely, they send the canonical generators of the $2k$-th braid group Br_{2k} to a $2k$ Dehn twists along interlocking simply-closed curves in an oriented surface of genus $k-1$. The non-trivial generator $w_3 \in H_4(\mathfrak{M}^1_{2,1};\mathbb{Q})$ is the image of the generator in $H_4(Br_6;\mathbb{Z}) \cong \mathbb{Z}_3$ under their map.

Acknowledgements

First and foremost I thank Carl-Friedrich Bödigheimer for his constant encouragement, for many valuable and illuminating conversations and for discussing various drafts of my thesis with me. I am grateful to Daniela Egas Santander for introducing me to various aspects of string topology and for plenty detailed and extensive discussions on different models of moduli spaces and related topics. I thank Nathalie Wahl for her interest in my project and for fruitful discussions on string operations. I am thankful to Andrea Bianchi and Martin Palmer for helpful discussions on various details of my thesis. My thanks go to Oscar Randal-Williams for useful conversations on methods to prove homological stability. I thank Alexander Kupers for conversations on homological stability and for answering my questions on the history of string topology. Furthermore, I thank Benson Farb for discussing methods to find unstable homology classes in the moduli spaces and the harmonic compactifications. Finally, I am thankful to David Sprehn for discussing methods to detect certain unstable homology classes.

Table of Contents

1

Background and results

In this chapter, we describe the context of this thesis and present our results. To begin with, we give in Section 1.1 a brief introduction to the moduli spaces of Riemann surfaces. Then, in Section 1.2, we sketch certain classifying maps from the moduli spaces to explicit models of $BU(1)^m$ and introduce our model for the universal torus bundle. In Section 1.3, we review the recent developments in the field of string topology and the applications of the theory of moduli spaces to these studies. Our own results are presented in Section 1.4.

1.1. The moduli spaces of Riemann surfaces

On a closed (orientable) surface, every conformal structure defines a unique complex structure and vice versa. Therefore, such a surface is a Riemann surface. More generally, we define a Riemann surface to be a smooth and compact surface with a fixed conformal structure such that, near the boundary, the metric is the product metric. Below we impose certain conditions on some of the boundaries components: We allow the boundary components to be enumerated and each boundary is allowed to come with a parametrization (which is a distinguished point on the boundary).

By $\mathfrak{M}^{\bullet}_{g,k}$ we denote the moduli space of Riemann surfaces of genus $g \geq 0$ with $k \geq 0$ parametrized and enumerated boundary components. For each $g \geq 0$, $m \geq 1$ and $n \geq 1$, we consider the moduli space of conformal bordisms of genus g with n parametrized and enumerated *incoming* boundaries and with m additional *outgoing* boundaries, namely

1. m parametrized and enumerated additional boundaries, denoted by $\mathfrak{M}^{\bullet}_{g}(m,n)$;

2. m unparametrized and enumerated additional boundaries, denoted by $\mathfrak{M}^{\circ}_{g}(m,n)$;

3. m parametrized and unenumerated additional boundaries, denoted by $\mathfrak{M}^{\blacksquare}_{g}(m,n)$;

4. m unparametrized and unenumerated additional boundaries, denoted by $\mathfrak{M}^{\square}_{g}(m,n)$.

These moduli spaces are related by the diagram below. The horizontal maps are $m!$-fold

coverings and the vertical map on the left is an m-dimensional torus bundle.

$$\begin{array}{ccc} \mathfrak{M}_g^{\bullet}(m,n) & \longrightarrow & \mathfrak{M}_g^{\blacksquare}(m,n) \\ \downarrow & & \downarrow \\ \mathfrak{M}_g^{\circ}(m,n) & \longrightarrow & \mathfrak{M}_g^{\square}(m,n) \end{array}$$

More precisely, on $\mathfrak{M}_g^{\bullet}(m,n) = \mathfrak{M}_{g,m+n}^{\bullet}$, the m-dimensional torus acts freely and properly discontinous by rotating around the parametrization of the m outgoing boundaries. The orbit space is $\mathfrak{M}_g^{\circ}(m,n)$. On $\mathfrak{M}_g^{\bullet}(m,n)$ resp. $\mathfrak{M}_g^{\circ}(m,n)$ the m-th symmetric group acts faithfully by permuting the m outgoing boundaries. The orbit space is $\mathfrak{M}_g^{\blacksquare}(m,n)$ resp. $\mathfrak{M}_g^{\square}(m,n)$.

These moduli spaces admit various (relative) cellular models and, in this thesis, we study two models in detail. The theory of quadratic differentials yields a space of metric ribbon graphs, see Section 1.1.1 and, using harmonic potentials, Bödigheimer constructs spaces of slit configurations in [Bö90a] and [Bö06], see Section 1.1.2 and Chapter 3. Both models admit a canonical compactification and the study of the homology of these compactifications has interesting applications in the field of string topology, see Section 1.3. In Sections 1.1.3 and 1.1.4, we briefly recall what is known about the homology of the moduli spaces.

1.1.1. Metric ribbon graphs

Ribbon graph models play a prominent role in the study of moduli spaces and rely on the works of [Str84], [Pen87], [BE88], [Har86], [Igu02] and [God04]. For convenience of the reader, we review some facts from the theory of Strebel differentials and discuss a space of metric ribbon graphs. A detailed discussion can be found in [Loo95].

A quadratic differential ϕ on a Riemann surface F (with k parametrized and enumerated boudaries) is a section of $(TF^*)^{\otimes 2}$, i.e., it is of the form $\phi(z)dz^2$ in local coordinates. The horizontal trajectories of ϕ are the closed curves along which $\phi(z)dz^2$ is real and positive. The Jenkins–Strebel quadratic differentials (short: JS differential) are the holomorphic quadratic differentials for which the union of the non-closed horizontal trajectories have measure zero. A JS differential ϕ defines a flat metric away from the discrete set of its zeros. The non-closed (horizontal) trajectories of a JS differential cut the surface into finitely many closed cylinders. Each of the cylinders has exactly one boundary component that is a union of non-closed trajectories; the cylinder is exhausted by closed trajectories whose length is the circumference of the cylinder and its other boundary component agrees with a boundary component of F. Therefore, the union of the non-closed trajectories define an embedded graph $G_\phi \subset F$ such that the edges are equiped with a positive length and, using the orientation of the surface F, the set of edges at each vertex is ordered cyclically. Such a (connected) graph is called metric ribbon graph. In G_ϕ, consider a closed path $\gamma = (v_0, e_0, v_1, \ldots, v_{n-1}, e_n, v_0)$ that constists of egdes e_i starting in the vertex v_{i-1} and ending in the vertex v_i. A closed path $\gamma = (v_0, e_1, \ldots, e_n, v_0)$ is called boundary component of the ribbon graph if, for each $i = 0, \ldots, n$, the succesor of the edge e_i with respect to the cyclic operation at v_{i+1} is e_{i+1}. The boundary components of the metric ribbon graph are in one-to-one correpondence with the boundary components of F. See Figure 1.1 for an example.

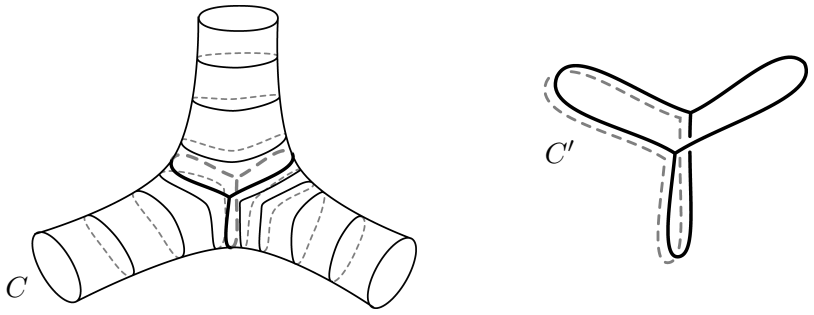

Figure 1.1.: On the left, we sketch the trajectories of a JS differential ϕ on a surface S of genus zero with three boundary components. One of the boundary component is called C. The non-closed trajectories are thick. On the right, we sketch the metric ribbon graph G_ϕ corresponding to the non-closed trajectories. Hereby, the boundary component C of S corresponds to the boundary component C' of G_ϕ.

The parametrization of every boundary component $C \subset F$ is a choice of basepoint $p_C \in C$. Following the vertical trajectory of $p_C \in C$ towards the embedded graph G_ϕ yields a marked point in every boundary component of G_ϕ. A metric ribbon graph with a distinguished point per boundary component is called marked metric ribbon graph. Given an arbitrary marked metric ribbon graph G, we can replace its edges by thin stripes (respecting the cyclic orientation at each vertex) to obtain a conformal surface F_G of genus g with k parametrized boundary components. Consequently, we say that G has genus g and k boundary components. The space of marked metric ribbon graphs of genus g and k parametrized and enumerated boundaries is denoted $Rib^\bullet_{g,k}$ and its topology is induced by the lenghts of the edges of its graphs. It is homotopy equivalent to the respective moduli space, see [God04]:

$$Rib^\bullet_{g,k} \simeq \mathfrak{M}^\bullet_{g,k}\,. \tag{1.1}$$

Selecting a partition $k = m + n$ of the boundaries into n incoming and m outgoing components, we denote the space of marked metric ribbon graphs by $Rib^\bullet_g(m,n) := Rib^\bullet_{g,n+m}$. The m-dimensional torus acts on $Rib^\bullet_g(m,n)$ by sliding each parametrization point along its boundary component. The orbit space is a space of metric ribbon graphs with n parametrized enumerated boundaries and m unparametrized enumerated boundaries denoted by $Rib^\circ_g(m,n)$. Variations of these spaces of ribbon graphs are used in the study of string topology, see Section 1.3.

1.1.2. Radial slit configurations

In this section, we briefly discuss Bödigheimer's spaces of radial slit configurations [Bö90a, Bö06] which model the moduli spaces $\mathfrak{M}^\bullet_g(m,n)$, $\mathfrak{M}^\circ_g(m,n)$, $\mathfrak{M}^\blacksquare_g(m,n)$ or $\mathfrak{M}^\square_g(m,n)$. We postpone the presentation of some technical details of this model to Chapter 3.

Given a Riemann surface F with $n \geq 1$ incoming and $m \geq 1$ outgoing boundaries, we choose a harmonic function $u\colon F \to \mathbb{R}_{\leq 0}$ that is zero on the incoming boundaries and constant on each outgoing boundary. The function u is a solution to a Dirichlet problem. It always exists and is uniquely determined by F and its values on the outgoing boundaries

(see e.g. [For81, Theorem 22.17] or [Tsu59, Theorem I.25]). The union of all gradient flow lines that leave a critical point define a possibly disconnected graph in F, called the critical graph. After removing the critical graph, we are left with an open possibly disconnected subsurface of F. Pulling the remaining flow lines straight defines a biholomorphic map whose image is a disjoint union of n annuli with pairs of radial slits removed, see Figure 1.2 for an example. The distribution of these pairs over the annuli define a combinatorial

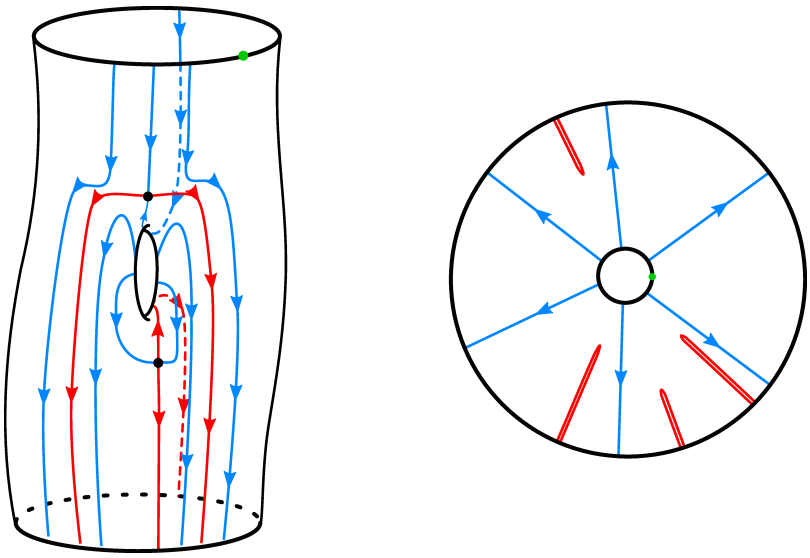

Figure 1.2.: On the left, we sketch the flow lines of a harmonic function defined on a Riemann surface F of genus one with one incoming and one outgoing boundary curve. The critical points are black, the flow lines leaving a critical point are red and all other flow lines are blue. On the right, we sketch the image of F under the process described above. It is an annulus with red pairs of radial slit removed and one pair is shorter than the other.

datum. The end points of the slits define barycentric coordinates in the interior of a multi-simplex. Sending a Riemann surface to its radial slit configuration defines the Hilbert uniformization $\Phi\colon \mathfrak{M}_g^\bullet(m,n)\times\mathbb{R}^m_{<0}\to R_g(m,n)$. The codomain is a multi-simplicial space, the image of Φ is the complement of a subcomplex $R'_g(m,n)\subset R_g(m,n)$ and the Hilbert uniformization restricts to a homeomorphism $\mathfrak{M}_g^\bullet(m,n)\times\mathbb{R}^m_{<0}\cong R_g(m,n)-R'_g(m,n)$.

We remark that there are at least two variations of the complex $R_g(m,n)$: In [Bö06, Section 8], the complex $R_g(m,n)$ is obtained by adding certain degenerate surfaces to $\mathfrak{M}_g^\bullet(m,n)$. It is called the harmonic compactification of the moduli space because it is the space of (possibly degenerate) surfaces admitting a real function that is harmonic on the smooth points. In Section 1.3, we discuss the role of the harmonic compactification in the studies of string topology. Most importantly, by [EK14], it has the homotopy type of a space of Sullivan diagrams and therefore it approximates the space of all higher string operations by [Wah16].

In [Bö07], another compactification is introduced. It admits a more elegant presentation as it is made from subspaces of bar resulutions of symmetric groups. This description is used by several authors to compute the integral homology of the moduli spaces for small parameters g and m, see Section 1.1.4, Section 7.3 and Appendix E.4.

Albeit we have two versions of $R_g(m,n)$, their differences shall not play any role here. Most importantly, the moduli space $\mathfrak{M}_g^\bullet(m,n)$ is a relative manifold, i.e., it is an oriented manifold that is homeomorphic to an open and dense subspace of a compact cell complex $R_g(m,n)$ and its boundary is a subcomplex of codimension one. Therefore, $H_*(\mathfrak{M}_g^\bullet(m,n);\mathbb{Z})$ is Poincaré-dual to $H^*(R_g(m,n), R'_g(m,n);\mathbb{Z})$.

1.1.3. Homological stability

Here, we state the most important facts about homological stability and the Madsen–Weiss theorem. For an introduction to the field, we refer the reader to [Hat11], [Wah13] and [Gal13].

Given a compact surface $F_{g,k}$ of genus g with k enumerated and parametrized boundary components, the mapping class group of $F_{g,k}$ is defined to be the group of all orientation preserving diffeomorphisms (that restrict to the identity near each boundary component) up to isotopy, i.e., $\Gamma_{g,k} := \mathit{Diff}^+(F_{g,k}, \partial F_{g,k})/_{\mathit{isotopy}}$. For $k \geq 1$ the mapping class group $\Gamma_{g,k}$ acts freely and properly discontinous via isometries on its corresponding contractible Teichmüller space and the orbit space is $\mathfrak{M}_{g,k}^\bullet$. Therefore, there is a natural isomorphism $H_*(\mathfrak{M}_{g,k}^\bullet) \cong H_*(\Gamma_{g,k})$.

Sewing a surface of genus one with two boundary components to a surface with $k \geq 1$ boundary components identifies $\Gamma_{g,k}$ with a subgroup of $\Gamma_{g+1,k}$ and the union of these is the stable mapping class group $\Gamma_{\infty,k}$. By [Har85], the inclusion $\Gamma_{g,k} \hookrightarrow \Gamma_{g+1,k}$ induces an isomorphism in homology in a range of the homological degree $*$ depending on g. The slope of this range has been improved in the last years and it is known to be at least $* \leq \frac{2(g-1)}{3}$ by [RW16]. Consequently, the inclusion of groups induces an isomorphism $H_*(\mathfrak{M}_{g,k}^\bullet) \cong H_*(\Gamma_{g,k}) \cong H_*(\Gamma_{\infty,k})$ in this range.

The stable moduli space $\mathfrak{M}_{\infty,1}^\bullet := B\Gamma_{\infty,1}$ is an infinite loop space by [Til97] (after applying the Quillen plus construction) and, as an infinite loop space, it is homotopy equivalent to the loop space of a certain Thom-spectrum by the famous Madsen–Weiss theorem, see [MW05] and also [GTMW]. The homology of the latter has been computed rationally by Madsen and Weiss in [MW05] and with coefficients in finite fields by Galatius in [Gal04].

Adding a point near the boundary of a surface induces maps $\mathfrak{M}_g^\square(m,n) \to \mathfrak{M}_g^\square(m+1,n)$. This leads to another result in terms of homological stability: In homology, the induced map is split injective by [BT01] and by [Til16] it an isomorphism in a range where the homological degree $*$ does not exceed $* \leq \frac{m}{2}$.

1.1.4. Unstable homology

The unstable homology of the moduli spaces is almost unkown. Here, we summarize what is known about the unstable homology, see also Appendix E.

The virtual cohomological dimension of the moduli spaces has been determined by Harer in [Har86, Theorem 4.1]. For example, if $g > 0$ and $k > 0$, then $\mathrm{vcd}(\Gamma_{g,k}) = 4(g-1) + 2k$. Moreover, the rational homology vanishes on its virtual cohomological dimension by [CFP12].

Using various techniques, the integral or rational homology groups of the moduli spaces $\mathfrak{M}_{g,k}^\bullet$ for arbitrary g and k are well understood in homological degrees of at most three.

Among others, there are results by Mumford in [Mum67], Powell in [Pow78, Theorem 1] and Korkmaz–McCarthy in [KM00, Theorem 3.12] on the first integral homology; results on the second integral homology are due to Harer in [Har91, Theorem 0.a] and Korkmaz–Stipsicz in [KS03]; and the third rational homology is trivial for $g \geq 6$ by [Har91, Theorem 0.b]. For the convenience of the reader, we spell out their results in Appendix E.

The moduli space of a disc with $m \geq 1$ (un)permutable punctures is the classifying space of the m-th (pure) braid group. A complete description of the integral homology of the pure braid group is due to Arnold in [Arn70]. Denoting the field with p elements by $\mathbb{F}_p$ for p a prime, the $\mathbb{F}_p$-homology of the braid groups has been determined by Fuks in [Fuk70] for $p = 2$ and by Cohen in [CLM76] for $p > 2$.

The following results on the homology groups $H_*(\mathfrak{M}_{g,k})$ for small parameters g and k and with coefficients in the integers or a field have been computed using Bödigheimer's models for the moduli spaces. In his Ph.D. thesis [Ehr97], Ehrenfried determines the complete integral homology $H_*(\mathfrak{M}_1^{\square}(2,1), \mathbb{Z})$ and $H_*(\mathfrak{M}_{2,1}; \mathbb{Z})$, see also [Abh05, ABE08]. Using Visy's theory of factorable groups introduced in [Vis10], Mehner computes the integral homology $H_*(\mathfrak{M}_g^{\square}(m,1); \mathbb{Z})$ for $2g + m \leq 5$ in [Meh11] and provides a list of generators for roughly half of the homology groups. Let us mention two examples.

Proposition (Bödigheimer, Ehrenfried, Mehner)**.** *The integral homology of* $\mathfrak{M}_{2,1}$ *and* $\mathfrak{M}_1^{\square}(2,1)$ *is as follows.*

$$H_*(\mathfrak{M}_{2,1}; \mathbb{Z}) = \begin{cases} \mathbb{Z}\langle c^2 \rangle & * = 0 \\ \mathbb{Z}_{10}\langle cd \rangle & * = 1 \\ \mathbb{Z}_2\langle d^2 \rangle & * = 2 \\ \mathbb{Z}\langle ? \rangle \oplus \mathbb{Z}_2\langle t \rangle & * = 3 \\ \mathbb{Z}_6\langle ? \rangle & * = 4 \\ 0 & * \geq 5 \end{cases} \qquad H_*(\mathfrak{M}_1^{\square}(2,1); \mathbb{Z}) = \begin{cases} \mathbb{Z}\langle a^2 c \rangle & * = 0 \\ \mathbb{Z}\langle a^2 d \rangle \oplus \mathbb{Z}_2\langle bc \rangle & * = 1 \\ \mathbb{Z}_2\langle a^2 e \rangle \oplus \mathbb{Z}_2\langle bd \rangle & * = 2 \\ \mathbb{Z}_2\langle ? \rangle & * = 3 \\ 0 & * \geq 4 \end{cases}$$

Here, the known generators a, b, c, d, e, t and their products are described in [Meh11, Kapitel 1] or [BH14, Chapter 4] see also [BB18a]. The other generators are denoted by ?.

To their findings, we will add three new generators, see Section 1.4 and Chapter 7.

For genus three, computations with coefficients in finite field $H_*(\mathfrak{M}_{3,1}; \mathbb{F}_p)$ where carried out by Wang in [Wan11]. In [BH14], the author and Anna Hermann determine $H_*(\mathfrak{M}_g^{\square}(m,1); \mathbb{F})$ for coefficients in finite fields and the rationals for $2g + m \leq 6$.

Let us mention more results. In [LW85, Corollary 5.2.3], Lee–Weintraub show that $\tilde{H}_*(\Gamma_{2,0}; \mathbb{Z})$ is all p-torsion with $p = 2,3$ or 5 and, in [BC91] Benson–Cohen, derive the Poincaré-series for $H^*(\Gamma_{2,0}; \mathbb{F}_p)$ with $p = 2$, 3 and 5. In her Ph.D. thesis [God04], Godin uses a ribbon graph model of the moduli space to compute the integral homology $H_*(\mathfrak{M}_{1,1}^{\bullet}; \mathbb{Z})$, $H_*(\mathfrak{M}_{2,1}^{\bullet}; \mathbb{Z})$ (agreeing with Ehrenfried's results) and $H_*(\mathfrak{M}_{1,2}^{\bullet}; \mathbb{Z})$. The mapping class group is perfect for $g \geq 3$ by [Pow78, Theorem 1], hence $H_1(\mathfrak{M}_{3,1}^{\bullet}; \mathbb{Z}) = 0$. The second homology group $H_2(\mathfrak{M}_{3,1}^{\bullet}; \mathbb{Z}) \cong \mathbb{Z} \oplus \mathbb{Z}_2$ has been determined by [Sak12, Theorem 4.9]. The rational cohomology of $\mathfrak{M}_{4,0}^{\bullet}$ resp. $\mathfrak{M}_3^{\square}(2,0)$ is determined by Tommasi in [Tom05] resp. [Tom07].

1.2. Maps to $BU(1)^m$

Forgetting the parametrization of the m enumerated parametrized outgoing boundaries defines an m-dimensional torus bundle $U(1)^m \to \mathfrak{M}_g^\bullet(m,n) \to \mathfrak{M}_g^\circ(m,n)$. The classifying map to the universal bundle $EU(1)^m \to BU(1)^m$ has been studied and we recall an important result by Looijenga [Loo95, Proposition 2.1] concerning the stable cohomology of moduli spaces:

Proposition 1.2.1. *There is a graded isomorphism of algebras over $H^*(\mathfrak{M}_\infty^\bullet(m,n);\mathbb{Z})$*

$$H^*(\mathfrak{M}_\infty^\bullet(m,n);\mathbb{Z})[u_1,\dots,u_m] \cong H^*(\mathfrak{M}_\infty^\circ(m,n);\mathbb{Z})\,, \tag{1.2}$$

where $u_i \in H^*(\mathfrak{M}_\infty^\circ(m,n);\mathbb{Z})$ is the pullback of $e_i \in H^*(BU(1)^m;\mathbb{Z}) \cong \mathbb{Z}[e_1,\dots,e_m]$ along the classifying map of the m-dimensional torus bundle $\mathfrak{M}_g^\bullet(m,n) \to \mathfrak{M}_g^\circ(m,n)$.

Using explicit (rational) models, both for the moduli spaces and the universal bundle $EU(1)^m \to BU(1)^m$, the classifying map has been made explicit by Kontsevich in [Kon92] and Bödigheimer in [Bö93b]. We use their ideas to construct yet another model for the classifying space in Chapter 2. Our model plays a role in the study of the harmonic compactifications of the moduli spaces, see Section 1.4, Chapter 5 and Chapter 6. For convenience of the reader, we discuss the main ideas of the three models here.

1.2.1. Finite subset spaces, polygon bundles and metric ribbon graphs

In this section, we discuss the relations between the space of finite subset space in the circle $\mathbb{S}^1 = U(1)$, Kontsevich's polygon bundles and spaces of (marked) metric ribbon graphs. More precisely, we recall the definitions of the spaces not yet introduced and discuss the following known fact.

Proposition (Kontsevich, Tuffley)**.** *There diagram below is commutative. The maps in the top row are $U(1)$-equivariant and the vertical maps are the orbit projections. The projection $Rib_g^\bullet(1,n) \to Rib_g^\circ(1,n)$ is a circle bundle.*

$$\begin{array}{ccccc} Rib_g^\bullet(1,n) & \longrightarrow & EU(1)^{comb} & \xrightarrow{\cong} & \mathbb{R}_{>0} \times exp(\mathbb{S}^1) \\ \downarrow & & \downarrow & & \downarrow \\ Rib_g^\circ(1,n) & \longrightarrow & BU(1)^{comb} & \xrightarrow{\cong} & \mathbb{R}_{>0} \times exp(\mathbb{S}^1)/U(1) \end{array}$$

Given a topological space X and an integer $N > 0$, the space of non-empty subsets of X of cardinality at most N is denoted by $exp_N(X)$. It is topologised as a quotient of the N-fold product X^N. Elementary properties and relations to configurations spaces are derived in [Han00]. For example, (1) the configuration spaces $\mathrm{Conf}^n(X)$ are open subspaces of $exp_N(X)$; (2) for X a compact Hausdorff space, $exp_N(X)$ is a compactification of $\mathrm{Conf}^N(X)$ and (3) for any $N \geq 1$ the subset spaces are homotopy functors.

The subset spaces $exp_N(\mathbb{S}^1)$ and variations of those are of particular interest for us. We know that $exp_N(\mathbb{S}^1)$ is homotopy equivalent to an odd dimensional sphere of dimension N

respectively $N-1$ if N is odd respectively even, see [Tuf02, Theorem 4]. Therefore the union

$$exp(\mathbb{S}^1) := \bigcup_{N\geq 1} exp_N(\mathbb{S}^1)$$

is contractible. In [Kon92, Section 2.2], Kontsevich introduces a contractible space with a faithful circle action called $EU(1)^{comb}$. It is homeomorphic to $\mathbb{R}_{>0} \times exp(\mathbb{S}^1)$ via an $U(1)$-equivariant map. Observe that the $U(1)$-action is faithful but not free: the vertices of a regular k-gon define a point in $EU(1)^{comb}$ with stabilizer $\mathbb{Z}_k \subset U(1)$. The orbit space is $BU(1)^{comb} \cong \mathbb{R}_{>0} \times exp(\mathbb{S}^1)/U(1)$.

Consider a metric ribbon graph $G \in Rib_g^\bullet(1,n)$ of genus g with one parametrized outgoing boundary and n enumerated parametrized incoming boundary components. The parametrized outgoing boundary is obviously isometric to an oriented parametrized circle consisting of k edges for some integer $k > 0$. The endpoints of these edges define a set $C(G)$ of k points on this circle, i.e., $C(G) \in \mathbb{R}_{>0} \times exp_N(\mathbb{S}^1)$. Sending G to $C(G)$ defines a continous map $Rib_g^\bullet(1,n) \to EU(1)^{comb}$. This map is $U(1)$-equivariant and therefore, it induces a map of orbit spaces $Rib_g^\circ(1,n) \to BU(1)^{comb}$.

1.2.2. Interval exchange spaces

In [Bö93b] Bödigheimer introduces several spaces of interval exchanges as a device to study moduli spaces of Riemann surfaces using his model of parallel slit configurations [Bö90a, Bö90b]. Here, we discuss the space of interval exchanges $\mathfrak{Er}(\infty) = \cup_n \mathfrak{Er}(n)$ and $\mathcal{E}(\infty)$.

Geometrically speaking, an interval exchange of the real line is given by cutting $\mathbb{R}$ into finitely many intervals and reglueing the bounded pieces in a different order. More pedantically, an interval exchange is an orientation preserving local isometry defined on the real line minus a finite number of points (that restricts to the identity on both ends of the real line). An interval exchange is determined by a sequence of points $y_0 \leq y_1 \leq \ldots \leq y_{n-1}$ and a permutation π of the $n-2$ bounded intervals $Y_i := [y_i, y_{i+1}]$, $0 \leq i \leq n-2$. Fixing the number of (bounded) intervals to be at most $n-2$, this space of interval exchanges retracts onto the subspace of normalized interval exchanges denoted by

$$\mathfrak{Er}(n) := \{[y_0, \ldots, y_{n-1}; \pi] \mid y_0 = 0, y_{n-1} = 1\}\,.$$

It is a semi-simplical space of dimension $n-2$, its top cells are indexed by the symmetric group on $n-1$ letters and it is homotopy equivalent to a bouquet of spheres of dimension $n-2$ by [Bö93b, Theorem 5.1]. Moreover, the family of spaces $\mathfrak{Er}(n)$ form an H-monoid with multiplication

$$\mathfrak{Er}(n) \times \mathfrak{Er}(m) \to \mathfrak{Er}(n+m)\,.$$

Using his parallel model of the moduli spaces of Riemann surfaces, c.f. [Bö90a, Bö90b], Bödigheimer constructs a map of H-monoids

$$\bigsqcup_{g\geq 0} \mathfrak{M}_{g,1} \to \bigsqcup_{g\geq 0} \mathfrak{Er}(4g)\,.$$

Furthermore, we have an inclusion $\iota\colon \mathfrak{Er}(n) \to \mathfrak{Er}(n+1)$ by sending $[y_0, \dots, y_{n-1}; \pi]$ to $[y_0, \dots, y_{n-1}, y_{n-1}; S_n(\pi)]$, where $S_n(\pi)$ is the permutation of the intervals $Y_0, \dots, Y_n$ that sends the degenerate interval $Y_n = [y_{n-1}, y_{n-1}]$ to itself and whose action on $Y_0, \dots, Y_{n-1}$ agrees with the action of π. The union $\mathfrak{Er}(\infty) = \cup_n \mathfrak{Er}(n)$ is contractible.

By construction, the space $\mathfrak{Er}(\infty)$ is the space of all normalized interval exchanges. It has the same homotopy type as the space of all (unnormalized) interval exchanges $\mathcal{E}(\infty)$ which is a space of all L^2-classes of functions $\phi\colon \mathbb{R} \to \mathbb{R}$ that have finitely many points of discontinuity C_ϕ, that restrict to an orientation preserving isometry on $\mathbb{R} - C_\phi$ and that restrict to the identity near $\pm\infty$. Observe that the composition of functions make $\mathcal{E}(\infty)$ into a group. The real line acts by translation on $\mathcal{E}(\infty)$ and it follows that $\mathcal{E}(\infty)$ is a model for the total space of the universal bundle $E\mathbb{R} \to B\mathbb{R}$.

In this thesis, we show that an analogously defined space of orientation preserving local isometries from $n \geq 1$ enumerated circles to $m \geq 1$ enumerated circles leads to an elegant model for $EU(1)^m \to BU(1)^m$ and we obtain an explicit description of the classifying map of the bundle $\mathfrak{M}^\bullet(m,n) \to \mathfrak{M}^\circ(m,n)$.

1.2.3. The spaces of polygons

For each $m \geq 1$ and $n \geq 1$, we define a model $\mathcal{P}ol^\bullet(m,n) \to \mathcal{P}ol^\circ(m,n)$ for the universal torus bundle $EU(1)^m \to BU(1)^m$. We see our construction as a natural generalization of Bödigheimer's space of interval exchanges discussed in Section 1.2.2. We give the basic idea of the construction of $\mathcal{P}ol^\bullet(m,n) \to \mathcal{P}ol^\circ(m,n)$ here. The details are found in Chapter 2.

Let us treat the case $m = n = 1$ at first. Following Bödigheimer, a point in $\mathcal{P}ol^\bullet(1,1)$ is an L^2 class of orientation preserving isometries ϕ between two circles that have a finite number of points of discontinuity. The domain is the "incoming circle" and the target is the "outgoing circle". On $\mathcal{P}ol^\bullet(1,1)$, there is a canonical $U(1)$-action by postcomposing isometries with a given rotation. Let us study the orbit space $\mathcal{P}ol^\circ(1,1)$. The incoming circle is $\mathbb{S}^1_{in} = [0,1]/_\sim$ and the points of discontinuity are $C_\phi \subset \mathbb{S}^1_{in}$. Note that C_ϕ is invariant under the $U(1)$-action, i.e., $C_\phi = C_{\alpha\phi}$ for every rotation $\alpha \in U(1)$ of the outgoing circle. For technical reasons, let us assume that $0 \in C_\phi$. After removing C_ϕ from $\mathbb{S}^1_{in}$, we are left with a sequence of oriented intervals $e_0 = (0, t_1), e_1 = (t_0, t_0 + t_1), \dots, e_k = (1 - t_k, 1)$ of total length $\sum t_i = 1$. By construction, ϕ maps the intervals isometrically into the outgoing circle. Using the orientation of the outgoing circle, we regard ϕ as a cyclic permutation σ_ϕ of the intervals. Observe that the combinatorial datum $\sigma = \sigma_\phi$ together with the lengths $t = (t_0, \dots, t_k)$ of the intervals defines a point in the orbit space $(\sigma; t) \in \mathcal{P}ol^\circ(1,1)$. This leads to a simplicial structure on $\mathcal{P}ol^\circ(1,1)$. In Section 2.6 we show that the orbit map $\mathcal{P}ol^\bullet(1,1) \to \mathcal{P}ol^\circ(1,1)$ is a universal circle bundle, c.f. Theorem 2.6.2.

The case $m \geq 1$ and $n = 1$ is treated similarly: The space $\mathcal{P}ol^\bullet(m,1)$ is the space of all orientation preserving isometries from one circle to m enumerated circles (having possibly different circumferences) up to a finite set of points. The domain is the "incoming circle" and the circles in the target are the "outgoing circles". The action of the m-dimensional torus $U(1)^m$ on $\mathcal{P}ol^\bullet(m,1)$ is by postcomposing isometries with a given sequence of m rotations. As before, by removing the points of discontinuity, the orbit projection sends $\phi \in \mathcal{P}ol^\bullet(m,1)$ to a point $(\sigma, t) \in \mathcal{P}ol^\circ(m,1)$ where $t \in \Delta^k$ and $\sigma \in \mathfrak{S}([k])$ is a permutation with exactly m enumerated cycles. Again, the orbit projection $\mathcal{P}ol^\bullet(1,1) \to \mathcal{P}ol^\circ(1,1)$ is a universal m-dimensional torus bundle by Theorem 2.6.2.

More generally, for each $m \geq 1$ and $n \geq 1$, there is an universal m-dimensional torus bundle $\mathcal{P}ol^\bullet(m,n) \to \mathcal{P}ol^\circ(m,n)$, with $\mathcal{P}ol^\bullet(m,n)$ the space of all orientation preserving isometries from n enumerated incoming circles to m enumerated outgoing circles up to a finite set of points and with $\mathcal{P}ol^\circ(m,n)$ made from points (σ, t) with $t \in \Delta^{k_1} \times \ldots \times \Delta^{k_n}$ and σ a permutation with exactly m enumerated cycles.

1.2.4. From moduli to polygons

Following [Bö06], a Riemann surface $F \in \mathfrak{M}_g^\bullet(m,n)$ admits a unique harmonic potential $f\colon F \to \mathbb{R}$ that is zero on the incoming boundaries and one on the outgoing boundaries. Let $\Phi = \operatorname{grad}(f)$ denote the gradient flow of f. We define the complete critical graph $K \subset F$ to consists of all gradient flow lines that enter or leave a critical point of u or that enter or leave a parametrization point in the outgoing or incoming boundaries. Most importantly, the complement $F - K$ is a disjoint union of half open rectangles $R = [0,1] \times (a,b)$. Such a rectangle R has exactly two boundary components $\partial R = \{0\} \times (a,b) \sqcup \{1\} \times (a,b)$. One boundary component is part of an incoming boundary while the other boundary component is part of an outgoing boundary. Moreover, these boundary components are isometric (flowing the one boundary through the rectangle defines an isotopy from the inclusion of the one boundary component to the inclusion of the other boundary component). Consequently, these pairs define an orientation preserving isometry from the incoming boundaries of F to the outgoing boundaries of F up to a finite set of points. Sending a Riemann surface to this isometry defines a continous map $\mathfrak{M}_g^\bullet(m,n) \to \mathcal{P}ol^\bullet(m,n)$ that commutes with the map forgetting the parametrizations, i.e., we have the following map of m-dimensional torus bundles.

$$\begin{array}{ccc} \mathcal{P}ol^\bullet_{\mathfrak{M}}\colon \mathfrak{M}_g^\bullet(m,n) & \longrightarrow & \mathcal{P}ol^\bullet(m,n) \simeq EU(1)^m \\ \downarrow & & \downarrow \\ \mathcal{P}ol^\circ_{\mathfrak{M}}\colon \mathfrak{M}_g^\circ(m,n) & \longrightarrow & \mathcal{P}ol^\circ(m,n) \simeq BU(1)^m \end{array} \tag{1.3}$$

In particular, $\mathcal{P}ol^\circ_{\mathfrak{M}}\colon \mathfrak{M}_g^\circ(m,n) \to \mathcal{P}ol^\circ(m,n)$ classifies the torus bundle $\mathfrak{M}^\bullet(m,n) \to \mathfrak{M}^\circ(m,n)$ which is a highly non-trivial bundle (see [Loo95, Proposition 2.1] or Proposition 1.2.1).

The inclusion of the moduli space into its harmonic compactification is of particular interest in the study of string topology, see Section 1.3. Our spaces of polygons turn out to be useful in understanding these inclusions. The moduli space $\mathfrak{M}^\bullet(m,n)$ deformation retracts onto the subspace $N\mathfrak{M}^\bullet(m,n)$ where all incoming resp. outgoing boundaries have equal lengths. The space of polygons $\mathcal{P}ol^\bullet(m,n)$ deformation retracts onto a corresponding subspace denoted by $N\mathcal{P}ol^\bullet(m,n)$. Both retractions are equivariant with respect to the torus action. In Chapter 5, we show that the classifying map factors through the inclusion into the harmonic compactification of $N\mathfrak{M}^\bullet(m,n)$, i.e., we have the following maps of m-dimension torus bundles.

$$\begin{array}{ccccc} N\mathfrak{M}_g^\bullet(m,n) & \longrightarrow & \overline{N\mathfrak{M}}_g^\bullet(m,n) & \longrightarrow & N\mathcal{P}ol^\bullet(m,n) \simeq EU(1)^m \\ \downarrow & & \downarrow & & \downarrow \\ N\mathfrak{M}_g^\circ(m,n) & \longrightarrow & \overline{N\mathfrak{M}}_g^\circ(m,n) & \longrightarrow & N\mathcal{P}ol^\circ(m,n) \simeq BU(1)^m \end{array} \tag{1.4}$$

In Chapter 5 and Chapter 6, we compare these bundle maps with the stabilization maps of the moduli spaces and their harmonic compactifications, see also Section 1.4.

1.3. Applications to string topology

The subject of string topology is the study of algebraic properties of the based loop space ΩM, the free loop space $LM = \mathrm{Map}(\mathbb{S}^1, M)$ and, more generally, the space of paths in a manifold M. In this article, we restrict our attention to the rational homology $H_*(-) := H_*(-;\mathbb{Q})$ of the free loop space of a closed, oriented, d-dimensional, simply connected manifold M.

The study of moduli spaces of Riemann surfaces and their compactifications is strongly related to its applications to string topology. In this section, we give a brief overview of this relation. An introduction to the aspects of string topology presented here can be found in [CHV06, Abb15, Fé15]. For a broad overview that covers more aspects of string topology we refer the reader to [Sul07].

1.3.1. String operations

In [CS99], Chas and Sullivan discovered rich algebraic structures in the homology of the free loop space LM. There are several approaches and conjectures connecting these algebraic structures with algebraic structures on the Hochschild cohomology of algebras related to M, see e.g. [Jon87, CJ02, Vai07, Kau07, Kau08a, Kau10].

To begin with, Chas–Sullivan construct the loop product

$$\circ\colon H_i(LM) \otimes H_j(LM) \to H_{i+j-d}(LM)\,. \tag{1.5}$$

In order to give the geometric construction of this map we consider the bouquet $\mathbb{S}^1 \vee \mathbb{S}^1$ (which is often called "figure-8"), the canonical map $\mathbb{S}^1 \sqcup \mathbb{S}^1 \to \mathbb{S}^1 \vee \mathbb{S}^1$ and the pinch map $\mathbb{S}^1 \to \mathbb{S}^1 \vee \mathbb{S}^1$. The loop product of two homology classes x and y is the transverse intersection of $x \times y \in \mathrm{Map}(\mathbb{S}^1, M) \times \mathrm{Map}(\mathbb{S}^1, M) \cong \mathrm{Map}(\mathbb{S}^1 \sqcup \mathbb{S}^1, M)$ with the codimension d submanifold $\mathrm{Map}(\mathbb{S}^1 \vee \mathbb{S}^1, M)$ followed by the restriction ρ^{out} that is induced by the pinch map, c.f. [Cha05]. Equivalently, the restriction ρ^{in} to the two "inner" circles of the figure-8 admits an Umkehr (or wrong way) map $\rho^{in}_!$ and the loop product is the composition

$$\circ\colon H_i(LM) \otimes H_j(LM) \xrightarrow{\rho^{in}_!} H_{i+j-d}(\mathrm{Map}(\mathbb{S}^1 \vee \mathbb{S}^1, M)) \xrightarrow{\rho^{out}_*} H_{i+j-d}(LM)\,. \tag{1.6}$$

After adjusting the grading $\mathbb{H}_* = H_{*-d}$, the loop product turns $\mathbb{H}_*(LM)$ into an associative, commutative algebra. Moreover, the evaluation map $LM \to M$, $\gamma \mapsto \gamma(1)$ induces a homomorphism of algebras where $\mathbb{H}_*(M)$ is the intersection algebra

$$ev_*\colon \mathbb{H}_*(LM) \to \mathbb{H}_*(M)\,. \tag{1.7}$$

The circle action $\mathbb{S}^1 \times LM \to LM$ induces an operator

$$\Delta\colon \mathbb{H}_*(LM) \to \mathbb{H}_{*+1}(LM) \tag{1.8}$$

that turns $\mathbb{H}_*(LM)$ into a Batalin–Vilkovisky algebra (short: BV-algebra), i.e., $\mathbb{H}_*(LM)$ is graded commutative, $\Delta^2 = 0$ and the binary operator, called bracket,

$$\{x, y\} := (-1)^{|x|}\Delta(x \circ y) - (-1)^{|x|}\Delta(x) \circ y - x \circ \Delta(y) \tag{1.9}$$

is a derivation in each variable. The bracket satisfies the (graded) Jacobi identities and therefore $\mathbb{H}_*(LM)$ is also a graded Lie algebra. Over a field of characteristic different from 2, the category of BV-algebras is equivalent to the category of algebras over the (homology of the) operad of little framed 2-discs $\mathcal{D}_2$ by [Get94, Theorem 4.5]. In other words, $\mathbb{H}_*(LM)$ is an algebra over the operad $H_*(\mathcal{D}_2)$. Voronov gives an explicit description of this action, c.f. [Vor05, Theorem 2.3].

In [CJ02], Cohen and Jones give a homotopy theoretic realization of the structures found by Chas–Sullivan and Voronov. The loop operation and the operadic action are both realized on the Thom spectrum of a certain virtual bundle defined over LM. In particular, the above structures are present on all generalized homology theories. Moreover, they establish an isomorphism of graded algebras between the Hochschild cohomology of the singular cochains of M and $\mathbb{H}_*(LM)$

$$HH^*(C^\bullet(M), C^\bullet(M)) \cong \mathbb{H}_*(LM)\,. \tag{1.10}$$

For finite dimensional symmetric Frobenius algebras[1] or, more generally, a possibly infinite dimensional A_∞-Frobenius algebras A over $\mathbb{Q}$, the Hochschild cohomology carries a natural BV-algebra structure, see [Tra08] and [Kau08b]. The cochains $C^\bullet(M)$ of a closed, oriented manifold M carry a natural A_∞-Frobenius algebra structure that is compatible with the BV-algebra structure on the Hochschild cohomology and the loop homology. With rational coefficients and for a simply connected manifold M, the isomorphism (1.10) of Cohen–Jones is an isomorphism of BV-algebras by [FT08, Theorem 1], [LS08, Section 1.1] and [Men09, Corollary 20].

The $H_*(\mathcal{D}_2)$-algebra structure on $HH^*(C^\bullet(M), C^\bullet(M))$ depends only on the homotopy type of M, whereas on $\mathbb{H}_*(LM)$ the smooth structure of M is involved. However, the action of $H_*(\mathcal{D}_2)$ on $\mathbb{H}_*(LM)$ is independent up to orientation preserving homotopy equivalences, see [CKS08, Theorem 1].

1.3.2. Higher string operations

Observe that $H_*(\mathcal{D}_2)$ and $H_*(\sqcup_q \mathfrak{M}_0^\bullet(q, 1))$ are isomorphic operads, where the operadic action on the right is induced by sewing surfaces along parametrized boundaries. Consequently, denoting the surface PROP by $\mathfrak{M}^\bullet := \sqcup_{g,n,m}\mathfrak{M}_g^\bullet(m, n)$, we have an inclusion of a suboperad $H_*(\mathcal{D}_2) \subset H_*(\mathfrak{M}^\bullet)$. The homology of little framed 2-discs $H_*(\mathcal{D}_2)$ acts on the homology of the free loop space $\mathbb{H}_*(LM)$ and on the Hochschild cohomology of an algebra $HH^*(A, A)$ in a natural way. There are various extensions this action. By an extension of the action we mean a factorization of the operadic action of $H_*(\mathcal{D}_2)$ on $\mathbb{H}_*(LM)$ or $HH^*(A, A)$ through a PROPeradic action of $H_*(X)$, with X a suitable subspace (or componentwise compactification) of $\mathfrak{M}^\bullet$. The extensions reviewed in this subsection are

[1] An algebra A over $\mathbb{Q}$ is a Frobenius algebra if it is a unital, associative algebra with symmetric, non-degenrate inner product $\langle -, - \rangle$ satisfying $\langle a \cdot b, c\rangle = \langle a, b \cdot c\rangle$ for all $a, b, c \in A$, see Appendix C.

summarized in the following diagram, where the labels on the vertical arrows are indicating in which subsection the extension is discussed.

$$\begin{array}{ccc} H_*(\mathcal{D}_2) \curvearrowright \mathbb{H}_*(LM) & \xleftarrow[(1.10)]{\cong} & H_*(\mathcal{D}_2) \curvearrowright HH^*(C^\bullet(M), C^\bullet(M)) \\ \downarrow{\scriptstyle 1.3.2.1} & & \downarrow{\scriptstyle 1.3.2.2} \\ H_*(U\mathfrak{M}^\bullet) \curvearrowright \mathbb{H}_*(LM) & & H_*(\mathfrak{M}^\bullet) \curvearrowright HH^*(C^\bullet(M), C^\bullet(M)) \\ \downarrow{\scriptstyle 1.3.2.5} & & \downarrow{\scriptstyle 1.3.2.3 \text{ and } 1.3.2.4} \\ H_*(\overline{\mathfrak{M}}^\bullet) \curvearrowright \mathbb{H}_*(LM) & & H_*(\overline{\mathfrak{M}}^\bullet) \curvearrowright HH^*(C^\bullet(M), C^\bullet(M)) \end{array}$$

1.3.2.1. An extension by Godin–Cohen

In [CG04], Cohen and Godin provide an extension of the action on the homology of the free loop space (up to a shift in the homological degree)

$$H_*(URib_g^\bullet(m,n)) \otimes H_*(LM)^{\otimes n} \to H_*(LM)^{\otimes m} \tag{1.11}$$

for a subspace $URib_g^\bullet(m,n) \subset Rib_g^\bullet(m,n)$ that is defined as follows. A marked metric ribbon graph $G \in Rib_g^\bullet(m,n)$ is said to be of type (g,m,n) if two conditions are met. Firstly, we require the subgraph $G' \subset G$ corresponding to the n incoming boundaries to be a disjoint union of n circles; and secondly, we require the complement of G' in G to be a disjoint union of trees $T_1, \ldots, T_k$. The marked ribbon graphs of type (g,m,n) define the subspace $URib_g^\bullet(m,n) \subset Rib_g^\bullet(m,n)$. In order to define the action of $URib_g(m,n)$ in the loop homology, we contract each of the trees $T_i \subset G$ to obtain a new marked metric ribbon graph $S(G)$ called the reduction of G. The reduction of G has the same genus as G and there is a canonical decomposition of its boundary components into $n+m$ pieces. However it is not of type (g,m,n) any more. In Section 1.3.1, we reviewed the geometric definition of the Chas–Sullivan loop product using the transverse intersection with a certain submanifold followed by a restriction map. Here, we also have a submanifold $\mathrm{Map}(S(G), M) \subset \mathrm{Map}(\sqcup_n \mathbb{S}^1, M)$ of codimension $\chi(G)d$ and the transverse intersection with this induces an operation:

$$H_*(LM)^{\otimes n} \xrightarrow{\rho_!^{in}} H_{*+\chi(G)d}(\mathrm{Map}(S(G), M)) \xrightarrow{\rho_*^{out}} H_{*+\chi(G)d}(LM)^{\otimes m}\,. \tag{1.12}$$

Given two ribbon graphs G_1 and G_2, the induced operations agree whenever $[G_1] = [G_2] \in H_0(URib_g^\bullet(m,n))$ and there is an operation for each homology class $H_*(URib_g^\bullet(m,n))$.

Under the homotopy equivalence $Rib_g^\bullet(m,n) \simeq \mathfrak{M}_g^\bullet(m,n)$, the subspace $URib_g^\bullet(m,n)$ is sent to a subspace of the moduli space which we denote by $U\mathfrak{M}_g^\bullet(m,n) \subset \mathfrak{M}_g^\bullet(m,n)$. The homology groups $H_*(U\mathfrak{M}^\bullet) = H_*(\sqcup_{g,m,n} U\mathfrak{M}_g^\bullet(m,n))$ form a PROP and the PROPeradic composition is induced by sewing surfaces along boundaries. Consequently, the inclusion $U\mathfrak{M}^\bullet \subset \mathfrak{M}^\bullet$ induces a map of PROPs $H_*(U\mathfrak{M}^\bullet) \to H_*(\mathfrak{M}^\bullet)$. Voronovs model for the operad of little framed 2-discs $\mathcal{D}^2$ has the same homotopy type as $\sqcup_m U\mathfrak{M}_0^\bullet(m,1)$ and the actions (of their homologies) on $H_*(LM)$ agree. In other words, the operadic action of $H_*(\mathcal{D}_2)$ is extended to a PROPeradic action of $H_*(U\mathfrak{M}^\bullet)$.

1.3.2.2. An extension by Costello and Kontsevich–Soibelman

Costello constructs a model for the moduli space $\mathfrak{M}$ using a dual version of the ribbon graph decomposition, see [Cos07a] and [Ega14a, Theorem B]. Following [WW16], we call his model the chain complex of black and white graphs and denote it by $BW(\mathfrak{M})$. In [Cos07b] Costello constructs an action of the homology of $BW(\mathfrak{M})$ on the Hochschild cohomology of any A_∞-Frobenius algebra. This action is compatible with glueing surfaces along intervals and boundary components (see [Cos07b] and [Ega14a, Theorem D]). Moreover, the action of $H_*(\mathfrak{M}^\bullet)$ restricts to the usual action of $H_*(\mathcal{D}_2)$.

Using yet another chain complex model of the moduli spaces, Kontsevich and Soibelman let these chains act on the Hochschild cohomology of a finite dimensional A_∞-algebra with scalar product in [KS09, Section 11.6]. The two actions agree in case of A_∞-Frobenius algebras by [WW16, Section 6].

1.3.2.3. An extension by Tradler–Zeinalian

In [TZ06], Tradler and Zeinalian construct a PROP of chain complexes $\mathcal{SD}$ whose cells are in one to one correpondence to certain combinatorial graphs called Sullivan diagrams. The chain complex of Sullivan diagrams is a quotient of Costellos chain complex of black and white graphs, see [WW16, Theorem 2.9]. The corresponding space of Sullivan diagrams has the homotopy type of Bödigheimer's harmonic compactification of the moduli spaces, see [Bö06] and [EK14, Proposition 5.1]. The Hochschild homology of a finite dimensional Frobenius algebra A is an algebra over the PROP $H_*(\mathcal{SD})$ and the dual action on the Hochschild cohomology of a Frobenius algebra extends the action of Costello and Kontsevich–Soibelman by [WW16, Theorem 5.13].

1.3.2.4. An extension by Kaufmann

Another extension of the action of $H_*(\mathcal{D}_2)$ on the Hochschild cohomology of a Frobenius algebra has been provided by Kaufmann in [Kau07], [Kau08a] and [Kau10]. He constructs a model for the moduli space by means of embedded arcs running from the incoming boundaries to the outgoing ones. In his model, he allows open and closed boundaries. The closed part is a model for spaces of Sullivan diagrams and the actions agree with the ones above.

1.3.2.5. An extension by Drummond-Cole–Poirier–Rounds

In [PR11, DPR15], Drummond-Cole, Poirier and Rounds consider a compactification of the space of reduced ribbon graphs used by Cohen and Godin. This compactification is homeomorphic to the space of Sullivan diagrams defined by Tradler and Zeinalian. Using this identification, Poirer and Rounds define an action of the cellular chains $C_*(\mathcal{SD})$ on (a tensor product of) the singular chains $C_*(LM)$. After taking homology, the actions of Cohen–Godin and Poirer–Rounds agree in homological degree zero. However, it is not known to us wether the action of Cohen–Godin factors through the action of $C_*(\mathcal{SD})$ in all homological degrees.

1.3.3. Open questions and partial answers

In the above subsections, we gave a brief overview of the extensions of the action of the framed disc operad on the loop homology of a closed manifold M and on the Hochschild cohomology of an A_∞-Frobenius algebra. Up to identifications, the action on the loop homology resp. the Hochschild cohomology comes from subspaces $\mathcal{D}_2 \subset U\mathfrak{M}^\bullet \subset \overline{\mathfrak{M}}^\bullet$ resp. $\mathcal{D}_2 \subset \mathfrak{M}^\bullet \subset \overline{\mathfrak{M}}^\bullet$ of the harmonic compactification. Moreover, there is an isomorphism of $H_*(\mathcal{D}_2)$-algebras by [CJ02].

$$\mathbb{H}_*(LM) \cong HH^*(C^\bullet(M), C^\bullet(M))\,. \tag{1.13}$$

It is an open question wether or not the extension of the action of $H_*(\mathcal{D}_2)$ to an action of $H_*(\overline{\mathfrak{M}}^\bullet)$ is maximal or not; we do not know if the isomorphism of Cohen–Jones is an isomorphism of $H_*(\overline{\mathfrak{M}}^\bullet)$-algebras; and a description of the homology of $H_*(\overline{\mathfrak{M}}^\bullet)$ is also unkown. In what follows, we discuss some partial answers to these interrelated questions.

The question wether or not the harmonic compactification of the moduli space is the largest PROP through which the action factors has been partially answered by Wahl in [Wah16]: All natural operations on the Hochschild homology of Frobenius algebras form a chain complex. As an approximation of this, Wahl introduces her chain complex of all formal operations. The chain complex of Sullivan diagrams $\mathcal{SD}$ is a subcomplex of the complex of all formal operations and the inclusion is a split-injective quasi-isomorphism, see [Wah16, Theorem 2.9]. We believe this is a big step towards a complete answer of the first question.

The action of a homology class in $H_*(\mathscr{SD})$ on $HH_*(A, A)$ is made explicit in [WW16, Section 6.2]. Moreover, the space of Sullivan diagrams $\mathscr{SD}$ is homotopy equivalent to the (componentwise) harmonic compactification $\overline{\mathfrak{M}}^\bullet$ of $\mathfrak{M}^\bullet$ by [EK14]. Therefore, a better understanding of the extension of actions is strongly related to deeper understandin of the homology of the moduli spaces, their harmonic compactifications and the inclusion

$$\mathfrak{M}^\bullet \hookrightarrow \overline{\mathfrak{M}}^\bullet\,. \tag{1.14}$$

Wahl and Westerland showed that every stable class of the moduli space of surfaces with at least one parametrized outgoing boundary component vanishes in its harmonic compactification, see [WW16, Theorem 2.19]. However, there are unstable classes that are detected in the harmonic compactification, e.g., in case of a single incoming boundary and m outgoing boundaries, the harmonic compactification can be identified with a deformation retraction of its moduli space by the work of [EK14]. In this thesis, we provide some insights on the homotopy type of $\overline{\mathfrak{M}}^\bullet$.

1.4. Results

In this section, we state the most important results of our thesis. Some of the results in this thesis are published in the article [BE17] with Egas Santander. Here, these results are marked as "B.+Egas".

1.4.1. On the stable homotopy type of the harmonic compactification

Let $g \geq 0$, $m \geq 0$, $n = 1$ and $\star \in \{\bullet, \blacksquare, \circ, \square\}$. Recall that the stabilization map of the moduli spaces $\varphi_g \colon \mathfrak{M}_g^\star(m, n) \to \mathfrak{M}_{g+1}^\star(m, n)$ induces isomorphisms in integral homology in

the range $* \leq 2(g-1)/3$. We show that the stabilization map φ_g extends to the harmonic compactification and that this extension is highly connected connected with respect to the genus and the number of outgoing boundary curves.

Theorem 4.4.1 and Theorem 5.2.11 (B.+Egas)**.** *Let $g \geq 0$, $m \geq 1$, $\star \in \{\bullet, \blacksquare, \circ, \square\}$ and denote the stabilization maps of the moduli spaces by $\varphi_g \colon \mathfrak{M}_g^\star(m,1) \to \mathfrak{M}_{g+1}^\star(m,1)$ resp. $\varphi_g \colon N\mathfrak{M}_g^\star(m,1) \to N\mathfrak{M}_{g+1}^\star(m,1)$. The stabilization maps extend to the harmonic compactification, i.e., there is a maps $\overline{\varphi}_g \colon \overline{\mathfrak{M}}_g^\star(m,1) \to \overline{\mathfrak{M}}_{g+1}^\star(m,1)$ resp. $\overline{\varphi}_g \colon \overline{N\mathfrak{M}}_g^\star(m,1) \to \overline{N\mathfrak{M}}_{g+1}^\star(m,1)$ making the following diagrams commutative. The diagram on the right hand side is the restriction of the diagram on the left hand side.*

$$\begin{array}{ccc} \mathfrak{M}_g^\star(m,1) & \xrightarrow{\varphi_g} & \mathfrak{M}_{g+1}^\star(m,1) \\ \downarrow & & \downarrow \\ \overline{\mathfrak{M}}_g^\star(m,1) & \xrightarrow{\overline{\varphi}_g} & \overline{\mathfrak{M}}_{g+1}^\star(m,1) \end{array} \qquad \begin{array}{ccc} N\mathfrak{M}_g^\star(m,1) & \xrightarrow{\varphi_g} & N\mathfrak{M}_{g+1}^\star(m,1) \\ \downarrow & & \downarrow \\ \overline{N\mathfrak{M}}_g^\star(m,1) & \xrightarrow{\overline{\varphi}_g} & \overline{N\mathfrak{M}}_{g+1}^\star(m,1) \end{array}$$

The stabilization map $\overline{\varphi}_g$ induces an isomorphism in homology in the degrees $* \leq g+m-2$ resp. $* \leq g-1$. Moreover, if $m > 2$, the stabilization map $\overline{\varphi}_g$ is $(g+m-2)$-connected resp. $(g-1)$-connected.

The usual framework that is used to proof homological stability cannot be applied to our situation because the harmonic compactifications are highly connected (see the theorem below). Our proof of the above theorem in the case of $\overline{\mathfrak{M}}_g^\star(m,1)$ is as follows. The stabilization map $\overline{\varphi}_g$ identifies the cellular chain complex $C_*(\overline{\mathfrak{M}}_g^\star(m,1))$ with a subcomplex of $C_*(\overline{\mathfrak{M}}_{g+1}^\star(m,1))$. On the pair $(C_*(\overline{\mathfrak{M}}_g^\star(m,1), \overline{\mathfrak{M}}_{g+1}^\star(m,1))$, we construct a discrete Morse flow that is perfect in the degrees $* \leq (g+m-1)$. Consequently, the stabilization map induces an integral homology isomorphism in the degrees $* \leq g+m-2$. By the Theorem below, $\mathfrak{M}_g^\star(m,1)$ is $(g+m-2)$-connected and so is $\overline{\varphi}_g$. For $m=1$ and $m=2$, we believe that the stabilization maps $\overline{\varphi}_g$ are also highly connected with respect to the genus.

The harmonic compactifications are highly connected with respect to the number of outgoing boundaries.

Theorem 4.4.2 (B.+Egas)**.** *Let $g \geq 0$ and $m > 2$. The spaces $\overline{\mathfrak{M}}_g^\bullet(m,1)$, $\overline{\mathfrak{M}}_g^\blacksquare(m,1)$, $\overline{\mathfrak{M}}_g^\circ(m,1)$ or $\overline{\mathfrak{M}}_g^\square(m,1)$ are highly connected with respect to m, i.e.,*

$$\pi_*(\overline{\mathfrak{M}}_g^\bullet(m,1)) = 0 \qquad \textit{and} \qquad \pi_*(\overline{\mathfrak{M}}_g^\circ(m,1)) = 0 \qquad \textit{for} \qquad * \leq m-2$$

and

$$\pi_*(\overline{\mathfrak{M}}_g^\blacksquare(m,1)) = 0 \qquad \textit{and} \qquad \pi_*(\overline{\mathfrak{M}}_g^\square(m,1)) = 0 \qquad \textit{for} \qquad * \leq m'$$

where m' is the largest even number strickly smaller than m.

In addition to the above theorem, let us discuss the connectivity of $\overline{\mathfrak{M}}_g^\star(2,1)$ and $\overline{\mathfrak{M}}_g^\star(1,1)$ for a fixed $g \geq 0$. The space $\mathfrak{M}_g^\star(2,1)$ is not in general simply-connected, see Subsection 1.4.3. From the construction, it is clear that the moduli spaces with one parametrized incoming boundary $\mathfrak{M}_g^\bullet(1,1)$, $\mathfrak{M}_g^\blacksquare(1,1)$, $N\mathfrak{M}_g^\bullet(1,1)$ and $N\mathfrak{M}_g^\blacksquare(1,1)$ are all equal and so are their harmonic compactifications. Analogously, the moduli spaces $\mathfrak{M}_g^\circ(1,1)$, $\mathfrak{M}_g^\square(1,1)$,

$N\mathfrak{M}_g^\circ(1,1)$ and $N\mathfrak{M}_g^\square(1,1)$ are all equal and so are their harmonic compactifications. Therefore, it follows from the next Theorem, that $\overline{\mathfrak{M}}_g^\star(1,1)$ is also simply-connected.

The forgetful map $\overline{\mathfrak{M}}_g^\bullet(m,1) \to \overline{\mathfrak{M}}_g^\circ(m,1)$ is not a fibration (the homotopy type of the fibres is not even constant). However, the restriction to the harmonic compactification of $N\mathfrak{M}_g^\star(m,1)$ is an m-dimensional torus bundle $U(1)^m \to \overline{N\mathfrak{M}}_g^\bullet(m,1) \to \overline{N\mathfrak{M}}_g^\circ(m,1)$. The forgetful map commutes with the stabilization maps, the stabilization maps are highly connected and we determine its stable homotopy type of $\overline{N\mathfrak{M}}_g^\star(m,1)$.

Theorem 5.2.11 (B.)**.** *Let $m \geq 1$, $g \geq 0$. Forgetting the parametrization of the outgoing boundaries defines m-dimensional torus fibrations*

$$\begin{array}{ccccccc} N\mathfrak{M}_g^\bullet(m,1) & \longrightarrow & \overline{N\mathfrak{M}}_g^\bullet(m,1) & \xhookrightarrow{\overline{\varphi}_g} & \overline{N\mathfrak{M}}_\infty^\bullet(m,1) & \xrightarrow{\mathcal{P}ol} & N\mathcal{P}ol^\bullet(m,1) \simeq EU(1)^m \\ \downarrow{\scriptstyle \pi_\circ^\bullet} & & \downarrow{\scriptstyle \pi_\circ^\bullet} & & \downarrow{\scriptstyle \pi_\circ^\bullet} & & \downarrow{\scriptstyle \pi_\circ^\bullet} \\ N\mathfrak{M}_g^\circ(m,1) & \longrightarrow & \overline{N\mathfrak{M}}_g^\circ(m,1) & \xhookrightarrow{\overline{\varphi}_g} & \overline{N\mathfrak{M}}_\infty^\circ(m,1) & \xrightarrow{\mathcal{P}ol} & N\mathcal{P}ol^\circ(m,1) \simeq BU(1)^m \end{array}$$

with $\overline{\varphi}_g$ the extension of the stabilization map of the moduli spaces. The maps $\overline{\varphi}_g$ are $(g-1)$-connected and the maps $\mathcal{P}ol$ are homotopy equivalences.

The next theorem is of particular interest to string topologists, because the main result of [Wah16] suggests that all higher string operations are parametrized by the spaces $\overline{\mathfrak{M}}_g^\bullet(m,n)$.

Theorem 6.1 (B.)**.** *Let $g \geq 2$ and $m \geq 1$ or $g \geq 0$ and $m \geq 3$. The harmonic compactification $\overline{\mathfrak{M}}_g^\bullet(m,1)$ is $(g+m-2)$-connected. In particular, $\overline{\mathfrak{M}}_\infty^\bullet(m,1)$ is contractible.*

As a corollary, we obtain not only the vanishing result by Tamanoi [Tam09, Theorem 4.4 (ii)] (stating that all stable string operations are trivial) but the stronger statement that all string operations that are parametrized by the harmonic compactification $\mathfrak{M}_g^\bullet(m,1)$ are trivial if their homological degrees do not exceed $(g+m-2)$.

1.4.2. On the homology of the harmonic compactification

In this section, we present our results on the homology of the harmonic compactification.

We have the following generalization of the desuspension theorem by Klamt in [Kla13].

Theorem 5.1.22 (B.)**.** *Let $m \geq 1$ and $g \geq 0$. There are isomorphisms*

$$\begin{aligned} H_*(\overline{N\mathfrak{M}}_g^\bullet(m,1);\mathbb{Z}) &\cong \Sigma^{-m+1} H_*(\overline{\mathfrak{M}}_g^\bullet(m,1), D\overline{\mathfrak{M}}_g^\bullet(m,1);\mathbb{Z}) \\ H_*(\overline{N\mathfrak{M}}_g^\circ(m,1);\mathbb{F}_2) &\cong \Sigma^{-m+1} H_*(\overline{\mathfrak{M}}_g^\circ(m,1), D\overline{\mathfrak{M}}_g^\circ(m,1);\mathbb{F}_2) \\ H_*(\overline{N\mathfrak{M}}_g^\blacksquare(m,1);\mathbb{F}_2) &\cong \Sigma^{-m+1} H_*(\overline{\mathfrak{M}}_g^\blacksquare(m,1), D\overline{\mathfrak{M}}_g^\blacksquare(m,1);\mathbb{F}_2) \\ H_*(\overline{N\mathfrak{M}}_g^\square(m,1);\mathbb{F}_2) &\cong \Sigma^{-m+1} H_*(\overline{\mathfrak{M}}_g^\square(m,1), D\overline{\mathfrak{M}}_g^\square(m,1);\mathbb{F}_2) \end{aligned}$$

where $D\overline{\mathfrak{M}}^\star(m,1)$ denotes the subspace of all moduli (or Sullivan diagrams) having at least one degenerate outgoing boundary.

Roughly speaking, the theorem follows from the following observation. The subspace $D\overline{\mathfrak{M}}_g^\bullet(m,1) \subset \overline{\mathfrak{M}}_g^\bullet(m,1)$ is the closed subspace of all moduli with at least one degenerate outgoing boundary. The harmonic compactification of the moduli space with normalized

outgoing boundaries $\overline{N\mathfrak{M}^\bullet}_g(m,1)$ is a deformation retract of $\overline{\mathfrak{M}}^\bullet_g(m,1) - D\overline{\mathfrak{M}}^\bullet_g(m,1)$. The retraction together with measuring the circumference of the outgoing boundaries defines a homeomorphism $\overline{\mathfrak{M}}^\bullet_g(m,1) - D\overline{\mathfrak{M}}^\bullet_g(m,1) \cong \overline{N\mathfrak{M}}^\bullet_g(m,1) \times \mathrm{int}(\Delta^{m-1})$ that extends to the quotient $\overline{\mathfrak{M}}^\bullet_g(m,1)/D\overline{\mathfrak{M}}^\bullet_g(m,1) \cong \Sigma^{m-1}\overline{N\mathfrak{M}}^\bullet_g(m,1)$.

It is a non-trivial task to find non-trivial classes in the homology of the spaces of the harmonic compactification. We show that every homology class is represented by a chain of moduli without degenerate outgoing boundaries.

Proposition 4.4.3 (B.+Egas)**.** *Let $g \geq 0$, $m \geq 1$ and $\star \in \{\bullet, \blacksquare, \circ, \square\}$. Denote the cellular chain complex of $\overline{\mathfrak{M}}^\star_g(m,1)$ by C and let R be an arbitrary coefficient group. Denote the sub-complex of moduli with at least 1 degenerate boundaries by $D \subset C$. Every homology class $x \in H_*(\overline{\mathfrak{M}}; R)$ is represented by a chain $\sum \kappa_i c_i$ with $c_i \notin D$.*

Forgetting the enumeration of the outgoing boundaries is not a covering for moduli having more then two degenerate outgoing boundaries. Nontheless, using the above theorem, the forgetful maps behave like coverings in homology.

Proposition 4.4.4 (B.+Egas)**.** *In homology there are maps*

$$tr\colon H_*(\overline{\mathfrak{M}}^\blacksquare_g(m,1);\mathbb{Z}) \to H_*(\overline{\mathfrak{M}}^\bullet_g(m,1);\mathbb{Z})$$

respectively

$$tr\colon H_*(\overline{\mathfrak{M}}^\square_g(m,1);\mathbb{Z}) \to H_*(\overline{\mathfrak{M}}^\circ_g(m,1);\mathbb{Z})$$

where $(\pi^\bullet_\blacksquare)_* \circ tr$ respectively $(\pi^\circ_\square)_* \circ tr$ is the multiplication by $m!$.

1.4.3. Non-trivial families in the homology of the harmonic compactification

In this section, we present our non-trivial families in the homology of the harmonic compactification.

Denote the surface of genus g, with one incoming and one outgoing boundary by $S_g(1,1)$. Glueing the k-th punctured disc to the outgoing boundary induces the canonical inclusion of the k-th group into the mapping class group

$$Br_k \hookrightarrow \Gamma^k_{g,1} \quad \text{or equivalently} \quad \mathfrak{M}^\square_0(k,1) \hookrightarrow \mathfrak{M}^\square_g(k,1)\,.$$

By construction, these inclusion are compatible with respect to the stabilization of the genus.

Proposition 4.4.5 (B.+Egas)**.** *The fundamental group of $\overline{\mathfrak{M}}^\square_0(2,1)$ is*

$$\pi_1(\overline{\mathfrak{M}}^\square_0(2,1)) \cong \begin{cases} \mathbb{Z}\langle\alpha_0\rangle & g = 0 \\ \mathbb{Z}_2\langle\alpha_g\rangle & g > 0 \end{cases}.$$

The homomorphism on fundamental groups induced by the stabilization map

$$\pi_1(\overline{\varphi}_g)\colon \pi_1(\overline{\mathfrak{M}}^\square_g(2,1)) \to \pi_1(\overline{\mathfrak{M}}^\square_{g+1}(2,1))$$

sends α_g to α_{g+1}. Furthermore, the class α_g is in the image of the braid generator under the canonical map

$$\pi_1(\mathfrak{M}^\square_0(2,1)) \hookrightarrow \pi_1(\mathfrak{M}^\square_g(2,1)) \to \pi_1(\overline{\mathfrak{M}}^\square_g(2,1))\,.$$

Using the methods of [WW16] and [Wah16], we construct infinite families of non-trivial classes of infinite order that correspond to non-trivial higher string operations.

Proposition 4.4.6 (B.+Egas)**.** *Let $m > 0$, $1 \leq i \leq m$, $c_i > 1$ and $c = \sum_i c_i$.*

(*i*) *There are classes of infinite order*

$$\widetilde{\Gamma}_m \in H_{4m-1}(\overline{\mathfrak{M}}^{\bullet}_m(m,1);\mathbb{Z})$$

and

$$\widetilde{\Omega}_{(c_1,\ldots,c_m)} \in H_{2c-1}(\overline{\mathfrak{M}}^{\bullet}_0(c,1);\mathbb{Z})\,.$$

All these classes correspond to non-trivial higher string topology operations.

(*ii*) *There are classes of infinite order*

$$\Gamma_m \in H_{4m-1}(\overline{\mathfrak{M}}^{\blacksquare}_m(m,1);\mathbb{Z})$$

and

$$\Omega_{(c_1,\ldots,c_m)} \in H_{2c-1}(\overline{\mathfrak{M}}^{\blacksquare}_0(c,1);\mathbb{Z})$$

and

$$\zeta_{2m} \in H_{2m-1}(\overline{\mathfrak{M}}^{\blacksquare}_0(2m,1);\mathbb{Z})\,.$$

Furthermore, we use a computer program to determine the integral homology of the harmonic compactifications $\overline{\mathfrak{M}}^{\square}_g(m,1)$ and $\overline{\mathfrak{M}}^{\blacksquare}_g(m,1)$ for small parameters g and m.

Proposition 4.4.7 and Proposition 4.4.8 (B.+Egas)**.** *For small parameters $2g+m$, the integral homology of $\overline{\mathfrak{M}}^{\square}_g(m,1)$ and $\overline{\mathfrak{M}}^{\blacksquare}_g(m,1)$ is given by the tables 4.1, 4.2, 4.3, 4.4, 4.5, 4.6 and 4.7 in Section 4.4.4.*

1.4.4. On the unstable homology of the moduli spaces

Recall that, in Section 1.1.4, we stated the result by Ehrenfried and Mehner. To their findings, we add three more generators.

Theorem 7.0.1 (B., Bödigheimer, Ehrenfried, Mehner)**.** *The integral homology of $\mathfrak{M}_{2,1}$ and $\mathfrak{M}^2_{1,1}$ is as follows.*

$$H_*(\mathfrak{M}_{2,1};\mathbb{Z}) = \begin{cases} \mathbb{Z}\langle c^2\rangle & *=0 \\ \mathbb{Z}_{10}\langle cd\rangle & *=1 \\ \mathbb{Z}_2\langle d^2\rangle & *=2 \\ \mathbb{Z}\langle \lambda s\rangle \oplus \mathbb{Z}_2\langle T(e)\rangle & *=3 \\ \mathbb{Z}_3\langle w_3\rangle \oplus \mathbb{Z}_2\langle ?\rangle & *=4 \\ 0 & *\geq 5 \end{cases} \qquad H_*(\mathfrak{M}^2_{1,1};\mathbb{Z}) = \begin{cases} \mathbb{Z}\langle a^2c\rangle & *=0 \\ \mathbb{Z}\langle a^2d\rangle \oplus \mathbb{Z}_2\langle bc\rangle & *=1 \\ \mathbb{Z}_2\langle a^2e\rangle \oplus \mathbb{Z}\langle bd\rangle & *=2 \\ \mathbb{Z}_2\langle f\rangle & *=3 \\ 0 & *\geq 4 \end{cases}$$

Here, the known generators a, b, c, d, e, t and their products have been described in [Meh11, Kapitel 1] or [BH14, Chapter 4], see also [BB18a]. The generators s, w_3 and f will be described in Chapter 7. The only generator remaining unknown is denoted by $?$.

Firstly, we obtain a generator of the third rational homology of $\mathfrak{M}_{2,1}$ as follows.

Proposition 7.1.2 (B.)**.** *The moduli space $\mathfrak{M}_{2,1}$ is the total space of a rational fibration $U \to \mathfrak{M}_{2,1} \to \mathfrak{M}_{2,0}$ with U the unit tangent bundle over the closed surface of genus two. The inclusion of the fibre $U \hookrightarrow \mathfrak{M}_{2,1}$ induces an isomorphism*

$$H_3(U;\mathbb{Q}) \xrightarrow{\cong} H_3(\mathfrak{M}_{2,1};\mathbb{Q})\,.$$

We do not know, wether or not $[U]$ is an integral generator.

Secondly, we obtain the 3-torsion of the fourth integral homology via what we call a Segal–Tillmann map.

Proposition 7.2.2 (B.)**.** *Sending the braid generators $\sigma_1, \dots, \sigma_5 \in Br_6$ to a certain system of five Dehn twists along an interlocking chain of simply closed curves defines a Segal–Tillmann map $ST\colon Br_{2g+2} \to \Gamma_{g,1}$. This Segal–Tillman map induces an isomorphism*

$$H_4(\mathrm{Conf}^6(\mathbb{D}^2);\mathbb{F}_3) \to H_4(\mathfrak{M}_{2,1};\mathbb{F}_3)\,.$$

Lastly, we describe an integral class $f \in H_3(\mathfrak{M}^2_{1,1};\mathbb{Z})$ by an embedded torus $U(1)^3 \subset \mathfrak{M}^2_{1,1}$. Using a computer programm we show that this class is an integral generator.

Proposition 7.3.1 (B.)**.** *It is $H_3(\mathfrak{M}^2_{1,1};\mathbb{Z}) \cong \mathbb{Z}_2\langle f\rangle$ and f is represented by an embedded 3-dimensional torus.*

2

The spaces of polygons

In this chapter, we introduce our spaces of polygons. We see our construction as the natural generalization of Bödigheimer's spaces of interval exchanges, see [Bö93b] or Section 1.2.2. The space $\mathcal{P}ol^\bullet(m,n)$ is thought of as a space of (certain L^2 classes of) isometries mapping $n \geq 1$ enumerated incoming circles to $m \geq 1$ enumerated outgoing circles (up to a finite set of points). As such, $\mathcal{P}ol^\bullet(m,n)$ admits a free action of the m-dimensional torus by postcomposing isometries with a given sequence of m rotations. The quotient map to the orbit space $\mathcal{P}ol^\circ(m,n)$ is a universal m-torus bundle. In Chapter 3 we will construct maps of torus fibrations

$$\begin{array}{ccc} \mathfrak{M}_g^\bullet(m,1) & \longrightarrow & \mathcal{P}ol^\bullet(m,1) \simeq EU(1)^m \\ \downarrow & & \downarrow \\ \mathfrak{M}_g^\circ(m,1) & \longrightarrow & \mathcal{P}ol^\circ(m,1) \simeq BU(1)^m \end{array} \tag{2.1}$$

and these fibrations commute (up to homotopy) with the stabilization maps of the moduli spaces. Aside from these properties, we use (a deformation retraction of) our polygon spaces to study the harmonic compactifications of the moduli spaces in question, see Chapter 4, Chapter 5 and Chapter 6. Let us mention the following variation of these spaces of polygons. The maps in Diagram (2.1) are all equivariant with respect to permuting the outgoing boundaries resp. outgoing circles. The orbit projection of the spaces of polygons are denoted by $\mathcal{P}ol^\blacksquare(m,n) \to \mathcal{P}ol^\square(m,n)$ and we obtain the following diagram.

$$\begin{array}{ccc} \mathfrak{M}_g^\blacksquare(m,n) & \longrightarrow & \mathcal{P}ol^\blacksquare(m,n) \\ \downarrow & & \downarrow \\ \mathfrak{M}_g^\square(m,n) & \longrightarrow & \mathcal{P}ol^\square(m,n) \end{array} \tag{2.2}$$

Thus these spaces of polygons are suitable to study the moduli spaces of Riemann surfaces with unenumerated outgoing boundaries.

We will define the spaces of polygons as the realization of a corresponding simplicial set. The simplicial structure of the spaces $\mathcal{P}ol^\bullet(m,n)$, $\mathcal{P}ol^\blacksquare(m,n)$, $\mathcal{P}ol^\circ(m,n)$ and $\mathcal{P}ol^\square(m,n)$ is very similar. However, the combinatorics of $\mathcal{P}ol^\square(m,n)$ is the least technical.

Let us discuss the simplicial structure of the space of unenumerated and unparametrized polygons $\mathcal{P}ol^\square = \cup_m \mathcal{P}ol^\square(m,1)$ here. The k-dimensional simplices of $\mathcal{P}ol^\square$ are the permutations $\sigma \in \mathfrak{S}([k])$ on the symbols $[k] = \{0,\dots,k\}$. Let us describe the points of

an open k-simplex in the geometric realization before discussing the faces and degeneracies. To this end, let $\sigma \in \mathfrak{S}([k])$ with exactly m cycles $\mathrm{cyc}(\sigma) = \{\sigma_1, \ldots, \sigma_m\}$ and fix a point $t = (t_0, \ldots, t_k) \in \mathrm{int}(\Delta^k)$. Cutting the circle $\mathbb{S}^1 = [0,1]/_\sim$ into $k+1$ intervals $e_0 = [0, t_0], e_1 = [t_0, t_0 + t_1], \ldots, e_n = [1 - t_k, 1]$ of length $t_0, \ldots, t_k$, we obtain a set of m polygons by glueing the end of the edge e_i to the start of the edge $e_{\sigma(i)}$. Note that this defines an orientation preserving isomoetry from $\mathbb{S}^1$ to m unparametrized and unenumerated circles up to a finite set of points (which is the set of cut points). Observe that each orientation preserving isomoetry from $\mathbb{S}^1$ to m unparametrized and unenumerated circles up to a finite set of points is obtained this way. Removing i from its cycle representation and renormalizing all other symbols afterwards, defines the i-th face of σ. Geometrically speaking, the i-th face of (σ, t) is obtained by collapsing the edge e_i. In the special case, where i is a fixed point of σ, the i-th face is regarded as isomoetry from $\mathbb{S}^1$ to $m-1$ circles. The i-th degeneracy of σ is obtained by increasing all symbols $j \geq i$ by one in the cycle representation and making i the predecessor of $i+1$. Geometrically speaking, the i-th degeneracy splits the edge e_i into two pieces introducing a superfluous cut point. This space of polygons admits a stratification by the spaces of exactly m polygons. The m-th stratum is denoted $\mathcal{P}ol^{\square}(m,1)$. The construction of the spaces $\mathcal{P}ol^{\bullet}(m,n)$, $\mathcal{P}ol^{\blacksquare}(m,n)$ and $\mathcal{P}ol^{\circ}(m,n)$ will be similar.

Overview of the results of this chapter

The space of m polygons $\mathcal{P}ol^{\bullet}(m,1)$ deformation retracts onto the subspace where all circumferences are equal, see Proposition 2.3.12. This space is the space of m normalized polygons $N\mathcal{P}ol^{\bullet}(m,1)$ and the deformation retraction induces a homeomorphism $\mathcal{P}ol^{\bullet}(m,1) \cong N\mathcal{P}ol^{\bullet}(m,1) \times \mathrm{int}(\Delta^{m-1})$, see Proposition 2.3.13. The space of m normalized, enumerated and parametrized polygons $N\mathcal{P}ol^{\bullet}(m,1)$ admits the structure of an m-fold multi-cyclic set, see Proposition 2.4.1. The quotient by the m-fold torus action defines a m-fold torus bundle with base $N\mathcal{P}ol^{\circ}(m,1)$.

Theorem 2.6.2. *The m-fold torus bundles $\mathcal{P}ol^{\bullet}(m,1) \to \mathcal{P}ol^{\circ}(m,1)$ and $N\mathcal{P}ol^{\bullet}(m,1) \to N\mathcal{P}ol^{\circ}(m,1)$ are universal.*

Let us mention another result which is similar to [Kla13, Theorem C] and which is used in the study of the harmonic compactifications, see Chapter 5 and Chapter 6. For each $n \geq 1$, the space $\mathcal{P}ol^{\bullet} = \cup_k \mathcal{P}ol^{\bullet}(k,n)$ is filtered by the closed subspaces $F_m\mathcal{P}ol^{\bullet} = \overline{\mathcal{P}ol^{\bullet}}(m,n) = \cup_{k \leq m} \mathcal{P}ol^{\bullet}(k,n)$. Roughly speaking, there is an extension of the homeomorphism

$$F_m\mathcal{P}ol^{\bullet} - F_{m-1}\mathcal{P}ol^{\bullet} = \mathcal{P}ol^{\bullet}(m,1) \cong N\mathcal{P}ol^{\bullet}(m,n) \times \Delta^{m-1}$$

to $F_m\mathcal{P}ol^{\bullet}/F_{m-1}\mathcal{P}ol^{\bullet} \to \Sigma^{m-1} N\mathcal{P}ol^{\bullet}(m,n)$ which leads to our desuspension theorem for the spaces of polygons.

Theorem 2.5.2 and 2.5.1. *There are isomorphisms of cellular chain complexes*

$$\begin{aligned}
C_*(N\mathcal{P}ol^{\bullet}(m,1); \mathbb{Z}) &\cong \Sigma^{-m+1} C_*(F_m\mathcal{P}ol^{\bullet}, F_{m-1}\mathcal{P}ol^{\bullet}; \mathbb{Z}) \\
C_*(N\mathcal{P}ol^{\blacksquare}(m,1); \mathbb{F}_2) &\cong \Sigma^{-m+1} C_*(F_m\mathcal{P}ol^{\blacksquare}, F_{m-1}\mathcal{P}ol^{\blacksquare}; \mathbb{F}_2) \\
C_*(N\mathcal{P}ol^{\circ}(m,1); \mathbb{F}_2) &\cong \Sigma^{-m+1} C_*(F_m\mathcal{P}ol^{\circ}, F_{m-1}\mathcal{P}ol^{\circ}; \mathbb{F}_2) \\
C_*(N\mathcal{P}ol^{\square}(m,1); \mathbb{F}_2) &\cong \Sigma^{-m+1} C_*(F_m\mathcal{P}ol^{\square}, F_{m-1}\mathcal{P}ol^{\square}; \mathbb{F}_2)
\end{aligned}$$

The isomorphism is made explicit in Proposition 2.5.7 and a variation of the arguments are used to prove our desuspension Theorem for the harmonic compactifications, see Theorem 5.1.22. Lastly, in Section 2.7, we construct an explicit rational homotopy equivalence between our space of polygons $\mathcal{P}ol^{\circ}(1,1)$ and Kontsevich's polygon bundle $BU(1)^{comb}$.

Organization of the chapter

In Section 2.1, we fix our notations for the symmetric groups and define sets $\mathfrak{S}^{\star}$ of (un)enumerated and (un)parametrized permutations with $\star \in \{\bullet, \blacksquare, \circ, \square\}$. In Section 2.2 we define the spaces of (un)enumerated and (un)parametrized polygons $\mathcal{P}ol^{\star}$ as the geometric realization of $(\mathfrak{S}^{\star}([n]))_{n\in\mathbb{N}}$. It is stratified by the spaces of m polygons $\mathcal{P}ol^{\star}(m,1)$. For the sake of completeness, we make the definition of the four variations of the space of polygons explicit. In Section 2.3, we define the space of normalized polygons $N\mathcal{P}ol^{\star}(m,1) \subset \mathcal{P}ol^{\star}(m,1)$, discuss our interpretation of its points and establish a canonical homeomorphism $\mathcal{P}ol^{\star}(m,1) \cong N\mathcal{P}ol^{\star}(m,1) \times \mathrm{int}(\Delta^{m-1})$ in the enumerated cases. In Section 2.4, we use the projection $\mathcal{P}ol^{\bullet}(m,1) \cong N\mathcal{P}ol^{\bullet}(m,1) \times \mathrm{int}(\Delta^{m-1}) \to N\mathcal{P}ol^{\bullet}(m,1)$ to define an m-multi-cyclic structure on $N\mathcal{P}ol^{\bullet}(m,1)$ and a cellular structure on the other spaces of m normalized polygons $N\mathcal{P}ol^{\star}(m,1)$. Moreover, we prove our desuspension theorem for the spaces of polygons in Section 2.5 In Section 2.6, we study the homotopy type of the spaces of polygons. Most importantly, we prove that the m-dimensional torus bundle $\mathcal{P}ol^{\bullet}(m,1) \to \mathcal{P}ol^{\circ}(m,1)$ is universal. In Section 2.7, we construct a zig-zag of rational homotopy equivalence between $\mathcal{P}ol^{\circ}(1,1)$ and Kontsevich's polygon bundle $BU(1)^{comb}$.

2.1. The symmetric group

In this section we fix our notation. The definitions and propositions in this section are well known.

Definition 2.1.1. We denote the category of finite sets with injective maps by $\mathcal{F}in_{inj}$. The *symmetric group* on a finite set A is the group of automorphisms $\mathfrak{S}(A) := \mathrm{Aut}_{\mathcal{F}in_{inj}}(A)$. Consequently, in our notation, the product $\beta \cdot \alpha$ agrees with the composition $\beta \circ \alpha$ of maps.

Definition 2.1.2. Given an injection $f\colon A \to B$, the set A is identified with a subset of B and so every permutation on A is extended to a permutation of B by fixing $B - f(A)$ pointwise. More pedantically, the induced group homomorphism $\mathfrak{S}(f)\colon \mathfrak{S}(A) \hookrightarrow \mathfrak{S}(B)$ is defined by

$$\mathfrak{S}(f)(\sigma)(b) = \begin{cases} f(\sigma(s)) & \text{if } b = f(s) \text{ for some } s \in A, \\ b & \text{else.} \end{cases} \tag{2.3}$$

Proposition 2.1.3. *The symmetric groups define a faithful functor into the category of groups with monomorphisms*

$$\mathfrak{S}\colon \mathcal{F}in_{inj} \to \mathcal{G}rp_{inj}. \tag{2.4}$$

Definition 2.1.4. The *support* of a permutation $\sigma \in \mathfrak{S}(A)$ is the set of non-trivially permuted symbols

$$\mathrm{supp}(\sigma) = \{s \in A \mid \sigma(s) \neq s\}. \tag{2.5}$$

The *set of fixed points* of a permutation $\sigma \in \mathfrak{S}(A)$ is

$$\mathrm{fix}(\sigma) = \{s \in A \mid \sigma(s) = s\} = A - \mathrm{supp}(\sigma)\,. \tag{2.6}$$

Definition 2.1.5. The *long cycle of degree* $n \geq 0$ is the permutation $\omega_n \in \mathfrak{S}([n])$ sending k to $k+1$ modulo $n+1$. We write $\omega_n = \langle 0 \ \ldots \ n \rangle$ up to cyclic permutation of the symbols.

Definition 2.1.6. A permutation $\mathrm{id}_A \neq \sigma \in \mathfrak{S}(A)$ is *cyclic* if there exists $0 \leq n \leq \#A$ and an injective map $f \in \mathcal{F}in_{inj}([n], A)$ such that $\sigma = \mathfrak{S}(f)(\omega_n)$. In this case, the *cycle representation* of σ is the word $\langle f(0)\ f(1)\ \ldots\ f(n) \rangle$ up to cyclic permutation of the entries. Abusing notation, a non-trivial cyclic permutation is identified with its cycle representation.

Definition 2.1.7. Let A be a finite set and $n \geq 0$. Given a word $s = \langle s_0 \ \ldots \ s_n \rangle$ up to cyclic permutation and without reoccurring letters $s_i \in A$, the permutation associated with s is $\mathfrak{S}(f)(\omega_n)$ where $f(i) = s_i$. Abusing notation, such a word is identified with its associated permutation.

Remark 2.1.8. Clearly, a non-trivial cyclic permutation is uniquely given by its cycle representation. Observe that, in Definition 2.1.6, the cycle representation is only defined for non-trivial permutations. However, in Definition 2.1.7, we are more generous and allow words of length one. In this case, the associated permutation is the identity and we regard a word of length one as a chosen fixed point of the identity. In other words, a fixed point b is seen as a trivial cyclic permutation, its cycle representation is $\langle b \rangle$ and the product of a permutation σ with the trivial cyclic permutation $\langle b \rangle$ is σ.

Definition 2.1.9. The *set of non-trivial cycles* of a permutation $\sigma \in \mathfrak{S}(A)$ is the set of non-trivial cyclic permutations $\mathrm{cyc}^\dagger(\sigma) = \{\sigma_1, \ldots, \sigma_t\}$ with $\sigma = \sigma_1 \cdots \sigma_t$ and $\mathrm{supp}(\sigma_i) \cap \mathrm{supp}(\sigma_j) = \emptyset$ for all $i \neq j$.

Definition 2.1.10. The *set of cycles* of a permutation $\sigma \in \mathfrak{S}(A)$ is $\mathrm{cyc}(\sigma) = \mathrm{cyc}^\dagger(\sigma) \sqcup \mathrm{fix}(\sigma)$, where each fixed point i is regarded as cycle $\langle i \rangle$. The elements of $\mathrm{cyc}(\sigma)$ are the *cycles of* σ. The *number of cycles* of a permutation σ is the cardinality of $\mathrm{cyc}(\sigma)$.

Definition 2.1.11. Let $\sigma \in \mathfrak{S}(A)$ and $\mathrm{cyc}(\sigma) = \{\sigma_1, \ldots, \sigma_k\}$ be its set of cycles. The symbol $s \in A$ *belongs to* σ_k if it occurs in the cycle representation of σ_k.

Remark 2.1.12. Observe that, by Remark 2.1.8 and Definition 2.1.11, each symbol $s \in A$ belongs to exactly one cycle of a given permutation σ. Here, we demonstrate that each fixed point belongs to exactly one cycle. By definition, the set of cycles $\mathrm{cyc}(\sigma) = \{\sigma_1, \ldots, \sigma_k\}$ is the union of the set of non-trivial cycles and the set of fixed points. Following Remark 2.1.8, we emphasize that we identify a fixed point $s \in \mathrm{fix}(\sigma)$ with the cycle representation $\langle s \rangle$ and therefore, we write $\sigma_i = \langle s \rangle$, for a unique i. In particular, s occurs in the cycle representation of σ_i and, according to Definition 2.1.11, we say that s belongs to σ_i.

Definition 2.1.13. A permutation σ is *enumerated* if its set of cycles is equipped with a linear order.

$$\mathrm{cyc}(\sigma) = \{\sigma_1 < \cdots < \sigma_k\}\,. \tag{2.7}$$

The *set of enumerated permutations on* A is the set $\mathfrak{S}^\circ(A)$.

Definition 2.1.14. A permutation σ is *parametrized* if each cycle has a distinguished element. Given a parametrized permutation σ, denote the distinguished symbol of a cycle τ by τ_0 and denote the i-th successor of τ_0 by $\tau_i := \tau^i(\tau_0)$. The *parametrized cycle representation* of τ is $\tau = \langle \tau_0\ \tau_1\ \dots \rangle$. The set of parametrized permutations on A is the set $\mathfrak{S}^{\blacksquare}(A)$.

Remark 2.1.15. By definition, the cycle representation of an unparametrized permutation is unique up to cyclic permutation of its symbols. However, the parametrized cycle representation of a parametrized permutation is unique as the distinguished symbol comes first.

Definition 2.1.16. A permutation σ is *enumerated and parametrized*, if its cycles are enumerated (in the sense of Definition 2.1.13) and if each cycle has a distinguished element (in the sense of Definition 2.1.14).

The *set of enumerated and parametrized permutations on* A is the set $\mathfrak{S}^{\bullet}(A)$.

Notation 2.1.17. By abuse of notation, the term *permutation* refers to an ordinary permutation, an enumerated permutation, a parametrized permutation or an enumerated and parametrized permutation.

Definition 2.1.18. For each A, forgetting the enumeration or the parametrization of its permutations defines a commutative diagram of sets:

$$\begin{array}{ccc} & \mathfrak{S}^{\blacksquare}(A) & \\ {\scriptstyle \pi^{\bullet}_{\blacksquare}} \nearrow & & \searrow {\scriptstyle \pi^{\blacksquare}_{\square}} \\ \mathfrak{S}^{\bullet}(A) & \xrightarrow{\quad \pi^{\bullet}_{\square} \quad} & \mathfrak{S}^{\square}(A) \\ {\scriptstyle \pi^{\bullet}_{\circ}} \searrow & & \nearrow {\scriptstyle \pi^{\circ}_{\square}} \\ & \mathfrak{S}^{\circ}(A) & \end{array} \tag{2.8}$$

2.2. The space of polygons as simplicial spaces

In this section, we equip the sets of (un)enumerated and (un)parametrized permutations on $[n]$ with the structure of a cyclic set. For convenience of the reader, we provide the definitions and facts about (multi)cyclic sets used in this thesis in Appendix A.1. Let us describe informally the faces, degeneracies and the action of the cyclic operator on a permutation $\sigma \in \mathfrak{S}([n])$. To this end, we represent σ as a product of cycles $\sigma = \langle \sigma_{1,0}\ \dots \rangle \cdots \langle \sigma_{m,0}\ \dots \rangle$. The i-th face of σ deletes the symbol i from its cycle representation and renormalizes the other symbols afterwards. The i-th degeneracy map increases all symbols $j \geq i$ by one in the cycle representation and makes i the predecessor of $i+1$ afterwards. The cyclic operator increases all symbols in the cycle representation by one (with the convention that $n+1 = 0$). For a precise definition, see Definitions 2.2.1, 2.2.6, 2.2.10 and 2.2.14.

The spaces of (un)enumerated and (un)parametrized polygons is the geometric realization of the simplicial set underlying the cyclic set. This space is stratified by the number of cycles of a permutation and the m-th stratum is the space of m (un)enumerated and (un)parametrized polygons. Let us repeat that we make the definitions of the four variations of these spaces of polygons explicit for the sake of completeness. After reading Subsection 2.2.1 carefully, it is enough to skim the Subsections 2.2.2, 2.2.3 and 2.2.4.

2.2.1. The space of unenumerated unparametrized polygons

Definition 2.2.1. Denote the i-th face map in the simplicial category by $\delta_i\colon [n-1] \to [n]$. By Definition 2.1.2, the induced map $F_i := \mathfrak{S}^{\square}(\delta_i)\colon \mathfrak{S}^{\square}([n-1]) \hookrightarrow \mathfrak{S}^{\square}([n])$ regards a permutation $\sigma \in \mathfrak{S}^{\square}([n-1])$ as a permutation of $[n]$ that has i as a fixed point.

The i-th face map $D_i\colon \mathfrak{S}^{\square}([n]) \to \mathfrak{S}^{\square}([n-1])$ is

$$D_i(\sigma) := F_i^{-1}(\langle \sigma(i)\ i\rangle \cdot \sigma) \tag{2.9}$$

where $\langle \sigma(i)\ i\rangle$ is the permutation exchanging $\sigma(i)$ and i (if $\sigma(i) \neq i$; and it is the identity otherwise). The i-th degeneracy map $S_i\colon \mathfrak{S}^{\square}([n]) \to \mathfrak{S}^{\square}([n+1])$ is

$$S_j(\sigma) := \langle j+1\ j\rangle \cdot F_j(\sigma). \tag{2.10}$$

The cyclic operator $T\colon \mathfrak{S}^{\square}([n]) \to \mathfrak{S}^{\square}([n])$ is

$$T(\sigma) := \omega_n \cdot \sigma \cdot \omega_n^{-1} \tag{2.11}$$

with ω_n the long cycle $\omega_n = \langle 0\ 1\ 2\ \dots\ n\rangle$.

Lemma 2.2.2. *Let $\sigma \in \mathfrak{S}^{\square}([n])$ and consider its set of cycles $\mathrm{cyc}(\sigma) = \{\sigma_1, \dots, \sigma_k\}$. Let $0 \leq i \leq n$ and assume that i belongs to σ_j. Then*

$$\mathrm{cyc}(D_i(\sigma)) = \begin{cases} \{D_i(\sigma_1), \dots, D_i(\sigma_k)\} & \text{if } \sigma(i) \neq i \\ \{D_i(\sigma_1), \dots, D_i(\sigma_{j-1}), D_i(\sigma_{j+1}), \dots, D_i(\sigma_k)\} & \text{if } \sigma(i) = i \end{cases} \tag{2.12}$$

and

$$\mathrm{cyc}(S_i(\sigma)) = \{S_i(\sigma_1), \dots, S_i(\sigma_k)\} \tag{2.13}$$

and

$$\mathrm{cyc}(T(\sigma)) = \{T(\sigma_1), \dots, T(\sigma_k)\}. \tag{2.14}$$

We do not give a proof of this Lemma because the proof is straight forward.

Definition 2.2.3. The sets $\{\mathfrak{S}^{\square}([n])\}_{n\in\mathbb{N}}$ together with the face maps D_i, the degeneracy maps S_j and the cyclic operators T form a cyclic set denoted by $\mathfrak{S}^{\square}$.

Definition 2.2.4. The *space of unenumerated unparametrized polygons* $\mathcal{P}ol^{\square}$ is the geometric realization of the (underlying simplicial set of the) cyclic set

$$\mathcal{P}ol^{\square} := |\mathfrak{S}^{\square}|. \tag{2.15}$$

Definition 2.2.5. The cyclic set $\mathfrak{S}^{\square}$ has for each $m \geq 1$ a cyclic subset $F_m\mathfrak{S}^{\square} \subset \mathfrak{S}^{\square}$ consisting in degree n of all permutations $\sigma \in \mathfrak{S}^{\square}([n])$ that have at most m cycles (where fixed points count as cycles). This induces a filtration of the space of polygons $\mathcal{P}ol^{\square}$ by closed subspaces $F_m\mathcal{P}ol^{\square} := |F_m\mathfrak{S}^{\square}| \subset \mathcal{P}ol^{\square}$.

Let $m \geq 1$. The *space of m unenumerated unparametrized polygons* is the m-th stratum

$$\mathcal{P}ol^{\square}(m,1) := F_m\mathcal{P}ol^{\square} - F_{m-1}\mathcal{P}ol^{\square}. \tag{2.16}$$

2.2.2. The space of enumerated unparametrized polygons

Definition 2.2.6. Let $\sigma \in \mathfrak{S}^\circ([n])$ and consider its ordered set of cycles $\mathrm{cyc}(\sigma) = \{\sigma_1 < \ldots < \sigma_k\}$. Let $0 \leq i \leq n$ and $1 \leq j \leq k$ such that i belongs to σ_j. Then the structure maps D_i, S_i or T applied to σ give the permutations $D_i(\sigma)$, $S_i(\sigma)$ or $T(\sigma)$ and the enumeration of the cycles is as follows.

$$\mathrm{cyc}(D_i(\sigma)) = \begin{cases} \{D_i(\sigma_1) < \ldots < D_i(\sigma_k)\} & \text{if } \sigma(i) \neq i \\ \{D_i(\sigma_1) < \ldots < D_i(\sigma_{j-1}) < D_i(\sigma_{j+1}) < \ldots < D_i(\sigma_k)\} & \text{if } \sigma(i) = i \end{cases} \tag{2.17}$$

and

$$\mathrm{cyc}(S_i(\sigma)) = \{S_i(\sigma_1) < \ldots < S_i(\sigma_k)\} \tag{2.18}$$

and

$$\mathrm{cyc}(T(\sigma)) = \{T(\sigma_1) < \ldots < T(\sigma_k)\}. \tag{2.19}$$

Definition 2.2.7. The sets $\{\mathfrak{S}^\circ([n])\}_{n\in\mathbb{N}}$ together with the face maps D_i, the degeneracy maps S_j and the cyclic operators T form a cyclic set, denoted by $\mathfrak{S}^\circ$.

Definition 2.2.8. The *space of enumerated unparametrized polygons* $\mathcal{P}ol^\circ$ is the geometric realization of the (underlying simplicial set of the) cyclic set

$$\mathcal{P}ol^\circ := |\mathfrak{S}^\circ|. \tag{2.20}$$

Definition 2.2.9. The cyclic set $\mathfrak{S}^\circ$ has for each $m \geq 1$ a cyclic subset $F_m\mathfrak{S}^\circ \subset \mathfrak{S}^\circ$ consisting in degree n of all permutations $\sigma \in \mathfrak{S}^\circ([n])$ that have at most m cycles (where fixed points count as cycles). This induces a filtration of the space of polygons $\mathcal{P}ol^\circ$ by closed subspaces $F_m\mathcal{P}ol^\circ := |F_m\mathfrak{S}^\circ| \subset \mathcal{P}ol^\circ$.

Let $m \geq 1$. The *space of m enumerated unparametrized polygons* is the m-th stratum

$$\mathcal{P}ol^\circ(m, 1) := F_m\mathcal{P}ol^\circ - F_{m-1}\mathcal{P}ol^\circ. \tag{2.21}$$

2.2.3. The space of unenumerated parametrized polygons

Definition 2.2.10. Let $\sigma \in \mathfrak{S}^\blacksquare([n])$ and consider its set of cycles $\mathrm{cyc}(\sigma) = \{\sigma_1, \ldots, \sigma_k\}$. Let $0 \leq i \leq n$ and $1 \leq j \leq k$ such that i belongs to $\sigma_j = \langle \sigma_{j,0}\ \sigma_{j,1}\ \ldots \rangle$. Then the structure maps D_i, S_i or T applied to σ give the permutations $D_i(\sigma)$, $S_i(\sigma)$ or $T(\sigma)$ and the set of cycles is

$$\mathrm{cyc}(D_i(\sigma_j)) = \begin{cases} \{D_i(\sigma_1), \ldots, D_i(\sigma_k)\} & \text{if } \sigma(i) \neq i \\ \{D_i(\sigma_1), \ldots, D_i(\sigma_{j-1}), D_i(\sigma_{j+1}), \ldots, D_i(\sigma_k)\} & \text{if } \sigma(i) = i \end{cases} \tag{2.22}$$

and

$$\mathrm{cyc}(S_i(\sigma)) = \{S_i(\sigma_1), \ldots, S_i(\sigma_k)\} \tag{2.23}$$

and

$$\mathrm{cyc}(T(\sigma)) = \{T(\sigma_1), \ldots, T(\sigma_k)\}. \tag{2.24}$$

The parametrization of the permutations $D_i(\sigma)$, $S_i(\sigma)$ or $T(\sigma)$ is (up to possible renormalization) as follows: The first symbol of $D_i(\langle \sigma_{j,0}\ \sigma_{j,1}\ \ldots\ \rangle)$ is $\sigma_{j,0}$ if $i \neq \sigma_{j,0}$ and it is $\sigma_{j,1}$ otherwise. The first symbol of $S_i(\langle \sigma_{j,0}\ \sigma_{j,1}\ \ldots\ \rangle)$ is $\sigma_{j,0}$. The first symbol of $T(\langle \sigma_{j,0}\ \sigma_{j,1}\ \ldots\ \rangle) = \langle \omega_n(\sigma_{j,0})\ \omega_n(\sigma_{j,0})\ \ldots\ \rangle$ is $\omega_n(\sigma_{j,0})$.

Definition 2.2.11. The sets $\{\mathfrak{S}^{\blacksquare}([n])\}_{n\in\mathbb{N}}$ together with the face maps D_i, the degeneracy maps S_j and the cyclic operators T form a cyclic set, denoted by $\mathfrak{S}^{\blacksquare}$.

Definition 2.2.12. The *space of unenumerated parametrized polygons* $\mathcal{P}ol^{\blacksquare}$ is the geometric realization of the (underlying simplicial set of the) cyclic set

$$\mathcal{P}ol^{\blacksquare} := |\mathfrak{S}^{\blacksquare}|. \tag{2.25}$$

Definition 2.2.13. The cyclic set $\mathfrak{S}^{\blacksquare}$ has for each $m \geq 1$ a cyclic subset $F_m\mathfrak{S}^{\blacksquare} \subset \mathfrak{S}^{\blacksquare}$ consisting in degree n of all permutations $\sigma \in \mathfrak{S}^{\blacksquare}([n])$ that have at most m cycles (where fixed points count as cycles). This induces a filtration of the space of polygons $\mathcal{P}ol^{\blacksquare}$ by closed subspaces $F_m\mathcal{P}ol^{\blacksquare} := |F_m\mathfrak{S}^{\blacksquare}| \subset \mathcal{P}ol^{\blacksquare}$.

Let $m \geq 1$. The *space of m unenumerated parametrized polygons* is the m-th stratum

$$\mathcal{P}ol^{\blacksquare}(m,1) := F_m\mathcal{P}ol^{\blacksquare} - F_{m-1}\mathcal{P}ol^{\blacksquare}. \tag{2.26}$$

2.2.4. The space of enumerated parametrized polygons

Definition 2.2.14. Let $\sigma \in \mathfrak{S}^{\bullet}$ and consider its set of cycles $\mathrm{cyc}(\sigma) = \{\sigma_1 < \ldots < \sigma_k\}$. Let $0 \leq i \leq n$ and $1 \leq j \leq k$ such that i belongs to $\sigma_j = \langle \sigma_{j,0}\ \sigma_{j,1}\ \ldots\ \rangle$. Then the structure maps D_i, S_i or T applied to σ give the permutations $D_i(\sigma)$, $S_i(\sigma)$ or $T(\sigma)$ and the enumeration of the cycles is as follows.

$$\mathrm{cyc}(D_i(\sigma_j)) = \begin{cases} \{D_i(\sigma_1) < \ldots < D_i(\sigma_k)\} & \text{if } \sigma(i) \neq i \\ \{D_i(\sigma_1) < \ldots < D_i(\sigma_{j-1}) < D_i(\sigma_{j+1}) < \ldots < D_i(\sigma_k)\} & \text{if } \sigma(i) = i \end{cases} \tag{2.27}$$

and

$$\mathrm{cyc}(S_i(\sigma)) = \{S_i(\sigma_1) < \ldots < S_i(\sigma_k)\} \tag{2.28}$$

and

$$\mathrm{cyc}(T(\sigma)) = \{T(\sigma_1) < \ldots < T(\sigma_k)\}. \tag{2.29}$$

The parametrization of the permutations $D_i(\sigma)$, $S_i(\sigma)$ or $T(\sigma)$ is (up to possible renormalization) as follows: The first symbol of $D_i(\langle \sigma_{j,0}\ \sigma_{j,1}\ \ldots\ \rangle)$ is $\sigma_{j,0}$ if $i \neq \sigma_{j,0}$ and it is $\sigma_{j,1}$ otherwise. The first symbol of $S_i(\langle \sigma_{j,0}\ \sigma_{j,1}\ \ldots\ \rangle)$ is $\sigma_{j,0}$. The first symbol of $T(\langle \sigma_{j,0}\ \sigma_{j,1}\ \ldots\ \rangle) = \langle \omega_n(\sigma_{j,0})\ \omega_n(\sigma_{j,0})\ \ldots\ \rangle$ is $\omega_n(\sigma_{j,0})$.

Definition 2.2.15. The sets $\{\mathfrak{S}^\bullet([n])\}_{n\in\mathbb{N}}$ together with the face maps D_i, the degeneracy maps S_j and the cyclic operators T form a cyclic set, denoted by $\mathfrak{S}^\bullet$.

Definition 2.2.16. The *space of enumerated parametrized polygons* $\mathcal{P}ol^\bullet$ is the geometric realization of the (underlying simplicial set of the) cyclic set

$$\mathcal{P}ol^\bullet := |\mathfrak{S}^\bullet|. \tag{2.30}$$

Definition 2.2.17. The cyclic set $\mathfrak{S}^\bullet$ has for each $m \geq 1$ a cyclic subset $F_m\mathfrak{S}^\bullet \subset \mathfrak{S}^\bullet$ consisting in degree n of all permutations $\sigma \in \mathfrak{S}^\bullet([n])$ that have at most m cycles (where fixed points count as cycles). This induces a filtration of the space of polygons $\mathcal{P}ol^\bullet$ by closed subspaces $F_m\mathcal{P}ol^\bullet := |F_m\mathfrak{S}^\bullet| \subset \mathcal{P}ol^\bullet$.

Let $m \geq 1$. The *space of m enumerated parametrized polygons* is the m-th stratum

$$\mathcal{P}ol^\bullet(m,1) := F_m\mathcal{P}ol^\bullet - F_{m-1}\mathcal{P}ol^\bullet. \tag{2.31}$$

2.2.5. Forgetful maps

Definition 2.2.18. The forgetful maps from Definition 2.1.18 induce quotient maps denoted as follows.

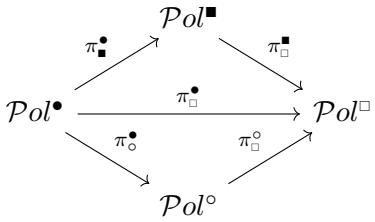

(2.32)

Remark 2.2.19. Let $m \geq 1$. Observe that both maps $\pi^\bullet_\blacksquare\colon \mathcal{P}ol^\bullet \to \mathcal{P}ol^\blacksquare$ and $\pi^\circ_\square\colon \mathcal{P}ol^\circ \to \mathcal{P}ol^\square$ restrict to an $m!$-fold covering

$$\mathcal{P}ol^\bullet(m,1) \to \mathcal{P}ol^\blacksquare(m,1) \tag{2.33}$$

and

$$\mathcal{P}ol^\circ(m,1) \to \mathcal{P}ol^\square(m,1) \tag{2.34}$$

whose group of Deck transformation is a symmetric group on m symbols. In Section 2.6, we show that $\pi^\bullet_\circ$ restricts to the m-dimensional torus fibration

$$: \mathcal{P}ol^\bullet(m,1) \to \mathcal{P}ol^\circ(m,1)\,. \tag{2.35}$$

2.3. The space of normalized polygons $N\mathcal{P}ol^\star(m,1)$

In this section, we introduce the space of m normalized polygons $N\mathcal{P}ol^\star(m,1) \subset \mathcal{P}ol^\star(m,1)$, see Definition 2.3.6. Most importantly, we will construct a homeomorphism

$$\mathcal{P}ol^\bullet(m,1) \cong N\mathcal{P}ol^\bullet(m,1) \times \mathrm{int}(\Delta^{m-1})\,, \tag{2.36}$$

see Proposition 2.3.13. This homeomorphism will be used Section 2.4 to equip these spaces of normalized polygons with an m-fold multi-simplicial structure and, in Section 2.5, it will be used to proof our desuspension theorem for our spaces of polygons.

Definition 2.3.1. Let $m \geq 1$ and consider a (representative of a) point $(\sigma; t) \in \mathcal{P}ol^{\circ}(m,1)$ or $(\sigma; t) \in \mathcal{P}ol^{\bullet}(m,1)$ with $\mathrm{cyc}(\sigma) = \{\sigma_1, \ldots, \sigma_m\}$. The *length of the i-th outgoing circle* is $l_i := l_i(\sigma, t) := \sum_{j \in \sigma_i} t_j$ and the *length of* (σ, t) is the tuple $l(\sigma, t) := (l_1, \ldots, l_m)$.

Remark 2.3.2. Observe that $l_i > 0$ for all i and that $\sum_{1 \leq i \leq m} l_i = 1$.

Definition 2.3.3. On the space of m enumerated (un)parametrized polygons, the *length* is the continous map

$$l \colon \mathcal{P}ol^{\circ}(m,1) \to \mathrm{int}(\Delta^{m-1}), \quad (\sigma, t) \mapsto l(\sigma, t) \tag{2.37}$$

respectively

$$l \colon \mathcal{P}ol^{\bullet}(m,1) \to \mathrm{int}(\Delta^{m-1}), \quad (\sigma, t) \mapsto l(\sigma, t)\,. \tag{2.38}$$

Remark 2.3.4. Clearly, the length does not depend on the parametrization of the outgoing circles. Therefore, the length commutes with the forgetful map $\pi^{\bullet}_{\circ} \colon \mathcal{P}ol^{\bullet}(m,1) \to \mathcal{P}ol^{\circ}(m,1)$.

In Remark 2.2.19 we saw that the map forgetting the enumeration of the m cycles is an $m!$-fold covering whose group of Deck transformations is isomorphic to $\mathfrak{S}[m-1]$. Observe that the length l is $\mathfrak{S}[m-1]$-equivariant (with respect to permuting the order of the cycles resp. the coordinates of the $(m-1)$-simplex).

Definition 2.3.5. On the space of m unenumerated (un)parametrized polygons, the *length* is the continous map

$$l \colon \mathcal{P}ol^{\blacksquare}(m,1) \to \mathrm{int}(\Delta^{m-1})/_{\mathfrak{S}[m-1]} \tag{2.39}$$

respectively

$$l \colon \mathcal{P}ol^{\square}(m,1) \to \mathrm{int}(\Delta^{m-1})/_{\mathfrak{S}[m-1]} \tag{2.40}$$

making the following diagram commutative.

$$\begin{array}{ccccc} \mathcal{P}ol^{\bullet}(m,1) & \xrightarrow{\pi^{\bullet}_{\circ}} & \mathcal{P}ol^{\circ}(m,1) & \xrightarrow{\quad l \quad} & \mathrm{int}(\Delta^{m-1}) \\ \downarrow{\scriptstyle /_{\mathfrak{S}[m-1]}} & & \downarrow{\scriptstyle /_{\mathfrak{S}[m-1]}} & & \downarrow{\scriptstyle /_{\mathfrak{S}[m-1]}} \\ \mathcal{P}ol^{\blacksquare}(m,1) & \xrightarrow{\pi^{\blacksquare}_{\square}} & \mathcal{P}ol^{\square}(m,1) & \dashrightarrow^{l} & \mathrm{int}(\Delta^{m-1})/_{\mathfrak{S}[m-1]} \end{array} \tag{2.41}$$

Definition 2.3.6. Let $m \geq 1$. The space of m *normalized enumerated or parametrized polygons* is the closed subspace of m polygons of the same length.

$$N\mathcal{P}ol^{\bullet}(m,1) := l^{-1}(\tfrac{1}{m}, \ldots, \tfrac{1}{m}) \subset \mathcal{P}ol^{\bullet}(m,1) \tag{2.42}$$

$$N\mathcal{P}ol^{\blacksquare}(m,1) := l^{-1}(\tfrac{1}{m}, \ldots, \tfrac{1}{m}) \subset \mathcal{P}ol^{\blacksquare}(m,1) \tag{2.43}$$

$$N\mathcal{P}ol^{\circ}(m,1) := l^{-1}(\tfrac{1}{m}, \ldots, \tfrac{1}{m}) \subset \mathcal{P}ol^{\circ}(m,1) \tag{2.44}$$

$$N\mathcal{P}ol^{\square}(m,1) := l^{-1}(\tfrac{1}{m}, \ldots, \tfrac{1}{m}) \subset \mathcal{P}ol^{\square}(m,1) \tag{2.45}$$

Definition 2.3.7. Abusing notation, the restrictions of the quotient maps in Definition 2.2.18 define quotient maps with the same names.

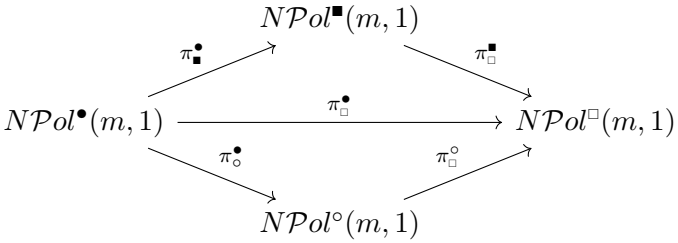

(2.46)

We will now show that $N\mathcal{P}ol^{\star}(m,1) \subset \mathcal{P}ol^{\star}(m,1)$ is a strong retract using a "normalization process".

Definition 2.3.8. Let $m \geq 1$ and $n \geq 0$. Let $\sigma \in \mathfrak{S}^{\bullet}([n])$ with m cycles and $t \in \mathrm{int}(\Delta^n)$. Each symbol $i \in [n]$ belongs to exactly one cycle, say $\sigma_{j(i)}$, and we denote the length of the $j(i)$-th outgoing circle by $l(i) := l_{j(i)}(\sigma,t) = \sum_{k\in\sigma_{j(i)}} t_k$. The *normalization of* (σ,t) is

$$r(\sigma,t) := (\sigma,t'), \quad t'_i = \frac{t_i}{m \cdot l(i)} \text{ for } 0 \leq i \leq n\,. \tag{2.47}$$

Remark 2.3.9. Note that the normalization of the simplices of $\mathcal{P}ol^{\bullet}(m,1)$ induces a continous self map of $\mathcal{P}ol^{\bullet}(m,1)$. Observe that $l(r(\sigma,t)) = (\frac{1}{m},\ldots,\frac{1}{m})$, i.e., the normalization maps to $N\mathcal{P}ol^{\bullet}(m,1) \subset \mathcal{P}ol^{\bullet}(m,1)$. Observe further that the normalization of $\mathcal{P}ol^{\bullet}(m,1)$ induces a normalization of the spaces of polygons $\mathcal{P}ol^{\circ}(m,1)$, $\mathcal{P}ol^{\blacksquare}(m,1)$ and $\mathcal{P}ol^{\square}(m,1)$.

Definition 2.3.10. Let $m \geq 1$ and $\star \in \{\bullet,\blacksquare,\circ,\square\}$. The *normalization* is the continous retraction

$$r\colon \mathcal{P}ol^{\star}(m,1) \to N\mathcal{P}ol^{\star}(m,1) \tag{2.48}$$

induced by the normalization of simplices.

Remark 2.3.11. By construction, the normalizations commute with the forgetful maps in Definition 2.3.7.

Proposition 2.3.12. *Let $m \geq 1$. The space of m normalized (enumerated and / or parametrized) polygons is a strong deformation retract of the space of m (enumerated and / or parametrized) polygons. The deformation retractions can be chosen to commute with the forgetful maps in Definition 2.3.7.*

Proof. On $\mathcal{P}ol^{\bullet}(m,1)$ we define the obvious homotopy on the level of n-dimensional simplices: On $\sigma \times \mathrm{int}(\Delta^n)$ the homotopy is

$$h_s(\sigma,t) := (\sigma,t^s_0,\ldots,t^s_n), \quad t^s_i = (1-s)\cdot t_j + s\cdot \tfrac{t_j}{m\cdot l(i)} \quad \text{for } 0 \leq i \leq n. \tag{2.49}$$

By construction, h_s induces strong deformation retractions $\mathcal{P}ol^{\blacksquare}(m,1) \to N\mathcal{P}ol^{\blacksquare}(m,1)$, $\mathcal{P}ol^{\circ}(m,1) \to N\mathcal{P}ol^{\circ}(m,1)$ and $\mathcal{P}ol^{\square}(m,1) \to N\mathcal{P}ol^{\square}(m,1)$ that commute with the forgetful maps. □

Proposition 2.3.13. *Let $m \geq 1$ and $\star \in \{\bullet, \circ\}$. The normalization and the length map induce a homeomorphism*

$$r \times l \colon \mathcal{P}ol^{\star}(m,1) \cong N\mathcal{P}ol^{\star}(m,1) \times int(\Delta^{m-1})\,. \tag{2.50}$$

Proof. The map $r \times l$ is a continous bijection. Its inverse is the continous map

$$(\sigma, t', l') \mapsto (\sigma, t), \quad t_i = t'_i \cdot m \cdot l'_{j(i)} \tag{2.51}$$

where $j(i)$ denotes the number of the cycle to which i belongs, i.e., $i \in \sigma_{j(i)}$. By construction, the length of the j-th cycle of (σ, t) is l'_j:

$$l_j(\sigma, t) = \sum_{i \in \sigma_j} t_i = \sum_{i \in \sigma_j} t'_i \cdot m \cdot l'_j = \frac{m \cdot l'_j}{m} = l'_j\,. \tag{2.52}$$

□

2.4. Cellular and multi-cyclic structures of $N\mathcal{P}ol^{\star}(m,1)$

In this section, we will use the projection to the left factor

$$\mathcal{P}ol^{\bullet}(m,1) \cong N\mathcal{P}ol^{\bullet}(m,1) \times \mathrm{int}(\Delta^{m-1}) \to N\mathcal{P}ol^{\bullet}(m,1)$$

to construct a multi-cyclic structure on $N\mathcal{P}ol^{\bullet}(m,1)$, see Proposition 2.4.1. This will lead to a cellular structure on $N\mathcal{P}ol^{\blacksquare}(m,1)$, $N\mathcal{P}ol^{\circ}(m,1)$ respectively $N\mathcal{P}ol^{\square}(m,1)$, see Proposition 2.4.5.

Proposition 2.4.1. *Let $m \geq 1$. The space $N\mathcal{P}ol^{\bullet}(m,1)$ is homeomorphic to the realization of an m-fold multi-cyclic set $N\mathfrak{S}^{\bullet}(m,1)$ whose multi-simplices of multi-degree $\underline{k} = (k_1, \ldots, k_m)$ and total degree n are*

$$N\mathfrak{S}^{\bullet}(m,1)_{\underline{k}} = \{\langle \sigma_{1,0} \ \ldots \ \sigma_{1,k_1} \rangle \cdots \langle \sigma_{m,0} \ \ldots \ \sigma_{m,k_m} \rangle\} \tag{2.53}$$

$$\subset F_m\mathfrak{S}^{\bullet}([n]) - F_{m-1}\mathfrak{S}^{\bullet}([n])\,. \tag{2.54}$$

The face maps $d_{j,i}$ remove the i-th symbol from the j-th cycle and renomalize the other symbols afterwards, i.e.,

$$d_{j,i}(\sigma) = D_{\sigma_{j,i}}(\sigma)\,, \tag{2.55}$$

the degeneracy maps $s_{j,i}$ are

$$s_{j,i}(\sigma) = S_{\sigma_{j,i}}(\sigma) \tag{2.56}$$

and the cyclic operator in the j-th component permutes the symbols in the j-th cycle cyclically.

Proof. Let us denote the interior of an n-simplex by Δ^n to simplify our notation. In this notation, the normalization of an n-dimensional cell $\sigma \times \Delta^n$ is

$$r(\sigma \times \Delta^n) = \sigma \times \{(t_0, \dots, t_n) \mid \textstyle\sum_{j \in \sigma_i} t_j = \frac{1}{m} \text{ for all } i\} \subset \sigma \times \Delta^n \,. \tag{2.57}$$

Consequently, denoting the norm of a permutation α by $N(\alpha)$, we obtain a canonical cell decomposition of $N\mathcal{P}ol^\bullet$ with open cells

$$\Delta(\sigma) := r(\sigma \times \Delta^n) \cong \sigma \times \Delta^{N(\sigma_1)} \times \ldots \times \Delta^{N(\sigma_m)} \,. \tag{2.58}$$

The dimension of the multi-simplex $\Delta(\sigma)$ is $n - m + 1$. Using the distinguished symbol of each cycle, we have canonical barycentric coordinates $(t_{j,0}, \dots, t_{j,N(\sigma_j)})_{j=1,\dots,m}$. From the construction it is clear that the i-th face in the j-coordinate is the cell $\Delta(D_{\sigma_{j,i}}(\sigma))$. With this at hand, it is easy to see that $N\mathcal{P}ol^\bullet(m,1)$ is the realization of the multi-simplicial space $N\mathfrak{S}^\bullet(m,1)$ with face maps $d_{j,i}(\sigma) = D_{\sigma_{j,i}}(\sigma)$ and with degeneracy maps $s_{j,i}(\sigma) = S_{\sigma_{j,i}}(\sigma)$.

We define the j-th cyclic operator t^j to act on $\sigma = \sigma_1 \cdots \sigma_m$ by $t^j \sigma_i = \sigma_i$ for $j \neq i$ and $t^j \langle \sigma_{j,0}\ \sigma_{j,1}\ \dots\ \sigma_{j,c} \rangle = \langle \sigma_{j,c}\ \sigma_{j,0}\ \dots\ \sigma_{j,c-1} \rangle$. A straight forward computation shows that these data equip $N\mathcal{P}ol^\bullet(m,1)$ with the structure of an m-fold multi-cyclic space. □

Discussion 2.4.2. We discuss our geometric interpretation of the points in $N\mathcal{P}ol^\bullet(m,1)$. For simplicity, assume $m = 1$ first. Given a point $x \in N\mathcal{P}ol^\bullet(1,1)$, consider a representative $x = (\sigma; u)$ with $u \in \mathrm{int}(\Delta^n)$. The permutation σ consists of a single cycle $\sigma = \sigma_1 = \langle \sigma_{1,0}\ \sigma_{1,1}\ \dots \rangle$. We dissect $\mathbb{S}^1 = [0,1]/_\sim$ into $n+1$ intervals $[t_i, t_{i+1}]$ where $t_i = \sum_{k<i} u_k$. The i-th interval is denoted by $e_i := \sigma_{1,i}$. Each interval e_i is oriented such that $t_i \in e_i$ is the starting point of e_i and $t_{i+1} \in e_i$ is the end point. The starting point of the interval e_0 is the distinguished point $0 \sim 1 \in \mathbb{S}^1$. See Figure 2.1 for two examples.

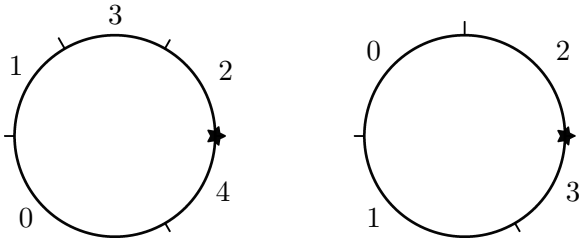

Figure 2.1.: In the left picture, we draw the point $x = (\sigma; u) \in N\mathcal{P}ol^\bullet(1,1)$ with $\sigma = \langle 4\ 0\ 1\ 3\ 2 \rangle$ and $u = (\frac{1}{6}, \frac{2}{6}, \frac{1}{6}, \frac{1}{6}, \frac{1}{6})$. In the right picture, we draw the point $y = (\sigma; u) \in N\mathcal{P}ol^\bullet(1,1)$ with $\sigma = \langle 3\ 1\ 0\ 2 \rangle$ and $u = (\frac{1}{6}, \frac{2}{6}, \frac{1}{4}, \frac{1}{4})$.

By construction, the lengths of the intervals are given by the barycentric coordinates u of $x = (\sigma, u)$ and if u tends towards the face $d_i \Delta^n$, the edge with label i degenerates to a point. Thus, our geometric interpretation of a point in $N\mathcal{P}ol^\bullet(1,1)$ behaves well with faces.

The geometric interpretation of a point $x = (\sigma, u)$ with $\sigma = s_i(\sigma')$ is a circle having consecutive edges with labels i and $i+1$. Regarding a point in $N\mathcal{P}ol^\bullet(1,1)$ as an orientation preserving isometry between two circles up to an unspecified configuration of points, the cutpoint between the two edges is superfluous, i.e., instead of two edges with labels i and $i+1$ we see a single edge with label i (and renormalize the labels of all other edges).

With this identification, our geometric interpretation is independent of representatives $x = (\sigma, u) = (s_i\sigma', s_i(u')) = (\sigma', u')$, see also Figure 2.2 left and middle.

Since $N\mathcal{P}ol^\bullet(1,1)$ is the realization of a cyclic space, we have a circle action: It is (up to introducing or forgetting cut points) the rotation of the distinguished point $1 \in \mathbb{S}^1$, see also Proposition A.1.7 and Figure 2.2.

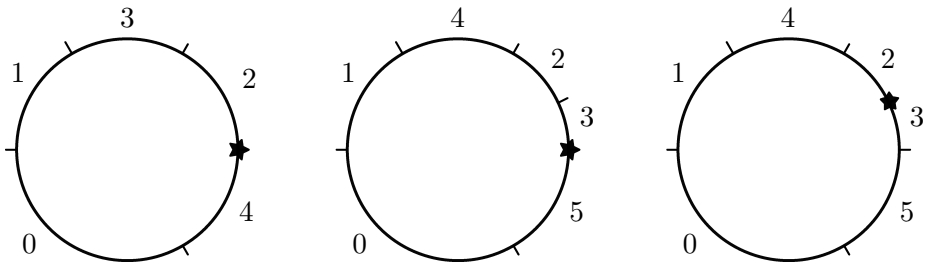

Figure 2.2.: Consider the point $x = (\sigma; u) \in N\mathcal{P}ol^\bullet(1,1)$ with $\sigma = \langle 4\ 0\ 1\ 3\ 2\rangle$ and $u = (\frac{1}{6}, \frac{2}{6}, \frac{1}{6}, \frac{1}{6}, \frac{1}{6})$ as it is seen on the left hand side on the left of this figure or of Figure 2.1. Let us demonstrate that the action of $z = \frac{1}{13} \in [0,1]/_\sim = \mathbb{S}^1$. It will be the rotation of the distinguished point in the circle by z. According to Proposition A.1.7, the new point $x.z$ is obtained as follows. In the first step we choose the degenerate representative $s_4\sigma$ of σ with degenerate coordinates $u' = (\frac{1}{6}, \frac{2}{6}, \frac{1}{6}, \frac{1}{6}, \frac{1}{6} - \frac{1}{13}, \frac{1}{13})$. This is seen in the middle. Then, we compute the action of t_5 on $s_4\sigma$ and the coaction of t_5^{-1} on u'. It is $t_5 s_4\sigma = \langle 3\ 5\ 0\ 1\ 4\ 2\rangle$ and $t_5^{-1}u = (\frac{1}{13}, \frac{1}{6}, \frac{2}{6}, \frac{1}{6}, \frac{1}{6}, \frac{1}{6} - \frac{1}{13})$. As it is seen on the right hand side, this is exactly the rotation of the distinguished point by z.

A point $x \in N\mathcal{P}ol^\bullet(m,1)$ is thought of cutting the circle into finitely many intervals and reglueing the pieces such that a collection of m enumerated circles of equal circumference is obtained. By symmetry, we can think of a point $x \in N\mathcal{P}ol^\bullet(m,1)$ as cutting m enumerated circles of equal circumference into intervals that are reglued to give a single circle. From this point of view, it is not surprising that $N\mathcal{P}ol^\bullet(m,1)$ admits not only a cyclic structure but also an m-fold multi-cyclic structure. Moreover, for arbitrary $m \geq 1$ and $n \geq 1$, it is straight forward to construct the spaces $N\mathcal{P}ol^\bullet(m,n)$ together with canonical n-fold multi-cyclic structure and m-fold multi-cyclic structure. We leave this to the reader.

Discussion 2.4.3. Recall that the spaces $N\mathcal{P}ol^\blacksquare(m,1)$, $N\mathcal{P}ol^\circ(m,1)$ and $N\mathcal{P}ol^\square(m,1)$ are quotients of $N\mathcal{P}ol^\bullet(m,1)$. It is easy to see that $\pi^\bullet_\blacksquare$ and $\pi^\circ_\square$ are $m!$-fold coverings whose group of Deck transformations is isomorphic to a symmetric group on m elements. After introducing an m-fold multi-cyclic structure on $N\mathcal{P}ol^\bullet(m,1)$, we give a full proof that $\pi^\bullet_\circ$ is an m-dimensional torus bundle in Section 2.6. In particular, one should expect to see these facts in our geometric interpretation of the points of $N\mathcal{P}ol^\blacksquare(m,1)$, $N\mathcal{P}ol^\circ(m,1)$ and $N\mathcal{P}ol^\square(m,1)$.

Firstly, fix a point $x \in N\mathcal{P}ol^\blacksquare(m,1)$. Consider a representative of $x = (\sigma, u)$ with $u \in \mathrm{int}(\Delta^n)$. Choosing an enumeration of the cycles of σ gives a point $\tilde{x} \in N\mathcal{P}ol^\circ(m,1)$ with $\pi^\bullet_\blacksquare(\tilde{x}) = x$. Therefore, a point $x \in N\mathcal{P}ol^\blacksquare(m,1)$ is thought of cutting the circle into finitely many intervals and reglueing the pieces such that a collection of m unenumerated circles of equal circumference is obtained.

Our geometric interpretation of a point $x \in N\mathcal{P}ol^\circ(1,1)$ is as follows. Consider a representative of $x = (\sigma, u)$ with $u \in \mathrm{int}(\Delta^n)$. We emphasize, that we allow σ to be simplicially

degenerated. By definition, σ has one cycle. Choosing a distinguished element of this cycle yields a point $\tilde{x} \in N\mathcal{P}ol^{\bullet}(1,1)$ with $\pi_{\circ}^{\bullet}(\tilde{x}) = x$. By Discussion 2.4.2, we view $\tilde{x}$ as a circle with decorated edges and the action of $\mathbb{S}^1$ on $\tilde{x}$ is the the rotation the distinguished point of this circle. It is straight forward to check that the preimage of x under $\pi_{\circ}^{\bullet}$ is exactly the orbit of $\tilde{x}$ of this action, see also Proposition A.1.7. Consequently, we interpret x as cutting a given circle into finitely many intervals and reglueing the pieces in a different order such that we obtain a circle but only up to rotation. See Figure 2.3 for an example. More generally, a point $x \in N\mathcal{P}ol^{\circ}(m,1)$ is thought of cutting a given circle into finitely

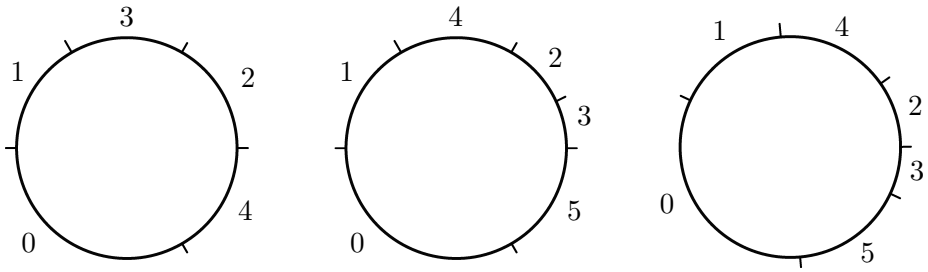

Figure 2.3.: The three pictures show the very same point $x \in N\mathcal{P}ol^{\circ}(1,1)$. It is the image of the points $\tilde{x}$ and $z.\tilde{x} \in N\mathcal{P}ol^{\bullet}(1,1)$ seen in Figure 2.2. The left picture represents the point $x = (\sigma; u)$ by $\sigma = \langle 4\ 0\ 1\ 3\ 2\rangle$ and $u = (\frac{1}{6}, \frac{2}{6}, \frac{1}{6}, \frac{1}{6}, \frac{1}{6})$. The middle picture represents the point $x = (\sigma'; u')$ by $\sigma' = \langle 5\ 0\ 1\ 4\ \ 2\ 3\rangle$ and $u' = (\frac{1}{6}, \frac{2}{6}, \frac{1}{6}, \frac{1}{6}, \frac{1}{6} - \frac{1}{13}, \frac{1}{13})$. The right picture represents the point $x = (\sigma''; u'')$ by $\sigma'' = \langle 3\ 5\ 0\ 1\ 4\ 2\rangle$ and $u'' = (\frac{1}{13}, \frac{1}{6}, \frac{2}{6}, \frac{1}{6}, \frac{1}{6}, \frac{1}{6} - \frac{1}{13})$.

many intervals and reglueing the pieces such that we obtain a collection of m enumerated circles of equal circumference but only up to rotation of each individual circle.

Lastly, a point $x \in N\mathcal{P}ol^{\square}(m,1)$ is thought of cutting a given circle into finitely many intervals and reglueing the pieces such that we obtain a collection of m unenumerated circles of equal circumference but only up to rotation of each individual circle.

Proposition 2.4.4. *Let $m \geq 1$. The induced action of the m-dimensional torus $U(1)^m$ on the space $N\mathcal{P}ol^{\bullet}(m,1)$ is free.*

Proof. From Discussion 2.4.2 and Proposition A.1.7 the action of the i-th factor of $U(1)^m$ on $N\mathcal{P}ol^{\bullet}(m,1)$ can be carried out explicitly: Let $\alpha \in U(1)$ be an arbitrary angle and let $x \in N\mathcal{P}ol^{\bullet}(m,1)$ be a collection of m normalized enumerated polygons with base points. Then, $\alpha.x$ is the very same collection of m enumerated polygons with the single exception that the base point of the i-th polygon has moved by the angle α. This is enough to prove the claim. □

Proposition 2.4.5. *Let $m \geq 1$ and $\star \in \{\bullet, \blacksquare, \circ, \square\}$. The space of m normalized polygons $N\mathcal{P}ol^{\star}(m,1)$ admits a cellular decomposition whose n cells are in one-to-one correspondence to*

$$F_m\mathfrak{S}^{\star}([n+m-1]) - F_{m-1}\mathfrak{S}^{\star}([n+m-1]) \tag{2.59}$$

and such that the quotient maps in Definition 2.3.7 are cellular.

Proof. First of all, note that Proposition 2.4.1 implies the desired result for $N\mathcal{P}ol^{\bullet}(m,1)$.

For the general case, recall that the normalization $\mathcal{P}ol^\bullet(m,1) \to N\mathcal{P}ol^\bullet(m,1)$ is cellular and that it sends every open cell $\sigma \times \Delta^n \subset \mathcal{P}ol^\bullet(m,1)$ onto the open multi-simplex $\sigma \times \Delta^{N(\sigma_1)} \times \ldots \times \Delta^{N(\sigma_m)} \subset N\mathcal{P}ol^\bullet(m,1)$. By construction, the vertices of the multi-simplex are given by the enumerated and parametrized cycles of σ. Moreover, the normalization $\mathcal{P}ol^\blacksquare(m,1) \to N\mathcal{P}ol^\blacksquare(m,1)$, $\mathcal{P}ol^\circ(m,1) \to N\mathcal{P}ol^\circ(m,1)$ and $\mathcal{P}ol^\square(m,1) \to N\mathcal{P}ol^\square(m,1)$ commute with the projection maps in Diagram 2.41. Therefore, the image of a cell $\sigma \times \Delta^n$ in $\mathcal{P}ol^\blacksquare(m,1)$, $\mathcal{P}ol^\circ(m,1)$ or $\mathcal{P}ol^\square(m,1)$ is homeomorphic to a multi-simplex $\sigma \times \Delta^{N(\sigma_1)} \times \ldots \times \Delta^{N(\sigma_m)}$ after choosing an enumeration of the cycles of σ and a parametrization of each cycle. The attaching maps of these cells are uniquely given by the choices of the enumerations and parametrizations of the cycles and the attaching maps of $\mathcal{P}ol^\blacksquare(m,1)$, $\mathcal{P}ol^\circ(m,1)$ or $\mathcal{P}ol^\square(m,1)$. □

2.5. The desuspension theorem for the spaces of polygons

The space of all enumerated and parametrized polygons $\mathcal{P}ol^\bullet$ is stratified by the spaces $\mathcal{P}ol^\bullet(m,1)$, i.e., (1) $\mathcal{P}ol^\bullet = \cup_k \mathcal{P}ol^\bullet(m,1)$ and (2) the closure of $\mathcal{P}ol^\bullet(m,1)$ in $\mathcal{P}ol^\bullet$ is $\overline{\mathcal{P}ol^\bullet}(m,1) = \cup_{k \leq m} \mathcal{P}ol^\bullet(k,1)$ and (3) $\mathcal{P}ol^\bullet(m,1)$ is open in $\overline{\mathcal{P}ol^\bullet}(m,1)$. In particular, $\mathcal{P}ol^\bullet$ is filtered by closed subspaces $F_m\mathcal{P}ol^\bullet = \overline{\mathcal{P}ol^\bullet}(m,1)$. Therefore, after fixing $m \geq 1$, we think of a point in $\overline{\mathcal{P}ol^\bullet}(m,1)$ as being non-degenerate if and only if it lies in $\mathcal{P}ol^\bullet(m,1)$. This idea of non-degenerate points is reflected by the moduli spaces and their harmonic compactifications in a precise sense, see Section 3.4 and Section 3.5.

The integral desuspension for the spaces of polygons $N\mathcal{P}ol^\bullet(m,1)$ relates the complement of the degenerate points $F_m\mathcal{P}ol^\bullet - F_{m-1}\mathcal{P}ol^\bullet = \mathcal{P}ol^\bullet(m,1) \cong N\mathcal{P}ol^\bullet(m,1) \times \mathrm{int}(\Delta^{m-1})$ with the quotient by the degenerate points $F_m\mathcal{P}ol^\bullet / F_{m-1}\mathcal{P}ol^\bullet$.

Theorem 2.5.1. *Let $m \geq 1$. There is an isomorphism*

$$H_*(N\mathcal{P}ol^\bullet(m,1);\mathbb{Z}) \cong \Sigma^{-m+1} H_*(F_m\mathcal{P}ol^\bullet, F_{m-1}\mathcal{P}ol^\bullet;\mathbb{Z})\,. \tag{2.60}$$

Moreover, without taking signs into account, we have a desuspension theorem for the spaces of polygons $\mathcal{P}ol^\star(m,1)$.

Theorem 2.5.2. *There are isomorphisms*

$$H_*(N\mathcal{P}ol^\bullet(m,1);\mathbb{F}_2) \cong \Sigma^{-m+1} H_*(F_m\mathcal{P}ol^\bullet, F_{m-1}\mathcal{P}ol^\bullet;\mathbb{F}_2) \tag{2.61}$$

$$H_*(N\mathcal{P}ol^\blacksquare(m,1);\mathbb{F}_2) \cong \Sigma^{-m+1} H_*(F_m\mathcal{P}ol^\blacksquare, F_{m-1}\mathcal{P}ol^\blacksquare;\mathbb{F}_2) \tag{2.62}$$

$$H_*(N\mathcal{P}ol^\circ(m,1);\mathbb{F}_2) \cong \Sigma^{-m+1} H_*(F_m\mathcal{P}ol^\circ, F_{m-1}\mathcal{P}ol^\circ;\mathbb{F}_2) \tag{2.63}$$

$$H_*(N\mathcal{P}ol^\square(m,1);\mathbb{F}_2) \cong \Sigma^{-m+1} H_*(F_m\mathcal{P}ol^\square, F_{m-1}\mathcal{P}ol^\square;\mathbb{F}_2) \tag{2.64}$$

Moreover, these isomorphisms commute with the forgetful maps (see Definitions 2.2.18 and 2.3.7).

Geometrically speaking, both theorems follow from an extension of the homeomorphism

$$F_m\mathcal{P}ol^\bullet - F_{m-1}\mathcal{P}ol^\bullet \cong N\mathcal{P}ol^\bullet(m,1) \times \mathrm{int}(\Delta^{m-1})$$

to the quotient

$$F_m\mathcal{P}ol^\bullet / F_{m-1}\mathcal{P}ol^\bullet \cong N\mathcal{P}ol^\bullet(m,1) \wedge \mathbb{S}^{m-1}\,.$$

However, we will give an algebraic proof, see also Proposition 2.5.7. The author would like to thank Andrea Bianchi for pointing out a closed formula for the signs, see (2.68) and (2.69).

Before going into the proofs, let us adumbrate how our desuspension theorem is related to the desuspension theorem of Klamt [Kla13, Theorem C]. She introduces a chain complex of certain loop diagrams that approximates the chain complex of all natural operations of certain commutative algebras. It is therefore related to the harmonic compactification of moduli spaces in a very precise meaning, see [Kla13, Section 2.4]. For sake of simplicity let us assume that every point in the harmonic compactification yields some sort of loop diagram and that a loop diagram is called degenerate, if it comes from a degenerate moduli. She shows that, in homology, the quotient of all loop diagrams by the subcomplex of degenerate loop diagrams is isomorphic to a (twisted) desuspension of the cacti operad.

Proof of Theorem 2.5.2 and Theorem 2.5.1. The desuspension theorem with coefficients in $\mathbb{F}_2$ follows immediately from the construction of the multi-cyclic structure on $N\mathcal{P}ol^\bullet(m,1)$ and the cell structures of $\mathcal{P}ol^\blacksquare(m,1)$, $\mathcal{P}ol^\circ(m,1)$ and $\mathcal{P}ol^\square(m,1)$. Up to shift in degrees, the cellular complex of the left hand side has the same cells and faces as the relative simplicial complex of the right hand side.

Introducing the correct signs, Theorem 2.5.1 follows immediately from Proposition 2.5.7. □

In order to define the correct signs mentioned in the proof of Theorem 2.5.1, we need to introduce some notation.

Definition 2.5.3. Let $m \geq 1$ and $\sigma = \langle \sigma_{1,0} \ \dots \ \rangle \cdots \langle \sigma_{m,0} \ \dots \ \rangle \in \mathfrak{S}^\bullet([k])$ be a multi-simplex of $N\mathcal{P}ol^\bullet(m,1)$ of multi-degree $(k_1, \dots, k_m)$.

Less pedantically, we say that l *is left of* u *in* σ, if l appears left of u in the parametrized enumerated cycle decomposition of σ.

More pedantically: For every $s \in [k]$, we have unique numbers $1 \leq j(s) \leq m$ and $0 \leq i(s) \leq k_{j(s)}$ with $u = \sigma_{j(s),i(s)}$ and we say that l *is left of* u *in* σ, in symbols $l \vdash_\sigma u$, if the following condition is satisfied:

$$l \vdash_\sigma u \quad :\Leftrightarrow \quad l \neq u \text{ and } \big(j(l) < j(u) \text{ or } j(l) = j(u) \text{ and } i(l) < i(u)\big)\,. \tag{2.65}$$

The *set of symbols left of* u *in* σ is

$$\{l \in [k] \mid l \vdash_\sigma u\}\,. \tag{2.66}$$

Example 2.5.4. Consider the parametrized enumerated permutation $\sigma = \langle 3\ 1\ 0\rangle\langle 2\ 5\rangle\langle 4\rangle$. Then, 3 is left of 0, 1, 2, 4 and 5. The set of symbols left of 5 is $\{0,1,2,3\}$.

Definition 2.5.5. Let $m \geq 1$ and $\sigma \in \mathfrak{S}^\bullet([k])$ be a multi-simplex of $N\mathcal{P}ol^\bullet(m,1)$. The *parity of* i *in* σ is

$$\mathrm{parity}(\sigma, i) := \#\{l \in [k] \mid l \vdash_\sigma i\} \in \mathbb{F}_2\,. \tag{2.67}$$

Having the inversion number of a permutation in mind, the *parity of* σ is

$$\mathrm{parity}(\sigma) := \#\{(l,u) \in [k]^2 \mid l < u, u \vdash_\sigma l\} \in \mathbb{F}_2 \tag{2.68}$$

and the *sign of* σ is

$$\operatorname{sign}(\sigma) := (-1)^{\operatorname{parity}(\sigma)} \in \mathbb{F}_2\,. \tag{2.69}$$

Example 2.5.6. Consider the parametrized enumerated permutation $\sigma = \langle 3\ 1\ 0\rangle\langle 2\ 5\rangle\langle 4\rangle$. Then, the parity of 5 in σ is

$$\operatorname{parity}(\sigma, 5) = \#\{0,1,2,3\} = 0\,. \tag{2.70}$$

The parity of σ is the number of pairs (l,u) with $l < u$ and $u \vdash_\sigma l$:

$$\operatorname{parity}(\sigma) = \#\{(0,1),(0,3),(1,3),(2,3),(4,5)\} = 1\,. \tag{2.71}$$

Therefore, the sign of σ is

$$\operatorname{sign}(\sigma) = (-1)^{\operatorname{parity}(\sigma)} = -1\,. \tag{2.72}$$

Proposition 2.5.7. *Let $m \geq 1$. Denote the cellular complex of the multi-simplicial space $N\mathcal{P}ol^\bullet(m,1)$ by $C_*(N\mathcal{P}ol^\bullet(m,1))$ and the relative simplicial complex associated to the simplicial pair $(F_m\mathcal{P}ol^\bullet, F_{m-1}\mathcal{P}ol^\bullet)$ by $C_*(F_m\mathcal{P}ol^\bullet, F_{m-1}\mathcal{P}ol^\bullet)$.*

The signs in (2.69) *define an isomorphism of chain complexes.*

$$C_*(F_m\mathcal{P}ol^\bullet, F_{m-1}\mathcal{P}ol^\bullet) \to \Sigma^{-m+1} C_*(N\mathcal{P}ol^\bullet(m,1)), \quad \sigma \mapsto \operatorname{sign}(\sigma)\cdot\sigma \tag{2.73}$$

Remark 2.5.8. The symmetric difference of two sets A and B is denoted by $A\Delta B$ and is clear that

$$\#A + \#B = \#(A\Delta B) \in \mathbb{F}_2\,. \tag{2.74}$$

We will use this fact in the proof of Proposition 2.5.7 implicitly.

Proof. Let $m \geq 1$ and $\sigma \in C_*(N\mathcal{P}ol^\bullet(m,1))$ a generator of multi-degree $(k_1,\dots,k_m)$. Usually, the sign of a face $d_{j,i}\sigma$ in the totalization of the multi-simplical complex is defined to be $(-1)^{k_1+\dots+k_{j-1}+i}$. However, we obtain an isomorphic chain complex by using the sign $(-1)^{\operatorname{parity}(\sigma,i)}$: An isomorphism is given by sending σ to $(-1)^{p(\sigma)}\sigma$ with $p(\sigma) = \sum_{k_j \text{ odd}} j - 1$.

With this convention, we will verify that $\sigma \mapsto \operatorname{sign}(\sigma)\sigma$ is a chain map: To this end, let $\sigma \in C_*(F_m\mathcal{P}ol^\bullet, F_{m-1}\mathcal{P}ol^\bullet)$ and assume $d_i\sigma$ is non-trivial. It is enough to show that the coefficients $\operatorname{sign}(d_i\sigma)\cdot(-1)^i$ and $(-1)^{\operatorname{parity}(\sigma,i)\}}\cdot\operatorname{sign}(\sigma)$ agree. This is the case if and only if the following expression vanishes in $\mathbb{F}_2$.

$$\operatorname{parity}(\sigma) + \operatorname{parity}(d_i\sigma) + \#\{l \mid l < i\} + \#\{l \mid l \vdash_\sigma i\} \tag{2.75}$$

In what follows, we abbreviate $\{l \in [k] \mid \dots\}$ by $\{l \mid \dots\}$ and $\{(l,u) \in [k]^2 \mid \dots\}$ by $\{l,u \mid \dots\}$. The symbols in $d_i\sigma$ correspond to the symbols in σ that are different from i. We use this correspondence to rewrite the parity of $d_i\sigma$.

$$= \#\{l,u \mid l < u, u \vdash_\sigma l\} + \#\{l,u \mid l < u, u \vdash_\sigma l, i \notin \{l,u\}\} + \#\{l \mid l < i\} + \#\{l \mid l \vdash_\sigma i\} \tag{2.76}$$

Computing the symmetric difference of the first two terms yields the following.

$$= \#\{l, u \mid l < u, u \vdash_\sigma l, i \in \{l, u\}\} + \#\{l \mid l < i\} + \#\{l \mid l \vdash_\sigma i\} \tag{2.77}$$
$$= \#\{l \mid l < i, i \vdash_\sigma l\} + \#\{l \mid i < l, l \vdash_\sigma i\} + \#\{l \mid l < i\} + \{l \mid l \vdash_\sigma i\} \tag{2.78}$$

Computing the symmetric difference of the first and the third term yields the following.

$$= \#\{l \mid l < i, l \vdash_\sigma i\} + \#\{l \mid i < l, l \vdash_\sigma i\} + \#\{l \mid l \vdash_\sigma i\} \tag{2.79}$$

Now we compute the symmetric difference of the first two terms.

$$= \#\{l \mid l \vdash_\sigma i\} + \#\{l \mid l \vdash_\sigma i\} \tag{2.80}$$
$$= 0 \tag{2.81}$$

□

2.6. On the homotopy type of the spaces of polygons

In this section, we study the homotopy type of the spaces of polygons. Most importantly, we will show that $\mathcal{P}ol^\bullet$ is contractible, see Proposition 2.6.3 and that the bundle $\mathcal{P}ol^\bullet(m,1) \to \mathcal{P}ol^\circ(m,1)$ is the universal torus bundle $EU(1)^m \to BU(1)^m$, see Theorem 2.6.2.

Proposition 2.6.1. *Let $m \geq 1$. The forgetful maps induce m-dimensional torus bundles.*

$$\begin{array}{ccccc} \mathcal{P}ol^\bullet(m,1) & \xrightarrow{\cong} & N\mathcal{P}ol^\bullet(m,1) \times int(\Delta^{m-1}) & \xrightarrow{\simeq} & N\mathcal{P}ol^\bullet(m,1) \\ \downarrow{\scriptstyle \pi_\circ^\bullet} & & \downarrow{\scriptstyle \pi_\circ^\bullet} & & \downarrow{\scriptstyle \pi_\circ^\bullet} \\ \mathcal{P}ol^\circ(m,1) & \xrightarrow{\cong} & N\mathcal{P}ol^\circ(m,1) \times int(\Delta^{m-1}) & \xrightarrow{\simeq} & N\mathcal{P}ol^\circ(m,1) \end{array} \tag{2.82}$$

Proof. The commutativity of the diagram follows from Proposition 2.3.12. The multi-cyclic structure of $N\mathcal{P}ol^\bullet(m,1)$ induces a free action by the m-dimensional torus by Proposition 2.4.4. Therefore $\pi_\circ^\bullet \colon N\mathcal{P}ol^\bullet(m,1) \to N\mathcal{P}ol^\circ(m,1)$ is a principle torus bundle.

By Proposition 2.3.13, the map $\pi_\circ^\bullet \colon \mathcal{P}ol^\bullet(m,1) \to \mathcal{P}ol^\circ(m,1)$ is the product of the torus fibration $\pi_\circ^\bullet \colon N\mathcal{P}ol^\bullet(m,1) \to N\mathcal{P}ol^\circ(m,1)$ with $\mathrm{id}_{\mathrm{int}(\Delta^{m-1})}$. This finishes the proof. □

Theorem 2.6.2. *The m-dimensional torus bundles*

$$\mathcal{P}ol^\bullet(m,1) \to \mathcal{P}ol^\circ(m,1) \quad \textit{and} \quad N\mathcal{P}ol^\bullet(m,1) \to N\mathcal{P}ol^\circ(m,1) \tag{2.83}$$

are universal.

Proof. The torus action is free by Proposition 2.4.4 and so it is enough to prove that $N\mathcal{P}ol^\bullet(m,1)$ is contractible. We show $N\mathcal{P}ol^\bullet(m,1) \simeq N\mathcal{P}ol^\bullet(m-1,1)$ for all $m \geq 1$ and $N\mathcal{P}ol^\bullet(0,1) := *$. To this end, observe that the simplicial set $N\mathcal{P}ol^\bullet(1,1)$ admits an extra degeneracy (see e.g. Appendix A.2) defined by

$$s_{-1}\langle i_0 \ \dots \ i_k\rangle = \langle -1 \ i_0 \dots \ i_k\rangle \tag{2.84}$$

followed by a renormalization of the symbols, i.e., $s_{-1}\langle i_0 \ \dots \ i_k\rangle = \langle 0 \ i_0+1 \dots \ i_k+1\rangle$. Moreover, $N\mathcal{P}ol^\bullet(1,1)$ has a single vertex $\langle 0\rangle$ and therefore, it is contractible. For $m>1$, there is an analogously constructed extra degeneracy on the first factor of the m-fold multisimplicial set $N\mathcal{P}ol^\bullet(m,1)$ defined by

$$s_{-1}\langle i_0 \ \dots \ i_k\rangle\sigma_2\cdots\sigma_m = \langle -1 \ i_0 \ \dots \ i_k\rangle\sigma_2\cdots\sigma_m \tag{2.85}$$

followed by a renormalization of the symbols. Consequently, $N\mathcal{P}ol^\bullet(m,1)$ is homotopy equivalent to the subspace consisting of all non-degenerate simplices of the form $\sigma_1\cdots\sigma_m$ with $\sigma_1=\langle 0\rangle$. This subspace is clearly homeomorphic to $N\mathcal{P}ol^\bullet(m-1,1)$. □

Proposition 2.6.3. *The space $\mathcal{P}ol^\bullet$ is contractible.*

Proof. Note that $\mathcal{P}ol^\bullet$ is simply connected: It has a single zero cell $\langle 0\rangle$ and the only non-degenerate one-dimensional cells are $\langle 1\ 0\rangle$, $\langle 0\rangle\langle 1\rangle$ and $\langle 1\rangle\langle 0\rangle$. The first loop is filled by the two-dimensional cell $\langle 0\ 2\ 1\rangle$, the second loop is filled by $\langle 0\rangle\langle 1\rangle\langle 2\rangle$ and the third loop is filled by $\langle 0\rangle\langle 2\rangle\langle 1\rangle$.

The filtration of $\mathcal{P}ol^\bullet$ by $F_m\mathcal{P}ol^\bullet$, see Definition 2.2.17, yields a spectral sequence with first page $E^1_{m,s}\cong H_{m+s}(F_m\mathcal{P}ol^\bullet, F_{m-1}\mathcal{P}ol^\bullet;\mathbb{Z})$. We have $E^1_{m,s}\cong H_{1+s}(N\mathcal{P}ol^\bullet(m,1);\mathbb{Z})$ by Theorem 2.5.1. But $N\mathcal{P}ol^\bullet(m,1)$ is contractible by Theorem 2.6.2. Therefore, $E^1_{m,s}$ is concentrated in a single row where $s=-1$ and $E^1_{m,-1}\cong H_0(N\mathcal{P}ol^\bullet(m,1);\mathbb{Z})$ is generated by the cell $\langle 0\rangle\cdots\langle m-1\rangle$. The differential d^1 is easily computed.

$$d^1(\langle 0\rangle\cdots\langle m-1\rangle) = \sum_i (-1)^i d_i(\langle 0\rangle\cdots\langle m-1\rangle) = \sum_i (-1)^i\langle 0\rangle\cdots\langle m-2\rangle \tag{2.86}$$

Thus, $E^1_{m,-1}$ is acyclic and so is $\mathcal{P}ol^\bullet$. □

2.7. Comparing $\mathcal{P}ol^\circ(1,1)$ with Kontsevich's $BU(1)^{comb}$

Let $m\geq 1$ and $\star\in\{\bullet,\circ,\blacksquare,\square\}$. Recall that the set of permutations with at most m cycles defines a simplicial subset $F_m\mathfrak{S}^\star\leq\mathfrak{S}^\star$. Note that, by definition, the realization of $F_1\mathfrak{S}^\star$ is $\mathcal{P}ol^\star(1,1)$. Denote the fat realization of $F_1\mathfrak{S}^\star$ by $\mathbb{P}ol^\star(1,1)$ and the canonical quotient by $q\colon \mathbb{P}ol^\star(1,1)\xrightarrow{\simeq}\mathcal{P}ol^\star(1,1)$. By definition of the fat realization, every point $x\in\mathbb{P}ol^\star(1,1)$ is uniquely represented by a pair $x=(\sigma,t)\in F_1\mathfrak{S}^\star([n])\times\mathrm{int}(\Delta^n)$ for some n.

Similarly to our geometric interpretation of points in $\mathcal{P}ol^\circ(1,1)$, we associate to $(\sigma,t)\in F_1\mathfrak{S}^\circ([n])\times\mathrm{int}(\Delta^n)$ an oriented polygon $P(x)$ with $n+1$ edges that are cyclically labeled by the symbols $0,\sigma(0),\dots,\sigma^n(0)$ and whose lengths are $t_0,t_{\sigma(0)},\dots,t_{\sigma^n(0)}$. This polygon is piecewise isometric to a circle and we regard the vertices of the polygons as set of $n+1$ points up to a rotation, i.e., $C(x)\in exp(\mathbb{S}^1)/U(1)$. This defines a continuous map

$$\theta\colon \mathbb{P}ol^\circ(1,1)\to exp(\mathbb{S}^1)/U(1)\,. \tag{2.87}$$

Proposition 2.7.1. *The zig-zag*

$$\mathcal{P}ol^\circ(1,1)\xleftarrow[\simeq]{q}\mathbb{P}ol^\circ(1,1)\xrightarrow[\simeq_{\mathbb{Q}}]{\theta} exp(\mathbb{S}^1)/U(1) \tag{2.88}$$

induces a rational homotopy equivalence.

Proof. Clearly, $exp(\mathbb{S}^1)$ is filtered by the closed subspaces $exp_N(\mathbb{S}^1) = \{C \subset \mathbb{S}^1 \mid \#C \leq N\}$. By [Tuf02, Theorem 4], the spaces $exp_{2k-1}(\mathbb{S}^1)$ and $exp_{2k}(\mathbb{S}^1)$ are odd dimensional spheres of dimension $2k-1$. Moreover, by [Tuf02, Theorem 5], the inclusion $exp_{2k-1}(\mathbb{S}^1) \subset exp_{2k}(\mathbb{S}^1)$ induces the multiplication by two in H_{2k-1}. From the long exact sequence of homotopy groups induced by the Borel construction

$$exp_{2k-1}(\mathbb{S}^1) \to EU(1) \times_{U(1)} exp_{2k-1}(\mathbb{S}^1) \to BU(1) \tag{2.89}$$

it follows that

$$EU(1) \times_{U(1)} exp_{2k-1}(\mathbb{S}^1) \to BU(1) \tag{2.90}$$

is $(2k-2)$-connected. Similarly, the inclusion $exp_{2k-1}(\mathbb{S}^1) \subset exp(\mathbb{S}^1)$ induces a $(2k-2)$-connected map

$$EU(1) \times_{U(1)} exp_{2k-1}(\mathbb{S}^1) \to EU(1) \times_{U(1)} exp(\mathbb{S}^1)\,. \tag{2.91}$$

The stabilizers of the action of $U(1)$ on $exp_{2k-1}(\mathbb{S}^1)$ and $exp(\mathbb{S}^1)$ are finite and it follows that both quotient maps

$$EU(1) \times_{U(1)} exp_{2k-1}(\mathbb{S}^1) \to exp_{2k-1}(\mathbb{S}^1)/U(1) \tag{2.92}$$

and

$$EU(1) \times_{U(1)} exp(\mathbb{S}^1) \to exp(\mathbb{S}^1)/U(1) \tag{2.93}$$

are rational equivalences. Consequently, the zig-zag

$$BU(1) \longleftarrow EU(1) \times_{U(1)} exp(\mathbb{S}^1) \longrightarrow exp(\mathbb{S}^1)/U(1) \tag{2.94}$$

induces a rational equivalence and the inclusion $exp_{2k-1}(\mathbb{S}^1)/U(1) \subset exp(\mathbb{S}^1)/U(1)$ is rationally a $(2k-2)$-connected map.

Observe that $\theta\colon \mathbb{P}ol^\circ(1,1) \to exp(\mathbb{S}^1)/U(1)$ maps the k-skeleton $\mathbb{P}ol^\circ_k(1,1)$ to $exp_{k+1}(\mathbb{S}^1)$. It is readily checked that $\mathbb{P}ol^\circ_2(1,1)$ is a sphere made a single 0-cell, a single 1-cell and two 2-simplices $\langle 0\ 1\ 2\rangle \times \Delta^2$ and $\langle 0\ 2\ 1\rangle \times \Delta^2$. Comparing the long exact sequences of the pair $(\mathbb{P}ol^\circ_3(1,1), \mathbb{P}ol^\circ_2(1,1))$ with the cellular chain complex it follows that the inclusion $\mathbb{P}ol^\circ_2(1,1) \subset \mathbb{P}ol^\circ_3(1,1) \subset \mathbb{P}ol^\circ(1,1) \simeq \mathbb{C}P^\infty$ induces an isomorphism in the second (co)homology.

By the above, we have the following commuting diagram.

$$\begin{array}{ccc} H^2(exp(\mathbb{S}^1)/U(1);\mathbb{Q}) & \xrightarrow{\theta^*} & H^2(\mathbb{P}ol^\circ(1,1);\mathbb{Q}) \\ \downarrow\cong & & \downarrow\cong \\ H^2(exp_3(\mathbb{S}^1)/U(1);\mathbb{Q}) & \xrightarrow{\theta^*} & H^2(\mathbb{P}ol^\circ_2(1,1);\mathbb{Q}) \end{array} \tag{2.95}$$

Since both $H^*(exp(\mathbb{S}^1)/U(1);\mathbb{Q})$ and $H^*(\mathbb{P}ol^\circ(1,1)\mathbb{Q})$ are polynomial algebras in one generator in degree two, it is enough to show that θ induces a rational isomorphism

$$\theta_*\colon H_2(\mathbb{P}ol^\circ_2(1,1);\mathbb{Q}) \cong H_2(exp_3(\mathbb{S}^1)/U(1);\mathbb{Q})\,. \tag{2.96}$$

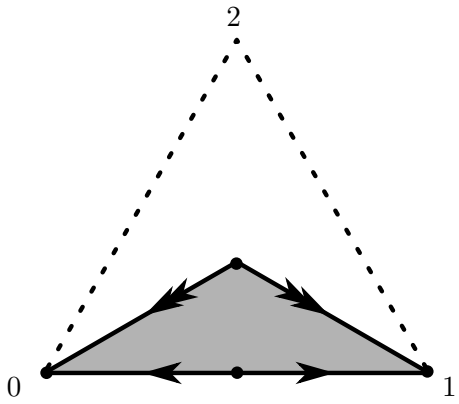

Figure 2.4.: The space $exp_3(\mathbb{S}^1)/\mathbb{S}^3$ is homeomorphic to a quotient of Δ^2. As such, it admits the following cellular decomposition. The barycenter $(\frac{1}{3}, \frac{1}{3}, \frac{1}{3})$, the point $(1, 0, 0)$ and the point $(\frac{1}{2}, \frac{1}{2}, 0)$ represent the three 0-cells. The segments $\{(t, \frac{1-t}{2}, \frac{1-t}{2}) \mid t \in [\frac{1}{3}, 1]\}$ and $\{(t, 1-t, 0) \mid t \in [\frac{1}{2}, 1]\}$ represent to two 1-cells and the 2-cell is represented by $\{(t_0, t_1, t_2) \mid t_0, t_1 \geq t_2\}$.

To this end, we choose the following cellular decomposition of $exp_3(\mathbb{S}^1)/U(1)$. Note that, given three distinct points on $\mathbb{S}^1$ up to rotation, measuring the distance of each pair of consecutive points defines a sequence $(t_0, t_1, t_2) \in \mathrm{int}(\Delta^2)/\mathbb{Z}_3$ up to cyclic permutation of the entries. This defines a homeomorphism $exp_3(\mathbb{S}^1)/U(1) - exp_2(\mathbb{S}^1)/U(1) \cong \mathrm{int}(\Delta^2)/\mathbb{Z}_3$. A fundamental domain of the action of $\mathbb{Z}_3$ on $\mathrm{int}(\Delta^2)$ is $\{(t_0, t_1, t_2) \in \mathrm{int}(\Delta^2) \mid t_0, t_1 \geq t_2\}$. From this, we obtain $exp_3(\mathbb{S}^1)$ as a quotient of Δ^2 with the cellular decomposition shown in Figure 2.4. With this identification, the map θ sends a point $(t_0, t_1, t_2) \in \langle 0\ 1\ 2\rangle \times \Delta^2 \subset \mathbb{P}ol_2^\circ(1,1)$ to $(t_0, t_1, t_2) \in exp_3(\mathbb{S}^1)/U(1)$ and a point $(t_0, t_1, t_2) \in \langle 0\ 2\ 1\rangle \times \Delta^2 \subset \mathbb{P}ol_2^\circ(1,1)$ is send to (t_0, t_2, t_1). Observe that θ is cellular and that its degree on $\langle 0\ 1\ 2\rangle$ is $+3$ whereas on $\langle 0\ 2\ 1\rangle$ it is -3. Observe further that $H_2(\mathbb{P}ol_2^\circ(1,1); \mathbb{Z})$ is generated by $\langle 0\ 1\ 2\rangle - \langle 0\ 2\ 1\rangle$. Therefore, (2.96) is a rational isomorphism which was left to show. □

3

The spaces of radial slit configurations

In [Bö90a, Bö06] Bödigheimer uses the theory of harmonic potentials to construct models for the moduli spaces in question. For the convenience of the reader and to fix our notation, we recall some of the details of the construction of one of his models. It is called the *space of radial slit configurations*. In Section 3.1, we discuss the construction of the model $\mathfrak{Rad}_g^{\square}(m,1) \simeq \mathfrak{M}_g^{\square}(m,1)$. The construction of the models $\mathfrak{Rad}_g^{\square}(m,1) \simeq \mathfrak{M}_g^{\square}(m,1)$, $\mathfrak{Rad}_g^{\bullet}(m,1) \simeq \mathfrak{M}_g^{\bullet}(m,1)$, $\mathfrak{Rad}_g^{\blacksquare}(m,1) \simeq \mathfrak{M}_g^{\blacksquare}(m,1)$ and $\mathfrak{Rad}_g^{\circ}(m,1) \simeq \mathfrak{M}_g^{\circ}(m,1)$ is similar and is discusses in fewer details in Section 3.2. These spaces of radial slit configurations admit at least two compactifications, see below.

Bödigheimer introduces the *bar compactification* in [Bö07]. In this thesis, we denote the bar compactification of $\mathfrak{M}_g^{\star}(m,1)$ by $Bar_g^{\star}(m,1)$. It is seen as the completion of the combinatorial aspects of radial slit configurations and as such it is a space made from subcomplexes of bar complexes of all symmetric groups, see Section 3.4, Appendix D and also [Vis10] and [BH14]. The bar compactification has been used by various authors to compute the unstable homology of the moduli spaces of Riemann surfaces for small parameters $m \geq 1$ and $g \geq 0$, see [Ehr97, Abh05, ABE08, Meh11, Wan11, BH14] and Section 7.3.

The *harmonic compactification* is introduced by Bödigheimer in [Bö06]. In this thesis, we denote the harmonic compactification of $\mathfrak{M}_g^{\star}(m,1)$ by $\overline{\mathfrak{M}}_g^{\star}(m,1)$. It is seen as the completion of the geometric aspects of the radial slit configurations, see Section 3.5 and also [Bö06] and [EK14]. The study of the harmonic compactification has important applications to the study of string topology, see Section 1.3 and Section 4.4. We study the homotopy type of the harmonic compactification in Chapters 4, 5 and 6.

In Section 3.6, we use the bar compactification and the spaces of polygons to classify the m-dimensional torus bundle $\mathfrak{Rad}_g^{\bullet}(m,1) \to \mathfrak{Rad}_g^{\circ}(m,1)$.

Theorem 3.6.8. *Let $m \geq 1$, $g \geq 0$. Forgetting the parametrization of the outgoing boundaries defines an m-dimensional torus bundle $\pi_{\circ}^{\bullet}\colon \mathfrak{Rad}_g^{\bullet}(m,1) \to \mathfrak{Rad}_g^{\circ}(m,1)$ that is classified by the restriction to the outgoing boundaries, see Definition 3.6.2:*

$$\begin{array}{ccc} \mathfrak{Rad}_g^{\bullet}(m,1) & \xrightarrow{\mathcal{P}ol_g^{\bullet}} & \mathcal{P}ol^{\bullet}(m,1) \simeq EU(1)^m \\ \downarrow{\scriptstyle \pi_{\circ}^{\bullet}} & & \downarrow{\scriptstyle \pi_{\circ}^{\bullet}} \\ \mathfrak{Rad}_g^{\circ}(m,1) & \xrightarrow{\mathcal{P}ol_g^{\circ}} & \mathcal{P}ol^{\circ}(m,1) \simeq BU(1)^m \end{array} \tag{3.1}$$

Denoting the stabilization map by $\varphi_g\colon \mathfrak{Rad}_g^{\star}(m,1) \to \mathfrak{Rad}_{g+1}^{\star}(m,1)$, it is $\mathcal{P}ol_g^{\star} = \mathcal{P}ol_{g+1}^{\star} \circ \varphi_g$.

Furthermore, in Section 3.6, we discuss the space of radial slit configurations with normalized boundaries — which is a model for the moduli space of Riemann surfaces whose outgoing boundaries have equal circumferences. Their harmonic compactifications will be studied in Chapter 5 and Chapter 6.

3.1. The space of radial slit configurations for $\mathfrak{M}_g^{\square}(m,1)$

In this section, we discuss the construction of Bödigheimer's radial model $\mathfrak{Rad}_g^{\square}(m,1) \simeq \mathfrak{M}_g^{\square}(m,1)$. Given a Riemann surface $F \in \mathfrak{M}_g^{\square}(m,1)$, we use the flow lines of a unique harmonic potential function $f\colon F \to [0,1]$ to associate a configuration of radial slits on a annulus with F, see Subsection 3.1.1. The combinatorics of such a radial slit configuration are encoded by a sequence of permutations that are subject to certain conditions, see Subsection 3.1.2. The space of all radial slit configurations satisfying these conditions constitute the space of radial slit configurations which is homeomorphic to the moduli space via the Hilbert uniformization map, see Subsection 3.1.3. For a topologist, there are two canonical compactifications of the space of radial slit configurations. Most of their features are described at the end of Subsection 3.1.3 and in Sections 3.4 and 3.5. The harmonic compactification is studied in greater detail via spaces of Sullivan diagrams in Chapter 4, Chapter 5 and Chapter 6.

3.1.1. From a Riemann surface to a radial slit configuration

Given a Riemann surface F with $n \geq 1$ parametrized and enumerated incoming and $m \geq 1$ unparametrized and unenumerated outgoing boundaries, we choose a harmonic function $f\colon F \to [0,1]$ that is equal to 0 on the incoming boundaries and one equal to 1 on the outgoing boundaries. The harmonic potential f is a solution to a Dirichlet problem. It always exists and is uniquely determined by F and its values on the boundary components, see e.g. [For81, Theorem 22.17] or [Tsu59, Theorem I.25]. Moreover, the harmonic potential has finitely many critical points and each of them is in the interior of F. The union of all critical points and of all gradient flow lines that leave a critical point define a possibly disconnected graph $K \subset F$, which is called the *unstable critical graph*. It is a subgraph of the *complete critical graph*[1] which consists of all critical points and of all flow lines that leave or enter a critical point or a parametrization point $P \in \partial_{in}F$. The preimage of a critical resp. regular value is a *critical level* resp. *regular level*. Observe that the union of the incoming boundaries is precisely $f^{-1}(0)$ whereas the union of the outgoing boundaries is precisely $f^{-1}(1)$ and for our purposes it is useful to call these levels also critical levels. The critical levels are ordered by their values, i.e., a critical level $f^{-1}(x)$ is smaller than a critical level $f^{-1}(y)$ if and only if $x < y$. Let us denote the number of critical levels by $q+2 \geq 2$ and index the critical levels by increasing order, i.e., the critical levels are $\mathfrak{l}_0 < \ldots < \mathfrak{l}_{q+1}$. By construction $\mathfrak{l}_0$ is the union of all incoming boundaries and $\mathfrak{l}_{q+1}$ is the union of all outgoing boundaries. We say that two critical levels $\mathfrak{l}_i < \mathfrak{l}_j$ are *consecutive* if and only if $j = i+1$. Given two consecutive critical levels $\mathfrak{l}_i = f^{-1}(x_i)$ and $\mathfrak{l}_{i+1} = f^{-1}(x_{i+1})$, the i-th intermediate (regular) level is $\mathfrak{r}_i := f^{-1}(\frac{x_i+x_{i+1}}{2})$.

[1] In Bödigheimer's original definition of the critical graph [Bö06, Section 6.2], the flow lines entering or leaving a parametrization point were not included in the complete critical graph.

Observe that the region between two consecutive critical levels is a disjoint union of open cylinders. Observe further that the region between the levels $\mathfrak{l}_0$ and $\mathfrak{r}_i$ for some $0 < i \leq q$ is a closed submanifold of F with Riemann structure, with n enumerated and parametrized incoming boundaries and with some number of outgoing boundaries that do not come with a natural parametrization or enumeration.

After removing the unstable critical graph, we are left with an open submanifold of F. The process of "pulling the remaining flow lines straight" defines a biholomorphic map whose image is a disjoint union of n annuli $A_1, \ldots, A_n$ with radial slits removed. More precisely, the inner radius of each annulus is $1 = \exp(0)$ and each outer radius is $\exp(1)$. Every flow line is mapped on a radiant, each incoming boundary $C_i^- \subset \partial_{in} F$ is mapped to the inner boundary of the annuli A_i and the parametrization point $P_i^- \in C_i^-$ is send to the complex number $1 \in A_i$. See Figure 3.1 for an example.

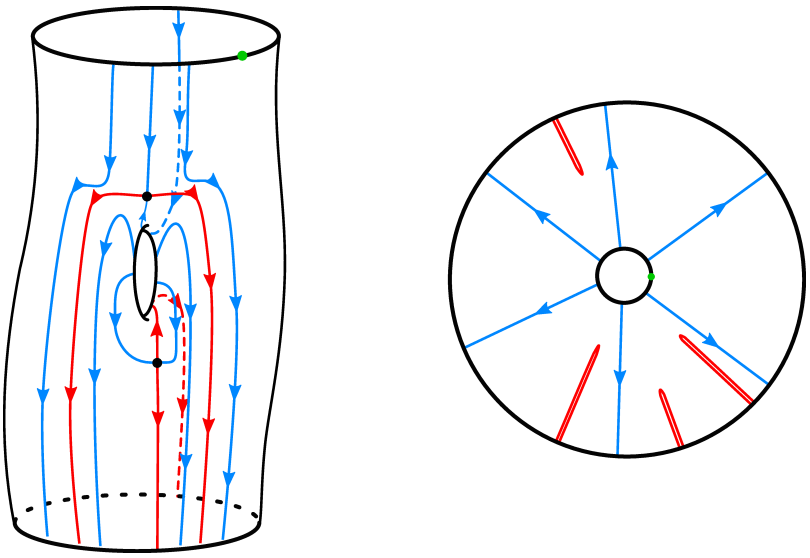

Figure 3.1.: On the left, we sketch the flow lines of a harmonic function defined on a Riemann surface $F \in \mathfrak{M}_1^{\square}(1,1)$ of genus one with one incoming and one outgoing boundary curve. The critical points are black, the paramatrization point on the incoming boundary is green, the flow lines leaving a critical point are red and all other flow lines are blue. On the right, we sketch the image of F under the process described above. It is an annulus with red pairs of radial slit removed and one pair is shorter than the other.

3.1.2. The combinatorial type of a radial slit configuration

Now, we discuss the combinatorics of the distribution of the pairs of radial slits over the annuli. For the sake of simplicity, we treat the case $F \in \mathfrak{M}_g^{\square}(m,1)$ at first, the other cases are treated later. By construction, a harmonic potential on a Riemann surface F induces a conformal map between $F - K$ and an annulus with pairs of radial slits removed. The complete critical graph and the critical levels give a grid of radial and concentric lines on this annulus. Recall that, by our definition of the complete critical graph, the positive

real axis[2] is part of the grid. The radial lines give $p+1$ radial segments. Using the clockwise orientation of the annulus, we number these segments by $0, \dots, p$ starting with the unique segment that begins on the positive real line. The critical levels give $q+1$ annuli of increasing size. We number the annuli by $0, \dots, q$ starting with the smallest one. The (bended) rectangle in the i-th sector of the j-th annulus is denoted by $R_{i,j}$. These rectangles correspond to (metric) rectangles on the surface such that the top edge of $R_{i,j}$ coincides with the bottom edge of $R_{i+1,j}$ and the right edge of $R_{i,j}$ coincides with the left edge of $R_{i,\sigma_i(j)}$ for some permutation $\sigma_i \in \mathfrak{S}([p])$. The sequence of permutations $(\sigma_0 : \dots : \sigma_q)$ is the *combinatorial type* of such a configuration of radial slits. In Figure 3.2, a radial slit configuration of combinatorial type $\Sigma = (\langle 0\ 1\ 2\ 3\ 4\rangle : \langle 0\ 3\ 4\rangle\langle 1\ 2\rangle : \langle 0\ 3\ 2\ 1\ 4\rangle)$ is shown.

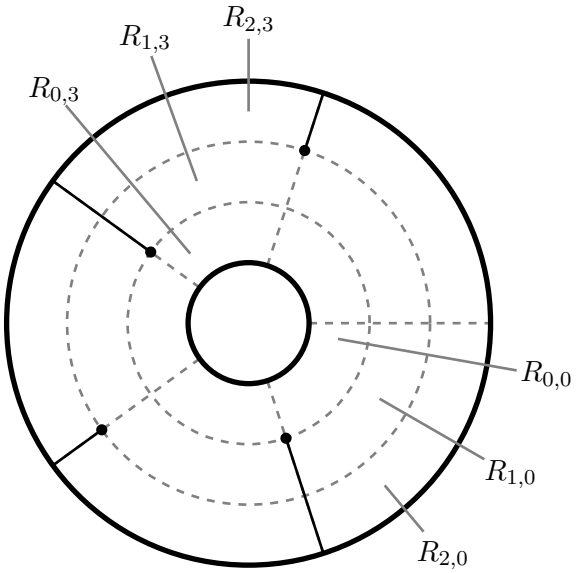

Figure 3.2.: A radial slit configuration whose grid is highlighted by dashed gray lines. Some of the (bended) rectangles are indicated. The combinatorial type of this radial slit configuration is $\Sigma = (\sigma_0 : \sigma_1 : \sigma_2)$ with $\sigma_0 = \langle 0\ 1\ 2\ 3\ 4\rangle$, $\sigma_1 = \langle 0\ 3\ 4\rangle\langle 1\ 2\rangle$ and $\sigma_2 = \langle 0\ 3\ 2\ 1\ 4\rangle$.

The combinatorial type is subject to three conditions: The parametrized incoming and the outgoing boundaries are encoded correctly, see (3.2) and (3.3); The combinatorial type encodes the Euler characteristic of the surface correctly, see (3.4); The configuration is non-degenerate in the simplicial sense, see (3.5), (3.6) and the subsequent paragraphs. More precisely: The region between the incoming boundary and the subsequent critical level $\mathfrak{l}_1$ is a cylinder (that comes with a parametrization of its incoming boundary), i.e., σ_0 is the long cycle

$$\sigma_0 = \omega_p = \langle 0\ 1\ \dots\ p\rangle\,; \tag{3.2}$$

The region between the outgoing boundaries and the preceding critical level $\mathfrak{l}_q$ is a disjoint union of m cylinders (that do not come with a natural ordering or a parametrization), i.e.,

[2]The intersection of the positive real axis with the annulus corresponds to the flow line that leaves the parametrization point of the incoming boundary.

σ_q has exactly m cycles

$$\mathrm{ncyc}(\sigma_q) = m\,. \tag{3.3}$$

Using the "triangulation" of F in terms of the rectangles $R_{i,j}$, observe that the curvature of F is concentrated in the corners of these rectangles. Observe further that the corner points in F are in one to one correspondence to the cycles of the permutations $\tau_i := \sigma_i\sigma_{i-1}^{-1}$ and each cycle c of length l contributes with an angle $l \cdot 2\pi$. Consequently, each cycle c of length l contributes to the Euler characteristic with $-(l-1) = -N(c)$, where $N(c)$ denotes the norm[3] of c. Therefore, the negative of the Euler characteristic of F is exactly

$$-\chi(F) = N(\tau_1) + \ldots + N(\tau_q) = 2g + m + n - 2\,. \tag{3.4}$$

By construction, neither does our grid give superflous annuli, i.e.,

$$\sigma_i \neq \sigma_{i+1} \text{ for all } i \tag{3.5}$$

nor does our grid give superflous radial segments, i.e.,

$$\text{for each } 1 \leq j+1 \leq p \text{ there is an } i \text{ with } \sigma_i(j) \neq j+1. \tag{3.6}$$

The first permutation σ_0 is always the long cycle by (3.2). Therefore, the sequence of permutations $(\sigma_0 : \ldots : \sigma_q)$ carries the same information as the sequence

$$(\tau_1 \mid \ldots \mid \tau_q) \qquad \text{with} \qquad \tau_i := \sigma_i\sigma_{i-1}^{-1}\,. \tag{3.7}$$

The former is called the *homogeneous notation* and the latter is called the *inhomogeneous notation* of a given combinatorial type.

3.1.3. The spaces of radial slit configurations $\mathfrak{Rad}_g^{\square}(m,1)$

Using the endpoints of the slits of a radial slit configuration as (bi-simplicial) barycentric coordinates, it is immediate that the subspace of all Riemann surfaces whose associated radial slit configuration has a fixed combinatorial type $(\sigma_0 : \ldots : \sigma_q)$ forms an open bi-simplex $\mathrm{int}(\Delta^p \times \Delta^q) \subset \mathfrak{M}_g^{\square}(m,1)$.

Given a radial slit configuration C of combinatorial type $\Sigma = (\sigma_0 : \ldots : \sigma_q)$ with bi-simplicial coordinates $(s,t) \in \mathrm{int}(\Delta^p \times \Delta^q)$, we write $C = (\Sigma; s; t)$. Letting the i-th coordinate in s tend to zero, the limit point is called the *i-th horizontal face* of $(\Sigma; s; t)$ if it exists. Similarly, letting the j-th coordinate in t tend to zero, the limit point is called the *j-th vertical face* of $(\Sigma; s; t)$ if it exists. Assuming that the j-th vertical face of $(\Sigma; s; t)$ exists, the resulting radial slit configuration is obtained by contracting the j-th annulus of $(\Sigma; s; t)$ and the combinatorial type is

$$d'_j(\sigma_0 : \ldots : \sigma_q) = (\sigma_0 : \ldots : \hat{\sigma_j} : \ldots : \sigma_q)\,. \tag{3.8}$$

Assuming that the i-th horizontal face of $(\Sigma; s; t)$ exists, the resulting radial slit configuration is obtained by contracting the i-th radial segment and its combinatorial type is

$$d''_i(\sigma_0 : \ldots : \sigma_q) = (D_i\sigma_0 : \ldots : D_i\sigma_q)\,. \tag{3.9}$$

[3]The norm of a permutation is the minimal word length in the generating set of all transpositions.

It is clear that not all faces of a given radial slit configuration exist in $\mathfrak{M}_g^{\square}(m,1)$ (e.g., the combinatorial type of the faces d_0' or d_q' will violate condition (3.2) or (3.3)). The radial slit configurations whose combinatorial type satisfies the conditions (3.2), (3.3), (3.4), (3.5) and (3.6) constitute the *space of radial slit domains* denoted by $\mathfrak{Rad}_g^{\square}(m,1)$. Its topology is such that sending a Riemann surface to its radial slit configuration defines a homeomorphism

$$\Phi\colon \mathfrak{M}_g^{\square}(m,1) \cong \mathfrak{Rad}_g^{\square}(m,1)\,. \tag{3.10}$$

This homeomorphism is called the *Hilbert uniformization map*, c.f. [Bö06, Theorem 1.1].

For a topologist, there are at least two canonical completions of the space of radial slit domains as a *relative multi-simplicial manifold*, i.e., there are two canonical choices of a space $R := R_g(m,1)$, such that (1) the space R is the realization of a (finite) multi-simplicial set and (2) $\mathfrak{Rad} \subset R$ is open and dense and the complement $R' := R - \mathfrak{Rad}$ is a codimension one subcomplex. Then, (3) $H_*(\mathfrak{Rad};\mathbb{Z})$ is Poincaré dual to $H^*(R,R';\mathcal{O})$ for an orientation system $\mathcal{O}$. The two completions are called the *harmonic compactification* and the *bar compactification* of the moduli space. The most important aspects of these compactifications are discussed in Section 3.4 and Section 3.5. Let us state their most important features here before discussing their details in the subsequent subsections.

The harmonic compactification, introduced in [Bö93a] see also [Bö06, Section 8], is obtained from $\mathfrak{Rad}_g^{\square}(m,1)$ by adding specific degenerate surfaces which admit a real function that is harmonic on its smooth points. The study of the harmonic compactification has important applications to the study of string topology, see Section 1.3.

The bar compactification, introduced in [Bö07], admits a more elegant presentation. Adding all iterated vertical and horizontal faces of all combinatorial types that occur in $\mathfrak{Rad}_g^{\square}(m,1)$ yields a multi-simplicial space with finitely many non-degenerate cells. We call this space the bar compactification of the moduli space because the vertical faces (3.8) make a connection to bar resolutions of all symmetric groups immediate. The bar compactification and its relations to group homology are used by several authors to compute the integral homology of the moduli spaces $\mathfrak{M}_g^{\square}(m,1)$ for small parameters g and m, see Section 1.1.4.

3.2. The space of radial slit configurations for $\mathfrak{M}_g^{\circ}(m,1)$, $\mathfrak{M}_g^{\blacksquare}(m,1)$ and $\mathfrak{M}_g^{\bullet}(m,1)$

Considering the moduli spaces $\mathfrak{M}_g^{\circ}(m,n)$, $\mathfrak{M}_g^{\blacksquare}(m,n)$ resp. $\mathfrak{M}_g^{\bullet}(m,n)$ with enumerated or parametrized outgoing boundaries, the theory of harmonic potentials is used to establish a homeomorphism between the moduli space and a space of radial slit configurations $\mathfrak{Rad}_g^{\circ}(m,n)$, $\mathfrak{Rad}_g^{\blacksquare}(m,n)$ resp. $\mathfrak{Rad}_g^{\bullet}(m,n)$. As before, each point in the respectively space of radial slit configurations has a combinatorial type and the points of the same combinatorial type form an open multi-simplex. We discuss the combinatorial types occuring in $\mathfrak{Rad}_g^{\circ}(m,1)$, $\mathfrak{Rad}_g^{\blacksquare}(m,1)$ resp. $\mathfrak{Rad}_g^{\bullet}(m,1)$ seperately.

3.2.1. The space of radial slit configurations $\mathfrak{Rad}_g^{\circ}(m,1)$

Using the same techniques as before, we associate to a Riemann surface $F \in \mathfrak{M}_g^{\circ}(m,1)$ with harmonic potential a radial slit configuration as follows. The union of all critical points and

of all gradient flow lines that leave a critical point constitute the *unstable critical graph* K and the *complete critical graph* consists of all critical points and of all flow lines that leave or enter a critical point or a parametrization point $P \in \partial_{in}F$. To $F - K$, we associate a radial slit configuration by pulling the remaining flow lines straight. The complete critical graph and the critical levels give a decomposition of the radial slit configuration (or the surface) into (bended) rectangles. The identifications of the lower and upper edges of these rectangles give a sequence of permutations $(\sigma_0 : \ldots : \sigma_q)$ with $\sigma_0, \ldots, \sigma_q \in \mathfrak{S}([p])$. The enumerated outgoing boundaries correspond to an enumeration of the cycles of σ_q which is an enumerated permutation $\sigma^\circ \in \mathfrak{S}^\circ([p])$ with $\sigma_q = \pi^\circ_\square(\sigma^\circ)$. The combinatorial type is $(\sigma_0 : \ldots : \sigma_q; \sigma^\circ)$ and $\mathfrak{Rad}^\circ_g(m,1)$ consists of all radial slit configurations whose combinatorial type $(\sigma_0 : \ldots : \sigma_q; \sigma^\circ)$ is subject to the conditions (3.2), (3.3), (3.4), (3.5) and (3.6). Its topology is such that the points in $\mathfrak{Rad}^\circ_g(m,1)$ with the same combinatorial type $(\sigma_0 : \ldots : \sigma_q; \sigma^\circ)$ form an open bi-simplex. If the j-th vertical face resp. the i-th horizontal face of a bi-simplex of combinatorial type $(\sigma_0 : \ldots : \sigma_q; \sigma^\circ)$ exsits in $\mathfrak{Rad}^\circ_g(m,1)$, the combinatorial type of the resulting face is as follows.

$$d'_j(\sigma_0 : \ldots : \sigma_q; \sigma^\circ) = (\sigma_0 : \ldots : \hat{\sigma_j} : \ldots : \sigma_q; \sigma^\circ) \tag{3.11}$$

$$d''_i(\sigma_0 : \ldots : \sigma_q; \sigma^\circ) = (D_i\sigma_0 : \ldots : D_i\sigma_q; D_i\sigma^\circ) \tag{3.12}$$

Sending a Riemann surface to its radial slit configuration defines a homeomorphism

$$\Phi \colon \mathfrak{M}^\circ_g(m,1) \cong \mathfrak{Rad}^\circ_g(m,1)\,. \tag{3.13}$$

This homeomorphism is called the *Hilbert uniformization map*. Moreover, $\mathfrak{Rad}^\circ_g(m,1)$ admits a bar compactification and an harmonic compactification.

3.2.2. The space of radial slit configurations $\mathfrak{Rad}^\blacksquare_g(m,1)$

Again, we associate to a Riemann surface $F \in \mathfrak{M}^\circ_g(m,1)$ with harmonic potential a radial slit configuration as follows. The union of all critical points and of all gradient flow lines that leave a critical point constitute the *unstable critical graph* K and the *complete critical graph* consists of all critical points and of all flow lines that leave or enter a critical point or a parametrization point $P \in \partial_{in}F \cup \partial_{out}F$. To $F - K$, we associate a radial slit configuration by pulling the remaining flow lines straight. The complete critical graph and the critical levels give a decomposition of the radial slit configuration (or the surface) into (bended) rectangles. The identifications of the lower and upper edges of these rectangles give a sequence of permutations $(\sigma_0 : \ldots : \sigma_q)$ with $\sigma_0, \ldots, \sigma_q \in \mathfrak{S}([p])$. The parametrization of the unenumerated outgoing boundaries correspond to an parametrization of the cycles of σ_q which is an parametrized permutation $\sigma^\blacksquare \in \mathfrak{S}^\blacksquare([p])$ with $\sigma_q = \pi^\blacksquare_\square(\sigma^\blacksquare)$. The combinatorial type is $(\sigma_0 : \ldots : \sigma_q; \sigma^\blacksquare)$ In order to deduce the conditions the combinatorial type satisfies, observe that the case, where all parametrization points are disjoint from the critical graph, is generic. In this case, whenever a parametrization point is inbetween the radial segments j and $j+1$, the parametrized permutation has $j+1$ as the distinguished element in its cycle and all permutation σ_i satisfy $\sigma_i(j) = j+1$. Now it is straight forward to check that $\mathfrak{Rad}^\blacksquare_g(m,1)$ consists of all radial slit configurations whose combinatorial type $(\sigma_0 : \ldots : \sigma_q; \sigma^\blacksquare)$ is subject to the conditions (3.2), (3.3), (3.4), (3.5) and (3.14).

$$\text{If } j+1 \text{ is not distinguished in } \sigma^\blacksquare, \text{ then there is an } i \text{ with } \sigma_i(j) \neq j+1. \tag{3.14}$$

Its topology is such that the points in $\mathfrak{Rad}^{\blacksquare}_g(m,1)$ with the same combinatorial type $(\sigma_0 : \ldots : \sigma_q; \sigma^{\blacksquare})$ form an open bi-simplex. If the j-th vertical face resp. the i-th horizontal face of a bi-simplex of combinatorial type $(\sigma_0 : \ldots : \sigma_q; \sigma^{\blacksquare})$ exsits in $\mathfrak{Rad}^{\blacksquare}_g(m,1)$, the combinatorial type of the resulting face is as follows.

$$d'_j(\sigma_0 : \ldots : \sigma_q; \sigma^{\blacksquare}) = (\sigma_0 : \ldots : \hat{\sigma_j} : \ldots : \sigma_q; \sigma^{\blacksquare}) \tag{3.15}$$

$$d''_i(\sigma_0 : \ldots : \sigma_q; \sigma^{\blacksquare}) = (D_i\sigma_0 : \ldots : D_i\sigma_q; D_i\sigma^{\blacksquare}) \tag{3.16}$$

Sending a Riemann surface to its radial slit configuration defines a homeomorphism

$$\Phi\colon \mathfrak{M}^{\blacksquare}_g(m,1) \cong \mathfrak{Rad}^{\blacksquare}_g(m,1)\,. \tag{3.17}$$

This homeomorphism is called the *Hilbert uniformization map*. Moreover, $\mathfrak{Rad}^{\blacksquare}_g(m,1)$ admits a bar compactification and an harmonic compactification.

3.2.3. The space of radial slit configurations $\mathfrak{Rad}^{\bullet}_g(m,1)$

Finally, as a combination of $\mathfrak{Rad}^{\circ}_g(m,1)$ and $\mathfrak{Rad}^{\blacksquare}_g(m,1)$, the combinatorial type of a radial slit domain in $\mathfrak{Rad}^{\bullet}_g(m,1)$ is a sequence of permutations $(\sigma_0 : \ldots : \sigma_q; \sigma^{\bullet})$ with $\sigma_0, \ldots, \sigma_q \in \mathfrak{S}([p])$, $\sigma^{\bullet} \in \mathfrak{S}^{\bullet}[p]$ and $\sigma_q = \pi^{\bullet}_{\square}(\sigma^{\bullet})$ and the space of radial slit domains $\mathfrak{Rad}^{\bullet}_g(m,1)$ consists of all radial slit configurations whose combinatorial type $(\sigma_0 : \ldots : \sigma_q; \sigma^{\bullet})$ is subject to the conditions (3.2), (3.3), (3.4), (3.5) and (3.18).

$$\text{If } j+1 \text{ is not distinguished in } \sigma^{\bullet}, \text{ then there is an } i \text{ with } \sigma_i(j) \neq j+1. \tag{3.18}$$

Its topology is such that the points in $\mathfrak{Rad}^{\bullet}_g(m,1)$ with the same combinatorial type $(\sigma_0 : \ldots : \sigma_q; \sigma^{\bullet})$ form an open bi-simplex. If the j-th vertical face resp. the i-th horizontal face of a bi-simplex of combinatorial type $(\sigma_0 : \ldots : \sigma_q; \sigma^{\bullet})$ exsits in $\mathfrak{Rad}^{\bullet}_g(m,1)$, the combinatorial type of the resulting face is as follows.

$$d'_j(\sigma_0 : \ldots : \sigma_q; \sigma^{\bullet}) = (\sigma_0 : \ldots : \hat{\sigma_j} : \ldots : \sigma_q; \sigma^{\bullet}) \tag{3.19}$$

$$d''_i(\sigma_0 : \ldots : \sigma_q; \sigma^{\bullet}) = (D_i\sigma_0 : \ldots : D_i\sigma_q; D_i\sigma^{\bullet}) \tag{3.20}$$

Sending a Riemann surface to its radial slit configuration defines a homeomorphism

$$\Phi\colon \mathfrak{M}^{\bullet}_g(m,1) \cong \mathfrak{Rad}^{\bullet}_g(m,1)\,. \tag{3.21}$$

This homeomorphism is called the *Hilbert uniformization map*. Moreover, $\mathfrak{Rad}^{\bullet}_g(m,1)$ admits a bar compactification and an harmonic compactification.

The rotation of the parametrization points of the m enumerated outgoing boundaries defines a free action of an m-dimensional torus $U(1)^m$. This action is induced by a multicyclic structure on an $U(1)^m$-equivariant retract of $\mathfrak{Rad}^{\bullet}_g(m,1)$, see Section 3.6.

3.3. The cluster filtration

In this section we recall the construction of the cluster filtration introduced in [BB18b], see also [BH14, Chapter 3]. The associated spectral sequence is used in [BH14], [BB18a] and in this thesis, to compute the homology of $\mathfrak{M}^{\square}_g(m,1)$ for small parameters g and m, see

Section 7.3 and Appendix E.4. In [BE17] the cluster filtration is used to make the cellular inclusion of the moduli space into its harmonic compactification explicit, see also Section 4.3.2.

Let $g \geq 0$, $m \geq 1$, $n \geq 1$ and $\star \in \{\bullet, \circ, \blacksquare, \square\}$. Let $F \in \mathfrak{M}_g^\star(m,1)$ and consider the unstable critical graph K of (the harmonic potential f of) F, see Section 3.1.1. The graph K is possibly disconnected. By $c(F)$ we denote the *cluster number of* F which is the number of the connected components of K. This gives a filtration of the moduli spaces called the *cluster filtration*:

$$Cl_c\mathfrak{M}_g^\star(m,n) = \{F \in \mathfrak{M}_g^\star(m,n) \mid c(F) \leq c\}\,. \tag{3.22}$$

Note that this filtration is bi-simplicial.

Theorem 3.3.1 (Bödigheimer)**.** *Let $g \geq 0$, $m \geq 1$, $n \geq 1$ and $\star \in \{\bullet, \circ, \blacksquare, \square\}$. The cluster filtration gives a first quadrant spectral sequence*

$$E^r_{c,t} \Rightarrow H_{c+t}(\mathfrak{M}_g^\star(m,n); \mathbb{Z}) \tag{3.23}$$

that collapses on the second page.

In terms of radial slit configurations, the cluster number is defined as follows. Let $\Sigma = (\tau_1 \mid \ldots \mid \tau_q)$ denote the combinatorial type of a cell of $\mathfrak{Rad}_g^\star(m,1)$ of bi-degree (p,q). On $[p]$ we declare the equivalence relation $\sim_{CL}$ as the transitive closure of the relation

$$s \sim t \quad \text{if } s \text{ and } t \text{ are in the same cycle of } \tau_i \text{ for some } 1 \leq i \leq q. \tag{3.24}$$

The equivalence classes of $\sim_{CL}$ are the *clusters of* Σ. The *number of clusters of* Σ is the number of equivalence classes of $\sim_{CL}$.

Proposition 3.3.2 (Bödigheimer)**.** *The number of clusters give a filtration of the spaces $\mathfrak{M}_g^\star(m,1)$ and $\mathfrak{Rad}_g^\star(m,1)$. The Hilbert uniformization $\mathfrak{M}_g^\star(m,1) \cong \mathfrak{Rad}_g^\star(m,1)$ induces a homeomorphism of the associated stratified spaces.*

The following Lemma is used to make the inclusion of the moduli space into its harmonic compactification explicit in Section 4.3.2.

Lemma 3.3.3. *Let $\Sigma = (\tau_1 \mid \ldots \mid \tau_q)$ denote the combinatorial type of a cell of $\mathfrak{Rad}_g^\star(m,1)$ of bi-degree (p,q). Let $\tau := \tau_q \cdots \tau_1$. On the set of cycles of τ, the relation*

$$\alpha \sim \beta \text{ if there exists } \alpha \ni i \sim_{CL} j \in \beta \tag{3.25}$$

is an equivalence relation.

Proof. Being in the same cycle of τ defines an equivalence relation $\sim_{cyc}$ on $[p]$. Moreover, two elements $i, j \in [p]$ are in the same cycle of τ only if they are in the same cycle of some τ_r. Therefore, $\sim_{CL}$ is coarser than $\sim_{cyc}$. This finishes the proof. □

3.4. The bar compactification of the moduli space

In this section, we introduce our notation and recall some of the details of the construction of the bar compactification of a given moduli space. In Section 7.3, we use the bar compactification to detect a generator in the unstable homology of the moduli space $\mathfrak{M}_1^{\square}(2,1)$. For more details and proofs, we refer the reader to [Bö90a, Bö93a, Bö07, Mü96, Meh11, BH14].

For the remainder of this section, we fix $g \geq 0$, $n = 1$, $m \geq 1$ and $\star \in \{\bullet, \circ, \blacksquare, \square\}$. Consider the multi-simplicial set S defined as follows.

1. $S_{p,q} := \{(\omega_p; \sigma_0 : \ldots : \sigma_q; \sigma^\star) \mid \omega_p = \langle 0 \ \ldots \ p\rangle \in \mathfrak{S}_p^{\square}; \sigma_0, \ldots, \sigma_q \in \mathfrak{S}_p^{\square}; \sigma^\star \in \mathfrak{S}_p^\star\}$
2. $d'_j \colon S_{p,q} \to S_{p,q-1}$, $d'_j(\omega_p; \sigma_0 : \ldots : \sigma_j : \ldots \sigma_q; \sigma^\star) = (\omega_p; \sigma_0 : \ldots : \hat{\sigma}_j : \ldots : \sigma_q; \sigma^\star)$
3. $s'_j \colon S_{p,q-1} \to S_{p,q}$, $s'_j(\omega_p; \sigma_0 : \ldots : \sigma_j : \ldots \sigma_q; \sigma^\star) = (\omega_p; \sigma_0 : \ldots : \sigma_j : \sigma_j : \ldots : \sigma_q; \sigma^\star)$
4. $d''_i \colon S_{p,q} \to S_{p-1,q}$, $d''_i(\omega_p; \sigma_0 : \ldots : \sigma_q; \sigma^\star) = (D_i\omega_p; D_i\sigma_0 : \ldots : D_i\sigma_q; D_i\sigma^\star)$
5. $s''_i \colon S_{p-1,q} \to S_{p,q}$, $s''_i(\omega_p; \sigma_0 : \ldots : \sigma_q; \sigma^\star) = (S_i\omega_p; S_i\sigma_0 : \ldots : S_i\sigma_q; S_i\sigma^\star)$

The *norm*

$$N(\omega_p; \sigma_0 : \ldots : \sigma_q; \sigma^\star) := N(\sigma_q\sigma_{q-1}^{-1}) + \ldots + N(\sigma_1\sigma_0^{-1}) \tag{3.26}$$

induces a filtration on the multi-simplicial set S that is weakly decreasing along the faces and constant along the degeneracies. Furthermore, the *number of non-degenerate outgoing boundaries*

$$m(\omega_p; \sigma_0 : \ldots : \sigma_q; \sigma^\star) := \mathrm{ncyc}(\sigma^\star) \tag{3.27}$$

induces another filtration that is weakly decreasing along the horizontal faces and constant along the vertical faces and along all degeneracies.

Denote the Euler characteristic of the surface of genus g with $n+m$ boundaries by $h = 2g+m+n-2$. In order to distinguish multi-simplicially degenerated radial slit configurations from those giving a degenerate surface, a multi-simplex $\Sigma = (\omega_p; \sigma_0 : \ldots : \sigma_q; \sigma^\star)$ is called *proper* (with respect to g, n, m and the boundary conditions) if the following conditions are satisfied:

$$N(\Sigma) = h = 2g + m + n - 2 \tag{3.28}$$
$$m(\Sigma) = m \tag{3.29}$$
$$\sigma_0 = \omega_p \tag{3.30}$$
$$\sigma_q = \pi_{\square}^\star(\sigma^\star) \tag{3.31}$$

The *bar compactification* $Bar_g^\star(m,1)$ of the moduli space $\mathfrak{M}_g^\star(m,1)$ is the realization of the multi-simplicial subset of S generated by all proper multi-simplices.

Sending the open cells of $\mathfrak{Rad}_g^\star(m,1)$ to the corresponding multi-simplices in $Bar_g^\star(m,1)$ defines an embedding. By construction, all faces and degeneracies of a non-proper multi-simplex are also non-proper. Therefore $DBar_g^\star(m,1) := Bar_g(m,1) - \mathfrak{Rad}_g^\star(m,1)$ is a subcomplex of $Bar_g^\star(m,1)$.

The orientation system on the bar compactification is constant if the outgoing boundaries are enumerated. For the unenumerated cases, we refer the reader to [Mü96].

Carrying out the details carefully leads to the following theorem.

Theorem 3.4.1 (Bödigheimer). *Let $g \geq 0$, $n \geq 1$, $m \geq 1$ and $\star \in \{\bullet, \circ, \blacksquare, \square\}$.*

1. *The Hilbert uniformization $\mathfrak{M}_g^\star(m,n) \to \mathfrak{Rad}_g^\star(m,n)$ is a homeomorphism between the moduli space $\mathfrak{M}_g^\star(m,n)$ and its corresponding space of radial slit domains $\mathfrak{Rad}_g^\star(m,n)$.*

2. *The space of radial slit domains is a relative multi-simplicial manifold inside the bar compactification $Bar_g^\star(m,n)$, i.e., the space $Bar_g^\star(m,n)$ is the realization of a (finite) multi-simplicial set; $\mathfrak{Rad}_g^\star(m,n) \subset Bar_g^\star(m,n)$ is open and dense and the complement $DBar_g^\star(m,n) = Bar_g^\star(m,n) - \mathfrak{Rad}_g^\star(m,n)$ is a subcomplex of codimension one;*

3. *$H_*(\mathfrak{Rad}_g^\star(m,n); \mathbb{Z})$ is Poincaré dual to $H^*(Bar_g^\star(m,n), DBar_g^\star(m,n); \mathcal{O})$ for an orientation system $\mathcal{O}$. The orientation system is constant in the enumerated cases.*

The relation between the bar compactification and the bar resolution of varying symmetric groups is discussed in Appendix D. This relation leads to the Ehrenfried complex $\mathbb{E}_g^\star(m,n)$ which is chain homotopy equivalent to the (total complex of the) relative multi-simplicial complex$(Bar_g^\star(m,n), DBar_g^\star(m,n))$. Its number of cells is considerably smaller and it is used by several authors to compute the integral homology of the moduli spaces in question, provided the genus and number of boundary components is small, see Section 1.1.4, Section 7.3 and Appendix E.4.

3.5. The harmonic compactification of the moduli space

For the remainder of this section, we fix $g \geq 0$, $n = 1$, $m \geq 1$ and $\star \in \{\bullet, \circ, \blacksquare, \square\}$. Given a Riemann surface $F \in \mathfrak{M}_g^\star(m,1)$, the complete critical graph and the critical levels of the harmonic potential give a decomposition of F: The complement of the complete critical graph is a disjoint union of open rectangles (that correspond to the radial segments of the radial slit configuration associated to F). The open region between two consecutive critical levels is a disjoint union of cylinders. Collapsing some of these regions eventually gives surfaces with the following degeneracies:

1. Handles degenerate to a line segment;

2. Outgoing boundaries collide or degenerate to a point, called degenerate point;

3. Non-separating closed curves degenerate to a point, also called degenerate point;

4. Degenerate points merge.

We advice the reader to study the pretty drawings of these degeneracies in [Bö06]. By construction, each degenerate surface comes with a continuous real function that is harmonic on the smooth points and so the surface corresponds to a radial slit configuration. Adding these surfaces to the moduli space yields its *harmonic compactification* $\overline{\mathfrak{M}}_g^\star(m,n)$. Using the space of radial slit domains $\mathfrak{Rad}_g^\star(m,n)$ as a model for the moduli space $\mathfrak{M}_g^\star(m,n)$ we have the following theorem due to Bödigheimer.

Theorem 3.5.1 (Bödigheimer). *Let $g \geq 0$, $n \geq 1$, $m \geq 1$ and $\star \in \{\bullet, \circ, \blacksquare, \square\}$. The moduli space $\mathfrak{M}_g^\star(m,n)$ is an open and dense subspace of the harmonic compactification $\overline{\mathfrak{M}}_g^\star(m,n)$. The harmonic compactification is a finite cell complex such that*

1. *the points in* $\mathfrak{M}_g^\star(m,n)$ *with common combinatorial type form an open cell inside* $\overline{\mathfrak{M}}_g^\star(m,n)$ *and*

2. *the complement* $\overline{\mathfrak{M}}_g^\star(m,n) - \mathfrak{M}_g^\star(m,n)$ *is a subcomplex of* $\overline{\mathfrak{M}}_g^\star(m,n)$ *of codimension one.*

In the subsequent chapters, we study the strong deformation retract $\overline{U\mathfrak{M}}_g^\star(m,1) \subset \overline{\mathfrak{M}}_g^\star(m,1)$ that is defined below. Most importantly, the combinatorics of $\overline{U\mathfrak{M}}_g^\star(m,n)$ are more accessible and the space $\overline{U\mathfrak{M}}_g^\star(m,n)$ is cellularly homeomorphic to a space of Sullivan diagrams that is used in the study of string topology, see Section 1.3 and Chapter 4.

Recall that each Riemann surface $F \in \mathfrak{M}_g^\star(m,n)$ comes with a unique harmonic potential $u\colon F \to [0,1]$ and the number of critical values of the harmonic potential gives a stratification of the moduli space $\mathfrak{M}_g^\star(m,n)$. Equivalently, we have a stratification of the corresponding space of radial slit configurations $\mathfrak{Rad}_g^\star(m,n)$ by the number of critical levels of a radial slit configuration. The bottom-stratum is the subspace of all radial slit configurations on a single critical level. It is denoted by $U\mathfrak{M}_g^\star(m,n) \subset \mathfrak{M}_g^\star(m,n)$ respectively $U\mathfrak{Rad}_g^\star(m,n) \subset \mathfrak{Rad}_g^\star(m,n)$. By construction, the Hilbert uniformization restricts to these subspaces. Applying Bödigheimer's construction of the harmonic compactification to the subspace $U\mathfrak{M}_g^\star(m,n)$, we obtain a compactification which is canonically homeomorphic to the closure of $U\mathfrak{M}_g^\star(m,n)$ in the harmonic combination $\overline{\mathfrak{M}}_g^\star(m,n)$. Therefore, $\overline{U\mathfrak{M}}_g^\star(m,n) \subset \overline{\mathfrak{M}}_g^\star(m,n)$ is seen as closed subspace without ambiguity.

The subspace $\overline{U\mathfrak{M}}_g^\star(m,n) \subset \overline{\mathfrak{M}}_g^\star(m,n)$ is a strong deformation retract. Roughly speaking, the retraction $r\colon \overline{\mathfrak{M}}_g^\star(m,1) \to \overline{U\mathfrak{M}}_g^\star(m,1)$ is defined as follows. A point x in $\overline{\mathfrak{M}}_g^\star(m,n)$ is a (possibly degenerate) configuration of pairs of radial slits on one annulus $\mathbb{A}$. The endpoints of these slits define critical levels in $\mathbb{A}$ and the critical levels give $q \geq 1$ subannuli of $\mathbb{A}$ of increasing size. The contraction of all but one subannus gives a (possibly degenerate) configuration of pairs of slits $r(x)$ whose endpoints share a common radius, i.e., $r(x) \in \overline{U\mathfrak{M}}_g^\star(m,1)$. A complete proof is found in [EK14, Lemma 2.23].

By [EK14, Theorem 1.1] the harmonic compactification $\overline{U\mathfrak{M}}_g^\star(m,n)$ is cellularly homeomorphic to the space of Sullivan diagrams $\mathscr{SD}_g^\star(m,n)$. In the literature, a Sullivan diagram is defined as a certain equivalence class of decorated ribbon graphs, see [EK14, Section 3] or Section 4.1. In this thesis, we use our combinatorial description of Sullivan diagrams, introduced in [BE17], see also Section 4.3. The space of Sullivan diagrams is defined as the realization of a simplicial set made from these Sullivan diagrams, see [EK14, Section 4] or Section 4.2.

3.6. Radial slit configurations with normalized boundaries

In this section, we discuss the spaces of radial slit configurations with normalized boundaries $N\mathfrak{Rad}_g^\star(m,n) \subset \mathfrak{Rad}_g^\star(m,n)$. The study of their harmonic compactifications will lead to new insights on the (usual) harmonic compactification of the moduli spaces, see Chapter 5 and Chapter 6. Here, we define the restriction to the outgoing boundaries $\mathcal{P}ol\colon \mathfrak{Rad}_g^\star(m,1) \to \mathcal{P}ol^\star(m,1)$, see Definition 3.6.2, and we measure the lengths of the outgoing boundaries, see Definition 3.6.3. Then, by Definition 3.6.4, the spaces $N\mathfrak{Rad}_g^\star(m,1) \subset \mathfrak{Rad}_g^\star(m,1)$ consist of all radial slit configurations (or moduli) whose outgoing boundary curves all share the same length. Then, we will prove Theorem 3.6.8.

Proposition 3.6.1. *Let $m \geq 1$, $g \geq 0$ and $\star \in \{\bullet, \circ, \blacksquare, \square\}$. The bar compactification of $\mathfrak{Rad}^\star_g(m,1)$ is $Bar^\star_g(m,1)$. The projection to the last factor*

$$S_{p,q} = (\mathfrak{S}^\square([p]))^q \times \mathfrak{S}^\star([p]) \to \mathfrak{S}^\star([p]) \tag{3.32}$$

induces a map of bi-simplicial sets whose geometric realization restricts to the following diagram.

$$\begin{array}{ccc} \mathfrak{Rad}^\star_g(m,1) & \xrightarrow{\mathcal{P}ol} & \mathcal{P}ol^\star(m,1) \\ \big\downarrow & & \big\downarrow \\ Bar^\star_g(m,1) & \xrightarrow{\mathcal{P}ol} & \mathcal{P}ol^\star \end{array} \tag{3.33}$$

Proof. Regarding $\mathfrak{S}^\star([n])$ as a bi-simplicial set that is constant in one direction, the projection to the last factor $S_{p,q} = (\mathfrak{S}^\square([p]))^q \times \mathfrak{S}^\star([p]) \to \mathfrak{S}^\star([p])$ is clearly a map of bi-simplicial sets. Its geometric realization is the map $\mathcal{P}ol\colon Bar^\star_g(m,1) \to \mathcal{P}ol^\star$.

The space of radial slit configurations $\mathfrak{Rad}_g(m,1)$ is an open subspace in $Bar^\star_g(m,1)$ consisting of all open simplices $(\omega_p; \sigma_0, \ldots, \sigma_q; \sigma^\star)$ that are proper. In particular, the number of non-degenerate outgoing boundaries is

$$m(\omega_p; \sigma_0, \ldots, \sigma_q; \sigma^\star) = \mathrm{ncyc}(\sigma^\star) = m\,. \tag{3.34}$$

Therefore, by definition of $\mathcal{P}ol^\star(m,1)$, the map $\mathcal{P}ol\colon Bar^\star_g(m,1) \to \mathcal{P}ol^\star$ restricts to $\mathcal{P}ol\colon \mathfrak{Rad}^\star_g(m,1) \to \mathcal{P}ol^\star(m,1)$. □

Having the geometric meaning of the map $\mathcal{P}ol$ in mind, it is called the restriction to the outgoing boundaries.

Definition 3.6.2. The map $\mathcal{P}ol$ is the *restriction to the outgoing boundaries.*

Having the lengths of a polygon and the space of normalized polygons at hand, the definition of the length of the outgoing boundaries and the space of radial slit configurations with normalized outgoing boundaries is straightforward.

Definition 3.6.3. Let $n \geq 1$, $m \geq 1$ and $\star \in \{\bullet, \circ, \blacksquare, \square\}$. The *length of the boundaries* is the composition

$$l\colon \mathfrak{Rad}^\star_g(m,1) \xrightarrow{\mathcal{P}ol} \mathcal{P}ol^\star(m,1) \xrightarrow{l} \mathrm{int}(\Delta^{m-1}) \tag{3.35}$$

for $\star \in \{\bullet, \circ\}$ respectively

$$l\colon \mathfrak{Rad}^\star_g(m,1) \xrightarrow{\mathcal{P}ol} \mathcal{P}ol^\star(m,1) \xrightarrow{l} \mathrm{int}(\Delta^{m-1})/_{\mathfrak{S}([m-1])} \tag{3.36}$$

for $\star \in \{\blacksquare, \square\}$.

Definition 3.6.4. Let $m \geq 1$, $g \geq 0$ and $\star \in \{\bullet, \circ, \blacksquare, \square\}$. The *space of radial slit configurations of genus g with (un)parametrized (un)enumerated normalized boundaries* is the subspace

$$N\mathfrak{Rad}^\star_g(m,1) := l^{-1}(\tfrac{1}{m}, \ldots, \tfrac{1}{m}) \subset \mathfrak{Rad}^\star_g(m,1) \tag{3.37}$$

Remark 3.6.5. Our notation agrees with the definition in [Bö06, Section 9].

Restricting the maps $\mathcal{P}ol$ to the spaces of normalized polygons gives the following corollary.

Corollary 3.6.6. *The maps $\mathcal{P}ol$ restrict as follows.*

$$\begin{array}{ccc} N\mathfrak{Rad}_g^\star(m,1) & \xrightarrow{\mathcal{P}ol} & N\mathcal{P}ol^\star(m,1) \\ \downarrow & & \downarrow \\ \mathfrak{Rad}_g^\star(m,1) & \xrightarrow{\mathcal{P}ol} & \mathcal{P}ol^\star(m,1) \end{array} \tag{3.38}$$

Proposition 3.6.7. *Let $g \geq 0$ and $m \geq 1$. In the parametrized case, the restriction to the outgoing boundaries defines a map of operads $\mathcal{P}ol\colon \mathfrak{Rad}_g^\bullet(m,1) \to \mathcal{P}ol^\bullet(m,1)$.*

Proof. It is well known that glueing surfaces along their parametrized boundaries defines the surface operad $\sqcup_{g,m}\mathfrak{M}_g^\bullet(m,1)$. Recall that the space of parametrized and enumerated polygons is a space of local isometries from one parametrized circle to many parametrized circles. The composition of local isometries defines an operad structure on $\sqcup_m\mathcal{P}ol^\bullet(m,1)$. Using Bödigheimer's spaces of radial slit configurations, it is clear that glueing surfaces along boundaries agrees with composing the corresponding local isometries. □

Theorem 3.6.8. *Let $m \geq 1$, $g \geq 0$. Forgetting the parametrization of the outgoing boundaries defines an m-dimensional torus bundle $\pi_\circ^\bullet\colon \mathfrak{Rad}_g^\bullet(m,1) \to \mathfrak{Rad}_g^\circ(m,1)$ that is classified by the restriction to the outgoing boundaries:*

$$\begin{array}{ccc} \mathfrak{Rad}_g^\bullet(m,1) & \xrightarrow{\mathcal{P}ol} & \mathcal{P}ol^\bullet(m,1) \simeq EU(1)^m \\ \downarrow{\scriptstyle \pi_\circ^\bullet} & & \downarrow{\scriptstyle \pi_\circ^\bullet} \\ \mathfrak{Rad}_g^\circ(m,1) & \xrightarrow{\mathcal{P}ol} & \mathcal{P}ol^\circ(m,1) \simeq BU(1)^m \end{array} \tag{3.39}$$

Moreover, denoting the stabilization map by φ, it is $\mathcal{P}ol = \mathcal{P}ol \circ \varphi$.

Proof. By construction, it is clear that $\mathcal{P}ol\colon \mathfrak{Rad}_g^\bullet(m,1) \to \mathcal{P}ol^\bullet(m,1)$ is equivariant with respect to the torus action. Consequently, $\mathfrak{Rad}_g^\bullet(m,1) \to \mathfrak{Rad}_g^\circ(m,1)$ is classified by $\mathcal{P}ol\colon \mathfrak{Rad}_g^\circ(m,1) \to \mathcal{P}ol^\circ(m,1) \simeq BU(1)^m$.

Observe that $\sqcup_{g,m}\mathfrak{Rad}_g^\circ(m,1)$ resp. $\sqcup_m\mathcal{P}ol^\circ(m,1)$ is an algebra over $\sqcup_{g,m}\mathfrak{Rad}_g^\bullet(m,1)$ resp. $\sqcup_m\mathcal{P}ol^\bullet(m,1)$ and that the restriction to the outgoing boundaries is a map of algebras. The stabilization map is defined by glueing a surface of genus one with two parametrized boundary components to a given surface, i.e., it is defined as the operadic action of a single point $S \in \mathfrak{Rad}_1^\bullet(1,1)$ on $\sqcup_{g,m}\mathfrak{Rad}_g^\circ(m,1)$. Here, we regard S as the radial slit picture corresponding to the barycenter of the $(2,2)$-simplex with combinatorial type $(\omega_2; \langle 0\ 1\ 2\rangle : \langle 0\ 2\rangle\langle 1\rangle : \langle 0\ 1\ 2\rangle; \langle 0\ 1\ 2\rangle)$, shown in Figure 3.3. Observe that $\mathcal{P}ol(S) = (\frac{1}{3}, \frac{1}{3}, \frac{1}{3}) \in \langle 0\ 1\ 2\rangle \times \Delta^2 \subset \mathcal{P}ol^\bullet(1,1)$ represents the local isometry $\mathrm{id}\colon \mathbb{S}^1 \to \mathbb{S}^1$. Since $\mathcal{P}ol$ is a map of algebras, it follows that

$$\mathcal{P}ol(\varphi(F)) = \mathcal{P}ol(F \cup S) = \mathcal{P}ol(F) \circ \mathcal{P}ol(S) = \mathcal{P}ol(F) \circ \mathrm{id} = \mathcal{P}ol(F)\,. \tag{3.40}$$

□

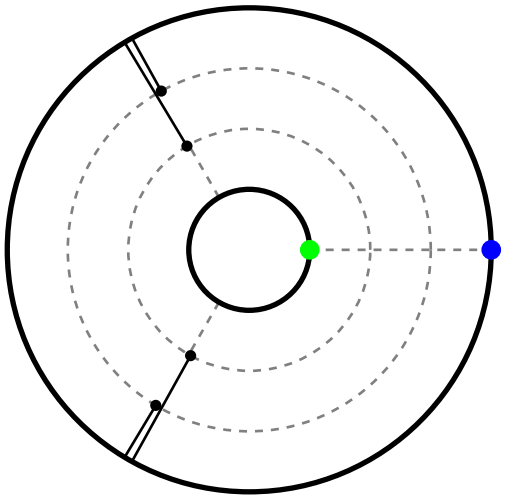

Figure 3.3.: The radial slit configuration S. The parametrization point of the incoming boundary is green and the parametrization on the outgoing boundary is blue.

Remark 3.6.9. Recall that, by Loojienga, there is a graded isomorphism of algebras over $H^*(\mathfrak{M}^\bullet_\infty(m,n);\mathbb{Z})$

$$H^*(\mathfrak{M}^\bullet_\infty(m,n);\mathbb{Z})[u_1,\dots,u_m] \cong H^*(\mathfrak{M}^\circ_\infty(m,n);\mathbb{Z}) \tag{3.41}$$

where u_i denote the characteristic classes of the m-dimensional torus bundle. Using the explicit cellular descriptions of $\mathfrak{Rad}$ and $\mathcal{P}ol$, the above Theorem allows explicit computations in low degrees.

4

On the spaces of Sullivan diagrams

In this chapter, we summarize the results of a joint-research project with Daniela Egas Santander that resulted in the article [BE17]. By [EK14], the spaces of Sullivan diagrams, denoted by $\mathscr{SD}_g^\star(m,n)$, have the same homotopy type as the harmonic compactifications, i.e., $\mathscr{SD}_g^\star(m,1) \simeq \overline{\mathfrak{M}}_g^\star(m,1)$. Usually, these spaces of Sullivan diagrams are defined as spaces of equivalence classes of combinatorial graphs, see Section 4.1 and Section 4.2. Inspired by the combinatorics of the Bödigheimer's spaces of radial slit configurations, we introduce an equivalent description of these spaces of Sullivan diagrams using bi-weighted partitions of permutations, see Section 4.3. With our notation of combinatorial Sullivan diagrams, we obtain results on homological stability and construct infinite families of non-trivial homology classes, see Section 4.4. Let us state the two most important results of [BE17] here.

Theorem 4.4.1 (B., Egas)**.** *Let $g \geq 0$, $m \geq 1$ and $\star \in \{\bullet, \blacksquare, \circ, \square\}$. The stabilization map $\varphi\colon \mathfrak{M}_g^\star(m,1) \to \mathfrak{M}_{g+1}^\star(m,1)$ extends to the harmonic compactifications, i.e., there is a map $\overline{\varphi}\colon \overline{\mathfrak{M}}_g^\star(m,1) \to \overline{\mathfrak{M}}_{g+1}^\star(m,1)$ making the following diagram commutative.*

$$\begin{array}{ccc} \mathfrak{M}_g^\star(m,1) & \xrightarrow{\varphi} & \mathfrak{M}_{g+1}^\star(m,1) \\ \downarrow & & \downarrow \\ \overline{\mathfrak{M}}_g^\star(m,1) & \xrightarrow{\overline{\varphi}} & \overline{\mathfrak{M}}_{g+1}^\star(m,1) \end{array}$$

The stabilization map $\overline{\varphi}$ induces an isomorphism in homology in the degrees $* \leq g+m-2$. Moreover, if $m > 2$, the stabilization map $\overline{\varphi}$ is $(g+m-2)$ connected.

Moreover, the harmonic compactification is highly connected with respect to m.

Theorem 4.4.2 (B., Egas)**.** *Let $g \geq 0$ and $m > 2$. Then*

$$\pi_*(\overline{\mathfrak{M}}_g^\bullet(m,1)) = 0 \qquad \text{and} \qquad \pi_*(\overline{\mathfrak{M}}_g^\circ(m,1)) = 0 \qquad \text{for} \qquad * \leq m-2$$

and

$$\pi_*(\overline{\mathfrak{M}}_g^\blacksquare(m,1)) = 0 \qquad \text{and} \qquad \pi_*(\overline{\mathfrak{M}}_g^\square(m,1)) = 0 \qquad \text{for} \qquad * \leq m'$$

where m' is the largest even number strictly smaller than m.

In Chapter 6, we will show that the harmonic compactification $\overline{\mathfrak{M}}_g^\bullet(m,1)$ is also highly connected with respect to g, see Theorem 6.1.

4.1. Ribbon graphs and Sullivan diagrams

For the convenience of the reader, we recall the notions of combinatorial graphs, ribbon graphs, their boundary cycles, Sullivan diagrams and their thickenings in this section.

Definition 4.1.1. A *combinatorial graph* G is a tuple $G = (V, H, s, i)$, with a finite set of vertices V, a finite set of *half-edges* H, a source map $s\colon H \to V$ and an involution $i\colon H \to H$. The source map s ties each half-edge to its source vertex and the involution i attaches half-edges together. The *valence* of a vertex $v \in V$ is the cardinality of the set $s^{-1}(v)$ and we denote it by $|v|$. A *leaf* of a graph is a fixed point of i. An *edge* of the graph is an orbit of i. Note that leaves are also edges. We call both leaves and edges connected to a vertex of valence one *outer-edges* all other edges are called *inner-edges*. See Figure 4.2.

Definition 4.1.2. A *ribbon graph* $\Gamma = (G, \sigma)$ is a combinatorial graph together with a cyclic orderings σ_v of the half edges incident at each vertex v. The cyclic orderings σ_v define a permutation $\sigma\colon H \to H, \sigma(h) := \sigma_{s(h)}(h)$ which satisfies $s\sigma = s$. This permutation is called the *ribbon structure* of the graph. Figure 4.1 shows some examples of ribbon graphs.

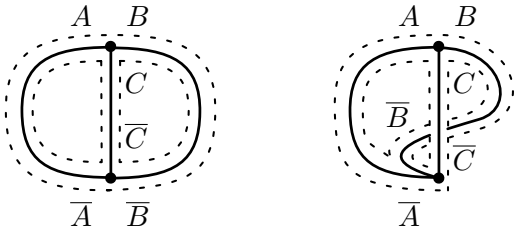

Figure 4.1.: The thick lines show two different ribbon graphs with the same underlying combinatorial graph. The ribbon structure is given by the clockwise orientation of the plane. The dotted lines indicate the boundary cycles. We make this graphical description precise using the names of the half edges indicated in the picture. (a) ribbon structure: $\sigma = (ABC)(\overline{ACB})$. Boundary cycles: $\omega = (A\overline{C})(B\overline{A})(C\overline{B})$. (b) ribbon structure: $\sigma = (ABC)(\overline{ABC})$. Boundary cycles: $\omega = (A\overline{B}C\overline{A}B\overline{C})$.

Definition 4.1.3. The *boundary cycles* of a ribbon graph $\Gamma = (G, \sigma)$ are the orbits of the permutation $\omega := \sigma \circ i\colon H \to H$. Let $c = (h_1, \ldots, h_k)$ be a boundary cycle of Γ. The *boundary cycle sub-graph* of c the sub-graph of Γ uniquely defined by the set of half-edges $\{h_1, i(h_1), h_2, i(h_2), \ldots \mid h_j \neq i(h_j)\}$. See Figure 4.1 for an example. When clear from the context, we will refer to a boundary cycle sub-graph simply as boundary cycle.

Definition 4.1.4 (Surface with decorations)**.** Given a ribbon graph $\Gamma = (V, H, s, i, \sigma)$, we construct a surface with marked points at the boundary by "fattening" the ribbon graph. More precisely, we start with a collection of oriented disks for every vertex

$$\{D_v \mid v \in V\} \tag{4.1}$$

and a collection of oriented strips for every half edge

$$\{I_h := [0, \tfrac{1}{2}] \times [-1, 1] \mid h \in H\}\,. \tag{4.2}$$

Preserving the orientations of the disks and the strips, we glue the boundary $\{0\} \times [-1, 1]$ of every strip I_h to the disk $D_{s(h)}$ in the cyclic order given by the ribbon structure of Γ. For each edge which is not a leaf, say $e = \{h, \overline{h}\}$, we glue $\{\frac{1}{2}\} \times [-1, 1]$ of I_h to $\{\frac{1}{2}\} \times [-1, 1]$ of $I_{\overline{h}}$ via $-\mathrm{id}$ in the second factor (see Figure 4.2 (b)).

We end our construction by collapsing each boundary component, which is not connected to a leaf or to a vertex of valence one, to a puncture. This procedure gives a surface with boundary, where each boundary component is connected to at least one leaf or one vertex of valence one. We interpret these as marked points on the boundary (see Figure 4.2 (c)).

We call this surface together with the combinatorial data of the marked points at the boundary a *surface with decorations* and denote it by S_Γ. The *topological type* of a surface with decorations S_Γ is its genus, number of boundary components and punctures together with the cyclic ordering of the marked points at the boundary.

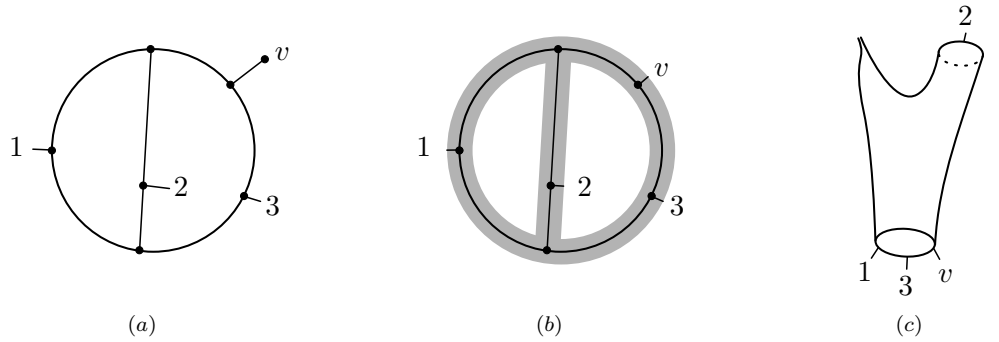

Figure 4.2.: The picture shows (a) a ribbon graph with 4 outer-edges and 7 inner-edges; (b) the surface obtained from the fattening procedure; (c) the surface with decorations obtained from (b) by labeling points at the boundary and collapsing unmarked boundary components to a puncture.

Remark 4.1.5. The topological type of S_Γ is completely determined by Γ. Moreover, given an inner-edge e of Γ which is not a loop, collapsing e gives a homotopy equivalence $S_\Gamma \xhookrightarrow{\simeq} S_{\Gamma/e}$ and does not change the number of boundary cycles or their decorations. Thus, the surfaces S_Γ and $S_{\Gamma/e}$ have the same topological type.

Remark 4.1.6. Usually, spaces of Sullivan diagrams are defined by geometric realization of certain semi-multi-simplicial sets. However, we will define the spaces of Sullivan diagrams as geometric realizations of certain multi-simplicial sets. In order to take simplicially degenerate Sullivan diagrams into account, we need to change the usual definition of "admissible fat graphs" by allowing vertices of valence two.

Definition 4.1.7. An *n-admissible ribbon graph* Γ consists of:

1. an (isomorphism class) of connected ribbon graphs such that all vertices have valence at least 2
2. an integer $k \geq n$ and an enumeration of a subset of the set of leaves by $\{1, 2, \ldots, k\}$

such that:

1. each of the first n leaves $L_1, \ldots, L_n$ is the only leaf in its boundary cycle c_i for $1 \leq i \leq n$,

2. their corresponding boundary cycle sub-graphs

$$\Gamma_{c_1}, \Gamma_{c_2}, \ldots, \Gamma_{c_n} \tag{4.3}$$

   are disjointly embedded circles in Γ.

We will refer to the first n leaves as *admissible leaves* and to their corresponding boundary cycles as *admissible cycles*. Figure 4.2 (a) shows a ribbon graph that is not 1-admissible because the leaf with number 1 is not the only leaf in its boundary cycle. Figure 4.3 shows an example of a 3-admissible ribbon graph.

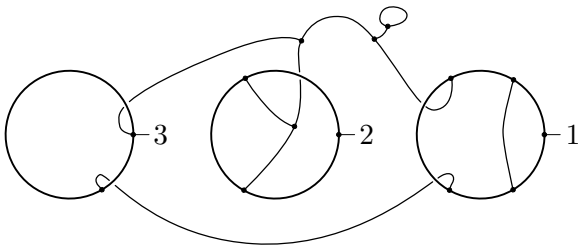

Figure 4.3.: An example of a 3-admissible ribbon graph.

Definition 4.1.8. Let Γ_1 and Γ_2 be n-admissible ribbon graphs. We say $\Gamma_1 \sim_{SD} \Gamma_2$ if Γ_1 and Γ_2 are connected by a zigzag of edge collapses where we only collapse inner edges that do not belong to the admissible cycles and which are not loops. Equivalently, we have $\Gamma_1 \sim_{SD} \Gamma_2$ if Γ_2 can be obtained from Γ_1 by sliding vertices along edges that do not belong to the admissible cycles. Figure 4.4 shows some examples of equivalent 1-admissible ribbon graphs.

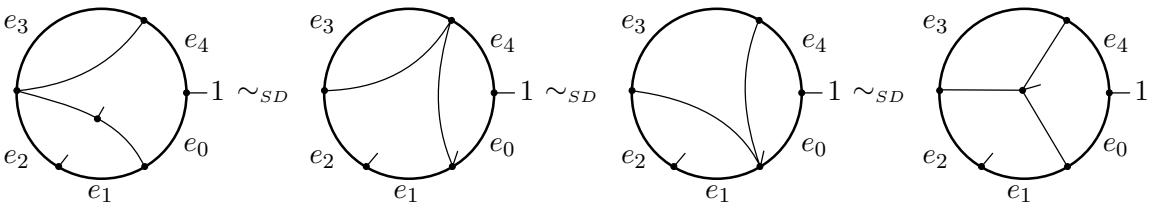

Figure 4.4.: Four equivalent 1-admissible ribbon graphs. Since there is only one admissible cycle, instead of labeling edges by e_j^1 (as described in Definition 4.2.1) they are just labeled by e_j.

Remark 4.1.9. Note that $\sim_{SD}$ is an equivalence relation.

Definition 4.1.10. An *n-Sullivan diagram* Σ is an equivalence class of n-admissible ribbon graphs under the equivalence relation $\sim_{SD}$.

4.2. The space of Sullivan diagrams

In this section, we define the space of n-Sullivan diagrams, denoted n-$\mathscr{SD}$, as the geometric realization of an n-fold multi-simplicial set, see Definition 4.2.1 and Definition 4.2.3. The space of Sullivan diagrams is the disjoint $\mathscr{SD} = \sqcup_n n$-$\mathscr{SD}$ and we define the chain complex of Sullivan diagrams as the corresponding cellular chain complex, see Definition 4.2.6. Our definition of the chain complex of Sullivan diagrams is equivalent to the one given by Tradler and Zeinalian in [TZ06] and by Wahl and Westerland in [WW16]. In [BE17] and in this thesis, we concentrate our study on the four families of spaces of Sullivan diagrams introduced in Section 4.2.1.

Definition 4.2.1. The *set of n-Sullivan diagrams* is

$$n\text{-}\mathfrak{SD} = \{\Sigma \mid \Sigma \text{ is an } n\text{-Sullivan diagram}\}/_{isomorphism}\,. \tag{4.4}$$

The *multi-degree of an n-Sullivan diagram* $\Sigma \in n$-$\mathfrak{SD}$ is

$$\deg(\Sigma) = (|E_1| - 1, |E_2| - 1, \ldots, |E_n| - 1) \tag{4.5}$$

where E_i is the set of inner-edges that belong to the i-th admissible cycle. The ribbon structure together with the admissible leaves give a natural ordering of the edges that belong to each admissible cycle. Let $e^i_0, e^i_1, \ldots, e^i_{|E_i|-1}$ denote the edges on the i-th admissible cycle in this induced order, see Figure 4.4 for an example.

For $1 \leq i \leq n$, $0 \leq j < |E_i|$ and $1 < |E_i|$, the *faces* of the Sullivan diagram Σ are given by

$$d^i_j(\Sigma) := \Sigma/e^i_j \tag{4.6}$$

where Σ/e^i_j is the Sullivan diagram obtained by collapsing the edge e^i_j. Note that Σ/e^i_j is well defined since we are only collapsing inner-edges on the admissible cycles and if $|E_i| = 1$ we do not collapse any edges on the i-th admissible cycle.

The *degeneracies* s^i_j of the Sullivan diagram Σ are given by splitting the edge e^i_j into two edges that meet at a vertex of valence two afterwards.

Remark 4.2.2. The maps d^i_j and s^i_j satisfy the multi-simplicial identities. Therefore, n-$\mathfrak{SD}$ is regarded as n-fold multi-simplicial set.

Definition 4.2.3. The *space of n-Sullivan diagrams*, denoted by n-$\mathscr{SD}$, is the geometric realization of the n-fold multi-simplicial set n-$\mathfrak{SD}$. In particular, the space of 1-Sullivan diagrams has a simplicial structure.

Definition 4.2.4. The *space of Sullivan diagrams* $\mathscr{SD}$ is

$$\mathscr{SD} := \coprod_n n\text{-}\mathscr{SD}\,. \tag{4.7}$$

Definition 4.2.5. The *chain complex of n-Sullivan diagrams*, denoted n-$\mathcal{SD}$, is the cellular complex of the space of n-Sullivan diagrams n-$\mathscr{SD}$. As a graded $\mathbb{Z}$-module it is freely generated by all (multi-simplicially non-degenerate) n-Sullivan diagrams. The total degree of an n-Sullivan diagram Σ is

$$\deg(\Sigma) := |E_a| - n \tag{4.8}$$

where E_a is the set of edges that belong to the admissible cycles. The differential of a Sullivan diagram Σ of multi-degree $(k_1, \dots, k_n)$ is

$$d(\Sigma) := \sum_{i=1}^{n} (-1)^{k_1+\dots+k_{i-1}} \sum_{j=0}^{k_i} (-1)^j d_j^i(\Sigma)\,. \tag{4.9}$$

Figure 4.5 gives and example of the differential.

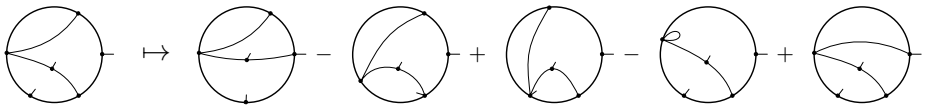

Figure 4.5.: The differential of a 1-Sullivan diagram of degree 4. The labeling of the first leaf is as in Figure 4.4. Here, it is omitted to improve the readability.

Definition 4.2.6. The *chain complex of Sullivan diagrams*, denoted $\mathcal{SD}$, is cellular complex of $\mathscr{S}\mathscr{D}$

$$\mathcal{SD} = \bigoplus_{n\geq 1} n\text{-}\mathcal{SD} \tag{4.10}$$

Remark 4.2.7. Given a n-Sullivan diagram Σ, observe that Σ is multi-simplicially degenerate if and only if one of the vertices on the admissible cycle has valence two. This implies that all faces of a multi-simplicially non-degenerate n-Sullivan diagram are also multi-simplicially non-degenerate.

In other words, the collection of all multi-simplicially non-degenerate n-Sullivan diagrams forms a semi-multi-simplicial set. Its realization is homeomorphic to n-$\mathscr{S}\mathscr{D}$.

Notation 4.2.8. By Remark 4.2.7 the faces of a multi-simplicially non-degenerate Sullivan diagram are multi-simplicially non-degenerate. From now on, a *Sullivan diagram* refers always to a Sullivan diagram that is multi-simplicially non-degenerate.

Remark 4.2.9. Recall that an n-Sullivan diagram Σ can be fattened, as in Remark 4.1.5, to give a topological type of a surface with decorations denoted by S_Σ. We call this *the topological type* of Σ. The surface with decorations S_Σ obtained by this fattening procedure must have either n boundary components and at least one puncture or at least $n+1$ boundary components. Moreover, n of its boundary components must have exactly one marked point and these parametrization points are enumerated by the set $\{1, 2, \dots, n\}$.

Since the face maps collapse an inner-edge which is not a loop, Σ and $d_j^i(\Sigma)$ have the same topological type for any i and j. Furthermore, any two n-Sullivan diagrams of the same topological type are connected by a zigzag of face maps. Therefore, the space of n-Sullivan diagrams splits into connected components given by the topological type of their diagrams. We denote these components by n-$\mathscr{S}\mathscr{D}(S)$, i.e.,

$$n\text{-}\mathscr{S}\mathscr{D} = \coprod_{S} n\text{-}\mathscr{S}\mathscr{D}(S) \tag{4.11}$$

where the disjoint union is taken over all topological types of surfaces with decorations that can be obtained by the fattening procedure.

We interpret the barycentric coordinates of a point in the space of a Sullivan diagrams as the lengths of the edges in the admissible cycles. Then one can intuitively think of $\mathscr{SD}$ as a space of metric admissible graphs were the topology is given by the lengths of the edges in the admissible cycles while all other edges are of length zero. We use this to motivate the following definition.

Definition 4.2.10. We call a boundary cycle of a Sullivan diagram *non-degenerate* if its boundary cycle sub-graph has at least one inner-edge which belongs to an admissible cycle and *degenerate* otherwise. In other words a boundary cycle is non-degenerate if it has at least one edge of "positive length", see also Definition 5.1.5. We call a Sullivan diagram *non-degenerate* if all its boundary cycles are non-degenerate.

Remark 4.2.11. Let $S_g^\bullet(m,n)$ be an oriented surface of genus g with $n+m$ boundary components each of which has exactly one marked point enumerated by the set $\{1,2,\dots,n+m\}$. Let $S_g^\circ(m,n)$ be the oriented surface obtained by collapsing each of the last m boundary components to a marked point. Then we have a central extension of the mapping class group $\Gamma_g^\bullet(m,n)$ by $\mathbb{Z}^m$

$$\mathbb{Z}^m \to \Gamma_g^\bullet(m,n) \to \Gamma_g^\circ(m,n) \tag{4.12}$$

which induces a fibration sequence of spaces

$$B\mathbb{Z}^m \to \mathfrak{M}_g^\bullet(m,n) \to \mathfrak{M}_g^\circ(m,n) \tag{4.13}$$

Similarly, we have a forgetful map

$$\pi\colon n\text{-}\mathscr{SD}(S_g^\bullet(m,n)) \to n\text{-}\mathscr{SD}(S_g^\circ(m,n)) \tag{4.14}$$

given by forgetting the parametrization of the last m boundaries, i.e., by forgetting the last m leaves of a Sullivan diagram in $n\text{-}\mathscr{SD}(S_g^\bullet(m,n))$. However, this map is not a fibration, see [BE17, Remark 2.13].

Remark 4.2.12. Let S be a connected surface with at least one boundary component. If S is not homeomorphic to the disk with one puncture it will follow that

$$\chi(n\text{-}\mathscr{SD}(S)) = 0\,. \tag{4.15}$$

In particular, $n\text{-}\mathscr{SD}(S)$ is not contractible. Otherwise, if S is homeomorphic to the disk with one puncture, then $n=1$ and

$$1\text{-}\mathscr{SD}(S) = *\,. \tag{4.16}$$

For a proof of this fact, see [BE17, Proposition 2.16].

4.2.1. The space of Sullivan diagrams with one incoming boundary curve

In what follows, we will study the homotopy type of the following four families of spaces of 1-Sullivan diagrams, that is, we study four families of spaces of Sullivan diagrams with one "incoming boundary curve". We emphasize that, what we call "incoming boundary curves" here is called "outgoing boundaries" in [BE17]. We choose this notation to fit better into the context of Bödigheimer's spaces of radial slit configurations.

Definition 4.2.13. Let S_Σ be the topological type of the surface with decorations obtained by thickening a Sullivan diagram Σ, see Definition 4.1.4. Let $g(\Sigma)$, $b(\Sigma)$ and $m(\Sigma)$ denote the genus, number of boundary components and number of punctures of S_Σ respectively. We define the following spaces.

The *space of 1-Sullivan diagrams with parametrized and enumerated outgoing boundaries* is the geometric realization of the simplicial set

$$\mathscr{SD}_g^\bullet(m,1) := \left| \left\{ \Sigma \;\middle|\; \begin{array}{l} \Sigma \text{ has exactly one leaf per boundary cycle;} \\ \text{all leaves are enumerated;} \\ g(\Sigma) = g, b(\Sigma) = m+1, m(\Sigma) = 0. \end{array} \right\} \right| \tag{4.17}$$

The *space of 1-Sullivan diagrams with unparametrized and enumerated outgoing boundaries* is the geometric realization of the simplicial set

$$\mathscr{SD}_g^\circ(m,1) := \left| \left\{ \Sigma \;\middle|\; \begin{array}{l} \text{the only leaf of } \Sigma \text{ is the admissible leaf;} \\ g(\Sigma) = g, b(\Sigma) = 1, m(\Sigma) = m; \\ \text{all boundary cycles are enumerated.} \end{array} \right\} \right| \tag{4.18}$$

The *space of 1-Sullivan diagrams with parametrized and unenumerated outgoing boundaries* is the geometric realization of the simplicial set

$$\mathscr{SD}_g^\blacksquare(m,1) := \left| \left\{ \Sigma \;\middle|\; \begin{array}{l} \Sigma \text{ has exactly one leaf per boundary cycle;} \\ \text{only the admissible leaf is enumerated;} \\ g(\Sigma) = g, b(\Sigma) = m+1, m(\Sigma) = 0. \end{array} \right\} \right| \tag{4.19}$$

The *space of 1-Sullivan diagrams with unparametrized and unenumerated outgoing boundaries* is the geometric realization of the simplicial set

$$\mathscr{SD}_g^\square(m,1) := \left| \left\{ \Sigma \;\middle|\; \begin{array}{l} \text{the only leaf of } \Sigma \text{ is the admissible leaf;} \\ g(\Sigma) = g, b(\Sigma) = 1, m(\Sigma) = m. \end{array} \right\} \right| \tag{4.20}$$

The spaces $\mathscr{SD}_g^\bullet(m,1)$, $\mathscr{SD}_g^\blacksquare(m,1)$ and $\mathscr{SD}_g^\square(m,1)$ are connected components of $\mathscr{SD}$. However, the space $\mathscr{SD}_g^\circ(m,1)$ is not a subspace of $\mathscr{SD}$ as we have defined it, since we only enumerate boundary cycles which are connected to a leaf and use the leaf to do so. Nevertheless, one could extended the definition of a ribbon graph to include this case by including additional data. Namely enumerating the boundary cycles of the ribbon graph and therefore of the Sullivan diagram. The topological type of such Sullivan diagrams would give surfaces with enumerated punctures.

Notation 4.2.14. From now onward, we will remove n from the notation and we will refer only to "the space of Sullivan diagrams" or a "Sullivan diagram" and it will be understood that $n = 1$ unless stated otherwise. By abuse of notation we write $\mathscr{SD}$ for the space of 1-Sullivan diagrams. Moreover, we exclude the enumeration of the admissible leaf in our drawings as it is the unique leaf on the admissible circle that "points outwards", see e.g. Figure 4.4 and Figure 4.5.

4.3. A combinatorial description for Sullivan diagrams

By Definition 4.1.10, the cells of the space of 1-Sullivan diagrams are given by equivalence classes of ribbon graphs. Here, we give a combinatorial description of the cells of $\mathscr{SD}_g^{\bullet}(m,1)$ and $\mathscr{SD}_g^{\circ}(m,1)$, see Definition 4.3.1, Definition 4.3.2 and Proposition 4.3.5. For combinatorial representatives of the cells of the spaces $\mathscr{SD}_g^{\blacksquare}(m,1)$ and $\mathscr{SD}_g^{\square}(m,1)$ see [BE17, Section 3]. In Section 4.3.1, we discuss the faces and degeneracies of our combinatorial representatives geometrically and algebraically. Using our combinatorial description, we describe the inclusion of the moduli space into its harmonic compactification followed by the homotopy equivalence to the space of Sullivan diagrams in Section 4.3.2. The stabilization map is described in Section 4.3.3.

The informal idea is that any Sullivan diagram is uniquely described by attaching onto a "ground circle" topological types of surfaces with decorations. These surfaces are determined by their genus, number of punctures, boundary components and the combinatorial data of marked points at the boundary. Inspired by [Bö90a, Bö90b, Bö06], we describe the combinatorial data of the marked points at the boundary and the way in which these surfaces are attached to the ground circle by permutations. Thereafter, we encode the genus and number of punctures as weights. Therefore, we give a presentation of Sullivan diagrams in terms of bi-weighted permutations subject to certain conditions. There are similarities to the the concept of stable graphs of [Kon92] and [Loo95].

For better readability we give separately the definition of combinatorial diagrams for the two cases in Definitions 4.3.1 and 4.3.2. In Section 4.3.2, we make the relation between the combinatorics of Bödigheimer's model for the moduli spaces and our description of 1-Sullivan diagrams explicit.

Definition 4.3.1. Let $n \geq 0, k \geq 1$ and let $L = \{L_1, \ldots, L_m\}$ be a non-empty finite set. A *parametrized enumerated combinatorial* 1*-Sullivan diagram* Σ of degree n with leaves L is a pair $(\lambda, \{S_1, \ldots, S_k\})$ consisting of the following data:

(1) the *ribbon structure* $\lambda \in \mathfrak{S}([n] \sqcup L)$,

(2) the set of cycles of λ is denoted by $\Lambda := \mathrm{cyc}(\lambda)$,

(3) the *outgoing boundary cycles* given by the permutation $\rho = \lambda^{-1}\langle 0\ 1\ \ldots\ n\rangle$,

(4) the *ghost surfaces* given by triples $S_i = (g_i, 0, A_i)$ where $A_i \subset \Lambda$ and $g_i \in \mathbb{N}$.

Subject to the following conditions:

(i) The A_i's form a partition of Λ, i.e., $A_i \cap A_j = \emptyset$ if $i \neq j$ and $\cup_i A_i = \Lambda$.

(ii) For each i the set A_i contains at least one cycle with an element in $[n]$.

(iii) Each cycle of ρ permutes exactly one leaf non-trivially or it is a fixed point $\langle L_i\rangle$ with $L_i \in L$.

We denote by $C_J^{\bullet}(n)$, the *set of parametrized enumerated combinatorial 1-Sullivan diagrams of degree n with leaves L.*

Definition 4.3.2. Let $n \geq 0$ and $k \geq 1$. An *unparametrized enumerated combinatorial* 1*-Sullivan diagram* Σ of degree n is a quadruple $(\lambda, \{S_1, \ldots, S_k\}, \beta_1, \beta_2)$ consisting of:

(1) the *ribbon structure* $\lambda \in \mathfrak{S}([n])$,

(2) the set of cycles of λ is denoted by $\Lambda := \mathrm{cyc}(\lambda)$,

(3) the *outgoing boundary cycles* given by the permutation $\rho = \lambda^{-1}\langle 0\ 1\ \ldots\ n\rangle$,

(4) the *ghost surfaces* given by triples $S_i = (g_i, m_i, A_i)$ where $A_i \subset \Lambda$ and $g_i, m_i \in \mathbb{N}$,

(5) the *enumerating data* given by injections

$$\beta_1 \colon \mathrm{cyc}(\rho) \hookrightarrow \{1, 2, \ldots, m\} \tag{4.21}$$

$$\beta_2 \colon \{1, 2, \ldots, m\} - \mathrm{im}(\beta_1) \hookrightarrow \{S_1, S_2, \ldots, S_k\}\,. \tag{4.22}$$

Subject to the following conditions:

(i) The A_i's form a partition of Λ, i.e., $A_i \cap A_j = \emptyset$ if $i \neq j$ and $\cup_i A_i = \Lambda$.

(iv) For every $1 \leq i \leq k$ it holds that $|\beta_2^{-1}(i)| = m_i$.

We denote by $C^\circ(n)$ the *set of unparametrized enumerated combinatorial 1-Sullivan diagrams of degree n*.

Remark 4.3.3. The names *ribbon structure* and *outgoing boundary cycles* come from the geometric interpretation of this description. Recall that each cycle λ_k of λ is contained in exactly ghost surface $S_i = (g_i, m_i, A_i)$ and we think of every such cycle as a boundary component of S_i that is attached to the ground circle, see Figure 4.6 for an example.

In the parametrized case, $\Sigma \in \mathscr{SD}_g^\bullet(m, 1)$, the *outgoing boundary cycles* ρ are in bijection with the cycles of Σ which are not the admissible cycle and which have either at least one edge on the admissible cycle or consist of a single leaf $\rho(L_i) = L_i$. Note that a Sullivan diagram $\Sigma \in \mathscr{SD}_g^\bullet(m, 1)$ is non-degenerate if and only if ρ has m cycles none of which consist of a single leave, see Definition 4.2.10 and Figure 4.6.

In the unparametrized case, $\Sigma \in \mathscr{SD}_g^\circ(m, 1)$, the *outgoing boundary cycles* ρ are in bijection with the cycles of Σ which are not the admissible cycle and have at least one edge on the admissible cycle. Note that a Sullivan diagram $\Sigma \in \mathscr{SD}_g^\circ(m, 1)$ is non-degenerate if and only if ρ has m cycles, see Definition 4.2.10

The maps β_1 and β_2 enumerate the non-degenerate outgoing boundaries and the degenerate outgoing boundaries respectively. In the case of $\mathscr{SD}_g^\bullet(m, 1)$, the role of β_1 resp. β_2, enumerating the non-degenerate resp. degenerate outgoing boundaries, is implicit in λ and the A_i's.

Notation 4.3.4. We refer by a *combinatorial 1-Sullivan diagram* to any of the two versions of given in Definitions 4.3.1 and 4.3.2. Abusing notation, we denote any combinatorial 1-Sullivan by a tuple $\Sigma = (\lambda, S_1, \ldots, S_k)$ and omit writing the enumerating data unless it is specifically necessary.

Consider two combinatorial 1-Sullivan diagrams $(\lambda, S_1, \ldots, S_k)$ and $(\lambda', S_1', \ldots, S_{k'}')$ of degree n. In the parametrized enumerated case, the two Sullivan diagrams are equal if and only if $\lambda = \lambda'$, $k = k'$ and the ghost surfaces agree up to reordering. In the unparametrized enumerated case, the two Sullivan diagrams are equal if and only if $\lambda = \lambda'$, $k = k'$, the ghost surfaces agree up to reordering and the enumeration data agree.

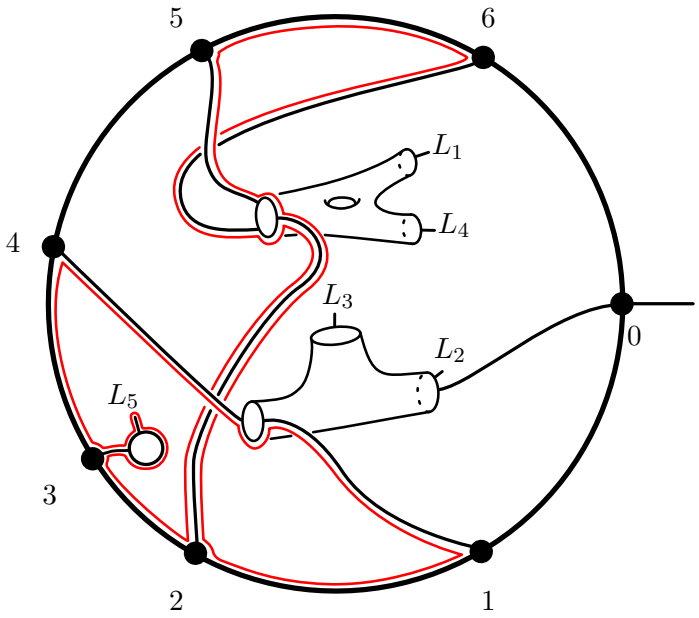

Figure 4.6.: We interpret a combinatorial 1-Sullivan diagram $\Sigma = (\lambda, S_1, S_2, S_3)$ as a cell of $\mathscr{SD}_g^\bullet(m,1)$. The ribbon structure is $\lambda = \langle 0\ L_2\rangle\langle 1\ 4\rangle\langle 2\ 6\ 5\rangle\langle 3\ L_5\rangle$ with fixed points L_1, L_3, L_4 and $\rho = \langle 0\ 4\ 6\ L_2\rangle\langle 1\ 5\ 2\ L_5\ 3\rangle$ with the same fixed points. The ghost surfaces are $S_1 = (0,0,\{\langle 0\ L_2\rangle, \langle L_3\rangle, \langle 1\ 4\rangle\})$, $S_2 = (1,0,\{\langle 2\ 6\ 5\rangle, \langle L_1\rangle, \langle L_4\rangle\})$ and $S_3 = (0,0,\{\langle 3\ L_5\rangle\})$. Consequently, we consider a surface of genus 0, no punctures and three boundary components for S_1, a surface of genus 1, no punctures and three boundary components for S_2 and a surface of genus 0, no punctures and one boundary component for S_3. The distribution of the leaves and the gluing of the surfaces to the ground cycle is prescribed by the ribbon structure λ. Moreover, we highlight one of the non-degenerate outgoing boundary curves.

Regarding a combinatorial 1-Sullivan diagram as a ground circle to which the topological types of decorated surfaces are attached and identifying a 1-Sullivan diagram (which is defined as equivalence class of graphs) with its fattening, we obtain the following Proposition.

Proposition 4.3.5 ([BE17, Proposition 3.8])**.** *Let $n \geq 0$, $m \geq 1$ and $L = \{L_1, \dots, L_m\}$. There exist bijections.*

$$C_L^\bullet(n) \xleftrightarrow{1:1} \{n\text{-simplices of } \coprod_g \mathscr{SD}_g^\bullet(m,1)\}$$
$$C^\circ(n) \xleftrightarrow{1:1} \{n\text{-simplices of } \coprod_{g,r} \mathscr{SD}_g^\circ(r,1)\}$$

Before discussing the faces and degeneracies in terms of the combinatorial representatives in Section 4.3.1, we want to make two remarks.

Remark 4.3.6 (Simplicial degenerate representatives). By Remark 4.2.7 and Notation 4.2.8, we discard simplicially degenerate Sullivan diagrams from our notation. Consequently, we will discard simplicially degenerate combinatorial 1-Sullivan diagrams from our notation. Under the bijection of Proposition 4.3.5, a combinatorial 1-Sullivan diagram $\Sigma = (\lambda, S_1, \dots, S_k)$ corresponds to a simplicially degenerate Sullivan diagram if and only if one

of its decorated surfaces is of the form $S_i = (0, 0, \langle r \rangle)$ with $r \neq 0$, c.f. [BE17, Section 3] and Discussion 4.3.9.

Remark 4.3.7 (Top degree and Euler characteristic). Consider a (simplicially non-degenerate) Sullivan diagram $\Sigma \in \mathcal{SD}_g^\circ(m, 1)$ and let S_Σ be the surface with decorations obtained by fattening it as in Definition 4.1.4. If Σ is of top degree, then all ghost surfaces S_i are all disks with exactly one or two attaching points at the boundary and no punctures or degenerate boundary. In other words, Σ is a graph given by a system of chords attached on the ground circle where the vertex attached to the admissible leaf is of valence three. See Figure 4.7 (b). Now, let c be the number of chords of Σ. The Euler characteristic of

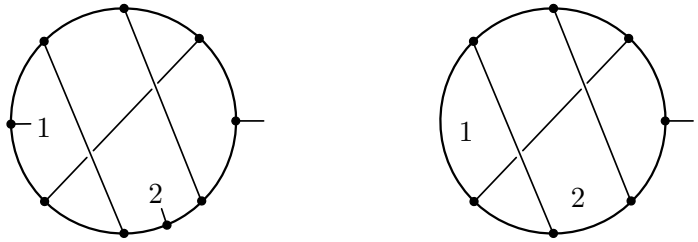

(a) (b)

Figure 4.7.: Two examples of top dimensional cells in $\mathscr{SD}_g^\bullet(2, 1)$ and $\mathscr{SD}_g^\circ(2, 1)$. The parametrized enumerated case is seen in (a) and the unparametrized enumerated case is seen in (b).

the circle is 0 and each time one adds a chord to the circle the Euler characteristic goes down by one. Therefore, we get

$$-c = \chi(\Sigma) = \chi(S_\Sigma)\,. \tag{4.23}$$

Thus, the degree of Σ is

$$\deg(\Sigma) = -2\chi(S_\Sigma)\,. \tag{4.24}$$

If $\Sigma \in \mathcal{SD}_g^\bullet(m, 1)$, then the top degree cell is a diagram with chords and leaves on the admissible cycles, exactly one per boundary cycle of Σ. See Figure 4.7 (a). Therefore, if Σ is of top degree, we have

$$\deg(\Sigma) = -2\chi(S_\Sigma) + m\,. \tag{4.25}$$

4.3.1. The simplicial structure on the space of Sullivan diagrams

By Proposition 4.3.5, a Sullivan diagram Σ is identified with a combinatorial 1-Sullivan diagram. We describe the face maps and the degeneracy maps both geometrically and algebraically.

Discussion 4.3.8 (The face map geometrically)**.** Geometrically, the i-th face of a combinatorial Sullivan diagram $\Sigma = (\lambda, S_1, \ldots, S_t)$ is given by collapsing the i-th edge of the ground circle. Hereby, the surfaces S_j and S_k attached to i and $i + 1$ are merged, i.e., the resulting surface is the connected sum of S_j and S_k at the corresponding boundary components. There are four possible cases:

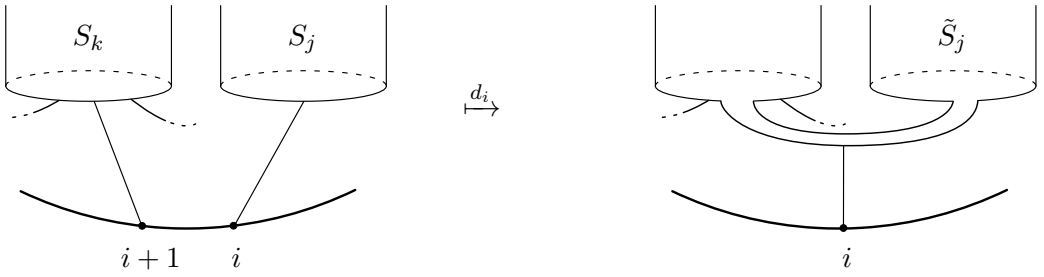

Figure 4.8.: The face map glues together the boundaries of two ghost surfaces S_j and S_k resulting in a ghost surface $\tilde{S}_j$.

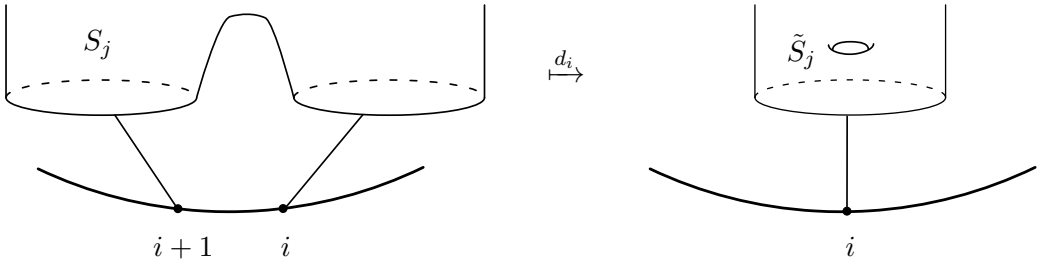

Figure 4.9.: The face map glues together two different boundary components of a ghost surface S_j resulting in a ghost surface $\tilde{S}_j$ having the same number of punctures while the genus is increased by one and the number of boundary components is decreased by one.

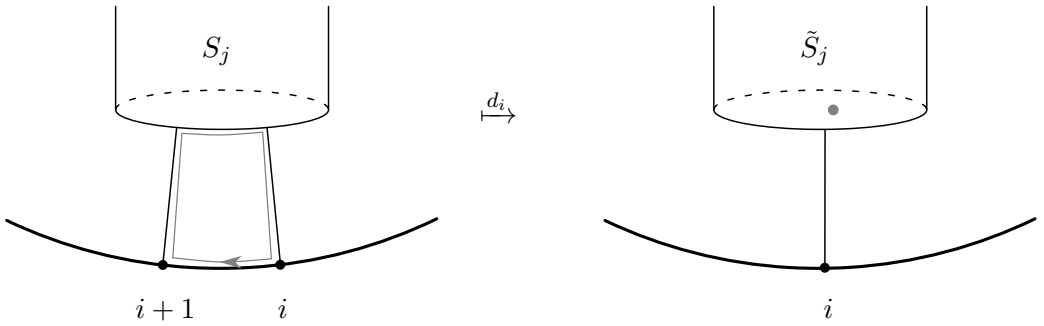

Figure 4.10.: The non-degenerate outgoing boundary cycle $\langle i \rangle$ of ρ degenerates to a puncture of $\tilde{S}_j$ which we indicate by a gray dot.

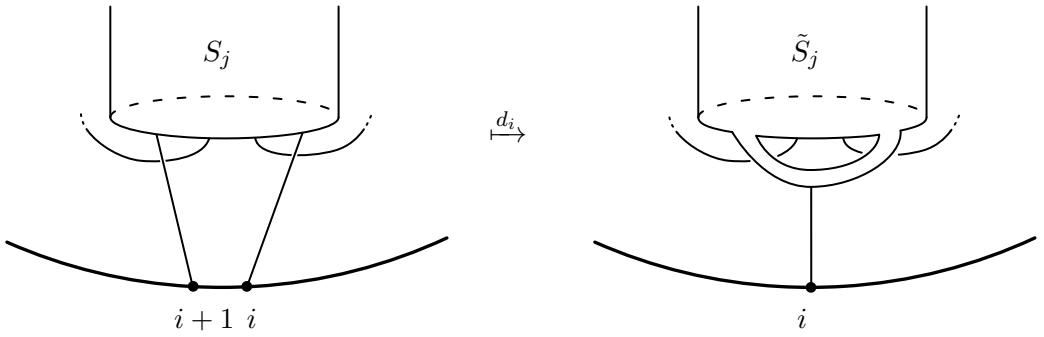

Figure 4.11.: The face map splits the boundary of a ghost surface into two parts.

Case (1): Assume that two different boundary components B and C are attached to i and $i+1$. There are two subcases.

(1.a) If B and C belong to different surfaces S_j and S_k, then d_i glues together two different surfaces. The resulting surface $\tilde{S}_j$ has genus $g(S_j)+g(S_k)$, number of punctures $m(S_j)+m(S_k)$ and one boundary component less than the total number of boundaries of S_j and S_k. See Figure 4.8.

(1.b) If B and C belong to the same surface S_j, then d_j glues together two different boundary components of the same surface. The resulting surface $\tilde{S}_j$ has genus $g(S_j)+1$, number of punctures $m(S_j)$ and one boundary component less than S_j. See Figure 4.9

Case (2): Assume that the same boundary B of a single surface S_j is attached to both i and $i+1$. There are two subcases:

(2.a) If S_j is attached to $i+1$ right after it is attached to i, i.e., $\lambda(i)=i+1$ or equivalently $\rho(i)=i$, then d_i collapses the boundary cycle $\langle i\rangle$ to a puncture. The resulting surface $\tilde{S}_j$ has genus $g(S_j)$, number of punctures $m(S_j)+1$ and one boundary component less than S_j. See Figure 4.10.

(2.b) If S_j is attached to $k\neq i+1$ right after i, i.e., $\lambda(i)\neq i+1$ or equivalently $\rho(i)\neq i$, then d_i splits the boundary of S_j into two parts. The resulting surface $\tilde{S}_j$ has genus $g(S_j)$, number of punctures $m(S_j)$ and one boundary component more than S_j. See Figure 4.11

Discussion 4.3.9 (The degeneracy map geometrically)**.** Geometrically speaking, the i-th degeneracy of $\Sigma=(\lambda,S_1,\dots,S_t)$ is given by splitting the i-th edge of the ground circle into two pieces. This is achieved by glueing a disc D to the splitting point. See Figure 4.12

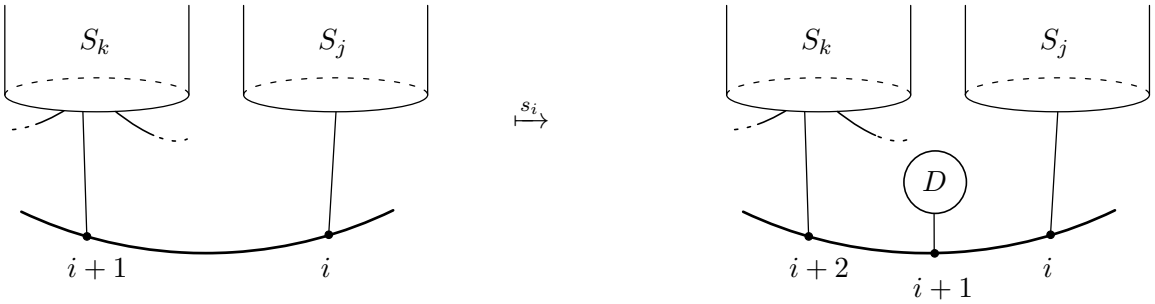

Figure 4.12.: The degeneracy map splits the i-th edge of the ground circle into two pieces and glues a disc D to the splitting point.

Before discussion the faces and degeneracies algebraically we need some notations. Analogously to Section 2.2, we define the face maps and degeneracy maps of symmetric groups as follows.

Definition 4.3.10. Let L be a finite set and $0\leq i\leq n$. By Definition 2.1.2, the induced map $F_i:=\mathfrak{S}(\delta_i\sqcup \mathrm{id}_L)\colon \mathfrak{S}([n-1]\sqcup L)\hookrightarrow \mathfrak{S}([n]\sqcup L)$ regards a permutation $\sigma\in\mathfrak{S}([n-1]\sqcup L)$ as a permutation of $[n]\sqcup L$ that has i as a fixed point.

The i-th face map $D_i\colon \mathfrak{S}([n]\sqcup L)\to\mathfrak{S}([n-1]\sqcup L)$ is

$$D_i(\sigma):=F_i^{-1}(\langle\sigma(i)\ i\rangle\cdot\sigma) \tag{4.26}$$

where $\langle\sigma(i)\ i\rangle$ is the permutation exchanging $\sigma(i)$ and i (if $\sigma(i)\neq i$; and it is the identity otherwise).

The i-th degeneracy map $S_i \colon \mathfrak{S}([n] \sqcup L) \to \mathfrak{S}([n-1] \sqcup L)$ is

$$S_j(\sigma) := \langle j+1 \ j \rangle \cdot F_j(\sigma). \tag{4.27}$$

The cyclic operator $T \colon \mathfrak{S}([n] \sqcup L) \to \mathfrak{S}([n] \sqcup L)$ is

$$T(\sigma) := \omega_n \cdot \sigma \cdot \omega_n^{-1} \tag{4.28}$$

with ω_n the long cycle $\omega_n = \langle 0 \ 1 \ 2 \ \dots \ n \rangle$.

Remark 4.3.11. Consider a (possibly empty) finite set L. The sets $\{\mathfrak{S}([n] \sqcup L)\}_{n \in \mathbb{N}}$ together with the face maps D_i, the degeneracy maps S_j and the cyclic operators T form a cyclic set.

Discussion 4.3.12 (The face map algebraically)**.** Let $\Sigma = (\lambda, S_1, S_2, \dots, S_t)$ be a combinatorial 1-Sullivan diagram of degree n and let $\rho = \lambda^{-1}\langle 0 \ 1 \ \dots \ n \rangle$ be the outgoing boundary cycles. The i-th face $d_i\Sigma = \tilde{\Sigma} = (\tilde{\lambda}, \tilde{S}_1, \dots, \tilde{S}_{\tilde{t}})$ is obtained as follows. The ribbon structure and the outgoing boundary cycles $\tilde{\rho}$ of $\tilde{\Sigma}$ are

$$\tilde{\rho} = D_i(\rho) \qquad \text{and} \qquad \tilde{\lambda} = D_i(\lambda \cdot \langle a \ i \rangle) \tag{4.29}$$

where $a = \rho(i)$. The ghost surfaces are obtained analogously to Discussion 4.3.8. There are four cases.

Case (1): Assume that $a = \rho(i)$ and i belong to different cycles of λ. Then, $\tilde{\lambda}$ has one cycle less than λ by (4.29). Moreover $\lambda(a) = \lambda\rho(i) = \lambda\lambda^{-1}\langle 0 \ 1 \ \dots \ n \rangle(i) = i+1$. Therefore, the map D_i induces a bijection

$$\Phi \colon \{\alpha \in \mathrm{cyc}(\lambda) \mid i, a \notin \alpha\} \cong \{\alpha \in \mathrm{cyc}(\tilde{\lambda}) \mid i \notin \alpha\}. \tag{4.30}$$

We have to distinguish two subcases.

(1.a) Assume that a and i belong to different cycles of different surfaces S_j and S_k. Then, $\tilde{\Sigma}$ has one surface less than Σ, i.e., $\tilde{t} = t - 1$. For sake of simplicity, let us assume that $j = t-1$ and $k = t$. For $1 \le r < \tilde{t}$ the surface $\tilde{S}_r$ is defined as

$$\tilde{S}_r = (g_r, m_r, \tilde{A}_r) \tag{4.31}$$

where

$$\tilde{A}_r = \{\Phi(\alpha) \mid \alpha \in A_r\}. \tag{4.32}$$

The surface $\tilde{S}_{\tilde{t}}$ is defined as

$$\tilde{S}_{\tilde{t}} = (g_{t-1} + g_t, m_{t-1} + m_t, \tilde{A}_{\tilde{t}}) \tag{4.33}$$

where

$$\tilde{A}_{\tilde{t}} = \{\Phi(\alpha) \mid a, i \notin \alpha \in A_{t-1} \cup A_t\} \cup \{i \in \alpha \in \mathrm{cyc}(\tilde{\lambda})\}. \tag{4.34}$$

(1.b) Assume further that a and i belong to different cycles of the same surface S_j. Then, $\tilde{\Sigma}$ has the same number of surfaces as Σ, i.e., $\tilde{t} = t$. For $r \neq j$ the surface $\tilde{S}_r$ is defined as

$$\tilde{S}_r = (g_r, m_r, \tilde{A}_r) \tag{4.35}$$

where

$$\tilde{A}_r = \{\Phi(\alpha) \mid \alpha \in A_r\}\,. \tag{4.36}$$

The surface $\tilde{S}_j$ is defined as

$$\tilde{S}_j = (g_j + 1, m_j, \tilde{A}_j) \tag{4.37}$$

where

$$\tilde{A}_j = \{\Phi(\alpha) \mid a, i \notin \alpha \in A_j\} \cup \{i \in \alpha \in \mathrm{cyc}(\tilde{\lambda})\}\,. \tag{4.38}$$

Case (2): Assume that $a = \rho(i)$ and i belong to the same cycle of λ. We distinguish two subcases.

(2.a) Assume that a and i belong to the same cycle of λ and that $\lambda(i) = i + 1$. Observe that this is the case if and only if $a = i$. Therefore $\lambda\langle a\ i\rangle = \lambda$ and $\tilde{\lambda}$ has the same number of cycles as λ and the map D_i induces an bijection

$$\Phi\colon \Lambda \cong \tilde{\Lambda} = \mathrm{cyc}(\tilde{\lambda})\,. \tag{4.39}$$

The i-th face $\tilde{\Sigma}$ has the same number of surfaces as Σ, i.e., $\tilde{t} = t$. For $r \neq j$ the surface $\tilde{S}_r$ is defined as

$$\tilde{S}_r = (g_r, m_r, \tilde{A}_r) \quad \text{where} \quad \tilde{A}_r = \{\Phi(\alpha) \mid \alpha \in A_r\}\,. \tag{4.40}$$

The surface $\tilde{S}_j$ is defined as

$$\tilde{S}_j = (g_j, m_j + 1, \tilde{A}_j) \quad \text{where} \quad \tilde{A}_j = \{\Phi(\alpha) \mid \alpha \in A_j\}\,. \tag{4.41}$$

(2.b) Assume that a and i belong to the same cycle of λ and that $\lambda(i) \neq i + 1$. Observe that this is the case if and only if $a \neq i$. It will follow that $\lambda\langle a\ i\rangle$ and $\tilde{\lambda}$ have one cycle more than λ and that the map D_i induces an injection

$$\Phi\colon \{\alpha \in \Lambda \mid i, a \notin \alpha\} \hookrightarrow \tilde{\Lambda} = \mathrm{cyc}(\tilde{\lambda})\,. \tag{4.42}$$

The i-th face $\tilde{\Sigma}$ has the same number of surfaces as Σ, i.e., $\tilde{t} = t$. For $r \neq j$ the surface $\tilde{S}_r$ is defined as

$$\tilde{S}_r = (g_r, m_r, \tilde{A}_r) \quad \text{where} \quad \tilde{A}_r = \{\Phi(\alpha) \mid \alpha \in A_r\}\,. \tag{4.43}$$

The surface $\tilde{S}_j$ is defined as

$$\tilde{S}_j = (g_j, m_j, \tilde{A}_j) \quad \text{where} \quad \tilde{A}_j = \{\Phi(\alpha) \mid i, a \notin \alpha \in A_j\} \cup (\tilde{\Lambda} - \mathrm{im}(\Phi))\,. \tag{4.44}$$

Discussion 4.3.13 (The degeneracy map algebraically)**.** Let $\Sigma = (\lambda, S_1, S_2, \ldots, S_t)$ be a combinatorial 1-Sullivan diagram of degree n and let $\rho = \lambda^{-1}\langle 0\ 1\ \ldots\ n\rangle$ its outgoing boundary cycles. The i-th degeneracy $s_i\Sigma = \tilde{\Sigma} = (\tilde{\lambda}, \tilde{S}_1, \ldots, \tilde{S}_{\tilde{t}})$ is obtained as follows. The ribbon structure and the outgoing boundary cycles $\tilde{\rho}$ of $\tilde{\Sigma}$ are

$$\tilde{\rho} = S_i(\rho) \qquad \text{and} \qquad \tilde{\lambda} = F_{i+1}(\lambda) \tag{4.45}$$

with F_{i+1} as in Definition 4.3.10. The ghost surfaces are obtained analogously to Discussion 4.3.9. The map F_{i+1} induces an injection

$$\Phi\colon \Lambda \hookrightarrow \tilde{\Lambda} \tag{4.46}$$

whose complement consists only of the cycle $\langle i+1\rangle$. The i-th degeneracy $\tilde{\Sigma}$ has one surface more than Σ, i.e., $\tilde{t} = t+1$. For $r \neq \tilde{t}$ the surface $\tilde{S}_r$ is defined as

$$\tilde{S}_r = (g_r, m_r, \tilde{A}_r) \quad \text{where} \quad \tilde{A}_r = \{\Phi(\alpha) \mid \alpha \in A_r\}\,. \tag{4.47}$$

The surface $\tilde{S}_{\tilde{t}}$ is defined as

$$\tilde{S}_{\tilde{t}} = (0, 0, \tilde{A}_{\tilde{t}}) \quad \text{where} \quad \tilde{A}_{\tilde{t}} = \tilde{\Lambda} - \mathrm{im}(\Phi) = \{\langle i+1\rangle\}\,. \tag{4.48}$$

The above discussions of the faces and degeneracies yield the following Proposition.

Proposition 4.3.14 (B., Egas)**.** *Let L be a finite, non-empty set of cardinality m. The sets of combinatorial 1-Sullivan diagrams $\{C^\bullet_L(n)\}_{n\in\mathbb{N}}$ together with the face maps d_i and degeneracies s_i define a simplicial set which is isomorphic to the simplicial set underlying $\sqcup_g \mathscr{SD}^\bullet_g(m,1)$. Similarly, the sets of combinatorial 1-Sullivan diagrams $\{C^\circ(n)\}_{n\in\mathbb{N}}$ together with the face maps d_i and degeneracies s_i define a simplicial set which is isomorphic to the simplicial set underlying $\sqcup_g \mathscr{SD}^\circ_g(m,1)$.*

4.3.2. The inclusion of the moduli space into its harmonic compactification

In [EK14], Egas–Kupers provide a cellular homotopy equivalence from the harmonic compactification to the space of Sullivan diagrams. The restriction to the moduli space

$$\mathfrak{M}^\star_g(m,1) \to \overline{\mathfrak{M}}^\star_g(m,1) \xrightarrow{\simeq} \mathscr{SD}^\star_g(m,1) \tag{4.49}$$

is given by sending a Riemann surface F to the union of its complete critical graph K and the incoming boundaries ∂_{in}. Here, we describe this map in terms of radial slit configurations and combinatorial Sullivan diagrams, see also [BE17, Remark 3.12].

In Section 3.4, the space of radial slit configurations $\mathfrak{Rad}^\star_g(m,1) \cong \mathfrak{M}^\star_g(m,1)$ is given as relative bi-simplicial set, i.e., it is a bi-simplicial set with some faces missing. An open cell of bi-degree (p,q) determines a sequence of permutations

$$\Sigma = (\tau_1|\ldots|\tau_q) \in \mathfrak{S}([p])^q \tag{4.50}$$

subject to certain conditions. By Section 3.3, the connected components of the complete graph corresponding to Σ defines partition of $[p]$ into clusters. Let $\tau := \tau_q \cdots \tau_1$. On the set of cycles $\Lambda := \mathrm{cyc}(\tau)$, the following relation

$$\alpha \sim \beta \text{ if there exists } \alpha \ni i \sim_{CL} j \in \beta \tag{4.51}$$

defines an equivalence relation by Lemma 3.3.3. We denote the partition of Λ into equivalence classes by

$$\Lambda = A_1 \sqcup \ldots \sqcup A_k\,. \tag{4.52}$$

The *radial projection* of Σ is the Sullivan diagram $\pi_{\mathcal{SD}}(\Sigma) = (\lambda, S_1, \ldots, S_k) \in \mathcal{SD}^\star_g(m,1)$ with $\lambda = \tau^{-1}$ and $S_i = (0,0,A_i)$. Using the cellular homotopy equivalence of Egas–Kupers, the next Proposition is an immediate consequence of the above.

Proposition 4.3.15 (B., Egas–Kupers)**.** *Let $g \geq 0$, $m \geq 0$ and $\star \in \{\bullet, \circ, \blacksquare, \square\}$. By*

$$\Phi \colon \mathfrak{Rad}_g^\star(m,1) \cong \mathfrak{M}_g^\star(m,1) \hookrightarrow \overline{\mathfrak{M}}_g^\star(m,1) \xrightarrow{\simeq} \mathscr{SD}_g^\star(m,1) \tag{4.53}$$

we denote the composition of the Hilbert uniformization map, the inclusion into the harmonic compactification and the cellular homotopy equivalence described by Egas–Kupers. The restriction of Φ to an open cell $\Sigma \times int(\Delta^p \times \Delta^q) \subset \mathfrak{Rad}_g^\star(m,1)$ is induced by the radial projection and the projection to the left simplex

$$\Phi|_{\Sigma \times int(\Delta^p \times \Delta^q)} = \pi_{\mathcal{SD}} \times pr_{int(\Delta^p)} \colon \Sigma \times int(\Delta^p \times \Delta^q) \to \pi_{\mathcal{SD}}(\Sigma) \times int(\Delta^p)\,. \tag{4.54}$$

4.3.3. The stabilization map

Let $g \geq 0$, $m \geq 1$, $n \geq 1$ and $\star \in \{\bullet, \circ, \blacksquare, \square\}$. The stabilization map $\varphi \colon \mathfrak{M}_g^\star(m,n) \to \mathfrak{M}_{g+1}(m,n)$ is given by sewing a surface of genus one with two boundary components to the first incoming boundary of $F \in \mathfrak{M}_g^\star(m,n)$, See Figure 4.13. In homology, the induced

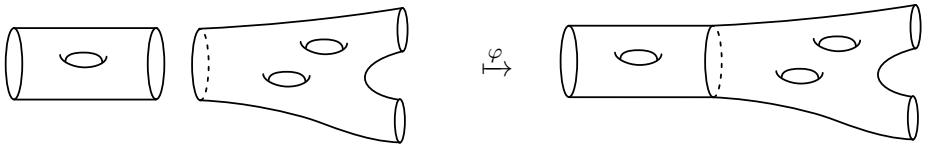

Figure 4.13.: The stabilization map is induced by sewing surfaces.

map in homology is an isomorphism for $g \geq \frac{3*+2}{2}$, see [Har85] and [RW16]. The stabilization map extends to the spaces of Sullivan diagrams as follows.

Definition 4.3.16. Let $g \geq 0$, $m \geq 1$, $n \geq 1$ and $\star \in \{\bullet, \circ, \blacksquare, \square\}$. The *stabilization map*

$$\overline{\varphi} \colon \mathscr{SD}_g^\star(m,1) \to \mathscr{SD}_{g+1}^\star(m,1) \tag{4.55}$$

is the simplicial map that increases the genus of the ghost surface attached to the vertex 0 by one, see Figure 4.14. More precisely, if $\Sigma = (\lambda, S_1, \ldots, S_t)$ and $S_1 = (g_1, m_1, A_1)$ such that A_1 contains the cycle to which 0 belongs, then $\overline{\varphi}(\Sigma) = (\lambda, (g_1+1, m_1, A_1), S_2, \ldots, S_t)$.

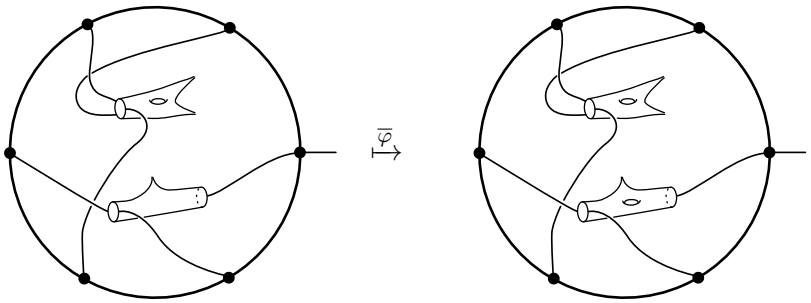

Figure 4.14.: The stabilization map increases the genus of the ghost surface attached to the vertex 0.

Remark 4.3.17. The stabilization map $\overline{\varphi} \colon \mathscr{SD}_g^\star(m,1) \to \mathscr{SD}_g^\star(m,1)$ is an injective simplicial map. In particular, it identifies $\mathcal{SD}_g^\star(m,1)$ with a sub-complex of $\mathcal{SD}_{g+1}^\star(m,1)$.

4.4. A summary of the results with Egas Santander

In this section, we provide the main results of our article with Egas Santander [BE17]. Recall that the harmonic compactification $\overline{\mathfrak{M}}_g^\star(m,1)$ is cellularly homotopy equivalent to the space of Sullivan diagrams $\mathscr{SD}_g^\star(m,1)$ by [EK14], see also Proposition 4.3.15. Therefore, the results presented below carry over to the harmonic compactifications.

The results on the stabilization map of the moduli spaces and its space of Sullivan diagrams are in Section 4.4.1. The results on structure of the homology of the space of Sullivan diagrams are in Section 4.4.2. The results on infinite families of non-trivial string operations are in Section 4.4.3. Lastly, we computed the homology of the space of Sullivan diagrams for small parameters g and m, see Section 4.4.4.

4.4.1. Homological stability and high connectivity

Using our combinatorial description of the spaces of Sullivan diagrams, we extend the stabilization map of the moduli spaces to their space of Sullivan diagrams.

Theorem 4.4.1 ([BE17, Theorem 4.1])**.** *Let $g \geq 0$, $m \geq 1$ and $\star \in \{\bullet, \blacksquare, \circ, \square\}$. The stabilization map $\varphi\colon \mathfrak{M}_g^\star(m,1) \to \mathfrak{M}_{g+1}^\star(m,1)$ extends to the space of Sullivan diagrams, i.e., there is a map $\overline{\varphi}\colon \mathscr{SD}_g^\star(m,1) \to \mathscr{SD}_{g+1}^\star(m,1)$ making the following diagram commutative.*

$$\begin{array}{ccc} \mathfrak{M}_g^\star(m,1) & \xrightarrow{\varphi} & \mathfrak{M}_{g+1}^\star(m,1) \\ \downarrow & & \downarrow \\ \mathscr{SD}_g^\star(m,1) & \xrightarrow{\overline{\varphi}} & \mathscr{SD}_{g+1}^\star(m,1) \end{array} \tag{4.56}$$

The stabilization map $\overline{\varphi}$ induces an isomorphism in homology in the degrees $* \leq g+m-2$. Moreover, if $m > 2$, the stabilization map $\overline{\varphi}$ is $(g+m-2)$ connected.

The usual framework that is used to proof homological stability cannot be applied to our situation because the spaces of Sullivan diagrams are highly connected (see Theorem 4.4.2). Our proof of the Theorem 4.4.1 is summarized as follows. The stabilization map $\overline{\varphi}_g$ identifies the cellular chain complex $\mathcal{SD}_g^\star(m,1)$ with a subcomplex of $\mathcal{SD}_{g+1}^\star(m,1)$. On the pair $(\mathcal{SD}_g^\star(m,1), \mathcal{SD}_{g+1}^\star(m,1))$, we construct a discrete Morse flow that is perfect in the degrees $* \leq (g+m-1)$. Consequently, the stabilization map induces an integral homology isomorphism in the degrees $* \leq g+m-2$. By Theorem 4.4.2, $\mathscr{SD}_g^\star(m,1)$ is 1-connected if $m > 2$ and, in this case, it follows that $\overline{\varphi}_g$ is $(g+m-2)$-connected. In Chapter 6, we will show that, in the parametrized enumerated case, the stabilization map $\overline{\varphi}_g$ is $(g+m-2)$-connected for all m and we believe that this holds true also in the (un)parametrized (un)enumerated cases.

Theorem 4.4.2 ([BE17, Theorem 4.2])**.** *Let $g \geq 0$ and $m > 2$. The spaces $\mathscr{SD}_g^\bullet(m,1)$, $\mathscr{SD}_g^\blacksquare(m,1)$, $\mathscr{SD}_g^\circ(m,1)$ or $\mathscr{SD}_g^\square(m,1)$ are highly connected with respect to m, i.e.,*

$$\pi_*(\mathscr{SD}_g^\bullet(m,1)) = 0 \qquad \text{and} \qquad \pi_*(\mathscr{SD}_g^\circ(m,1)) = 0 \qquad \text{for} \qquad * \leq m-2 \tag{4.57}$$

and

$$\pi_*(\mathscr{SD}_g^\blacksquare(m,1)) = 0 \qquad \text{and} \qquad \pi_*(\mathscr{SD}_g^\square(m,1)) = 0 \qquad \text{for} \qquad * \leq m' \tag{4.58}$$

where m' is the largest even number strictly smaller than m.

4.4.2. On the homology

It is a non-trivial task to find non-trivial classes in the homology of the spaces of Sullivan diagrams. We show that every homology class is represented by a chain of Sullivan diagrams without degenerate outgoing boundaries.

Proposition 4.4.3 ([BE17, Proposition 4.3])**.** *Let $g \geq 0$, $m \geq 1$ and $\star \in \{\bullet, \blacksquare, \circ, \square\}$. Let $\mathcal{SD} := \mathcal{SD}_g^\star(m,1)$ and let R be an arbitrary coefficient group. Denote the sub-complex of Sullivan diagrams with degenerate outgoing boundaries by D. Every homology class $x \in H_*(\mathcal{SD}; R)$ is represented by a chain $\sum \kappa_i c_i$ with $c_i \notin D$.*

The proof of Proposition 4.4.3 follows from the properties of the discrete Morse flows which we construct in the proofs of Theorem 4.4.1 and Theorem 4.4.1. In Chapter 5, we obtain another desuspension theorem, relating $\mathcal{SD}_g^\star(m,1)/D$ with an $(m-1)$-fold suspension of $\mathcal{SD}_g^\star(m,1) - D$.

Forgetting the enumeration of the outgoing boundaries is not a covering for Sullivan diagrams having more then two degenerate outgoing boundaries. Nonetheless, using Proposition 4.4.3, the forgetful maps behave like coverings in homology, i.e., there are "transfer maps". These "trace maps" are used to construct some of the non-trivial classes in Proposition 4.4.6.

Proposition 4.4.4 ([BE17, Proposition 5.13])**.** *In homology there are maps*

$$tr\colon H_*(\mathcal{SD}_g^\blacksquare(m,1);\mathbb{Z}) \to H_*(\mathcal{SD}_g^\bullet(m,1);\mathbb{Z}) \tag{4.59}$$

respectively

$$tr\colon H_*(\mathcal{SD}_g^\square(m,1);\mathbb{Z}) \to H_*(\mathcal{SD}_g^\circ(m,1);\mathbb{Z}) \tag{4.60}$$

where $(\pi_\blacksquare^\bullet)_* \circ tr$ respectively $(\pi_\square^\circ)_* \circ tr$ is the multiplication by $m!$.

4.4.3. Non-trivial families of higher string operations

Denote the surface of genus g, one parametrized incoming and one parametrized outgoing boundary by $S_{g,2}$. Glueing the k-th punctured disc to the outgoing boundary component of $S_{g,2}$ induces the canonical inclusion of the k-th Braid group resp. its classifying space:

$$Br_k \hookrightarrow \Gamma_{g,1}^k \quad \text{resp.} \quad \mathfrak{M}_0^\square(k,1) \hookrightarrow \mathfrak{M}_g^\square(k,1)\,. \tag{4.61}$$

By construction, these inclusions are compatible with respect to the stabilization of the genus. By α_g, we denote the image of the braid generator under the canonical map

$$Br_2 \cong \pi_1(\mathfrak{M}_0^\square(2,1)) \hookrightarrow \pi_1(\mathfrak{M}_g^\square(2,1)) \to \pi_1(\overline{\mathfrak{M}}_g^\square(2,1)) \cong \pi_1(\mathscr{SD}_g^\square(2,1))\,. \tag{4.62}$$

Proposition 4.4.5 ([BE17, Proposition 5.1])**.** *The fundamental group of the space of Sullivan diagrams $\mathscr{SD}_0^\square(2,1)$ is*

$$\pi_1(\mathscr{SD}_0^\square(2,1)) \cong \begin{cases} \mathbb{Z}\langle\alpha_0\rangle & g=0 \\ \mathbb{Z}_2\langle\alpha_g\rangle & g>0 \end{cases}. \tag{4.63}$$

The homomorphism on fundamental groups induced by the stabilization map

$$\varphi\colon \pi_1(\mathscr{SD}_g^\square(2,1)) \to \pi_1(\mathscr{SD}_{g+1}^\square(2,1)) \tag{4.64}$$

sends α_g to α_{g+1}.

Using the methods of [Wah16] and Proposition 4.4.4, we construct infinite families of non-trivial classes of infinite order that correspond to non-trivial higher string operations.

Proposition 4.4.6 ([BE17, Proposition 5.10 and Proposition 5.14])**.** *Let $m > 0$, $1 \leq i \leq m$, $c_i > 1$ and $c = \sum_i c_i$.*

(*i*) *There are classes of infinite order*

$$\widetilde{\Gamma}_m \in H_{4m-1}(\mathscr{SD}^{\bullet}_m(m,1);\mathbb{Z}) \tag{4.65}$$

and

$$\widetilde{\Omega}_{(c_1,\dots,c_m)} \in H_{2c-1}(\mathscr{SD}^{\bullet}_0(c,1);\mathbb{Z})\,. \tag{4.66}$$

All these classes correspond to non-trivial higher string operations.

(*ii*) *There are classes of infinite order*

$$\Gamma_m \in H_{4m-1}(\mathscr{SD}^{\blacksquare}_m(m,1);\mathbb{Z}) \tag{4.67}$$

and

$$\Omega_{(c_1,\dots,c_m)} \in H_{2c-1}(\mathscr{SD}^{\blacksquare}_0(c,1);\mathbb{Z}) \tag{4.68}$$

and

$$\zeta_{2m} \in H_{2m-1}(\mathscr{SD}^{\blacksquare}_0(2m,1);\mathbb{Z})\,. \tag{4.69}$$

The classes $\tilde{\Gamma}$ and $\tilde{\Omega}$ are constructed as follows. The PROP-structure of the surface PROP $\oplus_{g\geq 0,m\geq 1} H_*(\mathfrak{M}^{\bullet}_g(m,1);\mathbb{Z})$ extends to $\oplus_{g\geq 0,m\geq 1} H_*(\mathscr{SD}^{\bullet}_g(m,1);\mathbb{Z})$ and, roughly speaking, it is defined as follows. For a Sullivan diagram $\Sigma \in \mathscr{SD}^{\bullet}_g(m,1)$ with no degenerate boundary cycles and Sullivan diagrams $\Sigma_1,\dots,\Sigma_m \in \sqcup_{g'\geq 0,m'\geq 1}\mathscr{SD}^{\bullet}_{g'}(m',1)$, we cut open the ground circle of each Σ_i at the vertex 0 to obtain a "ground interval with decorated surfaces attached". These intervals are glued to the admissible edges of the i-th outgoing boundary of Σ. For a precise definition, see e.g. [BE17, Definition 2.17]. Using this PROP-structure, the classes $\tilde{\Gamma}$ and $\tilde{\Omega}$ are the products defined in (4.71) and (4.70). We begin with the basic building blocks. See Figure 4.15 for examples for small m.

1. For $m > 0$ consider the permutation $\widetilde{\lambda}_\zeta = \langle 0\ l_1\ 1\ l_2\ \dots\ l_{m-1}\ m-1\ l_m\rangle$ and let Λ_ζ denote its unique cycle. We define the chain $\widetilde{\zeta}_m := (\widetilde{\lambda}_\zeta, (0,0,\Lambda_\zeta)) \in \mathcal{SD}^{\bullet}_0(m,1)$.

2. For $m > 1$ we define the chain $\widetilde{\omega}_m := \widetilde{\omega}_{m,1} - \widetilde{\omega}_{m,2} \in \mathcal{SD}^{\bullet}_0(m,1)$, where $\widetilde{\omega}_{m,1} = (\lambda_1, S_{0,1}, S_{1,1}, S_2, \dots, S_m)$ and $\widetilde{\omega}_{m,2} = (\lambda_2, S_{0,2}, S_{1,2}, S_2, \dots, S_m)$ are given by the following data:

$$\begin{aligned}
\lambda_{0,1} &= \langle 0\rangle \text{ and } \lambda_{0,2} = \langle 0\ l_1\rangle\\
\lambda_{1,1} &= \langle 1\ 3\ \dots\ 2m-1\ l_1\rangle \text{ and } \lambda_{1,2} = \langle 1\ 3\ \dots\ 2m-1\rangle\\
\lambda_i &= \langle 2i-2\ l_i\rangle \text{ for } 2 \leq i \leq m\\
\lambda_1 &= \lambda_{0,1}\lambda_{1,1}\lambda_2\cdots\lambda_m\\
\lambda_2 &= \lambda_{0,2}\lambda_{1,2}\lambda_2\cdots\lambda_m\\
S_{i,j} &= (0,0,\lambda_{i,j}) \text{ for } i = 0,1 \text{ and } j = 1,2\\
S_i &= (0,0,\lambda_i) \text{ for } 2 \leq i \leq m
\end{aligned}$$

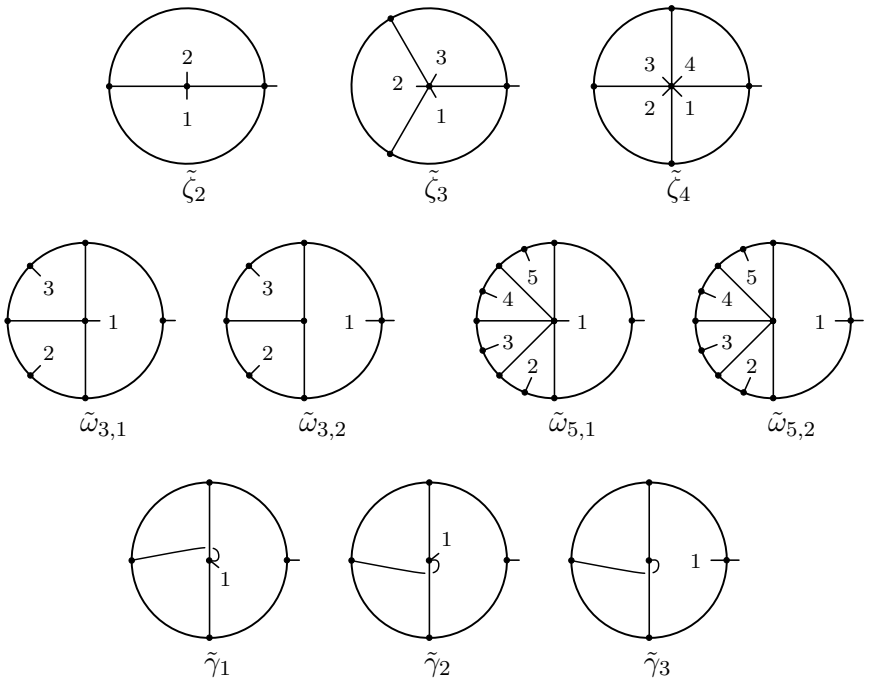

Figure 4.15.: The building blocks, where we abbreviate the name of a leaf l_i by i.

3. We define the chain $\widetilde{\gamma} := \widetilde{\gamma}_1 + \widetilde{\gamma}_2 - \widetilde{\gamma}_3 \in \mathcal{SD}_1^\bullet(m,1)$ where for $1 \leq i \leq 3$, $\widetilde{\gamma}_i = (\lambda_i, S_{1,i}, S_{2,i})$ and these are given by the following data:

$$\begin{aligned}
\lambda_{1,j} &= \langle 0 \rangle \text{ for } j = 1,2 \\
\lambda_{1,3} &= \langle 0\ l_1 \rangle \\
\lambda_{2,1} &= \langle l_1\ 1\ 3\ 2 \rangle \\
\lambda_{2,2} &= \langle 1\ 3\ l_1\ 2 \rangle \\
\lambda_{2,3} &= \langle 1\ 3\ 2 \rangle \\
\lambda_j &= \lambda_{1,j}\lambda_{2,j} \text{ for } j = 1,2,3 \\
S_{i,j} &= (0,0,\lambda_{i,j}) \text{ for } i = 1,2 \text{ and } j = 1,2,3
\end{aligned}$$

The chains $\widetilde{\omega}_m$ and $\widetilde{\gamma}$ are cycles in the chain complex of Sullivan diagrams. However, the chain $\widetilde{\zeta}_m$ is not a cycle.

Now, let $m > 0$ and let $(c_1, \ldots, c_m)$ be a tuple of integers with $c_i > 1$ for $1 \leq i \leq m$ and set $c := \sum_{i=1}^m c_i$. We define the chain $\widetilde{\Omega}_{(c_1,\ldots,c_m)} \in \mathcal{SD}_0^\bullet(c,1)$ to be

$$\widetilde{\Omega}_{(c_1,\ldots,c_m)} := \widetilde{\zeta}_m \circ (\widetilde{\omega}_{c_1} \otimes \widetilde{\omega}_{c_2} \otimes \ldots \otimes \widetilde{\omega}_{c_m}) \tag{4.70}$$

where $\circ$ denotes the PROPeradic multiplication. Note that $\widetilde{\Omega}_{(c)} = \widetilde{\zeta}_1 \circ \widetilde{\omega}_c = \widetilde{\omega}_c$. See Figure 4.16 for another example.

For $m > 0$ we define the chain $\widetilde{\Gamma}_m \in \mathcal{SD}_m^\bullet(m,1)$ to be

$$\widetilde{\Gamma}_m := \widetilde{\zeta}_m \circ (\widetilde{\gamma}^{\otimes m}) \tag{4.71}$$

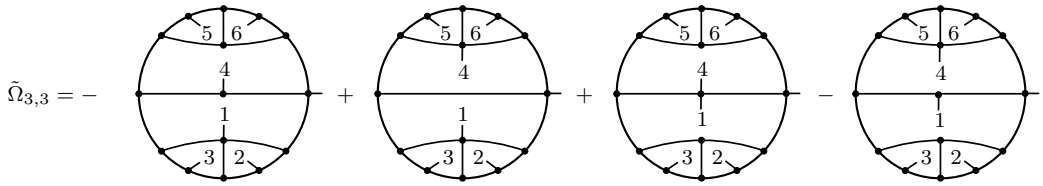

Figure 4.16.: The chain $\widetilde{\Omega}_{(3,3)}$.

Note that $\widetilde{\Gamma}_1 = \widetilde{\gamma}$.

The chains $\tilde{\Gamma}$ and $\tilde{\Omega}$ are cycles in the chain complex of Sullivan diagrams. Using the Kontsevich–Soibelman recipe (made explicit in [WW16, Section 6.2]), our classes act non-trivially on the Hochschild homology of the Frobenius algebra $H^*(\mathbb{S}^2;\mathbb{Q})$. This proofs part *(i)* of Proposition 4.4.6. Part *(ii)* follows the study of the string operations associated to the transfer of $\Omega_{(c_1,\ldots,c_m)}$, Γ_m and ζ_{2m}.

4.4.4. Computational results for small parameters g and m

We obtain the integral homology of $\mathscr{SD}_g^{\square}(m,1)$ and $\mathscr{SD}_g^{\blacksquare}(m,1)$ using computer software.

Proposition 4.4.7 ([BE17, Proposition A.1])**.** *The integral homology of $\mathscr{SD}_g^{\square}(m,1)$, for small parameters $2g+m$, is given by the tables 4.1, 4.2, 4.3 and 4.4.*

Proposition 4.4.8 ([BE17, Proposition A.2])**.** *The integral homology of $\mathscr{SD}_g^{\blacksquare}(m,1)$, for small parameters $2g+m$, is given by the tables 4.5, 4.6 and 4.7.*

Our program is mainly written in *Python 2.7*. Given parameters g and m it produces the integral chain complexes $\mathcal{SD}_g^{\square}(m,1)$ and $\mathcal{SD}_g^{\blacksquare}(m,1)$. Computing its integral homology is by far the most time consuming task. There is a zoo of programs and libraries for this purpose. We use a modified version of *The Original CHomP Software* by Paweł Pilarczyk [Pil13]. Even small parameter $2g+m$ lead to integer overflows in the current version of CHomP and we work around this issue by forcing CHomP to use the *GNU Multiple Precision Arithmetic Library* [GMP]. All results were produced on an *Intel i7-2670QM* and *Intel i5-4570* running *Debian Sid* and *Debian Jessie* with *Linux Kernel 4.2.0-1-amd64*. For the source code of our program, see [Boe18].

In [Ega14b], Egas Santander used a separate program in order to compute the integral homology of the genus zero case using the fact that every Sullivan diagram $\Sigma \in \mathcal{SD}_0^{\square}(m,1)$ is the same as a weighted, non-crossing partition. Her program is implemented in *Magma* [BCP97] and our results agree with these computations.

m	H_0	H_1	H_2	H_3	H_4	H_5	H_6	H_7	H_8	H_9	H_{10}
1	$\mathbb{Z}$										
2	$\mathbb{Z}$	$\mathbb{Z}$									
3	$\mathbb{Z}$			$\mathbb{Z}$							
4	$\mathbb{Z}$			$\mathbb{Z}$							
5	$\mathbb{Z}$					$\mathbb{Z}$					
6	$\mathbb{Z}$					$\mathbb{Z}$		$\mathbb{Z}$	$\mathbb{Z}$		
7	$\mathbb{Z}$							$\mathbb{Z}$			
8	$\mathbb{Z}$							$\mathbb{Z}$		$\mathbb{Z}$	$\mathbb{Z}$

Table 4.1.: The integral homology $H_*(\mathscr{SD}_0^{\square}(m,1);\mathbb{Z})$.

m	H_0	H_1	H_2	H_3	H_4	H_5	H_6	H_7	H_8	H_9
1	$\mathbb{Z}$			$\mathbb{Z}$						
2	$\mathbb{Z}$	$\mathbb{Z}_2$		$\mathbb{Z}$						
3	$\mathbb{Z}$			$\mathbb{Z}_3$		$\mathbb{Z}^2$	$\mathbb{Z}$			
4	$\mathbb{Z}$			$\mathbb{Z}_2$		$\mathbb{Z}\oplus\mathbb{Z}_2$	$\mathbb{Z}_2$	$\mathbb{Z}^2$	$\mathbb{Z}^2$	
5	$\mathbb{Z}$						$\mathbb{Z}$	$\mathbb{Z}^5$	$\mathbb{Z}^3$	$\mathbb{Z}_2$

Table 4.2.: The integral homology $H_*(\mathscr{SD}_1^{\square}(m,1);\mathbb{Z})$.

m	H_0	H_1	H_2	H_3	H_4	H_5	H_6	H_7	H_8	H_9	H_{10}
1	$\mathbb{Z}$		$\mathbb{Z}$	$\mathbb{Z}_5$		$\mathbb{Z}^2$	$\mathbb{Z}_3$				
2	$\mathbb{Z}$	$\mathbb{Z}_2$		$\mathbb{Z}_2$		$\mathbb{Z}\oplus\mathbb{Z}_2$	$\mathbb{Z}\oplus\mathbb{Z}_2$	$\mathbb{Z}^2$	$\mathbb{Z}\oplus\mathbb{Z}_2$	$\mathbb{Z}_2$	
3	$\mathbb{Z}$			$\mathbb{Z}_3$	$\mathbb{Z}_2$		$\mathbb{Z}^4$	$\mathbb{Z}^9\oplus\mathbb{Z}_2$	$\mathbb{Z}^4\oplus\mathbb{Z}_2\oplus\mathbb{Z}_3^2$	$\mathbb{Z}\oplus\mathbb{Z}_2$	$\mathbb{Z}$

Table 4.3.: The integral homology $H_*(\mathscr{SD}_2^{\square}(m,1);\mathbb{Z})$.

m	H_0	H_1	H_2	H_3	H_4	H_5	H_6	H_7	H_8	H_9	H_{10}	H_{11}
1	$\mathbb{Z}$		$\mathbb{Z}$		$\mathbb{Z}$	$\mathbb{Z}_{35}$	$\mathbb{Z}$	$\mathbb{Z}^5$	$\mathbb{Z}\oplus\mathbb{Z}_2^2\oplus\mathbb{Z}_3$		$\mathbb{Z}_2$	$\mathbb{Z}_2$

Table 4.4.: The integral homology $H_*(\mathscr{SD}_3^{\square}(m,1);\mathbb{Z})$.

m	H_0	H_1	H_2	H_3	H_4	H_5	H_6	H_7	H_8	H_9	H_{10}
1	$\mathbb{Z}$	$\mathbb{Z}$									
2	$\mathbb{Z}$	$\mathbb{Z}$	$\mathbb{Z}$	$\mathbb{Z}$							
3	$\mathbb{Z}$			$\mathbb{Z}^3$	$\mathbb{Z}^2$	$\mathbb{Z}$	$\mathbb{Z}$				
4	$\mathbb{Z}$			$\mathbb{Z}$	$\mathbb{Z}$	$\mathbb{Z}^6$	$\mathbb{Z}^5$	$\mathbb{Z}^2$	$\mathbb{Z}^2$		
5	$\mathbb{Z}$					$\mathbb{Z}^7$	$\mathbb{Z}^{10}$	$\mathbb{Z}^{13}$	$\mathbb{Z}^{11}$	$\mathbb{Z}^5$	$\mathbb{Z}^3$

Table 4.5.: The integral homology $H_*(\mathscr{SD}_0^{\blacksquare}(m,1);\mathbb{Z})$.

m	H_0	H_1	H_2	H_3	H_4	H_5	H_6	H_7	H_8	H_9	H_{10}
1	$\mathbb{Z}$	$\mathbb{Z}$		$\mathbb{Z}$	$\mathbb{Z}$						
2	$\mathbb{Z}$			$\mathbb{Z}^2$		$\mathbb{Z}^3$	$\mathbb{Z}^6$	$\mathbb{Z}^2$			
3	$\mathbb{Z}$				$\mathbb{Z}^2$	$\mathbb{Z}^{12}$	$\mathbb{Z}^{11}$	$\mathbb{Z}^9$	$\mathbb{Z}^{14}$	$\mathbb{Z}^8$	$\mathbb{Z}$

Table 4.6.: The integral homology $H_*(\mathscr{SD}_1^{\blacksquare}(m,1);\mathbb{Z})$.

m	H_0	H_1	H_2	H_3	H_4	H_5	H_6	H_7	H_8	H_9	H_{10}	H_{11}
1	$\mathbb{Z}$			$\mathbb{Z}$		$\mathbb{Z}^2$	$\mathbb{Z}^2$	$\mathbb{Z}_3$				
2	$\mathbb{Z}$				$\mathbb{Z}$	$\mathbb{Z}^3$	$\mathbb{Z}^2$	$\mathbb{Z}^{12}$	$\mathbb{Z}^{18}$	$\mathbb{Z}^{13} \oplus \mathbb{Z}_3^2$	$\mathbb{Z}^{10}$	$\mathbb{Z}^4$

Table 4.7.: The integral homology $H_*(\mathscr{SD}_2^{\blacksquare}(m,1);\mathbb{Z})$.

5

On the harmonic compactification with normalized boundaries

In this chapter, we introduce the spaces $N\mathscr{SD}_g^\star(m,1) \subset \mathscr{SD}_g^\star(m,1)$ which are the spaces of Sullivan diagrams of genus g with m (un)parametrized enumerated normalized outgoing boundaries. Using the homotopy equivalence of [EK14], see also Proposition 4.3.2, the spaces $N\mathscr{SD}_g^\star(m,1)$ are regarded as the harmonic compactification of the moduli spaces with normalized outgoing boundaries, i.e., $\overline{N\mathfrak{M}}_g^\star(m,1) \simeq N\mathscr{SD}_g^\star(m,1)$. Consequently, all results on the homotopy type of $N\mathscr{SD}_g^\star(m,1)$ also hold true for the harmonic compactification $\overline{N\mathfrak{M}}_g^\star(m,1)$. Let us state the main result of this chapter.

Theorem 5.2.11. *Let $m \geq 1$ and $g \geq 0$. There are maps of m-dimensional torus fibrations.*

$$\begin{array}{ccccccc} N\mathfrak{Rad}_g^\bullet(m,1) & \longrightarrow & N\mathscr{SD}_g^\bullet(m,1) & \xrightarrow{\overline{\varphi}_g} & N\mathscr{SD}_\infty^\bullet(m,1) & \xrightarrow{\mathcal{P}ol_{\mathscr{SD}}} & N\mathcal{P}ol^\bullet(m,1) \simeq EU(1)^m \\ \downarrow{\scriptstyle \pi_\circ^\bullet} & & \downarrow{\scriptstyle \pi_\circ^\bullet} & & \downarrow{\scriptstyle \pi_\circ^\bullet} & & \downarrow{\scriptstyle \pi_\circ^\bullet} \\ N\mathfrak{Rad}_g^\circ(m,1) & \longrightarrow & N\mathscr{SD}_g^\circ(m,1) & \xrightarrow{\overline{\varphi}_g} & N\mathscr{SD}_\infty^\circ(m,1) & \xrightarrow{\mathcal{P}ol_{\mathscr{SD}}} & N\mathcal{P}ol^\circ(m,1) \simeq BU(1)^m \end{array}$$

The composition $N\mathfrak{Rad}_g^\bullet(m,1) \to N\mathcal{P}ol^\bullet(m,1)$ respectively $N\mathfrak{Rad}_g^\circ(m,1) \to N\mathcal{P}ol^\circ(m,1)$ is the restriction to the outgoing boundaries (see Definition 3.6.2). The stabilization maps $\overline{\varphi}_g$ are $(g-2)$-connected and the maps $\mathcal{P}ol_{\mathscr{SD}}$ are homotopy equivalences.

The chapter is organized as follows. In Section 5.1, we introduce the spaces of Sullivan diagrams with normalized outgoing boundaries, denoted by $N\mathscr{SD}_g^\star(m,1)$, and relate these spaces to the spaces of normalized polygons. Using methods developed in Sections 2.3, 2.4, 2.5 and [BE17, Section 4], we construct an m-fold multi-cyclic structure on $N\mathscr{SD}_g^\bullet(m,1)$, see Proposition 5.1.17, we obtain the desuspension theorem for the spaces of Sullivan diagrams, see Theorem 5.1.22, and we show that the spaces $N\mathscr{SD}_g^\star(m,1)$ admit homological stability with respect to the genus, see Proposition 5.1.24.

In Section 5.2, we study the homotopy type of the spaces $N\mathscr{SD}_g^\star(m,1)$ using the "unreduced cluster spectral sequence". The main result of this chapter is Theorem 5.2.11 stated above.

5.1. The space of Sullivan diagrams with normalized boundaries

Using the ideas of Chapter 2, we introduce the spaces $N\mathscr{SD}_g^\star(m,1)$ which are called the space of Sullivan diagrams of genus g with m (un)parametrized enumerated normalized outgoing boundaries, see Definition 5.1.10. The spaces $N\mathscr{SD}_g^\star(m,1)$ and $N\mathcal{P}ol^\star(m,1)$ share important structural properties: The spaces $N\mathscr{SD}_g^\bullet(m,1)$ admit an m-fold multi-cyclic structure, see Proposition 5.1.17. There is a canonical map $\mathcal{P}ol_{\mathcal{SD}}\colon N\mathscr{SD}_g^\bullet(m,1)\to N\mathcal{P}ol^\bullet(m,1)$ of m-fold multi-cyclic spaces, that extends the restriction to the outgoing boundaries $\mathcal{P}ol_{\mathfrak{Rad}}\colon N\mathfrak{Rad}_g^\bullet(m,1)\to N\mathcal{P}ol^\bullet(m,1)$, see Theorem 5.1.21. The map $\mathcal{P}ol_{\mathcal{SD}}$ is investigated further in Section 5.2. Moreover, there is a desuspension theorem for spaces of Sullivan diagrams, see Theorem 5.1.22. Furthermore, using the methods of [BE17, Section 4], we show that the spaces of Sullivan diagrams with normalized boundaries admit homological stability, see Proposition 5.1.24.

5.1.1. Spaces of Sullivan diagrams with non-degenerate outgoing boundaries

Let $g\geq 0$, $m\geq 1$ and $\star\in\{\bullet,\circ\}$. Given a Sullivan diagram $(\Sigma;t)\in\mathscr{SD}_g^\star(m,1)$, each of its admissible edges has a length (determined by t) and is part of one of the m outgoing boundaries. We define the length of a fixed outgoing boundary as the sum of the lengths of the admissible edges belonging to this boundary cycle, see Definition 5.1.1 and Definition 5.1.3. The length of the outgoing boundaries defines a continuous map to the $(m-1)$-dimensional simplex, see Definition 5.1.5. An outgoing boundary cycle is said to be degenerate if its length is zero. This leads to a stratification of $\mathscr{SD}_g^\star(m,1)$ by the number of non-degenerate outgoing boundaries, see Definition 5.1.8. The space of Sullivan diagrams with non-degenerate outgoing boundaries $B\mathscr{SD}_g^\star(m,1)$ is the top stratum. It is open and dense. We define $N\mathscr{SD}_g^\star(m,1)\subset B\mathscr{SD}_g^\star(m,1)$ the space of Sullivan diagrams with normalized boundaries as the closed subspace where all outgoing boundaries have equal lengths, see Definition 5.1.10. Similarly to the spaces of polygons, the normalization of the outgoing boundaries of $B\mathscr{SD}_g^\star(m,1)$ defines a deformation retraction onto $N\mathscr{SD}_g^\star(m,1)$. By Proposition 5.1.15, the retraction and the length of the outgoing boundaries induce a homeomorphism $B\mathscr{SD}_g^\star(m,1)\cong N\mathscr{SD}_g^\star(m,1)\times\operatorname{int}(\Delta^{m-1})$. This homeomorphism will lead to an m-fold multi-cyclic structure on $N\mathscr{SD}_g^\bullet(m,1)$, see Proposition 5.1.17. Moreover, it is used to deduce the desuspension theorem for the spaces of Sullivan diagrams, see Theorem 5.1.22.

Definition 5.1.1. Let $g\geq 0$, $m\geq 1$ and $(\Sigma;t)\in\mathscr{SD}_g^\bullet(m,1)$ with $t\in\operatorname{int}(\Delta^k)$. Denote the labels of Σ by $L=\{L_1,\dots,L_m\}$. Its outgoing boundary cycles are ρ and we denote its set of cycles by $\operatorname{cyc}(\rho)=\{\sigma_1,\dots,\sigma_m\}$ such that $L_i\in\sigma_i$. The *length of the i-th outgoing boundary* is $l_i=l_i(\Sigma;t)=\sum_{j\in\sigma_i}t_j$ and the *length of* $(\Sigma;t)$ is the tuple $l(\Sigma;t)=(l_1,\dots,l_m)$.

Remark 5.1.2. Observe that $l_i>0$ if and only if $\rho_i\neq\langle L_i\rangle$ and that $\sum_{1\leq i\leq m}l_i=1$.

Definition 5.1.3. Let $g\geq 0$, $m\geq 1$ and $(\Sigma;t)\in\mathscr{SD}_g^\circ(m,1)$ with $t\in\operatorname{int}(\Delta^k)$. Denote the enumeration data of Σ by β_1 and β_2. Its non-degenerate boundary is ρ. The *length of the i-th outgoing boundary* is $l_i=l_i(\Sigma;t)=\sum_{j\in\beta_1^{-1}(i)}t_j$ and the *length of* $(\Sigma;t)$ is the tuple $l(\Sigma;t)=(l_1,\dots,l_m)$.

Remark 5.1.4. Observe that $l_i>0$ if and only if $i\in\operatorname{im}(\beta_1)$ and that $\sum_{1\leq i\leq m}l_i=1$.

Definition 5.1.5. On the space of Sullivan diagrams of genus g with m enumerated (un)parametrized outgoing boundaries, the *length of the outgoing boundaries* is the continuous map

$$l\colon \mathscr{SD}_g^\bullet(m,1) \to \Delta^{m-1}, \quad (\Sigma;t) \mapsto l(\Sigma;t) \tag{5.1}$$

respectively

$$l\colon \mathscr{SD}_g^\circ(m,1) \to \Delta^{m-1}, \quad (\Sigma;t) \mapsto l(\Sigma;t)\,. \tag{5.2}$$

Remark 5.1.6. The length of the outgoing boundaries l commutes with the forgetful map $\pi_\circ^\bullet\colon \mathscr{SD}_g^\bullet(m,1) \to \mathscr{SD}_g^\circ(m,1)$.

Remark 5.1.7. In Definition 4.2.10, we introduced the notion of degenerate (outgoing) boundary cycles of a Sullivan diagram. Given a point $(\Sigma;t) \in \mathscr{SD}_g^\bullet(m,1)$ or $\mathscr{SD}_g^\circ(m,1)$ with $t \in \operatorname{int}(\Delta^k)$, observe that the i-th boundary cycle of Σ is degenerate if and only if $l_i(\Sigma;t) = 0$. This leads to the following filtration.

Definition 5.1.8. Let $g \geq 0$, $m \geq 1$ and $\star \in \{\bullet, \circ\}$. The space of Sullivan diagrams of genus g with m (un)parametrized and enumerated outgoing boundaries is filtered by the closed subspaces of those Sullivan diagrams with at least $m-k$ degenerate outgoing boundaries

$$D_k\mathscr{SD}_g^\star(m,1) := l^{-1}(\operatorname{skel}_k \Delta^{m-1}) \quad \text{where } 0 \leq k \leq m\,. \tag{5.3}$$

The *space of Sullivan diagrams of genus g with m (un)parametrized, enumerated, partially degenerate outgoing boundaries* is the closed subspace

$$D\mathscr{SD}_g^\star(m,1) := l^{-1}(\partial\Delta^{m-1}) = D_{m-1}\mathscr{SD}_g^\star(m,1)\,. \tag{5.4}$$

The *space of Sullivan diagrams of genus g with m (un)parametrized enumerated, non-degenerate outgoing boundaries* is the open and dense subspace

$$B\mathscr{SD}_g^\star(m,1) := l^{-1}(\operatorname{int}(\Delta^{m-1})) = \mathscr{SD}_g^\star(m,1) - D\mathscr{SD}_g^\star(m,1)\,. \tag{5.5}$$

Remark 5.1.9. Let $g \geq 0$, $m \geq 1$ and $\star \in \{\bullet, \circ\}$. For $k = 0$, the space $D_k\mathscr{SD}_g^\star(m,1)$ is empty, for $k = 1$, it consists of exactly m discrete points and for $k > 1$, it is connected.

Definition 5.1.10. Let $g \geq 0$, $m \geq 1$ and $\star \in \{\bullet, \circ\}$. The *space of Sullivan diagrams of genus g with m (un)parametrized enumerated normalized boundaries* is the closed subspace of all Sullivan diagrams whose outgoing boundaries have equal length:

$$N\mathscr{SD}_g^\bullet(m,1) := l^{-1}(\tfrac{1}{m},\dots,\tfrac{1}{m}) \subset \mathscr{SD}_g^\bullet(m,1) \tag{5.6}$$

$$N\mathscr{SD}_g^\circ(m,1) := l^{-1}(\tfrac{1}{m},\dots,\tfrac{1}{m}) \subset \mathscr{SD}_g^\circ(m,1)\,. \tag{5.7}$$

On the space of Sullivan diagrams with non-degenerate outgoing boundaries, we introduce the normalization of the lengths of the outgoing boundaries analogously to the normalization of polygons, see Definition 2.3.8, Definition 2.3.10 and Proposition 2.3.13. To this end, we need a slight change in our notation for combinatorial Sullivan diagrams with non-degenerate boundary cycles.

Remark 5.1.11. Given a point $(\Sigma;t) \in B\mathscr{SD}_g^\bullet(m,1)$, denote the outgoing boundary cycles of Σ by ρ. It is clear that ρ has exactly m cycles, ρ does not have fixed points and each cycle permutes exactly one leaf in $L = \{L_1, \dots, L_m\}$ non-trivially. Therefore, each cycle $\rho_i = \langle L_i\ \rho_{i,0}\ \rho_{i,1}\ \dots\rangle \in \mathfrak{S}[n \sqcup L]$ describes a parametrized cyclic permutation $\tilde{\rho}_i = \langle \rho_{i,0}\ \rho_{i,1}\ \dots\rangle$. Using an enumeration of the leaves, ρ describes a parametrized enumerated permutation $\tilde{\rho} \in \mathfrak{S}^\bullet([n])$ with cycle decomposition $\tilde{\rho} = \tilde{\rho}_1 \cdots \tilde{\rho}_m$. Given two Sullivan diagrams $(\Sigma;t)$, $(\Sigma';t') \in B\mathscr{SD}_g^\bullet(m,1)$ with outgoing boundary cycles $\rho \neq \alpha$ it is clear that these give different parametrized enumerated permutations $\tilde{\rho} \neq \tilde{\alpha}$.

Given a point $(\Sigma;t) \in N\mathscr{SD}_g^\circ(m,1)$ and denoting the outgoing boundary cycles of Σ by ρ. It is clear that the enumeration data $\beta_1 \colon \mathrm{cyc}(\rho) \hookrightarrow \{1,2,\dots,m\}$ is a bijection. Therefore, ρ describes an unparametrized enumerated permutation $\tilde{\rho} \in \mathfrak{S}^\circ([n])$. As in the parametrized case, two outgoing boundary cycles $\rho \neq \alpha$ give different unparametrized enumerated permutations $\tilde{\rho} \neq \tilde{\alpha}$.

Notation 5.1.12. Let $g \geq 0$, $m \geq 1$ and $\star \in \{\bullet, \circ\}$. Given a Sullivan diagram $(\Sigma;t) \in B\mathscr{SD}_g^\star(m,1)$, we identify its outgoing boundary cycles ρ with its (un)parametrized enumerated permutation $\tilde{\rho} \in \mathfrak{S}^\star([n])$, see Remark 5.1.11.

Definition 5.1.13. Let $g \geq 0$, $m \geq 1$, $\star \in \{\bullet, \circ\}$ and $(\Sigma;t) \in B\mathscr{SD}_g^\star(m,1)$ with $t \in \mathrm{int}(\Delta^n)$. By $\rho = \rho_1 \cdots \rho_m$ we denote its outgoing boundary cycles. Each symbol $0 \leq i \leq n$ belongs to exactly one cycle of ρ, say $\rho_{j(i)}$, and we denote the length of the $j(i)$-th outgoing boundary by $l(i) := l_{j(i)}(\Sigma;t) = \sum_{k \in \rho_{j(i)}} t_k$. The *normalization of* $(\Sigma;t)$ is

$$r(\Sigma;t) := (\Sigma;t'), \quad t'_i = \frac{t_i}{m \cdot l(i)} \text{ for } 0 \leq i \leq n\,. \tag{5.8}$$

Definition 5.1.14. Let $g \geq 0$, $m \geq 1$, $\star \in \{\bullet, \circ\}$. The *normalization* is the continuous retraction

$$r \colon B\mathscr{SD}^\star(m,1) \to N\mathscr{SD}^\star(m,1) \tag{5.9}$$

induced by the normalization of simplices, see Definition 5.1.13.

Proposition 5.1.15. *Let $g \geq 0$, $m \geq 1$ and $\star \in \{\bullet, \circ\}$. The normalization and the length of the outgoing boundaries induce a homeomorphism*

$$r \times l \colon B\mathscr{SD}_g^\star(m,1) \cong N\mathscr{SD}_g^\star(m,1) \times \mathit{int}(\Delta^{m-1})\,. \tag{5.10}$$

Proof. Analogously to the proof of Proposition 2.3.13, the inverse of $r \times l$ is

$$((\Sigma;t'),l') \mapsto (\Sigma;t), \quad t_i = t'_i \cdot m \cdot l'_{j(i)} \tag{5.11}$$

where $j(i)$ denotes the number of the cycle to which i belongs, i.e., $i \in \rho_{j(i)}$. □

Remark 5.1.16. The m-dimensional torus $U(1)^m$ acts on $B\mathscr{SD}_g^\bullet(m,1)$ by rotating the leaves in their corresponding boundary cycles and is is clear that the orbit space is $B\mathscr{SD}_g^\circ(m,1)$, see Section 5.1.2. Observe that the normalization map $B\mathscr{SD}_g^\bullet(m,1) \to N\mathscr{SD}_g^\bullet(m,1)$ is equivariant with respect to this action and that the length of the outgoing boundaries is invariant under the action. Consequently, the homeomorphism $r \times l$ is an equivariant map (where $U(1)^m$ acts trivially on $\mathrm{int}(\Delta^{m-1})$).

5.1.2. Multi-cyclic structures and torus bundles

Recall that the m-dimensional torus acts on $N\mathcal{P}ol^\bullet(m,1)$ by rotating the m parametrization points. Moreover, the m parametrization points gave canonical barycentric coordinates in m enumerated simplices and this gave $N\mathcal{P}ol^\bullet(m,1)$ the structure of an m-fold multi-cyclic space, see Section 2.4. Regarding the leaves in a Sullivan diagram as parametrization point in its outgoing boundary, the methods used in Section 2.4 are used here to equip $N\mathscr{S}\mathscr{D}_g^\bullet(m,1)$ with the structure of an m-fold multi-cyclic space, see Proposition 5.1.17 and Discussion 5.1.18. The m-dimensional torus action if free by Proposition 5.1.19 and we have a canonical cell decomposition of the orbit space is $N\mathscr{S}\mathscr{D}_g^\circ(m,1)$, see Proposition 5.1.20. The restriction of a radial slit configuration to its outgoing boundaries factors through the spaces of Sullivan diagram with normalized boundaries, see Theorem 5.1.21.

Proposition 5.1.17. *Let $g \geq 0$ and $m \geq 1$. The space $N\mathscr{S}\mathscr{D}^\bullet(m,1)$ is homeomorphic to the realization of an m-fold multi-cyclic set whose multi-simplices of total degree k are the combinatorial Sullivan diagrams in*

$$\mathcal{SD}^\bullet(m,1)/D\mathcal{SD}^\bullet(m,1) \tag{5.12}$$

of degree $k+m-1$. Such a Sullivan diagram Σ has multi-degree $\underline{k} = (k_1,\dots,k_m)$ where k_i is the norm of the i-th cycle of the outgoing boundary cycles $\rho \in \mathfrak{S}^\bullet([k+m-1])$.

The face maps $d_{j,i}$ collapse the i-th admissible edge from the j-th outgoing boundary cycle, i.e.,

$$d_{j,i}(\Sigma) = d_{\rho_{j,i}}(\Sigma)\,, \tag{5.13}$$

the degeneracy maps $s_{j,i}$ are

$$s_{j,i}(\Sigma) = s_{\rho_{j,i}}(\Sigma) \tag{5.14}$$

and the cyclic operator in the j-th component is induced by cyclically permuting the leaf L_j in its cycle.

Proof. The proof is similar to the proof of Proposition 2.4.1. Let us denote the interior of an k-simplex by Δ^k for the sake of readability. The image of an open k-dimensional cell $\Sigma \times \Delta^k$ under the normalization map is the open multi-simplex

$$\Delta(\Sigma) := r(\Sigma \times \Delta^k) \cong \Sigma \times \Delta^{N(\rho_1)} \times \ldots \times \Delta^{N(\rho_m)} \tag{5.15}$$

of dimension $k-m+1$ where we regard $\rho = \langle \rho_{1,0}\ \ldots\rangle \cdots \langle \rho_{m,0}\ \ldots\rangle$ as permutation in $\mathfrak{S}^\bullet([k])$. Using the distinguished symbol of each cycle, we have canonical barycentric coordinates $(t_{j,0},\dots,t_{j,N(\rho_j)})_{j=1,\dots,m}$. From the construction it is clear that the i-th face in the j-coordinate of the multi-simplex $\Delta(\Sigma)$ is the multi-simplex $\Delta(D_{\rho_{j,i}}(\Sigma))$. With this at hand, it is easy to see that $N\mathscr{S}\mathscr{D}^\bullet(m,1)$ is the realization of the multi-simplicial space described in the Proposition.

Let $\Sigma = (\lambda, S_1,\dots,S_v) \in \mathcal{SD}^\bullet(m,1)/D\mathcal{SD}^\bullet(m,1)$ be a combinatorial Sullivan diagram and let $1 \leq j \leq m$. We define $t^j\Sigma := \tilde{\Sigma} := (\tilde{\lambda}, \tilde{S}_1, \dots \tilde{S}_v)$ algebraically. To this end, denote the outgoing boundary cycles of Σ by $\rho \in \mathfrak{S}([k] \cup L)$. The cycle decomposition of ρ is denoted by $\rho = \langle L_1\ \rho_{1,0}\ \ldots\ \rho_{1,k_1}\rangle \cdots \langle L_m\ \rho_{m,0}\ \ldots\ \rho_{m,k_m}\rangle$.

The outgoing boundary cycles of $\tilde{\Sigma}$ are defined as $\tilde{\rho} = \tilde{\rho}_1 \cdots \tilde{\rho}_m$ with $\tilde{\rho}_i = \rho_i$ for $i \neq j$ and $\tilde{\rho}_j = \langle \rho_{j,0}\ L_j\ \rho_{j,1}\ \dots\ \rho_{j,k_j} \rangle$. The ribbon structure of $\tilde{\Sigma}$ is defined as

$$\tilde{\lambda} = \langle 0\ \dots\ k \rangle \tilde{\rho}^{-1}\,. \tag{5.16}$$

We define the ghost surfaces of $\tilde{\Sigma}$ as follows. Since

$$\lambda^{-1} = \langle L_1\ \rho_{1,0}\ \dots \rangle \cdots \langle L_j\ \rho_{j,0}\ \rho_{j,1}\ \dots\ \rho_{j,k_j} \rangle \cdots \langle L_m\ \rho_{m,0}\ \dots \rangle \cdot \langle k\ \dots\ 0 \rangle \tag{5.17}$$

and

$$\tilde{\lambda}^{-1} = \langle L_1\ \rho_{1,0}\ \dots \rangle \cdots \langle \rho_{j,0}\ L_j\ \rho_{j,1}\ \dots\ \rho_{j,k_j} \rangle \cdots \langle L_m\ \rho_{m,0}\ \dots \rangle \cdot \langle k\ \dots\ 0 \rangle \tag{5.18}$$

differ only by the position of L_j in its cycle, deleting all leaves from λ and $\tilde{\lambda}$ gives the same permutation λ'. Observe that the permutation λ' has the same number of cycles as λ and $\tilde{\lambda}$: This is because $\rho(L_i) \neq L_i$ for any leaf L_i, since $\Sigma \notin D\mathcal{SD}^{\bullet}_g(m,1)$, and this implies $\lambda(L_i) \neq L_i$ for any leaf L_i. Therefore, deleting the leaves from λ and $\tilde{\lambda}$ induces a bijection

$$\Phi\colon\ \mathrm{cyc}(\lambda) \cong \mathrm{cyc}(\lambda') \cong \mathrm{cyc}(\tilde{\lambda})\,. \tag{5.19}$$

Denoting the ghost surfaces of $\Sigma = (\lambda, S_1, \dots, S_v)$ by $S_i = (g_i, m_i, A_i)$, the ghost surfaces of $\tilde{\Sigma} = (\tilde{\lambda}, \tilde{S}_1, \dots, \tilde{S}_v)$ are defined as

$$\tilde{S}_i = (g_i, m_i, \{\Phi(\alpha) \mid \alpha \in A_i\})\,. \tag{5.20}$$

A straight forward computation shows that these data equip $N\mathscr{S}\mathscr{D}^{\bullet}_g(m,1)$ with the structure of an m-fold multi-cyclic space. □

Discussion 5.1.18. Given a Sullivan diagram with parametrized enumerated normalized boundaries $\Sigma \in N\mathscr{S}\mathscr{D}^{\bullet}_g(m,1)$, each leaf L_i belongs to exactly one boundary cycle say ρ_i and each outgoing boundary cycle has length $\frac{1}{m}$, see Figure 5.1 for an example. Moving the m leaves clockwise in their respective boundary defines a free action by the m-dimensional torus on $N\mathscr{S}\mathscr{D}^{\bullet}_g(m,1)$. See Figure 5.2 for an example: The ribbon structure of Σ is $\lambda = \langle 0\ L_2 \rangle \langle 1\ 4 \rangle \langle 2\ 6\ 5 \rangle \langle 3\ L_1 \rangle$ and the outgoing boundary cycles are $\rho = \langle L_1\ 3\ 1\ 5\ 2 \rangle \langle L_2\ 0\ 4\ 6 \rangle$. The ghost surfaces are $S_1 = (0, 0, \{\langle 0\ L_2 \rangle, \langle 1\ 4 \rangle\})$, $S_2 = (0, 1, \{\langle 2\ 6\ 5 \rangle\})$ and $S_3 = (0, 0, \{\langle 3\ L_1 \rangle\})$. Given an angle $\alpha = e^{\frac{3}{4}\pi i} \in U(1)$, we move the leaf L_1 on its boundary cycle proportional to α. We denote the resulting Sullivan diagram by Σ_1. It is shown on the left of Figure 5.2.

Regarding the i-th leaf as a parametrization point in its boundary cycle leads to an m-fold multi-cyclic structure on $N\mathscr{S}\mathscr{D}^{\bullet}_g(m,1)$, see Proposition 5.1.17. The torus action described above agrees with the geometric realization of the multi-cyclic operation. Let us discuss the action of $\alpha = e^{\frac{3}{4}\pi i} \in U(1)$ on the first leaf of the Sullivan diagram Σ seen in Figure 5.1 in some detail. Using the multi-cyclic structure given in Proposition 5.1.17 and the formula in Proposition A.1.7, we obtain the Sullivan diagram $\alpha.\Sigma$ by in two steps: At first we split the admissible edge e_5 of Σ into two pieces (by using a degeneracy map s_5 which ties a disc to the splitting point). The outgoing boundary cycles of this Sullivan diagram $s_5(\Sigma)$ are $\langle L_1\ 3\ 1\ 5\ 6\ 2 \rangle \langle L_2\ 0\ 4\ 7 \rangle$. Rotating the leaf L_1 in its boundary cycle, the outgoing boundary cycles of $\alpha.\Sigma$ are $\langle L_1\ 6\ 2\ 3\ 1\ 5\ \rangle \langle L_2\ 0\ 4\ 7 \rangle$. This Sullivan diagram is denoted Σ_2 and it is shown on the right hand side of Figure 5.2.

Observe that the Sullivan diagrams Σ_1 and Σ_2 represent the same point in $N\mathscr{S}\mathscr{D}^{\bullet}_g(m,1)$ because $\Sigma_2 = s_2(\Sigma_1)$.

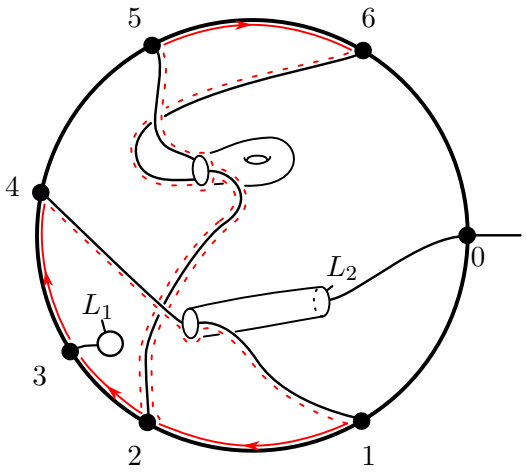

Figure 5.1.: The ribbon structure of this Sullivan diagram Σ is $\lambda = \langle 0\ L_2\rangle\langle 1\ 4\rangle\langle 2\ 6\ 5\rangle\langle 3\ L_1\rangle$ and the outgoing boundary cycles are $\rho = \langle L_1\ 3\ 1\ 5\ 2\rangle\langle L_2\ 0\ 4\ 6\rangle$. The ghost surfaces are $S_1 = (0, 0, \{\langle 0\ L_2\rangle, \langle 1\ 4\rangle\})$, $S_2 = (0, 1, \{\langle 2\ 6\ 5\rangle\})$ and $S_3 = (0, 0, \{\langle 3\ L_1\rangle\})$. We highlight the boundary cycle $\langle L_1\ 3\ 1\ 5\ 2\rangle$.

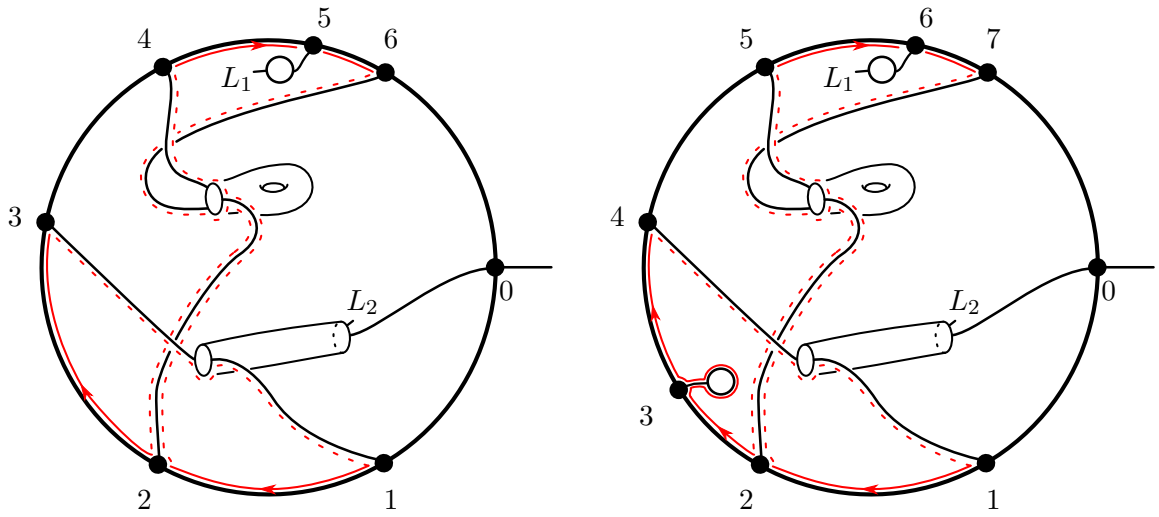

Figure 5.2.: Given the Sullivan diagram $\Sigma = (\lambda, S_1, S_2, S_3)$ seen in Figure 5.1 and the angle $\alpha = e^{\frac{3}{4}\pi i} \in U(1)$, we move the leaf L_1 (sitting on a disc between the admissible edges e_2 and e_3) in its boundary cycle (consisting of the admissible edges e_3, e_1, e_5 and e_2 in this order) by $\frac{3}{4}$ of the total length of the boundary cycle. The resulting Sullivan diagram $\Sigma_1 = \alpha.\Sigma$ is seen on the left.
Using the multi-cyclic structure and Proposition A.1.7 instead, we obtain the Sullivan diagram $\Sigma_2 = \alpha.\Sigma$ seen on the right. In $N\mathscr{S}\mathscr{D}_g^\bullet(m, 1)$ they represent the same point, because $\Sigma_2 = s_2(\Sigma_1)$.

Proposition 5.1.19. *Let $g \geq 0$ and $m \geq 1$. The induced action of the m-fold torus on the space $N\mathscr{SD}_g^\bullet(m,1)$ is free.*

Proof. The proof is similar to the proof of Proposition 2.4.4. Using Proposition A.1.7, the action of the i-th factor of the m-dimensional torus on $N\mathscr{SD}_g^\bullet(m,1)$ can be carried out explicitly: Let $\alpha \in U(1)$ be an arbitrary angle and let $\Sigma \in N\mathscr{SD}_g^\bullet(m,1)$. Then, $\alpha.\Sigma$ is obtained from Σ by moving the i-th leaf in its outgoing boundary cycle proportional to α. This is enough to proof the proposition. □

Proposition 5.1.20. *Let $g \geq 0$ and $m \geq 1$. The space of Sullivan diagrams $N\mathscr{SD}_g^\circ(m,1)$ admits a cellular decomposition whose k-dimensional cells are in one-to-one correspondence with the cellular generators of $\mathcal{SD}_g^\circ(m,1)/D\mathcal{SD}_g^\circ(m,1)$ of degree $k+m-1$. Forgetting the parametrizations defines a cellular quotient map $N\mathscr{SD}_g^\bullet(m,1) \to N\mathscr{SD}_g^\circ(m,1)$.*

Proof. The proof is similar to the proof of Proposition 2.4.5. The image of an open k-dimensional cell $\Sigma \times \Delta^k$ of $\mathscr{SD}_g^\circ(m,1)$ under the normalization map is the open cell

$$\Delta(\Sigma) := r(\Sigma \times \Delta^k) \cong \Sigma \times \Delta^{N(\rho_1)} \times \ldots \times \Delta^{N(\rho_m)} \tag{5.21}$$

of dimension $k-m+1$. Since ρ is an unparametrized enumerated permutation, the enumeration of the m simplices is determined by ρ but the barycentric coordinates in each simplex are only determined up to cyclic permutation. After choosing parametrizations for all open cells, the attaching maps of these cells are uniquely determined.

Forgetting the leaves defines the quotient map to the orbit space of the torus action and it is clear that this map sends (multi-simplicially non-degenerate) cells of $N\mathscr{SD}_g^\bullet(m,1)$ to (possibly multi-simplicially degenerate) cells of $N\mathscr{SD}_g^\circ(m,1)$. □

Given a radial slit configuration, the restriction to the outgoing boundaries defines a map to the spaces of polygons, see Definition 3.6.2 and Theorem 3.6.8. This map extends to the spaces of Sullivan diagrams with normalized boundaries.

Theorem 5.1.21. *Let $g \geq 0$, $m \geq 1$ and $\star \in \{\bullet, \circ\}$. Sending a Sullivan diagram $\Sigma \in N\mathscr{SD}_g^\star(m,1)$ to its outgoing boundary cycles $\rho \in \mathfrak{S}^\bullet([k])$ defines an m-fold multi-simplicial map*

$$\mathcal{P}ol_{\mathcal{SD}} \colon N\mathscr{SD}_g^\star(m,1) \to N\mathcal{P}ol^\star(m,1)\,. \tag{5.22}$$

It is an extension of the restriction to the outgoing boundaries $\mathcal{P}ol_{\mathfrak{Rad}} \colon N\mathfrak{Rad}_g^\star(m,1) \to N\mathcal{P}ol^\star(m,1)$, i.e., the following diagram of m-dimensional torus fibrations is commutative.

$$\begin{array}{ccccc}
\mathcal{P}ol_{\mathfrak{Rad}} \colon N\mathfrak{Rad}_g^\bullet(m,1) & \longrightarrow & N\mathscr{SD}_g^\bullet(m,1) & \xrightarrow{\mathcal{P}ol_{\mathcal{SD}}} & N\mathcal{P}ol^\bullet(m,1) \simeq EU(1)^m \\
\downarrow{\scriptstyle \pi_\circ^\bullet} & & \downarrow{\scriptstyle \pi_\circ^\bullet} & & \downarrow{\scriptstyle \pi_\circ^\bullet} \\
\mathcal{P}ol_{\mathfrak{Rad}} \colon N\mathfrak{Rad}_g^\circ(m,1) & \longrightarrow & N\mathscr{SD}_g^\circ(m,1) & \xrightarrow{\mathcal{P}ol_{\mathcal{SD}}} & N\mathcal{P}ol^\circ(m,1) \simeq BU(1)^m
\end{array} \tag{5.23}$$

Moreover, denoting the stabilization map of Sullivan diagrams by $\overline{\varphi}$, it holds $\mathcal{P}ol_{\mathcal{SD}} \circ \overline{\varphi} = \mathcal{P}ol_{\mathcal{SD}}$.

Proof. It is clear that sending $\Sigma = (\lambda, S_1, \ldots)$ of total degree k to $\rho \in \mathfrak{S}^\star([k+m-1])$ defines a map of m-fold multi-simplicial spaces, see Proposition 5.1.17 and Proposition 2.4.1. Moreover, $\mathcal{P}ol_{\mathcal{SD}} \circ \overline{\varphi} = \mathcal{P}ol_{\mathcal{SD}}$ follows from the definition of the stabilization map, see Definition 4.3.16.

In order to show that the diagram is commutatitive, recall that the restriction to the outgoing boundaries sends a radial slit configuration $(\sigma_0, \ldots, \sigma_q, \sigma^\star)$ to $\sigma^\star$. Moreover, by Section 4.3.2, the radial projection of $(\sigma_0, \ldots, \sigma_q, \sigma^\star)$ is a Sullivan diagram with outgoing boundary cycles $\rho = \sigma^\star$. □

In the next Sections, we investigate the map $\mathcal{P}ol_{\mathcal{SD}} \colon N\mathscr{S}\mathscr{D}^\star_g(m,1) \to N\mathcal{P}ol^\star(m,1)$ further and show that it is $(g-2)$-connected, see Theorem 5.2.11. This has interesting implications to the study of string topology, see Section 1.3.

5.1.3. The desuspension theorem for spaces of Sullivan diagrams

Recall that, for all $g \geq 0$, $m \geq 1$ and $\star \in \{\bullet, \circ\}$, the homeomorphism

$$\Phi \colon \mathscr{S}\mathscr{D}^\star(m,1) - D\mathscr{S}\mathscr{D}^\star(m,1) \cong N\mathscr{S}\mathscr{D}^\star(m,1) \times \mathrm{int}(\Delta^{m-1}) \tag{5.24}$$

lead to the cellular decomposition of $N\mathscr{S}\mathscr{D}^\star(m,1)$. The k-dimensional cells of $N\mathscr{S}\mathscr{D}^\star(m,1)$ are in canonical one-to-one correspondence to the $(k+m-1)$-dimensional cellular generators of $\mathcal{SD}^\star_g(m,1)/D\mathcal{SD}^\bullet_g(m,1)$. Extending the homeomorphism Φ to $\mathscr{S}\mathscr{D}^\star(m,1)/D\mathscr{S}\mathscr{D}^\star(m,1)$ yields our desuspension theorem for the spaces of Sullivan diagrams.

Theorem 5.1.22. *There are isomorphisms*

$$H_*(N\mathscr{S}\mathscr{D}^\bullet(m,1);\mathbb{Z}) \cong \Sigma^{-m+1} H_*(\mathscr{S}\mathscr{D}^\bullet(m,1), D\mathscr{S}\mathscr{D}^\bullet(m,1);\mathbb{Z}) \tag{5.25}$$

$$H_*(N\mathscr{S}\mathscr{D}^\circ(m,1);\mathbb{F}_2) \cong \Sigma^{-m+1} H_*(\mathscr{S}\mathscr{D}^\circ(m,1), D\mathscr{S}\mathscr{D}^\circ(m,1);\mathbb{F}_2) \tag{5.26}$$

Moreover, these isomorphisms commute with the stabilization maps $\overline{\varphi}$ and, with coefficients in $\mathbb{F}_2$, they commute with the forgetful map $\pi^\bullet_\circ$.

Proof. Given a combinatorial Sullivan diagram with non-degenerate boundaries, it is it has the same faces in $N\mathcal{SD}^\bullet_g(m,1)$ and $\Sigma^{-m+1}(\mathcal{SD}^\bullet_g(m,1)/D\mathcal{SD}^\bullet_g(m,1))$ up to signs. This proofs this desuspension theorem over $\mathbb{F}_2$. The integral desuspension theorem follows from introducing the correct signs, see Proposition 5.1.23. □

Proposition 5.1.23. *Let $g \geq 0$ and $m \geq 1$. The signs in* (2.69) *define an isomorphism of cellular chain complexes.*

$$\Phi \colon N\mathcal{SD}^\bullet_g(m,1) \to \Sigma^{-m+1}(\mathcal{SD}^\bullet_g(m,1)/D\mathcal{SD}^\bullet_g(m,1)) \tag{5.27}$$

$$(\lambda, S_1, \ldots, S_k) \mapsto \mathrm{sign}(\rho) \cdot (\lambda, S_1, \ldots, S_k)\,. \tag{5.28}$$

Proof. The proof of this proposition is analogous to the proof of Proposition 2.5.7. □

5.1.4. Homological stability for the spaces $N\mathscr{SD}^{\star}_{g}(m,1)$

Using a variation of the discrete Morse flows in [BE17], we obtain homological stability for the spaces of Sullivan diagrams with normalized boundaries.

Proposition 5.1.24. *Let $g \geq 0$, $m \geq 1$ and $\star \in \{\bullet, \circ\}$. The restriction of the stabilization map to the spaces of Sullivan diagrams with normalized boundaries*

$$\overline{\varphi}\colon N\mathscr{SD}^{\star}_{g}(m,1) \hookrightarrow N\mathscr{SD}^{\star}_{g+1}(m,1) \tag{5.29}$$

induces isomorphisms in homology in degrees $0 \leq * \leq g-2$.

Proof. The proof is analogous to the proof of the stability theorem of Sullivan diagrams, see Theorem 4.4.1. Using the same recipe as in [BE17, Section 4.4, Definition 4.27] we obtain a discrete Morse flow on $N\mathcal{SD}^{\star}_{g+1}(m,1)/N\mathcal{SD}^{\star}_{g}(m,1)$ such that all cells in degrees $0 \leq * \leq g-2$ are either collapsible or redundant. More precisely, using the notations introduced in [BE17, Section 4], a cell Σ is *collapsible* if has a surface S ending with an odd fence and every other surface S' of Σ with $ft(S) \neq 0$ and $end(S') > end(S) > 0$ has genus zero. Among the surfaces of Σ satisfying this condition, we pick S with $end(S)$ maximal. Then, the *redundant partner* of Σ is $d_{end(S)-1}(\Sigma)$. The arguments given in [BE17, Section 6.2], show that this defines a discrete Morse flow on $N\mathcal{SD}^{\star}_{g}(m,1)$ that is compatible with the stabilization map. From the construction it follows that $N\mathcal{SD}^{\star}_{g+1}(m,1)/N\mathcal{SD}^{\star}_{g}(m,1)$ does not have essential cells in degrees $0 \leq * \leq g-1$, i.e.,

$$H_*(N\mathcal{SD}^{\star}_{g+1}(m,1)/N\mathcal{SD}^{\star}_{g}(m,1)) = 0 \quad \text{for } 0 \leq * \leq g-1\,. \tag{5.30}$$

Now, the claim follows the long exact sequence of $\overline{\varphi}\colon N\mathcal{SD}^{\star}_{g}(m,1) \hookrightarrow N\mathcal{SD}^{\star}_{g+1}(m,1)$. □

Remark 5.1.25. We study the homomotopy type of these spaces of Sullivan diagrams in the subsequent sections. We will show that the stabilization maps are $(g-2)$-connected, see Theorem 5.2.11.

Note that the stabilization maps induces an inclusion of subspaces or subcomplexes. We define the spaces of Sullivan diagrams with stable genus as follows.

Definition 5.1.26. Let $g \geq 0$, $m \geq 1$ and $\star \in \{\bullet, \circ\}$. The *spaces of Sullivan diagrams of stable genus with m (un)parametrized enumerated (normalized) boundaries* are

$$\mathscr{SD}^{\star}_{\infty}(m,1) = \cup_{g\geq 0}\mathscr{SD}^{\star}_{g}(m,1) \tag{5.31}$$

respectively

$$N\mathscr{SD}^{\star}_{\infty}(m,1) = \cup_{g\geq 0}N\mathscr{SD}^{\star}_{g}(m,1) \tag{5.32}$$

Its cellular chain complex is denoted by

$$\mathcal{SD}^{\star}_{\infty}(m,1) = \cup_{g\geq 0}\mathcal{SD}^{\star}_{g}(m,1) \tag{5.33}$$

respectively

$$N\mathcal{SD}^{\star}_{\infty}(m,1) = \cup_{g\geq 0}N\mathcal{SD}^{\star}_{g}(m,1) \tag{5.34}$$

Abusing notation, the canonical inclusion into the (cellular complex of the) space of Sullivan diagrams with stable genus is denoted by $\overline{\varphi}$.

5.2. On the homotopy type of the spaces $N\mathscr{S}\mathscr{D}_g^\star(m,1)$

In this section, we study the homotopy type of the spaces of Sullivan diagram with normalized boundaries. Let us state our main result.

Theorem 5.2.11. *Let $m \geq 1$, $g \geq 0$ and consider the following maps of m-dimensional torus fibrations.*

$$\begin{array}{ccccc} N\mathscr{S}\mathscr{D}_g^\bullet(m,1) & \xhookrightarrow{\overline{\varphi}} & N\mathscr{S}\mathscr{D}_\infty^\bullet(m,1) & \xrightarrow{\mathcal{P}ol} & N\mathcal{P}ol^\bullet(m,1) \simeq EU(1)^m \\ \downarrow{\scriptstyle \pi_\circ^\bullet} & & \downarrow{\scriptstyle \pi_\circ^\bullet} & & \downarrow{\scriptstyle \pi_\circ^\bullet} \\ N\mathscr{S}\mathscr{D}_g^\circ(m,1) & \xhookrightarrow{\overline{\varphi}} & N\mathscr{S}\mathscr{D}_\infty^\circ(m,1) & \xrightarrow{\mathcal{P}ol} & N\mathcal{P}ol^\circ(m,1) \simeq BU(1)^m \end{array} \tag{5.35}$$

The stabilization maps $\overline{\varphi}$ are $(g-2)$-connected and the maps $\mathcal{P}ol$ are homotopy equivalences.

We obtain Theorem 5.2.11 by a careful study of the "unreduced cluster filtration" which is denoted by $Cl_p^- N\mathscr{S}\mathscr{D}_g^\bullet(m,1)$ of $N\mathscr{S}\mathscr{D}_g^\bullet(m,1)$. Our cluster filtration, introduced in Section 5.2.1, is an extension of Bödigheimer's filtration of the moduli spaces. The associated cluster spectral sequence is studied in Section 5.2.2 and we show that the inclusion $Cl_1^- N\mathscr{S}\mathscr{D}_g^\bullet(m,1) \subset N\mathscr{S}\mathscr{D}_g^\bullet(m,1)$ induces homology isomorphisms in the range $0 \leq * \leq g-2$, see Proposition 5.2.8. Then, in Section 5.2.3, we show that this inclusion and the map $\mathcal{P}ol\colon Cl_1^- N\mathscr{S}\mathscr{D}_g^\bullet(m,1) \to N\mathcal{P}ol_g^\bullet(m,1)$ are both $(g-2)$ connected. This will imply Theorem 5.2.11.

5.2.1. The (unreduced) cluster filtration of the spaces of Sullivan diagrams

In the section, we introduce the *cluster filtration* and the *unreduced cluster filtration*.

Definition 5.2.1. Let $\Sigma = (\lambda, S_1, \dots, S_v)$ be a combinatorial Sullivan diagram. A ghost surface S_i is a *non-essential cluster* if there exists $0 < r \leq \deg(\Sigma)$ and (in the parametrized case) a leaf L_j such that S_i is one of the following:

$$S_i = (0,0,\{\langle r\rangle\}) \text{ or } S_i = (0,0,\{\langle L_j\ r\rangle\})\,. \tag{5.36}$$

A ghost surface S_i is an *essential cluster* if it not a non-essential cluster.

Remark 5.2.2. Observe that the ghost surfaces $(0,0,\{\langle 0\rangle\})$ and $(0,0,\{\langle L_i\ 0\rangle\})$ are essential clusters. This is necessary in order to make the stabilization map and the torus action compatible with the cluster filtration, see below.

Definition 5.2.3. Let $\Sigma = (\lambda, S_1, \dots, S_v)$ be a combinatorial Sullivan diagram. The *cluster number of* Σ is its number of essential clusters:

$$c(\Sigma) = \#\{1 \leq i \leq v \mid S_i \text{ essential cluster}\}\,. \tag{5.37}$$

Let $g \geq 0$, $m \geq 1$ and $\star \in \{\bullet, \circ\}$. On the spaces of Sullivan diagrams (with normalized boundaries), the *cluster filtration* is

$$Cl_p\mathscr{S}\mathscr{D}_g^\star(m,1) = \{\Sigma \in \mathscr{S}\mathscr{D}_g^\star(m,1) \mid c(\Sigma) \leq p\} \tag{5.38}$$

respectively

$$Cl_p N\mathscr{S}\mathscr{D}_g^\star(m,1) = \{\Sigma \in N\mathscr{S}\mathscr{D}_g^\star(m,1) \mid c(\Sigma) \leq p\}\,. \tag{5.39}$$

Remark 5.2.4. Note that the cluster filtration of the spaces of Sullivan diagrams is induced by a cellular respectively multi-cyclic filtration of the underlying cellular respectively multi-cyclic structure. In particular, the torus action on $N\mathscr{S}\mathscr{D}_g^\bullet(m,1)$ restricts to each stratum of the cluster filtration.

Remark 5.2.5. Forgetting the parametrizations, the inclusion of the moduli space into its harmonic compactification and the stabilization maps respect the cluster filtration. More precisely, let $g \geq 0$, $m \geq 1$ and $\star \in \{\bullet, \circ\}$ and consider the following commutative diagram whose vertical maps are m-dimensional torus fibrations.

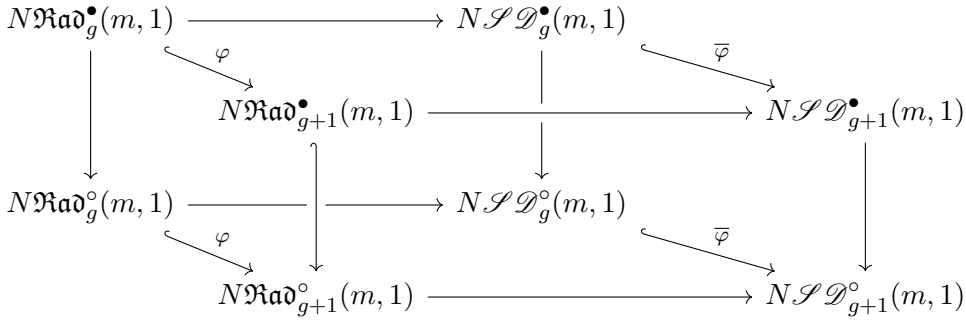

(5.40)

All maps in the diagram are compatible with the cluster filtration of radial slit configurations respectively Sullivan diagrams.

By construction, the cluster filtration behaves well with respect to the torus action. Clearly this is favorable for geometric arguments. However, in the study of the associated spectral sequence it leads to algebraic inconveniences. Therefore, we introduce the "unreduced" cluster filtration which is incompatible with the torus action but behaves well with our study of the spectral sequence.

Definition 5.2.6. Let $\Sigma = (\lambda, S_1, \ldots, S_v)$ be a combinatorial Sullivan diagram. The *unreduced cluster number of* Σ is its number of ghost surfaces:

$$c^-(\Sigma) = \#\{S_1, \ldots, S_v\} = v\,. \tag{5.41}$$

Let $g \geq 0$, $m \geq 1$ and $\star \in \{\bullet, \circ\}$. On the spaces of Sullivan diagrams (with possibly normalized boundaries), the *unreduced cluster filtration* is

$$Cl_p^- \mathscr{S}\mathscr{D}_g^\star(m,1) = \{\Sigma \in \mathscr{S}\mathscr{D}_g^\star(m,1) \mid c^-(\Sigma) \leq p\} \tag{5.42}$$

respectively

$$Cl_p^- N\mathscr{S}\mathscr{D}_g^\star(m,1) = \{\Sigma \in N\mathscr{S}\mathscr{D}_g^\star(m,1) \mid c^-(\Sigma) \leq p\}\,. \tag{5.43}$$

Remark 5.2.7. Forgetting the parametrizations and the stabilization maps respect the unreduced cluster filtration. More precisely, given $g \geq 0$, $m \geq 1$ and $\star \in \{\bullet, \circ\}$, all maps in the commutative diagrams below are compatible with the unreduced cluster filtration.

$$\begin{array}{ccc} N\mathscr{S}\mathscr{D}_g^\bullet(m,1) & \xrightarrow{\overline{\varphi}} & N\mathscr{S}\mathscr{D}_{g+1}^\bullet(m,1) \\ \downarrow & & \downarrow \\ N\mathscr{S}\mathscr{D}_g^\circ(m,1) & \xrightarrow{\overline{\varphi}} & N\mathscr{S}\mathscr{D}_{g+1}^\circ(m,1) \end{array} \qquad \begin{array}{ccc} \mathscr{S}\mathscr{D}_g^\bullet(m,1) & \xrightarrow{\overline{\varphi}} & \mathscr{S}\mathscr{D}_{g+1}^\bullet(m,1) \\ \downarrow & & \downarrow \\ \mathscr{S}\mathscr{D}_g^\circ(m,1) & \xrightarrow{\overline{\varphi}} & \mathscr{S}\mathscr{D}_{g+1}^\circ(m,1) \end{array} \tag{5.44}$$

5.2.2. The cluster spectral sequence of $N\mathscr{S}\mathscr{D}_g^\bullet(m,1)$

In this section, we investigate the unreduced cluster spectral sequence of $N\mathscr{S}\mathscr{D}_g^\bullet(m,1)$ and obtain the following result.

Proposition 5.2.8. *Let $m \geq 1$, $g \geq 0$ and consider the following diagrams of inclusions of subspaces.*

$$\begin{array}{ccc} Cl_1^- N\mathscr{S}\mathscr{D}_g^\bullet(m,1) & \xhookrightarrow{Cl_1^-\overline{\varphi}_g} & Cl_1^- N\mathscr{S}\mathscr{D}_\infty^\bullet(m,1) \\ \downarrow{\scriptstyle \alpha_g} & & \downarrow{\scriptstyle \alpha_\infty} \\ N\mathscr{S}\mathscr{D}_g^\bullet(m,1) & \xhookrightarrow{\overline{\varphi}_g} & N\mathscr{S}\mathscr{D}_\infty^\bullet(m,1) \end{array} \tag{5.45}$$

The maps α_g, $\overline{\varphi}_g$ and $Cl_1^-\overline{\varphi}_g$ induce isomorphisms in homology in the range $* \leq g-2$. The map α_∞ is a quasi-isomorphism.

Proof. Recall that, by Proposition 5.1.24, the stabilization map $\overline{\varphi}_g$ induces homology isomorphisms in the claimed range. Using the definition of a combinatorial Sullivan diagram with exactly one ghost surface, note that $Cl_1^-\overline{\varphi}\colon Cl_1^- N\mathscr{S}\mathscr{D}_g^\bullet(m,1) \hookrightarrow Cl_1^- N\mathscr{S}\mathscr{D}_\infty^\bullet(m,1)$ induces a map of cellular chain complexes that is an isomorphism in the claimed range. It remains to show that α_∞ is a quasi isomorphism.

By $E^r_{p,q}$ we denote the spectral sequence associated to the unreduced cluster filtration of $N\mathscr{S}\mathscr{D}_\infty^\bullet(m,1)$. Note that $E^0_{1,*} = (Cl_1^- N\mathcal{SD}_\infty^\bullet(m,1))_{*+1}$. For every $p \neq 1$, the p-th row $E^0_{p,*}$ is acyclic by Lemma 5.2.10. Consequently α_∞ induces an isomorphism:

$$H_{*+1}(Cl_1^- N\mathcal{SD}_\infty^\bullet(m,1);\mathbb{Z}) \cong E^1_{1,*} = E^\infty_{1,*} \cong H_{*+1}(N\mathcal{SD}_\infty^\bullet(m,1);\mathbb{Z})\,. \tag{5.46}$$

□

Definition 5.2.9. Let $m \geq 1$ and $N_* := N\mathcal{SD}_\infty^\bullet(m,1)$. By $E^r_{p,q}$ we denote the *cluster spectral sequence* associated to the unreduced cluster filtration of $N\mathcal{SD}_\infty^\bullet(m,1)$ with zero-th page $E^0_{p,q} = Cl_p^- N_{p+q}/Cl_{p-1}^- N_{p+q}$.

Lemma 5.2.10. *For every $p > 1$, the chain complex $E^0_{p,*}$ is acyclic .*

Proof. We construct a homotopy h from the identity to zero. Let $\Sigma = (\lambda, S_1, \dots, S_p)$ be a Sullivan diagram in $E^0_{p,*}$ such that S_1 is attached to the vertex zero. Note that S_1 is the unique ghost surface with infinite genus. Since $p \geq 2$, there is an attaching point $i(\Sigma)$ of minimal index such that S_1 is attached to $i(\Sigma)$ but not to $i(\Sigma)+1$. See the left hand side of Figure 5.3 for a local picture. Then, since S_1 has infinite genus, Σ is the face of the Sullivan diagram $h'(\Sigma)$ seen on the right hand side of Figure 5.3. Algebraically, $h'(\Sigma) = (\lambda', S_1', \dots S_p')$ is defined as follows. The ribbon structure λ' is obtained from λ by increasing all symbols $j > i(\Sigma)$ by one and then introducing the new fixed point $\langle i(\Sigma)+1\rangle$. This induces a canonical injection $\Phi\colon \mathrm{cyc}(\lambda) \hookrightarrow \mathrm{cyc}(\lambda')$ and we define the ghost surfaces of Σ' by

$$S_1' = (0, \infty, \Phi(A_1) \cup \{\langle i(\Sigma)+1\rangle\}) \tag{5.47}$$

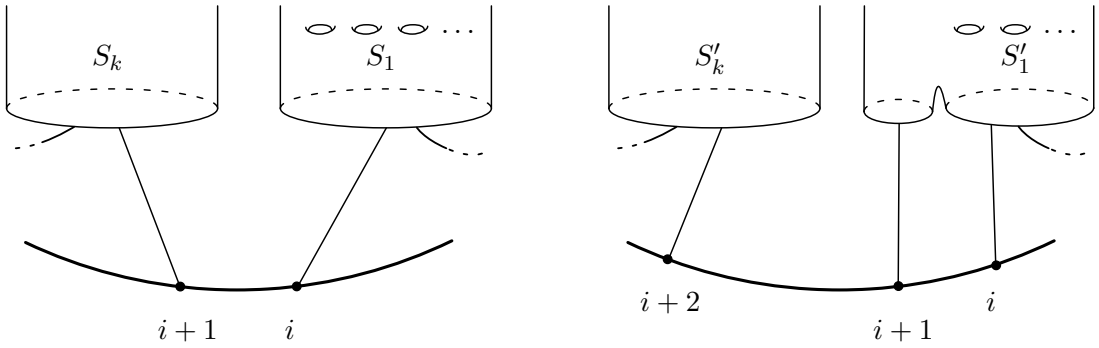

Figure 5.3.: On the left, we show the local picture around the attaching points $i = i(\Sigma)$ and $i+1$. Hereby, $i+1$ is the first vertex to which the ghost surface of infinite genus is not attached to. On the right, we show the local picture around the attaching points i, $i+1$ and $i+2$ of Σ'. By construction, we have $\Sigma = d_i(\Sigma')$.

and for $j > 1$ it is

$$S'_j = (0, g_i, \Phi(A_j))\,. \tag{5.48}$$

In order to define the homotopy $h(\Sigma) = \pm h'(\Sigma)$, we need to introduce the correct signs. Using Proposition 5.1.23, we can assume that the sign of the j-th face of a given Sullivan diagram is $(-1)^j$. With this sign convention, the homotopy is defined as

$$h(\Sigma) = (-1)^{i(\Sigma)} h'(\Sigma)\,. \tag{5.49}$$

Now, for a Sullivan diagram Σ of degree k with $i = i(\Sigma)$ we compute:

$$\begin{aligned} dh(\Sigma) &= \sum_{0\le j\le k+1} (-1)^{j+i} d_j h'\Sigma && (5.50)\\ &= \sum_{j<i} (-1)^{j+i} d_j h'\Sigma + \Sigma + \sum_{j>i} (-1)^{j+i} d_j h'\Sigma && (5.51)\\ &= \Sigma + \sum_{j<i} (-1)^{j+i} d_j h'\Sigma + \sum_{j>i} (-1)^{j+i} d_j h'\Sigma && (5.52) \end{aligned}$$

By definition of $h'\Sigma$ we have $d_j h'\Sigma = h' d_j \Sigma$ if $j < i$. By definition of the cluster spectral sequence, we delete all faces that merge two distinct surfaces. Therefore $d_{i+1} h'\Sigma = 0$, $h' d_i \Sigma = 0$ and $d_j h'\Sigma = h' d_{j-1}\Sigma$ for $j > i+1$.

$$\begin{aligned} &= \Sigma + \sum_{j<i} (-1)^{j+i} h' d_j \Sigma + \sum_{j>i} (-1)^{j+i} h' d_{j-1} \Sigma && (5.53)\\ &= \Sigma + \sum_{j<i} (-1)^{j+i} h' d_j \Sigma + \sum_{j\ge i} (-1)^{j+1+i} h' d_j \Sigma && (5.54) \end{aligned}$$

By definition of $h d_j \Sigma$, the sign of $h' d_j \Sigma$ is $(-1)^{i-1}$ if $j < i$ and $(-1)^i$ for $j \ge i$.

$$\begin{aligned} &= \Sigma + \sum_{j<i} (-1)^{j+1} h d_j \Sigma + \sum_{j\ge i} (-1)^{j+1} h d_j \Sigma && (5.55)\\ &= \Sigma - h d(\Sigma) && (5.56) \end{aligned}$$

This finishes the proof. □

5.2.3. The homotopy type of $N\mathscr{SD}^{\bullet}_{\infty}(m,1)$ and $N\mathscr{SD}^{\circ}_{\infty}(m,1)$

In this section, we detect the (stable) homotopy types of $N\mathscr{SD}^{\bullet}_{g}(m,1)$ and $N\mathscr{SD}^{\circ}_{g}(m,1)$.

Theorem 5.2.11. *Let $m \geq 1$, $g \geq 0$ and consider the following maps of m-dimensional torus fibrations.*

$$\begin{array}{ccccc} N\mathscr{SD}^{\bullet}_{g}(m,1) & \xhookrightarrow{\overline{\varphi}} & N\mathscr{SD}^{\bullet}_{\infty}(m,1) & \xrightarrow{\mathcal{P}ol} & N\mathcal{P}ol^{\bullet}(m,1) \simeq EU(1)^m \\ \downarrow{\scriptstyle \pi^{\bullet}_{\circ}} & & \downarrow{\scriptstyle \pi^{\bullet}_{\circ}} & & \downarrow{\scriptstyle \pi^{\bullet}_{\circ}} \\ N\mathscr{SD}^{\circ}_{g}(m,1) & \xhookrightarrow{\overline{\varphi}} & N\mathscr{SD}^{\circ}_{\infty}(m,1) & \xrightarrow{\mathcal{P}ol} & N\mathcal{P}ol^{\circ}(m,1) \simeq BU(1)^m \end{array} \tag{5.57}$$

The stabilization maps $\overline{\varphi}$ are $(g-2)$-connected and the maps $\mathcal{P}ol$ are homotopy equivalences.

Proof. To begin with, consider the following restiction of upper row of the diagram above:

$$\begin{array}{ccccc} Cl_1^- N\mathscr{SD}^{\bullet}_{g}(m,1) & \xhookrightarrow{Cl_1^-\overline{\varphi}_g} & Cl_1^- N\mathscr{SD}^{\bullet}_{\infty}(m,1) & \xrightarrow{Cl_1^-\mathcal{P}ol_{\infty}} & N\mathcal{P}ol^{\bullet}(m,1) \simeq EU(1)^m \\ \downarrow{\scriptstyle \alpha_g} & & \downarrow{\scriptstyle \alpha_{\infty}} & & \| \\ N\mathscr{SD}^{\bullet}_{g}(m,1) & \xhookrightarrow{\overline{\varphi}_g} & N\mathscr{SD}^{\bullet}_{\infty}(m,1) & \xrightarrow{\mathcal{P}ol_{\infty}} & N\mathcal{P}ol^{\bullet}(m,1) \simeq EU(1)^m \end{array} \tag{5.58}$$

Recall that, by Proposition 5.2.8, the maps α_g, $\overline{\varphi}_g$ and $Cl_1^-\overline{\varphi}_g$ induce isomorphisms in homology in the range $* \leq g-2$ and α_{∞} is a quasi-isomorphism. For $g \geq 2$, the inclusions α_g and α_{∞} induces a surjection on fundamental groups by Lemma 5.2.12. But, $Cl_1^- N\mathscr{SD}^{\bullet}_{g}(m,1)$ and $Cl_1^- N\mathscr{SD}^{\bullet}_{\infty}(m,1)$ are simply connected by Lemma 5.2.13. It follows that α_g is $(g-2)$-connected and that α_{∞} is a homotopy equivalence by the relative Hurewicz theorem.

By commutativity of the above diagram and by Theorem 5.1.21 we have:

$$Cl_1^-\mathcal{P}ol_{\infty} \circ Cl_1^-\overline{\varphi}_g = (\mathcal{P}ol_{\infty} \circ \overline{\varphi}_g) \circ \alpha_g = \mathcal{P}ol_g \circ \alpha_g \,. \tag{5.59}$$

Now, by Lemma 5.2.13, $\mathcal{P}ol_g \circ \alpha_g$ is $(g-1)$-connected and $Cl_1^-\mathcal{P}ol_{\infty} = \mathcal{P}ol_{\infty} \circ \alpha_{\infty}$ is a homotopy equivalence. In the preceding paragraph, we have seen that α_{∞} is a homotopy equivalence and we conclude that $\mathcal{P}ol_{\infty}$ is also a homotopy equivalence. Till this point, we have seen that α_g and $Cl_1^-\mathcal{P}ol_{\infty} \circ Cl_1^-\overline{\varphi}_g$ are $(g-2)$-connected and that $\mathcal{P}ol_{\infty}$ is a homotopy equivalence. It follows that $\overline{\varphi}_g$ is also $(g-2)$-connected.

The unparametrized case follows from the study of the long exact sequences of the m-dimensional torus fibrations $\pi^{\bullet}_{\circ}$. □

Lemma 5.2.12. *Let $1 \leq g \leq \infty$, $m \geq 1$ and $\star \in \{\bullet, \circ\}$. The inclusion*

$$Cl_1^- N\mathscr{SD}^{\star}_{g}(m,1) \hookrightarrow N\mathscr{SD}^{\star}_{g}(m,1) \tag{5.60}$$

induces a surjective homomorphism on fundamental groups.

Proof. Note that $Cl_1^- N\mathscr{SD}^{\star}_{g}(m,1) \subset N\mathscr{SD}^{\star}_{g}(m,1)$ is a cellular subcomplex. The one-dimensional cells not in $Cl_1^- N\mathscr{SD}^{\star}_{g}(m,1)$ are given by Sullivan diagrams Σ with exactly two ghost surfaces, see Figure 5.4. We denote the ghost surface attached to the vertex

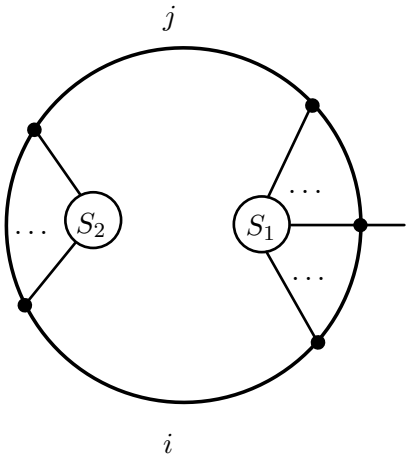

Figure 5.4.: We show a 1-cell $\Sigma = (\lambda, S_1, S_2)$ in the space of Sullivan diagram with normalized boundaries while suppressing the leaves and the genus of the two ghost surfaces. The cycles of ρ are all transpositions $\rho_r = \langle L_r\ i_r \rangle$ with the exception of a single three-cycle $\rho_v = \langle L_v\ i\ j \rangle$ or $\rho_v = \langle L_v\ j\ i \rangle$.

0 by S_1 and the other ghost surfaces is S_2. Assume that S_1 has positive genus. Then, the faces of the 2-cell seen on the left hand side of Figure 5.5 are Σ and two 1-cells in $Cl_1^- N\mathscr{S}\mathscr{D}_g^\star(m,1)$. Otherwise, if S_1 has genus zero, S_2 has to have positive genus (since $g \geq 1$). As before, the faces of the 2-cell seen on the right hand side of Figure 5.5 are Σ and two 1-cells in $Cl_1^- N\mathscr{S}\mathscr{D}_g^\star(m,1)$. This is enough to proof the Lemma. □

Lemma 5.2.13. *Let $1 \leq g \leq \infty$ and $m \geq 1$. The composition*

$$Cl_1^- \mathcal{P}ol_g \colon Cl_1^- N\mathscr{S}\mathscr{D}_g^\bullet(m,1) \xhookrightarrow{\alpha_g} N\mathscr{S}\mathscr{D}_g^\bullet(m,1) \xrightarrow{\mathcal{P}ol_g} N\mathcal{P}ol^\bullet(m,1) \simeq EU(1)^m \quad (5.61)$$

is $(g-1)$-connected. In particular, $Cl_1^- N\mathscr{S}\mathscr{D}_g^\bullet(m,1)$ is $(g-1)$-connected.

Proof. Recall that $\mathcal{P}ol \colon N\mathscr{S}\mathscr{D}_g^\bullet(m,1) \to N\mathcal{P}ol^\bullet(m,1)$ is defined by sending Σ to its outgoing boundary cycles ρ.

Observe that $Cl_1^- N\mathscr{S}\mathscr{D}_g^\bullet(m,1)$ is the realization of a semi-multi-simplicial subset of the multi-simplicial set underlying $N\mathscr{S}\mathscr{D}_g^\bullet(m,1)$: The multi-simplices in $Cl_1^- N\mathscr{S}\mathscr{D}_g^\bullet(m,1)$ are Sullivan diagrams with one surface and this condition is clearly closed under taking faces. However, every degeneracy map increase the number of ghost surfaces by one. Observe further that, $\mathcal{P}ol \colon Cl_1^- N\mathscr{S}\mathscr{D}_g^\bullet(m,1) \to N\mathcal{P}ol^\bullet(m,1)$ factors through the fat realization $N\mathbb{P}ol_g^\bullet(m,1)$ of $N\mathcal{P}ol^\bullet(m,1)$:

$$Cl_1^- \mathcal{P}ol_g \colon Cl_1^- N\mathscr{S}\mathscr{D}_g^\bullet(m,1) \to N\mathbb{P}ol_g^\bullet(m,1) \simeq N\mathcal{P}ol_g^\bullet(m,1)\,. \quad (5.62)$$

Given a combinatorial Sullivan diagrams with non-degenerate boundaries and a single surface, i.e., $\Sigma = (\lambda, S_1)$, note that $S_1 = (0, g_1, A_1)$ is uniquely determined by ρ and the genus of the Sullivan diagram. Therefore, $Cl_1^- \mathcal{P}ol \colon Cl_1^- N\mathscr{S}\mathscr{D}_g^\bullet(m,1) \to N\mathbb{P}ol_g^\bullet(m,1)$ is the realization of the injective semi-multi-simplicial map

$$\Phi \colon \Sigma = (\lambda, S_1) \mapsto \rho\,. \quad (5.63)$$

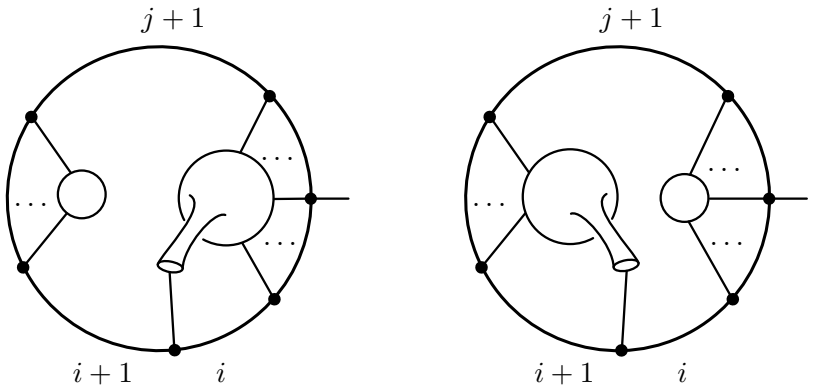

Figure 5.5.: We show two 2-cells in the space of Sullivan diagram with normalized boundaries while suppressing the leaves and the genus of the two ghost surfaces. On the left hand side, we show a Sullivan diagram whose right ghost surface has two boundary components and whose left ghost surface has one boundary component. On the right hand side, we show such a Sullivan diagram whose right ghost surface has one boundary components and whose left ghost surface has two boundary component.

It is enough to show that Φ is bijective in total degrees $0 \leq * \leq g$. Given a permutation ρ in $N\mathbb{P}ol_g^\bullet(m,1)$ of total degree $k \leq g$ there is a unique Sullivan diagram $\Sigma = (\lambda, S_1)$ of some genus g', with m normalized boundaries, with outgoing boundary cycles ρ and with ghost surface $S_1 = (0, 0, \mathrm{cyc}(\lambda))$. The genus g' of Σ is determined by taking k (multi-)faces of Σ leading to a Sullivan diagram $\Sigma' = (\lambda', S_1')$ of total degree zero. Then g' is the genus of S_1'. In this process of taking k faces of Σ, the genus of the unique ghost surface can only increase by one under a face map, i.e., $g' \leq k$. Therefore, the Sullivan diagram $(\lambda, (0, k-g', \mathrm{cyc}(\lambda))$ in $Cl^-1N\mathscr{S}\mathscr{D}_g^\bullet(m,1)$ is mapped to ρ in $N\mathbb{P}ol_g^\bullet(m,1)$. $\square$

6

The hamonic compactification $\overline{\mathfrak{M}}_g^\bullet(m,1)$ is highly connected

In this chapter, we show that the spaces of Sullivan diagrams with parametrized enumerated boundaries $\mathscr{SD}_g^\bullet(m,1)$ are highly connected with respect to the genus and the number of outgoing boundary curves. Using the homotopy equivalence of [EK14], see also Proposition 4.3.2, we regard the spaces $\mathscr{SD}_g^\bullet(m,1)$ as the harmonic compactification of the moduli spaces, i.e., $\overline{\mathfrak{M}}_g^\bullet(m,1) \simeq \mathscr{SD}_g^\bullet(m,1)$. Consequently, the harmonic compactifications $\overline{\mathfrak{M}}_g^\bullet(m,1)$ are highly connected with respect to the genus and the number of outgoing boundary curves.

Theorem 6.1. *Let $g \geq 2$ and $m \geq 1$ or $g \geq 0$ and $m \geq 3$. The spaces of Sullivan diagrams of genus g with m parametrized enumerated boundaries is $(g+m-2)$-connected. In particular, $\mathscr{SD}_\infty^\bullet(m,1)$ and $\overline{\mathfrak{M}}_\infty^\bullet(m,1)$ are contractible.*

Proof. The space $\mathscr{SD}_\infty^\bullet(m,1)$ is simply connected by Proposition 6.3. By Proposition 6.4, the inclusion

$$Cl_1^- \mathscr{SD}_\infty^\bullet(m,1) \hookrightarrow \mathscr{SD}_\infty^\bullet(m,1) \tag{6.1}$$

is a quasi isomorphism. But $Cl_1^- \mathscr{SD}_\infty^\bullet(m,1)$ is acyclic by Lemma 6.8. We conclude that $\mathscr{SD}_\infty^\bullet(m,1)$ is contractible. Finally, the inclusion $\mathscr{SD}_g^\bullet(m,1) \to \mathscr{SD}_\infty^\bullet(m,1) \simeq *$ is $(g+m-2)$-connected by Theorem 4.4.1, Proposition 6.3 and the relative Hurewicz theorem. □

The remainder of this chapter is devoted to the Lemmas and Propositions used in the proof of Theorem 6.1.

Lemma 6.2. *Let $1 \leq g \leq \infty$, $m \geq 1$ and $\star \in \{\bullet, \circ\}$. The inclusion*

$$Cl_1^- \mathscr{SD}_g^\star(m,1) \hookrightarrow \mathscr{SD}_g^\star(m,1) \tag{6.2}$$

induces a surjective homomorphism on fundamental groups.

Proof. The proof is similar to the proof of Lemma 5.2.12. The 1-cells of $\mathscr{SD}_g^\star(m,1)$ that are not in $Cl_1^- \mathscr{SD}_g^\star(m,1)$ are the Sullivan diagrams with two ghost surfaces, see the left hand side of Figure 6.1. Given such a Sullivan diagram $\Sigma = (\lambda, S_1, S_2)$, one of the two

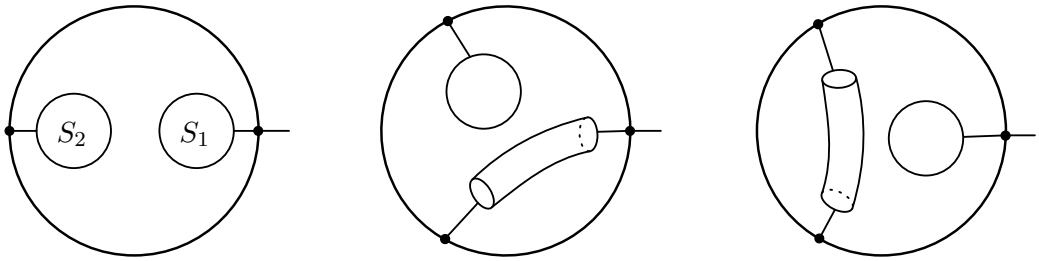

Figure 6.1.: We show three cells with two ghost surfaces while suppressing the leaves and the genus of the ghost surfaces. On the left, we show a 1-cell Σ. One of the ghost surfaces has to have positive genus since $g \geq 1$. On the middle and on the right, we show cofaces Σ' of Σ.

ghost surfaces has to have positive genus since $g \geq 1$. Therefore, Σ is a face of a Sullivan diagram Σ' seen in the middle or on the right hand side of Figure 6.1. The other two faces of Σ' are 1-cells in $Cl_1^- \mathscr{SD}_g^\star(m,1)$. This is enough to proof the Lemma. □

Proposition 6.3. *Let $2 \leq g \leq \infty$ and $m \geq 1$ or $0 \leq g \leq \infty$ and $m \geq 3$. Then, the space of Sullivan diagrams $\mathscr{SD}_g^\bullet(m,1)$ is simply connected.*

Proof. For $m = 1$, we have $\mathscr{SD}_g^\bullet(m,1) = N\mathscr{SD}_g^\bullet(m,1)$ and the claim follows from Lemma 5.2.12 and Lemma 5.2.13. For $m > 2$, the claim follows from Theorem 4.4.2.

It remains to study the case $m = 2$. Using Lemma 6.2, it enough to show that $Cl_1^- \mathcal{SD}_g^\bullet(m,1)$ has trivial fundamental group. To this end, note that a Sullivan diagram with a single ghost surface is completely determined by its outgoing boundary cycles ρ. This leads to the following partition of the 1-cells of $Cl_1^- \mathcal{SD}_g^\bullet(m,1)$ into three groups, see Figure 6.2. A 1-cell $\Sigma \in Cl_1^- \mathcal{SD}_g^\bullet(m,1)$ is of type α_1, α_2 respectively β if its outgoing boundary cycles ρ are $\rho(\alpha_1) = \langle L_i\ 0\ 1\rangle\langle L_j\rangle$, $\rho(\alpha_2) = \langle L_i\ 1\ 0\rangle\langle L_j\rangle$ respectively $\rho(\beta) = \langle L_i\ 0\rangle\langle L_j\ 1\rangle$.

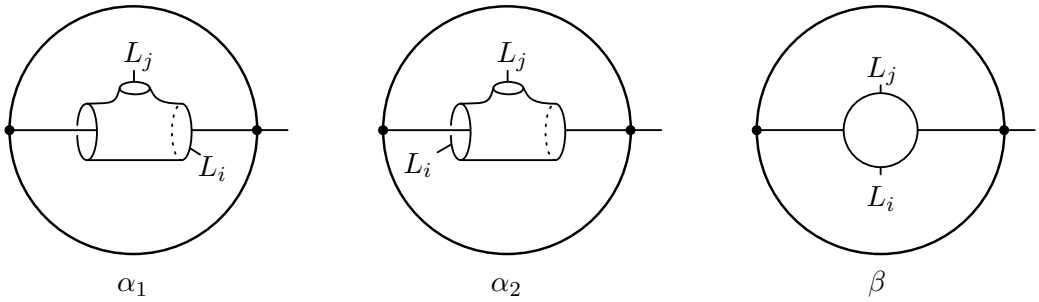

Figure 6.2.: We show the three types of 1-cells in $Cl_1^- \mathcal{SD}_g^\bullet(m,1)$ while suppressing the genus of the ghost surface. We denote the types by α_1, α_2 and β and the corresponding outgoing boundary cycles are $\rho(\alpha_1) = \langle L_i\ 0\ 1\rangle\langle L_j\rangle$, $\rho(\alpha_2) = \langle L_i\ 1\ 0\rangle\langle L_j\rangle$ respectively $\rho(\beta) = \langle L_i\ 0\rangle\langle L_j\ 1\rangle$.

Every cell of type α_1 is a loop in $Cl_1^- \mathcal{SD}_g^\bullet(m,1)$ because $D_0(\rho(\alpha_1)) = D_1(\rho(\alpha_1)) = \langle L_i\ 0\rangle\langle L_j\rangle$. This loop is filled by the 2-cell seen on the left of Figure 6.3: Its outgoing boundary cycles are $\tilde{\rho} = \langle L_i\ 0\ 1\ 2\rangle\langle L_j\rangle$ and we have $D_0(\tilde{\rho}) = D_1(\tilde{\rho}) = D_2(\tilde{\rho}) = \langle L_i\ 0\ 1\rangle\langle L_j\rangle = \rho(\alpha_1)$.

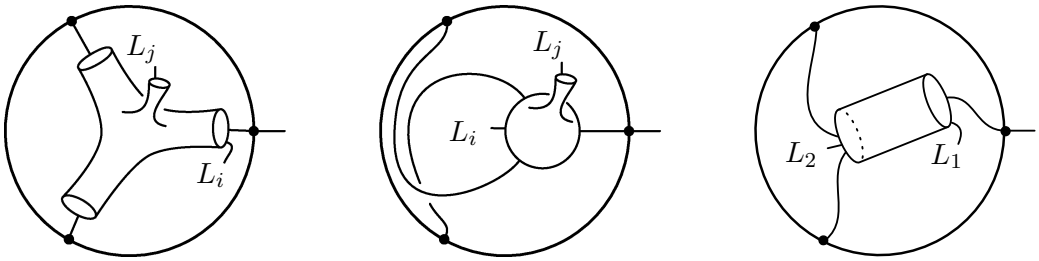

Figure 6.3.: We show three 2-cells in $Cl_1^- \mathcal{SD}_g^\bullet(m,1)$ while suppressing the genus of the ghost surface. On the left, the outgoing boundary cycles are $\langle L_i\ 0\ 1\ 2\rangle\langle L_j\rangle$. In the middle, the outgoing boundary cycles are $\langle L_i\ 2\ 1\ 0\rangle\langle L_j\rangle$. On the right, the outgoing boundary cycles are $\langle L_1\ 0\ 2\rangle\langle L_2\ 1\rangle$.

Similarly, α_2 is a loop in $Cl_1^- \mathcal{SD}_g^\bullet(m,1)$ that is filled by the 2-cell seen in the middle of Figure 6.3.

Observe that there are exactly two 1-cells of type β: The outgoing boundary cycles of β_1 are $\rho(\beta_1) = \langle L_1\ 0\rangle\langle L_2\ 1\rangle$ and the outgoing boundary cycles of β_2 are $\rho(\beta_2) = \langle L_1\ 1\rangle\langle L_2\ 0\rangle$. Observe further that both β_1 and β_2 are edges joining the two 0-cells. Therefore, the fundamental group is generated by the loop $\beta_2 \star \beta_1$. But the 2-cell on the right of Figure 6.3 show that $\beta_2 \star \beta_1$ is homotopic to a loop of type α_1, which is null-homotopic. □

Proposition 6.4. *Let $m \geq 1$, $g \geq 0$ and consider the following diagrams of inclusions of subspaces.*

$$\begin{array}{ccc} Cl_1^- \mathscr{S}\mathscr{D}_g^\bullet(m,1) & \xhookrightarrow{Cl_1^- \overline{\varphi}_g} & Cl_1^- \mathscr{S}\mathscr{D}_\infty^\bullet(m,1) \\ \downarrow{\scriptstyle \alpha_g} & & \downarrow{\scriptstyle \alpha_\infty} \\ \mathscr{S}\mathscr{D}_g^\bullet(m,1) & \xhookrightarrow{\overline{\varphi}_g} & \mathscr{S}\mathscr{D}_\infty^\bullet(m,1) \end{array} \tag{6.3}$$

The maps α_g, $\overline{\varphi}_g$ and $Cl_1\overline{\varphi}_g$ induce isomorphisms in homology in the range $* \leq m+g-2$. The map α_∞ is a quasi-isomorphisms.

Proof. The proof is similar to the proof of Proposition 5.2.8. Recall that, by Theorem 4.4.1, the stabilization map $\overline{\varphi}$ induces homology isomorphisms in the claimed range. From the definition of a combinatorial Sullivan diagram with exactly one ghost surface and the discrete Morse flow constructed in [BE17, Section 4.4], it is clear that $Cl_1^-\overline{\varphi}\colon Cl_1^- \mathscr{S}\mathscr{D}_g^\bullet(m,1) \hookrightarrow Cl_1^- \mathscr{S}\mathscr{D}_\infty^\bullet(m,1)$ induces a map of Morse complexes that is an isomorphism in the claimed range. It remains to show that α_∞ is a quasi isomorphism. This will follow from studying of the cluster spectral sequence $E^r_{p,q}$ of $\mathscr{S}\mathscr{D}_\infty^\bullet(m,1)$. Using the same recipe as in the proof of Lemma 5.2.10, the rows of $E^0_{p,q}$ are acyclic for $p > 0$. We leave this to the reader. □

Definition 6.5. Let $0 \leq g \leq \infty$ and $m \geq 1$. The space $Cl_1^- \mathscr{S}\mathscr{D}_g^\bullet(m,1)$ is filtered by the Sullivan diagrams with at least $m-k$ degenerate outgoing boundaries, i.e., for $0 \leq k \leq m$ it is

$$D_k Cl_1^- \mathscr{S}\mathscr{D}_\infty^\bullet(m,1) = Cl_1^- \mathscr{S}\mathscr{D}_\infty^\bullet(m,1) \cap D_k \mathscr{S}\mathscr{D}_\infty^\bullet(m,1) \tag{6.4}$$

$$= \{\Sigma \in Cl_1^- \mathscr{S}\mathscr{D}_\infty^\bullet(m,1) \mid l(\Sigma) \in \operatorname{skel}_k \Delta^{m-1}\}\,. \tag{6.5}$$

Remark 6.6. Let $g \geq 0$ and $m \geq 1$. For $k = 0$, the space $D_k Cl_1^- \mathscr{SD}_g^\bullet(m,1)$ is empty, for $k = 1$, it consists of exactly m discrete points and for $k > 1$, it is connected.

Remark 6.7. A Sullivan diagram $\Sigma \in D_k Cl_1^- \mathscr{SD}_\infty^\bullet(m,1)$ is always of the form $\Sigma = (\lambda, (0, \infty, \operatorname{cyc} \lambda))$. Therefore, it is uniquely determined by its ribbon structure λ or, equivalently, its outgoing boundary cycles ρ.

Lemma 6.8. *Let $m \geq 1$ and let $E^r_{p,q}$ be the spectral sequence associated to the filtration $D_p Cl_1^- \mathscr{SD}_\infty^\bullet(m,1)$. The spectral sequence collapses on the second page and is concentrated in $E^2_{1,-1} \cong \mathbb{Z}$. In particular $Cl_1^- \mathscr{SD}_\infty^\bullet(m,1)$ is acyclic.*

Proof. We denote the set of m leaves by $L = \{L_1, \dots, L_m\}$. By C_*, we denote the cellular chain complex $Cl_1^- \mathcal{SD}_\infty^\bullet(m,1)$ and by $E^r_{p,q}$ we denote the spectral sequence associated to the filtration $D_p Cl_1^- \mathcal{SD}_\infty^\bullet(m,1)$. The 0-th page is

$$E^0_{p,q} = D_p C_{p+q} / D_{p-1} C_{p+q} \,. \tag{6.6}$$

By definition, $E^0_{p,q}$ is generated by Sullivan diagrams $\Sigma = (\lambda, S_1)$ whose non-degenerate boundary cycle ρ has exactly p cycles not of the form $\langle L_i \rangle$ for some leaf $L_i \in L$. This gives a partition of L into $L = L' \sqcup L''$ with

$$L' = \{L_i \in L \mid \langle L_i \rangle \notin \operatorname{cyc}(\rho)\} \,. \tag{6.7}$$

Note that the partition is invariant under the face maps in $E^0_{p,q}$. Therefore, $E^0_{p,*}$ is a direct sum of $\binom{m}{p}$ chain complexes

$$E^0_{p,*} \cong \bigoplus_{L' \subset L, \# L' = p} K(L')_* \,. \tag{6.8}$$

For each $p \geq 1$, we will show now that each $K(L')$ is isomorphic to $Cl_1^- N\mathcal{SD}_\infty^\bullet(p,1)$. Given $L' \subset L$ the enumeration of L induces an enumeration of L' and we are safe to assume that $L' = \{L_1, \dots, L_p\} \subset \{L_1, \dots, L_m\} = L$. Given a Sullivan diagram $\Sigma \in K(L')$ having a single ghost surface and with outgoing boundary cycles

$$\rho = \rho_1 \cdots \rho_p \cdot \langle L_{p+1} \rangle \cdot \cdots \cdot \langle L_m \rangle \in \mathfrak{S}[k \sqcup L] \tag{6.9}$$

we define $\Phi(\Sigma)$ to be the Sullivan diagram with a single ghost surface and with outgoing boundary cycles

$$\Phi(\rho) = \rho_1 \dots \rho_p \in \mathfrak{S}[k \sqcup L'] \,. \tag{6.10}$$

From Discussion 4.3.12 it is clear that this defines a chain map

$$\Phi \colon K(L') \to Cl_1^- \mathcal{SD}_\infty^\bullet(p,1) / Cl_1^- D\mathcal{SD}_\infty^\bullet(p,1) \,. \tag{6.11}$$

Observe that Φ is bijective: Given a Sullivan diagram in $Cl_1^- \mathcal{SD}_\infty^\bullet(p,1)/Cl_1^- D\mathcal{SD}_\infty^\bullet(p,1)$, adding the $m - p$ degenerate cycles $\langle L_{p+1} \rangle, \dots, \langle L_m \rangle$ to the unique ghost surface defines the inverse chain map. By our desuspension theorem for the spaces of Sullivan diagrams and Proposition 5.1.23 we have an isomorphism

$$\mathcal{SD}_\infty^\bullet(p,1) / D\mathcal{SD}_\infty^\bullet(p,1) \cong \Sigma^{p-1} N\mathcal{SD}_\infty^\bullet(p,1) \tag{6.12}$$

that sends a Sullivan diagram (λ, S) to $\pm(\lambda, S)$. In particular, the isomorphism is compatible with the corresponding unreduced cluster filtrations, i.e.,

$$Cl_1^- \mathcal{SD}^\bullet_\infty(p,1)/Cl_1^- D\mathcal{SD}^\bullet_\infty(p,1) \cong \Sigma^{p-1} Cl_1^- N\mathcal{SD}^\bullet_\infty(p,1)\,. \tag{6.13}$$

The chain complexes $Cl_1^- N\mathcal{SD}^\bullet_\infty(p,1)$ are contractible by Proposition 5.2.8 and Theorem 5.2.11. Therefore,

$$E^1_{p,q} = \bigoplus_{L'\subset L, \#L'=p} H_{p+q}(K(L');\mathbb{Z}) \cong \bigoplus_{L'\subset L, \#L'=p} H_{p+q}(\mathbb{Z}[p-1]);\mathbb{Z}) \begin{cases} \mathbb{Z}^{\binom{m}{p}} & q=-1 \\ 0 & q\neq -1 \end{cases}. \tag{6.14}$$

Denote the single non-trivial row by $G_* = E^1_{*,-1}$. From the above it clear that

$$G_p \cong \mathbb{Z}\langle L' \subset L \mid \#L' = p\rangle \tag{6.15}$$

where we identify $L' = \{L_{i_1} < \ldots < L_{i_p}\} \subset \{L_1 < \ldots < L_m\} = L$ with the Sullivan diagram $\Sigma(L')$ having outgoing boundary cycles

$$\rho(L') = \langle 0\ L_{i_1}\rangle \cdots \langle p-1\ L_{i_p}\rangle \cdots . \tag{6.16}$$

With this identification, the differential $d\colon G_p \to G_{p-1}$ is

$$d(L') = \sum_{1\leq j\leq p} (-1)^j \{L_{i_1} < \ldots < \widehat{L_{i_j}} < \ldots < L_{i_p}\}\,. \tag{6.17}$$

We conclude that G_{*-1} is the cellular chain complex of an $(m-1)$-dimensional simplex. In particular, $E^2_{p,q}$ is concentrated in degree $E^2_{1,-1} \cong \mathbb{Z}$. □

7

Three new generators in the unstable homology of $\mathfrak{M}_{2,1}$ and $\mathfrak{M}^2_{1,1}$

This chapter is an excerpt of the article [BB18a] Here, we construct three homology classes in the unstable range, using various techniques. Our classes live in the moduli space with at most one parametrized incoming boundary curve and $m \geq 0$ unenumerated punctures. To simplify our notation, we write $\mathfrak{M}^m_{g,n}$ instead of $\mathfrak{M}^{\square}_g(m,n)$ and we drop the symbol n resp. m from the notation if $n = 0$ resp. $m = 0$. The corresponding mapping class group is denoted by $\Gamma^m_{g,n}$ and we drop the the symbol n resp. m from the notation if $n = 0$ resp. $m = 0$.

Using Bödigheimer's space of parallel slit configurations [Bö90a], the integral homology of $\mathfrak{M}_{2,1}$ has been computed by Ehrenfried in [Ehr97]. Based on Visy's results on factorable groups in [Vis10], Mehner applied discrete Morse theory to the Bödigheimer's model in [Meh11] and detected some of the generators of $H_*(\mathfrak{M}_{2,1};\mathbb{Z})$ and $H_*(\mathfrak{M}^2_{1,1};\mathbb{Z}_2)$, see also Appendix E.4. Adding our generators to their findings, we obtain the following result.

Theorem 7.0.1 (B., Bödigheimer, Ehrenfried, Mehner)**.** *The integral homology of $\mathfrak{M}_{2,1}$ and $\mathfrak{M}^2_{1,1}$ is as follows.*

$$H_*(\mathfrak{M}_{2,1};\mathbb{Z}) = \begin{cases} \mathbb{Z}\langle c^2\rangle & *=0 \\ \mathbb{Z}_{10}\langle cd\rangle & *=1 \\ \mathbb{Z}_2\langle d^2\rangle & *=2 \\ \mathbb{Z}\langle \lambda s\rangle \oplus \mathbb{Z}_2\langle T(e)\rangle & *=3 \\ \mathbb{Z}_3\langle w_3\rangle \oplus \mathbb{Z}_2\langle ?\rangle & *=4 \\ 0 & *\geq 5 \end{cases} \qquad H_*(\mathfrak{M}^2_{1,1};\mathbb{Z}) = \begin{cases} \mathbb{Z}\langle a^2c\rangle & *=0 \\ \mathbb{Z}\langle a^2d\rangle \oplus \mathbb{Z}_2\langle bc\rangle & *=1 \\ \mathbb{Z}_2\langle a^2e\rangle \oplus \mathbb{Z}_2\langle bd\rangle & *=2 \\ \mathbb{Z}_2\langle f\rangle & *=3 \\ 0 & *\geq 4 \end{cases}$$

Here, the known generators a,b,c,d,e,t and their products have been described in [Meh11, Kapitel 1] or [BH14, Chapter 4], see also [BB18a]. The generators $s \in H_3(\mathfrak{M}^1_{2,1};\mathbb{Q})$, $w_3 \in H_4(\mathfrak{M}^1_{2,1};\mathbb{Z})$ respectively $f \in H_3(\mathfrak{M}^2_{1,1};\mathbb{Z})$ will be described in Section 7.1, Section 7.2 respectively Section 7.3. The only unknown generator is denoted by the symbol ?.

In Section 7.1, we study $\mathfrak{M}_{2,1}$ as the total space of the fibration $U \hookrightarrow \mathfrak{M}_{2,1} \to \mathfrak{M}_{2,0}$ whose fiber is the unit tangent bundle of the closed oriented surface of genus two. We show that the image of the rational fundamental class $[U]$ is a rational generator denoted by $s \in H_3(\mathfrak{M}_{2,1};\mathbb{Q})$.

In Section 7.2, we study certain maps between the braid groups, spherical braid groups and mapping class groups. Sending the braid generators $\sigma_1, \dots, \sigma_5 \in Br_6$ to a certain system of five Dehn twists defines a Segal–Tillmann map $ST\colon \mathrm{Conf}^6(\mathbb{D}^2) \to \mathfrak{M}_{2,1}$. By a result of Cohen, see [CLM76, Theorem A.1.b], we know that $H_4(\mathrm{Conf}^6(\mathbb{D}^2); \mathbb{F}_3) \cong \mathbb{F}_3\langle \tilde{w}_3 \rangle$ where $\tilde{w}_3$ is the class of tree pairs of revolving particles that orbit the origin. We denote the image of $\tilde{w}_3$ under ST by w_3 and show w_3 generates the 3-torsion of $H_4(\mathfrak{M}_{2,1}; \mathbb{Z})$.

Finally, in Section 7.3, we define a homology class $f \in H_3(\mathfrak{M}^2_{1,1}; \mathbb{Z})$ by embedding a three dimensional torus $U(1)^3$ into Bödigheimer's space of parallel slit configurations $\mathfrak{Par}^2_{1,1} \simeq \mathfrak{M}^2_{1,1}$. The space of parallel slit configurations is a relative manifold in its bar compactification $Bar := Bar(\mathfrak{Par}^2_{1,1})$. We construct the Poincaré-dual $PD(f) \in H^9(Bar, Bar'; \mathcal{O})$ of f and show that $H^9(Bar, Bar'; \mathcal{O}) \cong \mathbb{Z}_2\langle PD(f) \rangle$.

7.1. The generator $s \in H_3(\mathfrak{M}_{2,1}; \mathbb{Q})$

Let us recall some well known facts (whose proofs can be found in [FM12, Section 4.2.5 and Section 12.6]). The moduli space $\mathfrak{M}_{2,1}$ is homotopy equivalent to the moduli space of all closed oriented surfaces of genus two together with a choice of tangential direction at some base point. Forgetting the tangential direction but keeping the base point defines a surjective map $\mathfrak{M}_{2,1} \to \mathfrak{M}^1_2$ to the moduli space of all closed oriented surfaces of genus two together with a choice of base point. The base is a rational classifying space for the mapping class group Γ^1_2, i.e., its rational homology is the rational homology of Γ^1_2. Performing only rational computations, we are safe to assume that $\mathfrak{M}_{2,1} \to \mathfrak{M}^1_2$ is a circle fibration. Forgetting the tangential direction and the base point, defines a surjective map $\mathfrak{M}_{2,1} \to \mathfrak{M}_2$ to the moduli space of all closed oriented surfaces of genus two. The base is a rational classifying space for the mapping class group Γ_2 and, performing only rational computations, we are safe to assume that $\mathfrak{M}_{2,1} \to \mathfrak{M}_2$ is a fibration whose fiber is the total space U of the unit tangent bundle $\mathbb{S}^1 \to U \to F$ over the closed oriented surface F of genus two.

Definition 7.1.1. The image of the (rational) fundamental class $[U]$ in $H_3(\mathfrak{M}_{2,1}; \mathbb{Q})$ is denoted by s.

A careful study of the rational spectral sequences associated to the diagram below will lead to Proposition 7.1.2.

$$\begin{array}{cccccc} & & & 3 & & 4 \\ 1 & & \mathbb{S}^1 & \longrightarrow & U & \longrightarrow & F \\ & & \downarrow{\scriptstyle \mathrm{id}} & & \downarrow & & \downarrow \\ 2 & & \mathbb{S}^1 & \longrightarrow & \mathfrak{M}_{2,1} & \longrightarrow & \mathfrak{M}^1_2 \\ & & & & \downarrow & & \downarrow \\ & & & & \mathfrak{M}_2 & \xrightarrow{\mathrm{id}} & \mathfrak{M}_2 \end{array} \tag{7.1}$$

Proposition 7.1.2. *The inclusion of the fiber $U \hookrightarrow \mathfrak{M}_{2,1}$ induces an isomorphism*

$$H_3(U; \mathbb{Q}) \xrightarrow{\cong} H_3(\mathfrak{M}_{2,1}; \mathbb{Q}) \cong \mathbb{Q}\langle s \rangle\,. \tag{7.2}$$

Proof. Let us investigate the four spectral sequences.

Spectral sequence 1

The first spectral sequence computes the homology of the unit tangent bundle $\mathbb{S}^1 \to U \to F$ of a surface of genus two. The action of $\pi_1(F)$ on $H_1(\mathbb{S}^1)$ is trivial because the bundle is oriented. The second page consists of two rows with three columns and a single non-trivial differential, see Figure 7.1. It is the multiplication with the Euler characteristic $\chi(F) = -2$.

$$\begin{array}{ccccccc} \mathbb{Q} & \mathbb{Q}^4 & \mathbb{Q} & & 0 & \mathbb{Q}^4 & \mathbb{Q} \\ \mathbb{Q} & \mathbb{Q}^4 & \mathbb{Q} & & \mathbb{Q} & \mathbb{Q}^4 & 0 \end{array}$$

Figure 7.1.: The second and third page of spectral sequence 1.

Spectral sequence 2

The second spectral sequence comes from a central extension of the mapping class groups Γ_2^1 by the integers. It is used in [Har91, p. 33] to compute certain rational Betti numbers. The second page has exactly two non-trivial columns and a single non-trivial differential, see Figure 7.2. Therefore, we obtain rational Betti numbers

$$\beta(\mathfrak{M}_2^1) = (1, 0, 1) \quad \text{and} \quad \beta(\mathfrak{M}_{2,1}) = (1, 0, 0, 1)\,. \tag{7.3}$$

$$\begin{array}{ccc} \mathbb{Q} & 0 & \mathbb{Q} \\ \mathbb{Q} & 0 & \mathbb{Q} \end{array}$$

Figure 7.2.: The second page of spectral sequence two.

Spectral sequence 3

The first page of the third spectral sequence is $E^1_{p,q} \cong C_p(\mathfrak{M}_2; \mathcal{H}_q(U; \mathbb{Q}))$ with $\mathcal{H}_q(U; \mathbb{Q})$ the canonical $\pi_1(\mathfrak{M}_2)$-module. We have $\pi_1(\mathfrak{M}_2) \cong \Gamma_2$, so we need to understand how an orientation preserving diffeomorphism f of the closed surface F acts on $H_*(U; \mathbb{Q})$. Clearly, f_* acts on $H_0(U; \mathbb{Q}) \cong \mathbb{Q} \cong H_3(U; \mathbb{Z})$ via the identity. By the discussion of spectral sequence 1, see Figure 7.1, we have isomorphisms

$$H_1(U; \mathbb{Q}) \cong H_1(F; H_0(\mathbb{S}^1; \mathbb{Q})) \cong H_1(F; \mathbb{Q}) \tag{7.4}$$

and

$$H_2(U; \mathbb{Q}) \cong H_1(F; H_1(\mathbb{S}^1; \mathbb{Q})) \cong H_1(F; \mathbb{Q})\,. \tag{7.5}$$

Note that these isomorphisms are Γ_2-equivariant. Therefore, the second page of spectral sequence 3 consists of four rows; rows 0 and 3 are isomorphic and rows 1 and 2 are isomorphic, see the left hand side of Figure 7.3.

Spectral sequence 4

The discussion of this spectral sequence is similar to the discussion of spectral sequence 3. The second page of spectral sequence 4 consists of three rows: Row number 0 (resp. 1, resp. 2) of spectral sequence 4 is identified with row 0 (resp. 2, resp. 3) of spectral sequence 3, see the right hand side of Figure 7.3

Rational computations

Denote $M_* = H_*(\Gamma_2; V)$ with V the symplectic representation. By the above, the middle row(s) of spectral sequences 3 and 4 are rationally isomorphic to M_*. In [LW85, Corollary 5.2.3], the authors show that the reduced integral homology of Γ_2 is all p-torsion for $p = 2, 3, 5$. Thus, the top and bottom rows are rationally trivial except for the trivial Γ_2-module $\mathbb{Q}$ sitting in column zero. With (7.3) it follows that $M_k = 0$ for all k. Therefore,

$$\begin{array}{ccccc} \mathbb{Q} & 0 & 0 & 0 & \dots \\ M_0 & M_1 & M_2 & M_3 & \dots \\ M_0 & M_1 & M_2 & M_3 & \dots \\ \mathbb{Q} & 0 & 0 & 0 & \dots \end{array} \qquad \begin{array}{ccccc} \mathbb{Q} & 0 & 0 & 0 & \dots \\ M_0 & M_1 & M_2 & M_3 & \dots \\ \mathbb{Q} & 0 & 0 & 0 & \dots \end{array}$$

Figure 7.3.: The second page of the spectral sequence $E^r_{*,*}(U \to \mathfrak{M}_{2,1} \to \mathfrak{M}_2)$ is seen on the left. The second page of the spectral sequence $E^r_{*,*}(F \to \mathfrak{M}^1_2 \to \mathfrak{M}_2)$ is seen on the right.

$H_3(\mathfrak{M}_{2,1}; \mathbb{Q}) \cong E^2_{0,3} \cong \mathbb{Q}$ which is generated by the image of the fundamental class of the fiber U in $\mathfrak{M}_{2,1}$. This ends the proof of Proposition 7.1.2. □

7.2. The generator $w_3 \in H_4(\mathfrak{M}_{2,1}; \mathbb{Z})$

In [ST07] and [ST08], the authors study maps $Br_{2g+2} \to \Gamma_{g,2}$ from the braid group on $2g+2$ strands to the mapping class group of a surface of genus g with two parametrized boundary curves. This braid group is generated by the braids $\sigma_1, \dots, \sigma_{2g+1}$ where σ_i interchanges the strands i and $i+1$. The mapping class group is generated by Dehn twists along finitely many, simple closed curves. Consider a sequence of simple closed curves $\alpha_1, \dots, \alpha_{2g+1}$ such that (1) each α_i is invariant under the hyperelliptic involution and such that (2) two consecutive curves intersect exactly once and with positive sign, while all other pairs of curves do not intersect at all, see Figure 7.5. Then, the Dehn twists $D_1, \dots D_{2g+1}$ along $\alpha_1, \dots, \alpha_{2g+1}$ satisfy the braid relations and we obtain the Segal–Tillmann map

$$ST_g \colon Br_{2g+2} \to \Gamma_{g,2}, \sigma_i \mapsto D_i \,. \tag{7.6}$$

Moreover, we call the composition of the Segal–Tillmann map ST_g with the forgetful map $\Gamma_{g,2} \to \Gamma_{g,i}, i = 0, 1$ also a Segal–Tillmann map.

The classifying space of the 6-th braid group is the configuration space of six points in the disc. By [CLM76, Theorem A.1.b], the 3-torsion of its fourth homology is $\mathbb{Z}_3\langle \tilde{w}_3 \rangle$,

where $\tilde{w}_3$ is the class of three pairs of revolving particles that orbit the origin, see Figure 7.4. By [Ehr97] we know that $H_4(\mathfrak{M}_{2,1};\mathbb{Z}) \cong \mathbb{Z}_2 \oplus \mathbb{Z}_3$.

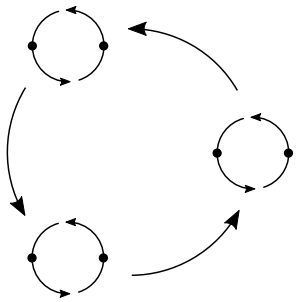

Figure 7.4.: The homology class $\tilde{w}_3 \in H_4(Br_6;\mathbb{Z})$.

Definition 7.2.1. Consider the Segal–Tillmann map $ST\colon Br_{2g+2} \to \Gamma_{g,1}$. By w_3 we denote the element $ST_*(\tilde{w}_3) \in H_4(\mathfrak{M}_{2,1};\mathbb{Z})$.

Proposition 7.2.2. *The Segal–Tillmann map* $ST\colon Br_{2g+2} \to \Gamma_{g,1}$ *induces a map*

$$ST\colon H_4(\mathrm{Conf}^6(\mathbb{D}^2);\mathbb{Z}) \to H_4(\mathfrak{M}_{2,1};\mathbb{Z}) \tag{7.7}$$

that sends the 3*-torsion of* $H_4(\mathrm{Conf}^6(\mathbb{D}^2);\mathbb{Z})$ *isomorphically to the* 3*-torsion of* $H_4(\mathfrak{M}_{2,1};\mathbb{Z})$.

In order to proof Proposition 7.2.2, we fix an explicit geometric setup and relate the Segal–Tillmann map to certain spherical braid groups and other mapping class groups, see Diagram 7.8. Then, Proposition 7.2.2 is follows immediately from Proposition 7.2.3.

Braid groups, spherical braid groups and other mapping class groups

Consider the disc $\mathbb{D} \subset \mathbb{C}$ of radius one, centered at the origin. In $\mathbb{D}$, consider six points $x_1,\dots,x_6$ all lying on the real line and such that $x_i < x_{i+1}$ for all i. The mapping class group $\Gamma^6_{0,1}$ of this disc is identified with the braid group on six strands Br_6 as follows. Two consecutive points x_i and x_{i+1} lie on a circle of diameter $|x_{i+1}-x_i|$. Rotating the circle by π in positive direction extends to a diffeomorphism f_i of the disc $\mathbb{D}$ that exchanges x_i with x_{i+1} while keeping the other x_j fixed. Sending the braid generator σ_i, exchanging the i-th strand with the $(i+1)$-th strand, to the mapping class of f_i, one obtains an isomorphism $Br_6 \cong \Gamma^6_{0,1}$, see e.g [KT08, Section 1.6].

In the surface of genus two and with one boundary component $F_{2,1}$, we pick five, oriented, simple closed curves $a_1,\dots,a_5$ with intersection number 1 as shown in Figure 7.5.

The Dehn twists D_i and D_j along a_i and a_j satisfy the braid relation if $j = i \pm 1$ and they commute if $|i-j| \geq 2$. Thus, we have the Segal–Tillmann map $\alpha\colon \Gamma^6_{0,1} \to \Gamma_{2,1}$ sending $[f_i]$ to D_i is well-defined.

Glueing a disc to the boundary curve of $F_{2,1}$ induces a surjective map $\beta\colon \Gamma_{2,1} \to \Gamma_{2,0}$. Abusing notation, we denote the Dehn twist $\beta(D_i)$ also by D_i.

The hyperelliptic involution $\tau\colon F_2 \to F_2$ has exactly six fixed points denoted by $y_1,\dots,y_6$, see Figure 7.6. The quotient F_2/τ is a sphere with six marked points also denoted by $y_1,\dots,y_6$. Observe that each Dehn twists $D_1,\dots,D_5$ of F_2 commutes with the hyperelliptic

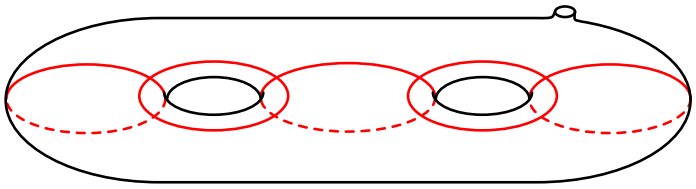

Figure 7.5.: The five closed curves $a_1, \dots, a_5$ in the surface of genus two with one boundary component. Observe that these curves are invariant under the hyperelliptic involution seen in Figure 7.6 (after glueing a disc to the outgoing boundary).

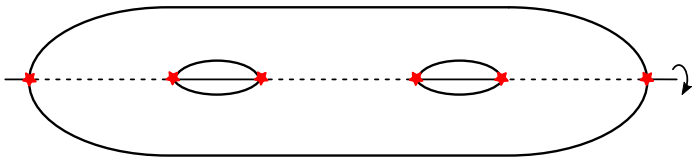

Figure 7.6.: We sketch the hyperelliptic involution of the closed surface of genus two. We highlight the 6 fixed points.

involution. Therefore, D_i induces the half Dehn twist $\tilde{D}_i$ on F_2/τ that exchanges y_i with y_{i+1} while leaving the other y_j fixed. It is well known that $\Gamma_{2,0}$ is generated the Dehn twists $D_1, \dots, D_5$, see e.g. [FM12, Section 5.1.3]. Therefore, we have a well defined homomorphism $\gamma\colon \Gamma_{2,0} \to \Gamma^6$ given by sending D_i to $\tilde{D}_i$.

Note that the composition $\gamma\beta\alpha\colon \Gamma^6_{0,1} \to \Gamma^6$ sends the half twist that interchanges the points x_i with x_{i+1} in the disc $\mathbb{D}$ to the half twist that interchanges the points y_i with y_{i+1} in the sphere $\mathbb{S}^2$. In other words, $\gamma\beta\alpha$ is induced by the inclusion $\mathbb{D} \subset \mathbb{S}^2$. Thus, the composite $\gamma\beta\alpha$ can be factored as follows. Glueing a punctured disc to the boundary of $\mathbb{D}$ induces a central extension $\mathbb{Z} \to \Gamma^6_{0,1} \xrightarrow{\delta} \Gamma^{6,1}$, where $\Gamma^{6,1} \subset \Gamma^7$ is the subgroup of mapping classes that leaves one distinguished point fixed. Forgetting the distinguished point we get another, non-central extension $\pi_1(\mathbb{S}^2 - 6) \to \Gamma^{6,1} \xrightarrow{\epsilon} \Gamma^6$, where $\mathbb{S}^2 - 6$ denotes the two-sphere with 6 points removed. We have the following commutative diagram.

$$\begin{array}{ccccc} \Gamma^6_{0,1} & \xrightarrow{\alpha} & \Gamma_{2,1} & \xrightarrow{\beta} & \Gamma_2 \\ \downarrow{\scriptstyle \delta} & & & & \downarrow{\scriptstyle \gamma} \\ \Gamma^{6,1} & & \xrightarrow{\quad\epsilon\quad} & & \Gamma^6 \end{array} \tag{7.8}$$

By [CLM76, Theorem A.1.b], we know that $H_4(Br_6; \mathbb{F}_3) = \mathbb{F}_3\langle \tilde{w}_3 \rangle$ and $\tilde{w}_3$ is obtained as iterated Dyer–Lashof operation, see Figure 7.4. Moreover, by [Ehr97], we know that $H_4(\mathfrak{M}_{2,1}; \mathbb{Z}) \cong \mathbb{Z}_2 \oplus \mathbb{Z}_3$. Observe that Proposition 7.2.2 is an immediate consequence of the following Proposition.

Proposition 7.2.3.

(*i*) *On 3-torsion, $H_4(\delta)$ is an isomorphism.*

(*ii*) *On 3-torsion, $H_4(\epsilon)$ is an isomorphism.*

The remainder of this section is the proof of Proposition 7.2.3.

The homomorphism $H_4(\delta)$

We study the spectral sequence of the central extension $\mathbb{Z} \to \Gamma^6_{0,1} \xrightarrow{\delta} \Gamma^{6,1}$. In order to detect the free part and the 3-torsion simultaneously, we use coefficients in the subring $\mathbb{Z}_{(3)} \subset \mathbb{Q}$ where all primes but 3 are invertible. Recall that $\mathbb{Z}_{(3)}$ is flat, see e.g. [Wei95, Theorem 3.2.2]. Therefore, the universal coefficient theorem gives a natural isomorphism of homology theories $H_*(-;\mathbb{Z}_{(3)}) \cong H_*(-;\mathbb{Z}) \otimes \mathbb{Z}_{(3)}$.

Proof of Proposition 7.2.3.(i). We deduce the first half of Proposition 7.2.3 from studying the 3-torsion and the free part of the cohomological spectral sequence of the central extension $\mathbb{Z} \to \Gamma^6_{0,1} \xrightarrow{\delta} \Gamma^{6,1}$. Observe that we have a cohomological spectral sequence with two non-trivial rows which are (in addition) isomorphic. By Lemma 7.2.4.(i) and the universal coefficient theorem for cohomology, the first column is trivial and the second column is $\mathbb{Z}_3 \oplus A$ for A to be determined. The free part and the 3-torsion of the cohomology of the braid group Br_6 is $(\mathbb{Z}_{(3)};\mathbb{Z}_{(3)};0;0;0;\mathbb{Z}_3)$. Therefore $A = 0$ and $d_2 \colon \mathbb{Z}_{(3)} \cong E_2^{0,1} \to E_2^{2,1} \cong \mathbb{Z}_3$ is surjective, i.e., $d_2(s) = r$ for generators s and r. This yields $d_2(s \cdot r^k) = \pm r^{k+1}$. Now, the shape of the second page is dictated by Lemma 7.2.4.(ii), the cohomology of Br_6 and the multiplicative structure, see Figure 7.7.

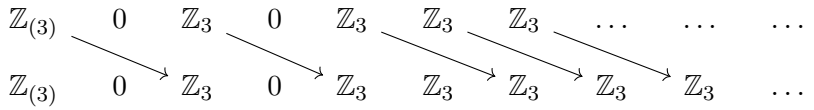

Figure 7.7.: The 3-torsion and the free part of $E_2^{**}(\mathbb{Z} \to \Gamma^6_{0,1} \to \Gamma^{6,1})$. All arrows are surjective.

We see that $E_\infty^{0,5} = E_2^{0,5} \cong \mathbb{Z}_3$ and $E_\infty^{1,4} = 0$. Thus, $\delta \colon \Gamma^6_{0,1} \to \Gamma^{6,1}$ induces an isomorphism

$$H^5(\delta) \colon H^5(\Gamma^{6,1};\mathbb{Z}_{(3)}) \cong E_\infty^{0,5} \cong H^5(\Gamma^6_{0,1};\mathbb{Z}_{(3)}) \cong \mathbb{Z}_3\,. \tag{7.9}$$

Now, by the universal coefficient theorem, $H_4(\delta)$ maps the 3-torsion of $H_4(\Gamma^6_{0,1};\mathbb{Z})$ isomorphically to the 3-torsion of $H_4(\Gamma^{6,1};\mathbb{Z})$. □

Lemma 7.2.4. *We have*

(i) $H_1(\Gamma^{6,1};\mathbb{Z}_{(3)}) = \mathbb{Z}_3$ *and*

(ii) $H_*(\mathbb{Z}_3;\mathbb{Z}_{(3)}) \leq H_*(\Gamma^{6,1};\mathbb{Z}_{(3)})$.

Proof. Let $\mathbb{Z} \subset \Gamma^6_{0,1}$ be the subgroup generated by the boundary twist θ. Recall that θ generates the center of $\Gamma^6_{0,1}$ and that θ is represented by a word of length 30 in the braid generators, see e.g. [KT08, Theorem 1.24]. Therefore, Hopf's exact sequence gives the short exact sequence

$$0 \to \mathbb{Z} \xrightarrow{\cdot 30} \mathbb{Z} \cong H_1(\Gamma^6_{0,1};\mathbb{Z}) \to H_1(\Gamma^{6,1};\mathbb{Z}) \to 0 \tag{7.10}$$

and hence $H_1(\Gamma^{6,1}) = \mathbb{Z}_{30}$. Consequently, the 3-torsion of $H_1(\Gamma^{6,1};\mathbb{Z})$ is $\mathbb{Z}_3$.

The forgetful map of classifying spaces $\mathrm{Conf}^{6,1}(\mathbb{S}^2) \to \mathrm{Conf}^7(\mathbb{S}^2)$ is a 7-sheeted covering. Thus, the transfer map yields an inclusion $H_*(\Gamma^7;\mathbb{F}_3) \hookrightarrow H_*(\Gamma^{6,1};\mathbb{F}_3)$. The abelianization

$\Gamma^7 \to (\Gamma^7)^{ab} \cong \mathbb{Z}_{12}$ sends each braid generator $\sigma_i \in \Gamma^7$ to $1 \in \mathbb{Z}_{12}$ and by the classification of the torsion elements of the spherical braid group Γ^n, see [Mur82, Theorem 4.2] and also [GG08, Theorem 1.2], the element $(\sigma_1 \cdots \sigma_6\sigma_1)^4 \in \Gamma^7$ has order three. Therefore,

$$\mathbb{Z}_3 \to \Gamma^7, \quad 1 \mapsto (\sigma_1 \cdots \sigma_6\sigma_1)^4 \tag{7.11}$$

is a section of $\Gamma^7 \to (\Gamma^7)^{ab} \cong \mathbb{Z}_{12} \to \mathbb{Z}_3$, $\sigma_i \mapsto 1$. Taking homology, we conclude that $H_*(\mathbb{Z}_3;\mathbb{F}_3) \hookrightarrow H_*(\Gamma^7;\mathbb{F}_3) \hookrightarrow H_*(\Gamma^{6,1};\mathbb{F}_3)$ is injective. Now, the second claim follows from the universal coefficient theorem. □

The homomorphism $H_4(\epsilon)$

To show that ϵ_* maps the 3-torsion of $H_4(\Gamma^{6,1};\mathbb{Z})$ isomorphically to the 3-torsion of $H_4(\Gamma^6;\mathbb{Z})$, we study the homological spectral sequence of the extension $\mathrm{Fr}_5 = \pi_1(\mathbb{S}^2 - 6) \to \Gamma^{6,1} \xrightarrow{\epsilon} \Gamma^6$, where $\mathbb{S}^2 - 6$ denotes the two-dimensional sphere with 6 points removed and Fr_5 is the free group on 5 generators. To detect the free part and the 3-torsion simultaneously, we use again coefficients in the subring $\mathbb{Z}_{(3)} \subset \mathbb{Q}$ where all primes but 3 are invertible.

Proof of Proposition 7.2.3.(ii). By Lemma 7.2.5 and the fact that $H_*(\mathbb{S}^2 - 6;\mathbb{Z}_{(3)}) \cong 0$ for $* \geq 2$, the second page of spectral sequence for the extension $\mathrm{Fr}_5 \to \Gamma^{6,1} \xrightarrow{\epsilon} \Gamma^6$, is as seen in Figure 7.8. We show that $E^2_{2,1}$ vanishes and this will imply Proposition 7.2.3.(ii).

$E^2_{0,1}$	$E^2_{1,1}$	$E^2_{2,1}$	$E^2_{3,1}$	$E^2_{4,1}$	$\dots$
$\mathbb{Z}_{(3)}$	0	0	$\mathbb{Z}_3$	$\mathbb{Z}_3$	$\dots$

Figure 7.8.: The second page of spectral sequence $E^r_{*,*}(\mathrm{Fr}_5 \to \Gamma^{6,1} \to \Gamma^6)$. The differentials are not shown.

To this end, consider $H = \mathfrak{A}_3 \times \mathfrak{A}_3 \leq \mathfrak{S}_6$ of index 80. The pullback of the canonical map $\Gamma^6 \to \mathfrak{S}_6$ to H yields a subgroup $\Gamma^6_H \leq \Gamma^6$ of index 80. Denoting $K = H_1(\mathbb{S}^2 - 6;\mathbb{Z}_{(3)})$, in homology with coefficients in K, the transfer associated to the subgroup $\Gamma^6_H \leq \Gamma^6$ yields an injection:

$$E^2_{2,1} = H_2(\Gamma^6;K) \leq H_2(\Gamma^6_H;K)\,. \tag{7.12}$$

For each of the four short exact sequences $A' \to A \to A''$ in Lemma 7.2.6, we get a long exact sequence:

$$\dots \to H_n(\Gamma^6_H;A') \to H_n(\Gamma^6_H;A) \to H_n(\Gamma^6_H;A'') \to \dots \tag{7.13}$$

But $H_*(\Gamma^6_H;\mathbb{Z}_{(3)}) = 0$ for $* = 1,2$ by Lemma 7.2.6 and this implies $H_*(\Gamma^6_H;B_l) = 0$ for $* = 1,2$ and $H_*(\Gamma^6_H;B_r) = 0$ for $* = 1,2$. Analogously, $H_*(\Gamma^6_H;B) = 0$ for $* = 1,2$ and therefore $H_*(\Gamma^6_H;K) = 0$ for $* = 1,2$. We end with

$$E^2_{2,1} = H_2(\Gamma^6;K) \leq H_2(\Gamma^6_H;K) = 0\,. \tag{7.14}$$

Therefore, $E^2_{4,0} \cong E^\infty_{4,0}$ survives.

By Proposition 7.2.3.(i), the 3-torsion of $H_4(\Gamma^{6,1};\mathbb{Z})$ is $\mathbb{Z}_3$ implying that $E^2_{3,1}=0$. Therefore, the induced map $H_4(\epsilon)$ is the composition:

$$H_4(\epsilon)\colon H_4(\Gamma^{6,1};\mathbb{Z}_{(3)}) \cong E^\infty_{4,0} \cong H_4(\Gamma^6;\mathbb{Z}_{(3)}) \cong \mathbb{Z}_3\,. \tag{7.15}$$

This finishes the proof of Proposition 7.2.3.(ii). □

Lemma 7.2.5. *For $* \leq 4$, the 3-torsion and the free part of $H_*(\Gamma^6;\mathbb{Z})$ is:*

$$\begin{cases} \mathbb{Z} & *=0 \\ 0 & *=1 \\ 0 & *=2 \\ \mathbb{Z}_3 & *=3 \\ \mathbb{Z}_3 & *=4 \\ 0 & *=5 \end{cases}. \tag{7.16}$$

Proof. Benson provides the Poincaré series of $H^*(\Gamma^6;\mathbb{F}_3)$ to be $\frac{1+t^3+t^4+t^5}{1-t^4} = 1+t^3+2t^4+t^5+t^7+\ldots$, see [BC91, Chapter 2, Theorem 1.1]. This and the universal coefficient theorem

$$0 \to \mathrm{Hom}_{\mathbb{Z}}(H_*(\Gamma^6;\mathbb{Z}),\mathbb{F}_3) \to H^*(\Gamma^6;\mathbb{F}_3) \to \mathrm{Ext}^{\mathbb{Z}}_1(H_{*-1}(\Gamma^6;\mathbb{Z}),\mathbb{F}_3) \to 0 \tag{7.17}$$

imply the claim for $* = 1,2$.

The virtual cohomological dimension is $vcd(\Gamma^6) \leq 3$ by [Har86, Theorem 4.1]. Combining this with the Poincaré series and the universal coefficient theorem above, the claim follows for $*=5$. Now, the claim follows analogously for $*=4$ and then for $*=3$. □

Lemma 7.2.6.

(i) *For $* = 1,2$ it is $H_*(\Gamma^6_H;\mathbb{Z}_{(3)}) = 0$.*

(ii) *There are Γ^6_H-modules B_l, B_r and B that fit into the following short exact sequences of Γ^6_H-modules, where $\mathbb{Z}_{(3)}$ comes with the trivial action:*

$$\begin{aligned} 0 &\longrightarrow \mathbb{Z}_{(3)} \longrightarrow B_l \longrightarrow \mathbb{Z}_{(3)} \longrightarrow 0 \\ 0 &\longrightarrow \mathbb{Z}_{(3)} \longrightarrow B_r \longrightarrow \mathbb{Z}_{(3)} \longrightarrow 0 \\ 0 &\longrightarrow B_l \longrightarrow B \longrightarrow B_r \longrightarrow 0 \\ 0 &\longrightarrow \mathbb{Z}_{(3)} \longrightarrow K \longrightarrow B \longrightarrow 0 \end{aligned}$$

Proof. By the universal coefficient theorem

$$0 \to \mathrm{Hom}_{\mathbb{F}_3}(H^*(\Gamma^6_H;\mathbb{F}_3),\mathbb{F}_3) \to H_*(\Gamma^6_H;\mathbb{F}_3) \to \mathrm{Ext}^{\mathbb{F}_3}_1(H^{*+1}(\Gamma^6_H;\mathbb{F}_3),\mathbb{F}_3) = 0 \tag{7.18}$$

we have $H_*(\Gamma^6_H;\mathbb{F}_3) \cong H^*(\Gamma^6_H;\mathbb{F}_3)$ for all $* \geq 0$. Moreover, $H_*(\Gamma^6_H;\mathbb{F}_3) \cong H^*(\Gamma^6_H;\mathbb{F}_3) = 0$ for $* = 1,2$ because $H^*(\Gamma^6_H;\mathbb{F}_3) \leq H^*(\Gamma^6;\mathbb{F}_3)$ by the transfer and, in the degrees $* = 1,2$, the latter homology groups are trivial by [BC91, Chapter 2, Theorem 1.1] or Lemma 7.2.5. Using the universal coefficient theorem

$$0 \to H_*(\Gamma^6_H;\mathbb{Z}) \otimes_{\mathbb{Z}} \mathbb{Z}_{(3)} \to H_*(\Gamma^6_H;\mathbb{Z}_{(3)}) \to \mathrm{Tor}^{\mathbb{Z}}_1(H_{*-1}(\Gamma^6_H;\mathbb{Z}),\mathbb{Z}_{(3)}) \to 0 \tag{7.19}$$

and the fact that $H_*(\Gamma^6_H;\mathbb{Z})$ contains neither 3-torsion nor free parts for $* = 1,2$ and $H_0(\Gamma^6_H;\mathbb{Z}) = \mathbb{Z}$, the first claim follows.

In order to show the second claim, we study the action of Γ^6 and Γ^6_H on K. Recall that the action of $\Gamma^6 = \pi_1(\mathrm{Conf}^6(\mathbb{S}^2))$ on $H_1(\mathbb{S}^2 - 6;\mathbb{Z}_{(3)}) = K$ comes from the extension $\mathrm{Fr}_5 \to \Gamma^{6,1} \to \Gamma^6$. Note that this extension is just the first three terms of the long exact sequence of homotopy groups associated to the following Fadel-Neuwirth fibration.

$$\mathbb{S}^2 - 6 \to \mathrm{Conf}^{6,1}(\mathbb{S}^2) \to \mathrm{Conf}^6(\mathbb{S}^2)\,. \tag{7.20}$$

In order to make the action explicit, we enumerate the six holes in $\mathbb{S}^2 - 6$ and we denote the closed loop running in positive orientation around the i-th hole by l_i. Then

$$K = \langle l_1, \ldots, l_6\rangle/\Delta^6 \tag{7.21}$$

as a $\mathbb{Z}_{(3)}$-module with $\Delta^6 = \langle(1,1,1,1,1,1)\rangle$ the diagonal . The mapping class group Γ^6 is generated by the half Dehn twists σ_i that interchange two consecutive punctures. Thus, σ_i acts on K as the transposition that interchanges l_i with l_{i+1}. Evidently, the action of Γ^6 factors the standard representation of $\mathfrak{S}_6$. The restriction of the action to Γ^6_H factors through the restriction of the standard representation of $\mathfrak{S}_6$ to $\mathfrak{A}_3 \times \mathfrak{A}_3$.

Next, consider the short exact sequence of Γ^6_H-modules $A \to K \to B$ where

$$A = \langle(1,1,1,0,0,0)\rangle/\Delta^6 \tag{7.22}$$

and $\Delta^6 = \langle(1,1,1,1,1,1)\rangle$ is the diagonal. Clearly, A is isomorphic to the trivial Γ^6_H-module $\mathbb{Z}_{(3)}$. Note that B splits as Γ^6_H-module into $\mathbb{Z}^3_{(3)}/\Delta^3 \oplus \mathbb{Z}^3_{(3)}/\Delta^3$, where Δ^3 denotes the diagonal in $\mathbb{Z}^3_{(3)}$. Let us study the left factor, which we call B_l, the right factor is treated similarly. By construction, the Γ^6_H-action factors as follows $\Gamma^6_H \to \mathfrak{A}_3 \times \mathfrak{A}_3 \xrightarrow{q} \mathfrak{A}_3$ with q the projection onto the left factor and B_l is the restriction of the standard representation of $\mathfrak{S}_3$ to $\mathfrak{A}_3$. Therefore, we have another short exact sequence of Γ^6_H-modules

$$C \to B_l \to D \tag{7.23}$$

with $C = \{(x,y,z) \mid x+y+z = 0\}/\Delta^3$. Both C and D are isomorphic to the trivial Γ^6_H-module $\mathbb{Z}^3_{(3)}$: To see that C is trivial, observe that $2x + y = 2x + y + (x + y + z) = 2y + z = 2y + z + (x + y + z) = 2z + x$ and that $\mathfrak{A}_3$ acts by permuting the coordinates x, y, z cyclically. To see that D is trivial, observe that $x = x + (x + y + z) = 2x + y + z = z$ and that $\mathfrak{A}_3$ acts by permuting the coordinates x, y, z cyclically. □

7.3. The generator $f \in H_3(\mathfrak{M}^2_{1,1};\mathbb{Z})$

The integral class $f \in H_3(\mathfrak{M}^2_{1,1};\mathbb{Z})$ is defined as the embedded three dimensional torus $U(1)^3 \subset \mathfrak{Par}^2_{1,1}$ that is shown in Figure 7.9.

Proposition 7.3.1. *It is $H_3(\mathfrak{M}^2_{1,1};\mathbb{Z}) \cong \mathbb{Z}_2\langle f\rangle$ where f is represented by the embedded 3-dimensional torus seen in Figure 7.9.*

We show that f is non-trivial as follows. Firstly, we construct its Poincaré-dual $PD(f) \in H^{12-3}(Bar, Bar'; \mathcal{O})$, with $Bar := Bar(\mathfrak{Par}^2_{1,1})$ the bar compactification of $\mathfrak{Par}^2_{1,1}$. Then, we compute the cohomology of this finitely generated cochain complex explicitly and compare the generators. For the convenience of the reader, we describe the construction of a Poincaré-dual of an embedded manifold below.

Denote the bar compactification of $\mathfrak{Par}^2_{1,1}$ by Bar and recall that the space of parallel slit configurations $\mathfrak{Par}^2_{1,1}$ is a relative manifold, i.e., $\mathfrak{Par}^2_{1,1} \subset Bar$ is open and dense in the finite complex Bar and its complement $Bar' = Bar - \mathfrak{Par}^2_{1,1}$ is a subcomplex of codimension one. The Poincaré dual of an embedded closed, d-dimensional manifold $M \subset \mathfrak{Par}^2_{1,1}$ is constructed as follows. We assume that M intersects every open cell $e \subset \mathfrak{Par}^2_{1,1}$ transversely. In particular, M does not meet any cell of codimension more then d. The intersection with an arbitrary cell $e \subset \mathfrak{Par}^2_{1,1}$ of codimension d is a finite number of points and for each $x \in M \cap e$, we set $\mathfrak{o}(e) = \pm 1$ according to the orientation of M at x relative e and $\mathfrak{Par}^2_{1,1}$. With this at hand, the Poincaré-dual of M is the cochain $PD(M) \in C^{12-d}(Bar, Bar'; \mathcal{O})$ defined by evaluation:

$$PD(M)(e) = \sum_{x \in M \cap e} \mathfrak{o}(x)\,. \tag{7.24}$$

We define $f \in H_3(\mathfrak{Par}^2_{1,1})$ by the embedded torus $U(1)^3 \hookrightarrow \mathfrak{Par}^2_{1,1}$ that is shown in Figure 7.9. Observe that $U(1)^3$ intersects all cells transversely. Observe further, that

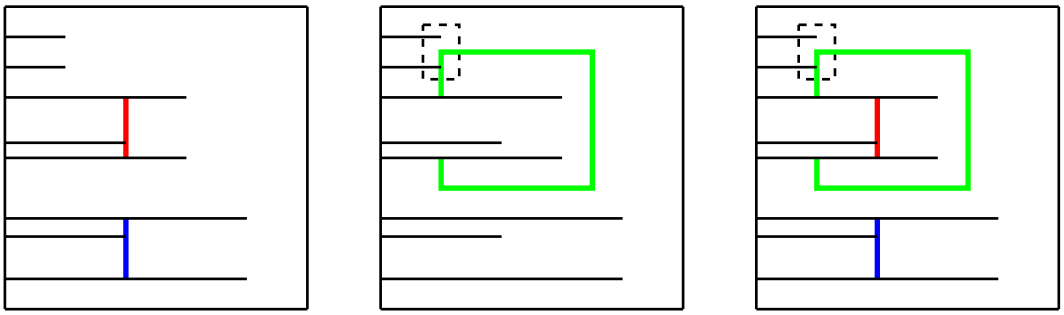

Figure 7.9.: On the left, we describe the embedded torus $U(1)^2 \times \{1\} \subset U(1)^3 \subset \mathfrak{Par}^2_{1,1}$. The first factor defines the rotation of a slit along the red line and the second factor defined the rotation of a slit along the blue line. In the middle, we describe the embedded circle $\{1\}^2 \times U(1) \subset U(1)^3 \subset \mathfrak{Par}^2_{1,1}$. It is the closed loop moving the pair of slits sitting in the dotted box along the green line. On the right, we describe the embedded torus $U(1)^3 \subset \mathfrak{Par}_1(2,1)$ as a combination of two independent movements shown on the left and in the middle.

$U(1)^3$ intersects exactly four cells of codimension three non-trivially and the intersection with each of these cells is a single point, see Figure 7.10. An explicit computation of the orientations at the intersection points yields the Poincaré-dual of $f\colon U(1)^3 \hookrightarrow \mathfrak{Par}^2_{1,1}$:

$$\begin{aligned} PD(f) = &(\langle 5\ 4\rangle|\langle 3\ 1\rangle|\langle 4\ 3\rangle|\langle 2\ 1\rangle) - (\langle 5\ 3\rangle|\langle 4\ 1\rangle|\langle 5\ 4\rangle|\langle 2\ 1\rangle) \\ &- (\langle 4\ 1\rangle|\langle 5\ 4\rangle|\langle 2\ 1\rangle|\langle 4\ 3\rangle) + (\langle 3\ 1\rangle|\langle 5\ 3\rangle|\langle 2\ 1\rangle|\langle 5\ 4\rangle) \end{aligned} \tag{7.25}$$

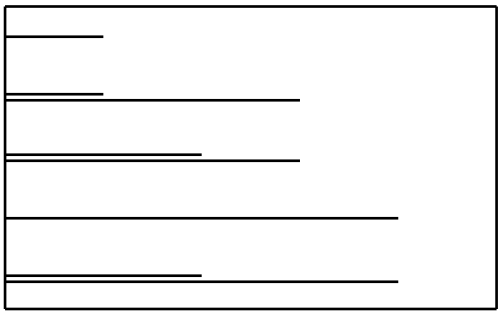

The intersection of $U(1)^3$ with cell of combinatorial type $(\langle 5\ 4\rangle|\langle 3\ 1\rangle|\langle 4\ 3\rangle|\langle 2\ 1\rangle)$.

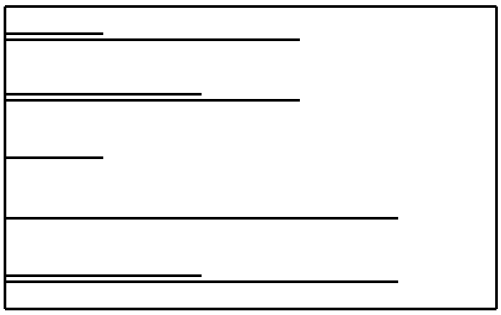

The intersection of $U(1)^3$ with cell of combinatorial type $(\langle 5\ 3\rangle|\langle 4\ 1\rangle|\langle 5\ 4\rangle|\langle 2\ 1\rangle)$.

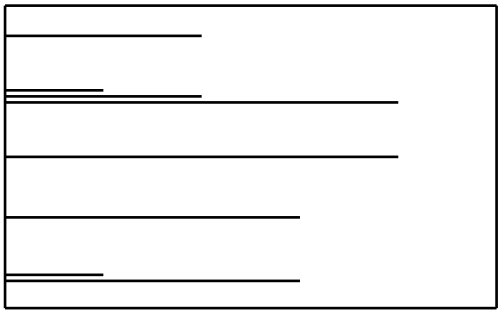

The intersection of $U(1)^3$ with cell of combinatorial type $(\langle 4\ 1\rangle|\langle 5\ 4\rangle|\langle 2\ 1\rangle|\langle 4\ 3\rangle)$.

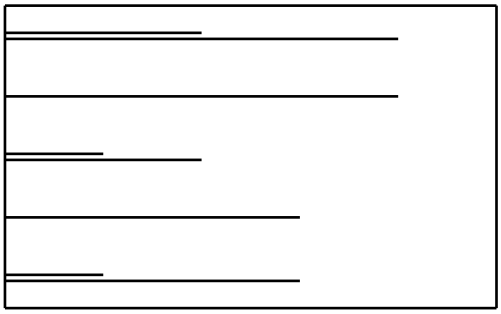

The intersection of $U(1)^3$ with cell of combinatorial type $(\langle 3\ 1\rangle|\langle 5\ 3\rangle|\langle 2\ 1\rangle|\langle 5\ 4\rangle)$.

Figure 7.10.: The torus $U(1)^3 \subset \mathfrak{Par}^2_{1,1}$ described in Figure 7.9 intersects exactly four cells of codimension three non-trivially. We draw the intersection points schematically here.

The Poincaré-dual is a cochain in the finitely generated chain complex $C^*(Bar, Bar'; \mathcal{O})$. Using a computer program based on [BH14], we verify

$$H^9(Bar(\mathfrak{Par}^2_{1,1}), Bar'(\mathfrak{Par}^2_{1,1}); \mathcal{O})) \cong \mathbb{Z}_2\langle PD(f)\rangle\,. \tag{7.26}$$

This proves Proposition 7.3.1.

Our program is mainly written in *C++11* and makes use of the *GNU Multiple Precision Arithmetic Library* [GMP] and the *Boost C++ Libraries* [Boost]. Given parameters g, m and a coefficient ring, it produces the corresponding chain complexes of the Ehrenfried complex associated to $\mathfrak{Rad}^{\square}_g(m, 1)$. Then, we compute its homology and the projection maps from the cycles to the homology. This task consumes by far the most time and memory. Using the projections, we test if our cycles are generators. The above results were produced on an *Intel i7-2670QM* and *Intel i5-4570* running *Debian Sid* and *Debian Jessie* with *Linux Kernel 4.2.0-1-amd64*. For the source code of our program, see [BH18].

A

Simplicial homotopy theory

For the convenience of the reader, we collect all definitions, formulas and facts from simplicial homotopy theory that might be lesser-known.

A.1. Multi-cyclic sets

The upcoming definitions are well known and discussed in great detail in [Lod92, Chapter 6.1].

Definition A.1.1. *Connes cyclic category* Δ_C has objects $[n] = \{0, \dots, n\}$ for $n \in \mathbb{N}$ and the following morphisms:

1. $\delta_i \colon [n-1] \to [n]$, $i = 0, \dots, n$ called faces,
2. $\sigma_i \colon [n+1] \to [n]$, $i = 0, \dots, n$ called degeneracies and
3. $\tau_n \colon [n] \to [n]$ called cyclic operators.

These satisfy the following relations.

1. $\delta_j \delta_i = \delta_i \delta_{j-1}$ for $i < j$,
   $\sigma_j \sigma_i = \sigma_i \sigma_{j+1}$ for $i \leq j$,
   $$\sigma_j \delta_i = \begin{cases} \delta_i \sigma_{j-1} & i < j, \\ \mathrm{id}_{[n]} & i = j, i = j+1, \\ \sigma_j \delta_{i-1} & i > j+1. \end{cases}$$
2. $\tau_n \delta_i = \delta_{i-1} \tau_{n-1}$ for $1 \leq i \leq n$,
   $\tau_n \delta_0 = \delta_n$,
   $\tau_n \sigma_i = \sigma_{i-1} \tau_{n+1}$ for $1 \leq i \leq n$,
   $\tau_n \sigma_0 = \sigma_n \tau_{n+1}^2$.
3. $\tau_n^{n+1} = \mathrm{id}_{[n]}$.

Definition A.1.2. The category Δ_C^{op} has objects $[n] = \{0, \dots, n\}$ for $n \in \mathbb{N}$ and the following morphisms:

1. $d_i \colon [n] \to [n-1]$, $i = 0, \ldots, n$ called faces,
2. $s_i \colon [n] \to [n+1]$, $i = 0, \ldots, n$ called degeneracies and
3. $t_n \colon [n] \to [n]$ called cyclic operators.

These satisfy the following relations.

1. $d_i d_j = d_{j-1} d_i$ for $i < j$,
   $s_i s_j = s_{j+1} s_i$ for $i \leq j$,
   $$d_i s_j = \begin{cases} s_{j-1} d_i & i < j, \\ \mathrm{id}_{[n]} & i = j, i = j+1, \\ s_j d_{i-1} & i > j+1. \end{cases}$$
2. $d_i t_n = t_{n-1} d_{i-1}$ for $1 \leq i \leq n$,
   $d_0 t_n = d_n$,
   $s_i t_n = t_{n+1} s_{i-1}$ for $1 \leq i \leq n$,
   $s_0 t_n = t_{n+1}^2 s_n$.
3. $t_n^{n+1} = \mathrm{id}_{[n]}$.

In this thesis, we are working with multi-simplicial sets that come with a cyclic action in each factor.

Definition A.1.3. The *multi-cyclic category*, denoted by $k\Delta_C$, is the k-fold product of categories $k\Delta_C := \Delta_C \times \ldots \times \Delta_C$. The objects of $k\Delta_C$ are denoted $[n_1, \ldots, n_k] := [n_1] \times \ldots \times [n_k]$.

The category $k\Delta_C^{op}$ is the k-fold product of categories $k\Delta_C^{op} := \Delta_C^{op} \times \ldots \times \Delta_C^{op}$ which is canonically isomorphic to $(\Delta_C \times \ldots \times \Delta_C)^{op}$. The objects of $k\Delta_C^{op}$ are denoted $[n_1, \ldots, n_k] := [n_1] \times \ldots \times [n_k]$.

Note that Proposition A.1.4, Proposition A.1.5 and Theorem A.1.6 justify our definition above. The proof of the case $k = 1$ can be found in [Lod92, Chapter 6 and Chapter 7]. The general case is proven analogously because all identities and relations that have to be satisfied can be verified in $\mathcal{S}et$.

Proposition A.1.4. *The category $k\Delta_C^{op}$ contains $k\Delta^{op} = \Delta^{op} \times \ldots \times \Delta^{op}$ as a subcategory. Moreover:*

1. *There are canonical isomorphisms $Aut_{k\Delta_C^{op}}([n_1, \ldots, n_k]) \cong \times_{i=1}^{k} \mathbb{Z}_{n_i+1}$.*
2. *In $k\Delta_C^{op}$, any morphism $\varphi \in \mathrm{Hom}_{k\Delta_C^{op}}([m_1, \ldots, m_k], [n_1, \ldots, n_k])$ admits a unique decomposition $\varphi = \sigma \circ f$ with $f \in \mathrm{Hom}_{k\Delta^{op}}([m_1, \ldots, m_k], [n_1, \ldots, n_k])$ and $\sigma \in \mathrm{Aut}_{k\Delta_C^{op}}([n_1, \ldots, n_k])$.*

Proposition A.1.5. *The family of cyclic groups $C_n := \mathrm{Aut}_{\Delta_C^{op}}([n])$ of order $n+1$ forms a cyclic set $C_\bullet \colon \Delta_C^{op} \to \mathcal{S}et$. Its geometric realization is homeomorphic to the circle $U(1)$.*

For $k \geq 1$, the family of multi-cyclic groups is defined to be the composition of functors

$$kC_\bullet \colon \Delta_C^{op} \times \ldots \times \Delta_C^{op} \xrightarrow{C_\bullet \times \ldots \times C_\bullet} \mathcal{S}et \times \ldots \times \mathcal{S}et \hookrightarrow \mathcal{S}et\,. \tag{A.1}$$

It is a multi-cyclic set. Its geometric realization is homeomorphic to the torus $U(1)^k$.

Theorem A.1.6. *Let X be a multi-cyclic set and let $|X|$ be the geometric realization of its underlying simplicial set. Then*

1. *the space $|X|$ is endowed with a canonical action of the torus $U(1)^k$ and*
2. *the geometric realization is a functor from the category of multi-cyclic spaces to the category of spaces with $U(1)^k$ action.*

Proposition A.1.7. *Let X be a cyclic set and let $|X|$ be its geometric realization. Consider a point $x = (\sigma; u_0, \ldots, u_n) \in |X|$ with σ not degenerate and with $0 < u_i$ for all i. For $z \in \mathbb{S}^1 = [0,1]/\sim$ with $0 \leq z \leq u_n$ the point $z.x$ is represented by*

$$(t_{n+1}s_n\sigma; z, u_0, \ldots, u_{n-1}, u_n - z)\,. \tag{A.2}$$

Proof. The proof uses notations and facts from [Lod92, Chapters 6.1, 7.1]. There is a functor $F\colon \mathrm{Fun}(\Delta^{op}, \mathcal{S}et) \to \mathrm{Fun}(\Delta_C^{op}, \mathcal{S}et)$ that is left adjoint to the forgetful functor. For a simplicial set Y it is defined as the simplicial set $F(Y)_n = C_n \times Y_n$. Here, we do not spell out the cyclic structure on $F(Y)$. For a cyclic space X, the evaluation $\mathrm{ev}\colon F(X) \to X$, $(g, x) = g.x$ is a morphism of cyclic spaces. The realization $|F(X)|$ is homeomorphic to $|C| \times |X|$ via $p_1 \times p_2$ for maps

$$p_1(g, x; u) = (g; u) \quad \text{and} \quad p_2(g, x; u) = (x; g^*u) \tag{A.3}$$

where g^*u is the cocylic action defined by $\tau_n(u_0, \ldots, u_n) := (u_1, \ldots, u_n, u_0)$. The action of $\mathbb{S}^1 \cong |C|$ on $|X|$ is $\mathrm{ev} \circ (p_1 \times p_2)^{-1}$.

With these facts at hand, the claim is readily checked: A point $x = (\sigma; u_0, \ldots, u_n)$ is also represented by $(s_n\sigma; u_0, \ldots, u_{n-1}, u_n - z, z)$ for $0 \leq z \leq u_n$. The point $z \in \mathbb{S}^1$ is represented by $(t_1, z, 1-z)$ which is also $(s_n \circ \ldots \circ s_1(t_1); z, u_0, \ldots, u_{n-1}, u_n - z)$. By [Lod92], we know that $s_n \circ \ldots \circ s_1(t_1) = t_{n+1}$. The point $(z, x) \in \mathbb{S}^1 \times |X|$ is hit by $(t_{n+1}, s_n\sigma; z, u_0, \ldots, u_{n-1}, u_n - z)$ under the homeomorphism $p_1 \times p_2$:

$$(z, x) = p_1 \times p_2(t_{n+1}, s_n\sigma; z, u_0, \ldots, u_{n-1}, u_n - z)\,. \tag{A.4}$$

Evaluating yields

$$\mathrm{ev}(t_{n+1}, s_n\sigma; z, u_0, \ldots, u_{n-1}, u_n - z) = (t_{n+1}s_n\sigma; z, u_0, \ldots, u_{n-1}, u_n - z)\,. \tag{A.5}$$

□

A.2. Extra degeneracies

For the convenience of the reader, we recall the definition of an *extra degeneracy*. A detailed discussion is found in [Bar02, Section 3.3.2].

Definition A.2.1. Let $X_\bullet$ be an augmented simplicial object. A sequence of maps $s^n_{-1}\colon X_n \to X_{n+1}$ for all $n \geq -1$ are called *extra degeneracies* if they satisfy:

1. $d^{n+1}_0 s^n_{-1} = \mathrm{id}$ for all $n \geq -1$
2. $d^{n+1}_{i+1} s^n_{-1} = s^{n-1}_{-1} d^n_i$ for all $n \geq i \geq 0$
3. $s^{n+1}_0 s^n_{-1} = s^{n+1}_{-1} s^n_{-1}$ for all $n \geq -1$
4. $s^{n+1}_i s^n_{-1} = s^{n+1}_{-1} s^n_{i-1}$ for all $n+1 \geq i > 0$

Proposition A.2.2. *Consider an augmented simplicial object $X_\bullet$ with extra degeneracies. Then, the underlying simplicial object is simplicially homotopy equivalent to the constant simplicial object X_{-1}.*

B

Discrete Morse Theory

Here, we review the elements of discrete Morse theory which was introduced by Forman in [For98]. We briefly recall the geometric motivation in a simplified setting. Consider a finite, regular simplicial complex X and assume we have a top dimensional simplex Δ of X with a free face $d_i\Delta$, i.e., $d_i\Delta$ appears exactly once as a face of a top dimensional simplex. Retracting Δ onto $\Lambda^i\Delta = \partial\Delta - d_i\Delta$ results in a finite, regular simplicial complex $X' \simeq X$ having two simplicies fewer then X. The cell Δ is called *collapsible* and $d_i\Delta$ is *redundant*. Repeating this process results in a sequence of pairs of collapsibles and redundants. This set of (disjoint) pairs is called *discrete Morse flow* and all non-paired simplices are called *essential*. Performing the collapses one gets a smaller simplicial complex $M \simeq X$ and M has as many simplices as there are essentials in X.

We need a more general version where a non-regular cell complex X and non-free faces are allowed. We only describe this in the algebraic setting.

Definition B.1 (Cellular Graph)**.** Let R be a coefficient ring. A directed graph $C = (V, E, d, \theta)$ with *vertices* V, *edges* $E \subseteq V \times V$, *degree* $d\colon V \to \mathbb{Z}$ and *coefficients* $\theta\colon E \to R$ is said to be *cellular* if it has only finitely many vertices in each grading and every edge $(v, w) \in E$ decreases the grading by one and has non-vanishing coefficient, i.e.,

$$d(v) = d(w) + 1 \qquad \text{and} \qquad \theta(v, w) \neq 0\,. \tag{B.1}$$

Let $K_\bullet$ be a chain complex of finite type that is free in each degree and has a distinguished choice of basis, e.g., the cellular complex of a CW complex of finite type. Its associated cellular graph has vertices given by the basis elements and edges given by the differential. The grading of the vertices is given by the degree of the basis elements in the chain complex and the coefficients of the edges by their coefficient in the differential.

Example B.2. Consider the integral chain complex $K_\bullet$ concentrated in degrees 0 and 1 with $K_0 = \mathbb{Z}\langle e_1, e_2, e_3\rangle$, $K_1 = \mathbb{Z}\langle f_1, f_2, f_3\rangle$; the only non-trivial differential is

$$\begin{pmatrix} 1 & -1 & 0 \\ 2 & 2 & 1 \\ 0 & 5 & -1 \end{pmatrix}. \tag{B.2}$$

The cellular graph is as follows:

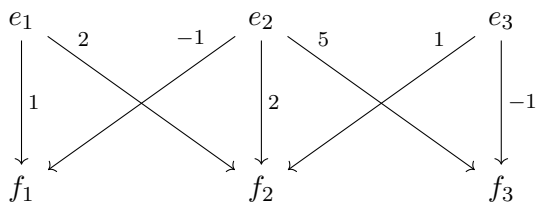

(B.3)

Definition B.3 (Matchings)**.** Let $C = (V, E, d, \theta)$ be a cellular graph. A collection of edges $F \subseteq E$ is a *matching* if any two edges in F have disjoint vertices and if $\theta(v, w)$ is invertible for every edge $(v, w) \in F$. In this case, a vertex $v \in V$ is called *collapsible* if there exists an edge $(v, w) \in F$, it is called *redundant* if there exists an edge $(u, v) \in F$ and it is called *essential* otherwise.

Definition B.4 (F-inverted graph)**.** Let $C = (V, E, d, \theta)$ be a cellular graph and $F \subseteq E$ a matching. The *F-inverted graph* $C[F^{-1}] = (V, E_F, d, \theta_F)$ is obtained from C by inverting the edges in F, i.e.,

$$E_F = (E - F) \sqcup \{(w, v) \mid (v, w) \in F\} \tag{B.4}$$

and inverting their coefficient in R, i.e.,

$$\theta_F(x, y) = \begin{cases} \theta(x, y) & (x, y) \in E - F \\ -\theta(y, x)^{-1} & (y, x) \in F \end{cases} \tag{B.5}$$

Every edge in the F-inverted graph either decreases or increases the grading by one and so we write $v \searrow w$ if $(v, w) \in E - F$ and $v \nearrow w$ else.

A path in $C[F^{-1}]$ from x to y is denoted by $\gamma \colon x \rightsquigarrow y$. The set of paths in the F-inverted graph is

$$P_F(y, x) = \{\gamma \colon x \rightsquigarrow y \text{ in } C[F^{-1}]\}\,. \tag{B.6}$$

The *coefficient* $\theta_F(\gamma)$ of a path $\gamma \in P_F(y, x)$ is the product of the coefficients θ_F of its edges.

Definition B.5 (Discrete Morse flow)**.** Let C be a cellular graph. A matching F is a *discrete Morse flow* if the F-inverted graph $C[F^{-1}]$ is *acyclic*, i.e., it does not contain oriented loops.

The following Lemma turns out to be helpful to deduce the acyclicity of a matching.

Lemma B.6. *Let C be a cellular graph and F a matching. The F-inverted graph is acyclic if and only if there exists a partial order $\leq$ on the collapsibles such that the existence of a path*

$$c_1 \searrow r_2 \nearrow c_2 \qquad \textit{with} \qquad c_i \textit{ collapsible} \tag{B.7}$$

implies $c_1 \lneqq c_2$.

Proof. If $C[F^{-1}]$ is acyclic, then the relation

$$c_1 \precneqq c_2 \text{ if and only if there exists a non-empty path from } c_1 \text{ to } c_2 \tag{B.8}$$

is a partial order. The converse is clear. □

Definition B.7 (Morse Complex)**.** Let $C = (V, E, d, \theta)$ be a cellular graph with Morse flow F. The *Morse complex* $M_\bullet = M(C, F)_\bullet$ of C and F is a chain complex freely generated by the essential vertices in each grading. The coefficient of an essential cell $y \in M_{n-1}$ in the boundary of an essential cell $x \in M_n$ is

$$\partial_{y,x} = \sum_{\gamma \in P_F(y,x)} \theta_F(\gamma)\,. \tag{B.9}$$

Theorem B.8 (Forman)**.** *Let C be the cellular graph of a chain complex $K_\bullet$. Let F be a discrete Morse flow on C. Then, the Morse complex $M(C, F)_\bullet$ is a homotopy retract of $K_\bullet$. The inclusion $\iota\colon M(C, F)_\bullet \to K_\bullet$ is given by sending essential cells x to*

$$\iota(x) = \sum_{\gamma \in P_x} \theta_F(\gamma) t(\gamma) \tag{B.10}$$

where $P_x = \{\gamma \in P_F(y, x) \mid \deg(y) = \deg(x), y \text{ not redundant}\}$ and $t(\gamma)$ denotes the endpoint of a path γ.

For a proof of Theorem B.8, we refer the reader to [Koz08, Chapter 11.3].

C

Symmetric Frobenius Algebras

In what follows, we denote by $\mathbb{K}$ a field of characteristic different from two. We give three equivalent definitions of symmetric Frobenius algebra. A detailed discussion of Frobenius algebras and their connections to two-dimensional field theories is found in [Koc04].

Definition C.1. A *symmetric Frobenius algebra* is a finite dimensional, unital, associative algebra A over $\mathbb{K}$ together with a non-degenerate, symmetric bilinear form $\sigma\colon A \otimes A \to A$ with $\sigma(xy, z) = \sigma(x, yz)$ for all $x, y, z \in A$.

Definition C.2. A *symmetric Frobenius algebra* is a finite dimensional, unital, associative algebra A over $\mathbb{K}$ together with a non-degenerate, symmetric linear functional $\epsilon\colon A \to \mathbb{K}$, i.e., $\{x \in A \mid \epsilon(x) = 0\}$ does not contain a proper left ideal and $\epsilon(xy) = \epsilon(yx)$ for all $x, y \in A$.

Definition C.3. A *symmetric Frobenius algebra* is a finite dimensional vector space A over $\mathbb{K}$ together with

1. a multiplication $\mu\colon A \otimes A \to A$ and unit $\eta\colon \mathbb{K} \to A$ making A a unital, associative algebra
2. a comultiplication $\delta\colon A \to A \otimes A$ and counit $\epsilon\colon A \to \mathbb{K}$ making A a counital, coassociative coalgebra

such that $\sigma := \epsilon\mu\colon A \otimes A \to \mathbb{K}$ is symmetric and such that the Frobenius relation

$$(\mathrm{id} \otimes \mu)(\delta \otimes \mathrm{id}) = \delta\mu = (\mu \otimes \mathrm{id})(\mathrm{id} \otimes \delta) \tag{C.1}$$

is satisfied.

Remark C.4. Let us say a few words why the three definitions give the same object. Consider a symmetric Frobenius algebra as defined in Definition C.1 the non-degenerate symmetric bilinear form σ defines a non-degenerate symmetric linear functional ϵ via

$$\epsilon(x) = \sigma(x, 1)\,. \tag{C.2}$$

Vice versa, the non-degenerate symmetric linear functional ϵ defines the non-degenerate symmetric bilinear form via

$$\sigma(x, y) = \epsilon(xy)\,. \tag{C.3}$$

Given a symmetric Frobenius algebra $A = (A, \mu, \eta, \delta, \epsilon)$ as in Definition C.3, the counit ϵ is a non-degenerate, symmetric linear functional. In order to construct the comultiplication and the counit from a given non-degenerate bilinear form, we refer the reader to [Koc04, Section 2.3].

Remark C.5. Using the Kozul-sign-convention, the definition of a graded symmetric Frobenius algebra agrees with the above Definitions.

Let us discuss two well known examples of Frobenius algebras.

Example C.6. Consider the cohomology ring $A := H^*(M; \mathbb{Q})$ of a connected, closed, oriented, n-dimensional manifold M with fundamental class $[M]$. We denote the Kronecker pairing by $\langle -, - \rangle$. The *Frobenius pairing of* A is

$$\sigma(\alpha, \beta) := \langle \alpha \cup \beta, [M] \rangle \in \mathbb{Q} \tag{C.4}$$

This makes the cohomology ring A into a graded symmetric Frobenius algebra by the Poincaré-duality Theorem.

If, in addition, all odd-dimensional cohomology groups vanish, we obtain an ungraded symmetric Frobenius algebra. In particular, the cohomology ring of an even-dimensional sphere is an ungraded symmetric Frobenius algebra. Let us spell out its structure in the sense of Definition C.3. As an algebra, it is an exteriour algebra $A = \Lambda[t]$ in one generator t in degree $2n$. The counit is given by $\epsilon(1) = 0$ and $\epsilon(t) = 1$. The comultiplication is given by $\delta(1) = 1 \otimes t + t \otimes 1$ and $\delta(t) = t \otimes t$.

Example C.7. Let G be a finite group with $n + 1$ elements $G = \{1, s_1, \ldots, s_n\}$. On its group ring $\mathbb{C}[G]$ we define the *Frobenius form* by $\epsilon(1) = 1$ and $\epsilon(s_i) = 0$. The associated bilinear form $\sigma(x, y) := \epsilon(xy)$ is non-degenerate since $\sigma(g, g^{-1}) = 1$ for all group elements $g \in G$. The Frobenius form is clearly symmetric.

D

Factorable groups

Here, we make the relation between the bar compactification and the (norm filtration of the reduced) bar resolution of varying symmetric groups explicit. To this end, we concentrate on the bar compactification $R := Bar(\mathfrak{M}_g^{\square}(m,1))$ of a fixed moduli space with unparametrized and unenumerated outgoing boundaries. As before, we denote the complement of $\mathfrak{Rad} \subset R$ by R' which is a subcomplex of R. The homology of $\mathfrak{M}$ is Poincaré dual to the cohomology of (R, R') with certain orientation coefficients. The orientation coefficients will not play a role in the subsequent discussion and are therefore suppressed in the notation.

Computing the horizontal faces of the reduced[1] bi-complex (R, R') gives rise to a spectral sequence $E^r_{p,q}$. Using the inhomogeneous notation, the q-th row of $E^0_{p,q}$ is the chain complex of all tuples $\Sigma = (\tau_1 \mid \ldots \mid \tau_q)$ such that $\tau_i \neq 1$, $N(\tau_1) + \ldots + N(\tau_q) = h = 2g + m - 2$ and $m(\Sigma) = \mathrm{ncyc}(\tau_q \cdots \tau_1 \cdot \omega_p) = m$. Observe that $d'_0\Sigma = 0 = d'_q\Sigma$ and that $m(\Sigma) = m(d'_i\Sigma)$ whenever $d'_i\Sigma \neq 0$. This chain complex is a direct summand of a row of a spectral sequence that computes the homology of the reduced bar resolution of the symmetric group $\mathfrak{S}_p$: Denote the reduced bar resolution of $\mathfrak{S}_p$ by $B_*\mathfrak{S}_p$. The set of all transpositions is a generating set $\mathcal{E}$ of $\mathfrak{S}_p$. The corresponding world length norm is denoted by $N^{\mathcal{E}}$. It induces a filtration F_s of $B_*\mathfrak{S}_p$. The associated shifted spectral sequence is denoted by $\mathcal{N}^r_{s,t}$ with $\mathcal{N}^0_{s,t} := F_sB_t\mathfrak{S}_p/F_{s-1}B_t\mathfrak{S}_p$. It is immediate that $(E^0_{p,*}, d') \subset (\mathcal{N}^0_{h,*}, d^0)$ is a direct summand and therefore, $E^1_{p,q} \subset \mathcal{N}^1_{h,q}$ is a direct summand.

The theory of factorable groups, introduced by Visy in [Vis10] and generalized by Alexander Heß and Rui Wang in [Heß12] and [Wan11], is used to show that $\mathcal{N}^1_{h,*}$ is concentrated in degree $\mathcal{N}^1_{h,h} = \ker(d^0_{h,h})$. By [Vis10, Theorem 5.2.1], the symmetric group $\mathfrak{S}_p$ is *factorable* with respect to the generating set of all transpositions $\mathcal{E}$, i.e., there is a factorization map $\eta\colon \mathfrak{S}_p \to \mathfrak{S}_p \times \mathcal{E}$ that splits off a generator while respecting the word length norm and such that a certain compatibility with the multiplication is achieved. More precisely, denote the multiplication by $\mu\colon \mathfrak{S}_p \times \mathfrak{S}_p \to \mathfrak{S}_p$ and consider the diagram below.

$$\begin{array}{ccccccc} \mathfrak{S}_p \times \mathfrak{S}_p & \xrightarrow{\eta\times\mathrm{id}} & \mathfrak{S}_p \times \mathfrak{S}_p \times \mathfrak{S}_p & \xrightarrow{\mathrm{id}\times\mu} & \mathfrak{S}_p \times \mathfrak{S}_p & \xrightarrow{\mathrm{id}\times\eta} & \mathfrak{S}_p \times \mathfrak{S}_p \times \mathfrak{S}_p \\ \downarrow{\scriptstyle \mu} & & & & & & \downarrow{\scriptstyle \mu\times\mathrm{id}} \\ \mathfrak{S}_p & & \xrightarrow{\qquad\qquad\qquad\eta\qquad\qquad\qquad} & & & & \mathfrak{S}_p \times \mathfrak{S}_p \end{array} \tag{D.1}$$

[1] The subcomplex generated by all simplicially degenerated bi-simplices is acyclic. The quotient by this subcomplex is the called the reduced bi-complex.

Then, the upper right composition of maps preserves the norm if and only if the lower left composition does and, in this case, the diagram commutes. Visualizing the multiplication as two strings that are merged and the factorization map as a single string that is split, the lower left and upper right composition of the diagram is visualized by Figure D.1.

Figure D.1.: The left picture visualizes $\eta \circ \mu$ and the right picture visualizes $\mu \times \mathrm{id} \circ \mathrm{id} \times \eta \circ \mathrm{id} \times \mu \circ \eta \times \mathrm{id}$.

Let us discuss another example of factorable groups, see [Vis10, Example 1.2.4]. Consider the free group Fr_n on n generators $\{s_1, \dots, s_n\}$. Taking the generating set $\mathcal{E} = \{s_1, \dots s_n, s_1^{-1}, \dots, s_n^{-1}\}$, any element $x \in \mathrm{Fr}_n$ is uniquely represented by a unique word of minimal length $x = s_{i_N}^{\epsilon_N} \cdots s_{i_1}^{\epsilon_1}$ with $s_j \in \mathcal{E}$. The factorization map η is defined by splitting of the right most generator of the unique word.

In general, for a factorable group (or monoid), the factorability structure leads to a discrete Morse flow on the complex $(\mathcal{N}^0_{h,*}, d^0)$ such that all basis elements in degree $* < h$ are either collapsible or redundant, see [Heß12, Chapter 3]. The norm filtration $\mathcal{N}^0_{h,*}$ of the reduced bar resolution does not have elements of degree $* > h$ by construction.

Theorem D.1 ([Vis10, Theorem 4.1.1])**.** *The homology of the norm filtration $(\mathcal{N}^0_{h,*}, d^0)$ is concentrated in degree h and $\mathcal{N}^1_{h,*} = \ker(d^0_{h,h})$.*

Moreover, using the discrete Morse flow, a canonical basis for $\mathcal{N}^1_{h,*}$ is constructed, see [Vis10, Remark 4.3.2] and also [Heß12, Proposition 2.3.36] or [BH14, Definition 2.8.5].

E

The unstable homology of the moduli spaces

Here, we collect most of what is known about the unstable homology of the moduli spaces in question. For the convenience of the reader, we include some results on the stable homology.

E.1. The virtual cohomological dimension

The virtual cohomological dimension of the moduli spaces has been determined by Harer in [Har86, Theorem 4.1].

Theorem E.1.1 (Harer)**.** *Let $g \geq 0$, $m \geq 0$, $n \geq 0$ and $2g + m + n > 2$. The virtual cohomological dimension of the moduli space $\mathfrak{M}_g^\bullet(m,n)$ is $d(g,m,n)$ with*

$$d(g,m,n) = \begin{cases} 4(g-1) + 2n + m & \text{if } g > 0 \text{ and } n + m > 0 \\ 4g - 5 & \text{if } g > 0 \text{ and } n = m = 0 \\ 2n + m - 3 & \text{else} \end{cases} . \tag{E.1}$$

Moreover, by [CFP12], the rational homology vanishes on its virtual cohomological dimension in the following cases.

Theorem E.1.2 (Church–Farb–Putman)**.** *For $g \geq 2$, $m + n \leq 1$ it is*

$$H^{d(g,m,n)}(\mathfrak{M}_g^\circ(m,n); \mathbb{Q}) = 0 . \tag{E.2}$$

E.2. Results on the first homology

Here, we spell out the results of [Bir74, Theorem 4.5], [Pow78, Theorem 1], [Ehr97], [KM00, Theorem 3.12], [KS03, Proposition 1.6] and [God07, Proposition 11] on the first homology of the mapping class group. We denote by $\Gamma_g^\star(m,n)$ the mapping class group of a surface of genus g with $n+m$ boundary components among which n are enumerated and parametrized whereas the other m component are (un)enumerated and unparametrized depending on $\star \in \{\circ, \square\}$.

Theorem E.2.1 (Birman, Powell, Ehrenfried, Korkmaz–McCarthy, Godin)**.** *It is*

$$H_1(\Gamma_g^{\square}(m,0);\mathbb{Z}) \cong \begin{cases} 0 & g=0, m=0,1 \\ \mathbb{Z}_{m-1} & g=0, m\geq 2, m \text{ odd} \\ \mathbb{Z}_{2m-2} & g=0, m\geq 2, m \text{ even} \\ \mathbb{Z}_{12} & g=1, m=0,1 \\ \mathbb{Z}_{12}\oplus\mathbb{Z}_2 & g=1, m\geq 2 \\ \mathbb{Z}_{10} & g=2, m=0,1 \\ \mathbb{Z}_{10}\oplus\mathbb{Z}_2 & g=2, m\geq 2 \\ 0 & g\geq 3, m=0,1 \\ \mathbb{Z}_2 & g\geq 3, m\geq 2 \end{cases} \tag{E.3}$$

and

$$H_1(\Gamma_g^{\circ}(m,n);\mathbb{Z}) \cong \begin{cases} \mathbb{Z}^2 & g=1, m=0, n=2 \\ \mathbb{Z}_{10} & g\geq 2, m\geq 0, n\geq 0 \\ 0 & g\geq 3, m\geq 0, n\geq 0 \end{cases}. \tag{E.4}$$

Recall that, for $n \geq 1$, the moduli space $\mathfrak{M}_g^{\star}(m,n)$ is a classifying space of $\Gamma_g^{\star}(m,n)$ and, for $n=0$, $\mathfrak{M}_g^{\star}(m,n)$ is still rationally a classifying space.

Corollary E.2.2. *Let $g \geq 1$, $m \geq 0$, $n \geq 1$ and $\star \in \{\circ, \square\}$. Then*

$$H_1(\mathfrak{M}_g^{\circ}(m,n);\mathbb{Z}) \cong \begin{cases} \mathbb{Z}^2 & g=1, m=0, n=2 \\ \mathbb{Z}_{10} & g\geq 2, m\geq 0, n\geq 1 \\ 0 & g\geq 3, m\geq 0, n\geq 1 \end{cases} \tag{E.5}$$

and

$$H_1(\mathfrak{M}_g^{\star}(m,0);\mathbb{Q}) \cong 0\,. \tag{E.6}$$

Moreover, we would like to add the following proposition which we believe is known. A proof of this fact will follow from the study of the spectral sequence of the fibration $\mathfrak{M}_g^{\square}(m,1) \to \mathfrak{M}_g^{\square}(0,1)$.

Proposition E.2.3. *Let $g \geq 0$ and $m \geq 0$. It is*

$$H_1(\mathfrak{M}_g^{\square}(m,1);\mathbb{Z}) \cong \begin{cases} \mathbb{Z} & g=0,1, m=0,1 \\ \mathbb{Z}\oplus\mathbb{Z}_2 & g=0,1, m\geq 2 \\ \mathbb{Z}_{10} & g=2, m=0,1 \\ \mathbb{Z}_{10}\oplus\mathbb{Z}_2 & g=2, m\geq 2 \\ 0 & g\geq 3, m=0,1 \\ \mathbb{Z}_2 & g\geq 3, m\geq 2 \end{cases}. \tag{E.7}$$

E.3. Results on the second homology

Let us spell out the results of [Har83], [Har91], [BC91], [Ehr97], [KS03], [God07, Proposition 11], [Meh11] and [Sak12, Theorem 4.9, Corollary 4.10] on the second homology of the mapping class group $\Gamma_g^\circ(m,n)$.

Theorem E.3.1 (Harer, Benson–Cohen, Ehrenfried, Korkmaz–Stipsicz, Godin, Mehner, Sakasai)**.** *It is*

$$H_2(\Gamma_g^\circ(m,n);\mathbb{Z}) \cong \begin{cases} \mathbb{Z}\oplus\mathbb{Z}_2 & g=1, m=0, n=2 \\ \mathbb{Z}_2 & g=2, m=0,1, n=0,1 \\ \mathbb{Z}\oplus\mathbb{Z}_2 & g=3, m=0, n=0,1 \\ \mathbb{Z}^2\oplus\mathbb{Z}_2 & g=3, m=1, n=0 \\ \mathbb{Z}^{n+1} & g\geq 4, m\geq 0, n\geq 0 \end{cases}. \tag{E.8}$$

Recall that, for $n \geq 1$, the moduli space $\mathfrak{M}_g^\circ(m,n)$ is a classifying space of $\Gamma_g^\circ(m,n)$ and, for $n=0$, $\mathfrak{M}_g^\circ(m,n)$ is still rationally a classifying space.

Corollary E.3.2. *It is*

$$H_2(\mathfrak{M}_g^\circ(m,n);\mathbb{Z}) \cong \begin{cases} \mathbb{Z}\oplus\mathbb{Z}_2 & g=1, m=0, n=2 \\ \mathbb{Z}_2 & g=2, m=0,1, n=1 \\ \mathbb{Z}\oplus\mathbb{Z}_2 & g=3, m=0, n=1 \\ \mathbb{Z}^{n+1} & g\geq 4, m\geq 0, n\geq 1 \end{cases} \tag{E.9}$$

and

$$H_2(\mathfrak{M}_g^\circ(m,n);\mathbb{Q}) \cong \begin{cases} \mathbb{Q} & g=1, m=0, n=2 \\ 0 & g=2, m=0,1, n=0,1 \\ \mathbb{Q} & g=3, m=0, n=0,1 \\ \mathbb{Q}^2 & g=3, m=1, n=0 \\ \mathbb{Q}^{n+1} & g\geq 4, m\geq 0, n\geq 0 \end{cases}. \tag{E.10}$$

E.4. Results on the homology of a single moduli space

The moduli spaces $\mathfrak{M}_0^\square(m,1)$ are classifying spaces for the braid groups Br_m. Their homology is well known by the results of [Arn70], [Fuk70] and [CLM76].

For coefficients in a field $\mathbb{F}$ with $\mathrm{char}(\mathbb{F}) \neq 2$, 3 or 5, the mapping class group $\Gamma_2^\square(0,0)$ is a classifying space for $\mathfrak{M}_2^\square(0,0)$. In this case, we have $H^*(\mathfrak{M}_2^\square(0,0);\mathbb{F}) = 0$ by [LW85, Corollary 5.2.3]. For coefficients in the field $\mathbb{F}$ with $\mathrm{char}(\mathbb{F}) = 2$, 3 or 5 elements, the Poincaré series of $\Gamma_2^\square(0,0)$ has been determined by [BC91, Theorem I.1.2, Theorem II.1.1, Theorem III.1.1].

Theorem E.4.1 (Lee–Weintraub, Benson–Cohen)**.** *Let p be a prime and denote the finite field with p elements by $\mathbb{F}_p$. The Poincaré series of $\Gamma_2^\square(0,0)$ are as follows.*

$$\sum_{n\geq 0} \dim_{\mathbb{F}_p} H^n(\Gamma_2^\square(0,0);\mathbb{F}_p)\cdot t^n = \begin{cases} (1+t^2+2t^3+t^4+t^5)/(1-t)(1-t^4) & p=2 \\ (1+t^3+t^4+t^5)/(1-t^4) & p=3 \\ 1/(1-t) & p=5 \\ 1 & \textit{else} \end{cases} \tag{E.11}$$

The rational homology of the moduli spaces $\mathfrak{M}_2^\square(3,0)$ respectively $\mathfrak{M}_4^\square(0,0)$ has been computed by Tommasi in [Tom05, Theorem 1.4] respectively [Tom07, Theorem 1.1]. We summarize her results as follows.

Theorem E.4.2 (Tommasi)**.** *The rational Betti numbers of the moduli space $\mathfrak{M}_2^\square(3,0)$ respectively $\mathfrak{M}_4^\square(0,0)$ are*

$$\beta(\mathfrak{M}_4^\square(0,0)) = (1,0,1,0,1,1) \tag{E.12}$$

respectively

$$\beta(\mathfrak{M}_2^\square(3,0)) = (1,0,3,0,2,1,1,0,2)\,. \tag{E.13}$$

Adding a point near the boundary of a given surface induces an inclusion of moduli spaces $a\colon \mathfrak{M}_g^\square(m,n) \to \mathfrak{M}_g^\square(m+1,n)$. The induced map in homology is split injective by [BT01, Theorem 1.3]. Using Bödigheimer's combinatorial models for the moduli spaces, [Ehr97], [Abh05], [Wan11], [Meh11], [BH14] and the author compute the rational and integral homology of $\mathfrak{M}_g^\square(m,1)$ for small parameters m. Moreover, [Meh11] and the author identified some of the generators.

Theorem E.4.3 (Bödigheimer, Ehrenfried, Abhau, Wang, Mehner, B.–Hermann, B.)**.** *The integral homology of the moduli space $\mathfrak{M}_1^\square(3,1)$ respectively $\mathfrak{M}_2^\square(2,1)$ is as follows.*

$$H_*(\mathfrak{M}_1^\square(3,1);\mathbb{Z}) \cong \begin{cases} \mathbb{Z}\langle a^3c\rangle & *=0 \\ \mathbb{Z}\langle a^3d\rangle \oplus \mathbb{Z}_2\langle abc\rangle & *=1 \\ \mathbb{Z}_2\langle a^2e\rangle \oplus \mathbb{Z}_2\langle abd\rangle & *=2 \\ \mathbb{Z}\langle ?\rangle \oplus \mathbb{Z}_2\langle be\rangle \oplus \mathbb{Z}_2\langle af\rangle & *=3 \\ \mathbb{Z}\langle ?\rangle \oplus \mathbb{Z}\langle ?\rangle & *=4 \\ \mathbb{Z}\langle ?\rangle & *=5 \\ 0 & \textit{else} \end{cases} \tag{E.14}$$

respectively

$$H_*(\mathfrak{M}_2^\square(1,1);\mathbb{Z}) \cong \begin{cases} \mathbb{Z}\langle ac^2\rangle & *=0 \\ \mathbb{Z}_2\langle acd\rangle & *=1 \\ \mathbb{Z}\langle ?\rangle \oplus \mathbb{Z}_2\langle ad^2\rangle & *=2 \\ \mathbb{Z}\langle \lambda as\rangle \oplus \mathbb{Z}\langle ?\rangle \oplus \mathbb{Z}_2\langle at\rangle \oplus \mathbb{Z}_2\langle de\rangle & *=3 \\ \mathbb{Z}_3\langle aw_3\rangle \oplus \mathbb{Z}_2\langle a?\rangle \oplus \mathbb{Z}_6\langle ?\rangle & *=4 \\ \mathbb{Z}\langle ?\rangle & *=5 \\ \mathbb{Z}\langle ?\rangle & *=6 \\ 0 & \textit{else} \end{cases} \tag{E.15}$$

Here, the known generators a,b,c,d,e,t and their products are described in [Meh11, Kapitel 1] or [BH14, Chapter 4], see also [BB18a]. The generators $s \in H_3(\mathfrak{M}_2^{\square}(1,1);\mathbb{Q})$, $w_3 \in H_4(\mathfrak{M}_2^{\square}(1,1);\mathbb{Z})$ *respectively* $f \in H_3(\mathfrak{M}_1^{\square}(2,1);\mathbb{Z})$ *are described in Section 7.1, Section 7.2 respectively Section 7.3. The other generators are denoted by the symbol ?. Moreover, a generator* $x \in H_*(\mathfrak{M}_g^{\square}(m,1);\mathbb{Z})$ *is in image of the split injective map* $a^k \colon H_*(\mathfrak{M}_g^{\square}(m-k,1);\mathbb{Z}) \to H_*(\mathfrak{M}_g^{\square}(m,1);\mathbb{Z})$ *if and only if it is denoted by* $x = a^k y$ *in the above description.*

Furthermore, the rational Betti numbers of the moduli space $\mathfrak{M}_1^{\square}(4,1)$, $\mathfrak{M}_2^{\square}(2,1)$ *respectively* $\mathfrak{M}_3^{\square}(0,1)$ *are*

$$\beta(\mathfrak{M}_1^{\square}(4,1)) = (1,1,0,2,3,2,1)\,, \tag{E.16}$$

$$\beta(\mathfrak{M}_2^{\square}(2,1)) = (1,0,1,3,1,2,2) \tag{E.17}$$

respectively

$$\beta(\mathfrak{M}_3^{\square}(0,1)) = (1,0,1,1,0,1,1,0,0,1)\,. \tag{E.18}$$

$$\tag{E.19}$$

Using a chain complex of ribbon graphs as a model for mapping class groups, Godin computes the integral homology of $\Gamma_g^{\square}(m,n)$ for small parameters g, m and n in [God07]. Her results match the results of Ehrenfried.

Theorem E.4.4 (Godin)**.** *The integral homology of the mapping class group* $\Gamma_1^{\square}(0,2)$, $\Gamma_1^{\square}(1,0)$ *respectively* $\Gamma_2^{\square}(1,0)$ *is as follows.*

$$H_*(\Gamma_1^{\square}(0,2);\mathbb{Z}) \cong \begin{cases} \mathbb{Z} & *=0 \\ \mathbb{Z}^2 & *=1 \\ \mathbb{Z}\oplus\mathbb{Z}_2 & *=2 \\ \mathbb{Z}_2 & *=3 \\ 0 & \textit{else} \end{cases} \tag{E.20}$$

respectively

$$H_*(\Gamma_1^{\square}(1,0);\mathbb{Z}) \cong \begin{cases} \mathbb{Z} & *=0 \\ \mathbb{Z}_{12} & *=2k+1 \\ 0 & *=2k+2 \end{cases} \tag{E.21}$$

respectively

$$H_*(\Gamma_2^{\square}(1,0);\mathbb{Z}) \cong \begin{cases} \mathbb{Z} & *=0 \\ \mathbb{Z}_{10} & *=1 \\ \mathbb{Z}\oplus\mathbb{Z}_2 & *=2 \\ \mathbb{Z}_{120}\oplus\mathbb{Z}_{10}\oplus\mathbb{Z}_2 & *=2k+3 \\ \mathbb{Z}_6\oplus\mathbb{Z}_2 & *=2k+4 \end{cases} \tag{E.22}$$

Recall that, for $n \geq 1$, the moduli space $\mathfrak{M}_g^{\square}(m,n)$ is a classifying space of $\Gamma_g^{\square}(m,n)$ and, for $n=0$, $\mathfrak{M}_g^{\square}(m,n)$ is still rationally a classifying space.

Corollary E.4.5. *It is*

$$H_*(\mathfrak{M}_1^{\square}(0,2);\mathbb{Z}) \cong \begin{cases} \mathbb{Z} & *=0 \\ \mathbb{Z}^2 & *=1 \\ \mathbb{Z}\oplus\mathbb{Z}_2 & *=2 \\ \mathbb{Z}_2 & *=3 \\ 0 & else \end{cases} \tag{E.23}$$

respectively

$$H_*(\mathfrak{M}_1^{\square}(1,0);\mathbb{Q}) \cong \begin{cases} \mathbb{Q} & *=0 \\ 0 & else \end{cases} \tag{E.24}$$

respectively

$$H_*(\mathfrak{M}_2^{\square}(1,0);\mathbb{Q}) \cong \begin{cases} \mathbb{Q} & *=0 \\ 0 & *=1 \\ \mathbb{Q} & *=2 \\ 0 & else \end{cases}. \tag{E.25}$$

Bibliography

[Abb15] Hossein Abbaspour. On algebraic structures of the Hochschild complex. In *Free loop spaces in geometry and topology*, volume 24 of *IRMA Lect. Math. Theor. Phys.*, pages 165–222. Eur. Math. Soc., Zürich, 2015.

[Abh05] Jochen Abhau. *Die Homologie von Modulräumen Riemannscher Flächen — Berechnungen für $g \leq 2$.* Rheinische Friedrich-Wilhelms-Universität Bonn, January 2005. Diplomarbeit.

[ABE08] Jochen Abhau, Carl-Friedrich Bödigheimer, and Ralf Ehrenfried. Homology of the mapping class group $\Gamma_{2,1}$ for surfaces of genus 2 with a boundary curve. In *The Zieschang Gedenkschrift*, volume 14 of *Geom. Topol. Monogr.*, pages 1–25. Geom. Topol. Publ., Coventry, 2008.

[Arn70] Vladimir I. Arnold. On some topological invariants of algebraic functions. In *Vladimir I. Arnold - Collected Works*, pages 199–221. Springer Berlin Heidelberg, 1970.

[Bar02] Michael Barr. *Acyclic models*, volume 17 of *CRM Monograph Series*. American Mathematical Society, Providence, RI, 2002.

[BC91] David. J. Benson and Frederick. R. Cohen. Mapping class groups of low genus and their cohomology. *Mem. Amer. Math. Soc.*, 90(443):iv+104, 1991.

[Bir74] Joan S. Birman. *Braids, links, and mapping class groups.* Princeton University Press, Princeton, N.J.; University of Tokyo Press, Tokyo, 1974. Annals of Mathematics Studies, No. 82.

[Boe18] Felix J. Boes. *Homology of Sullivan Diagrams – hosd*, 2015 - 2018. `https://github.com/felixboes/hosd`.

[BE17] Felix J. Boes and Daniela Egas Santander. On the homotopy type of the space of Sullivan diagrams. *preprint*, 2017, `arXiv:1705.07499 [math.AT]`.

[BH18] Felix J. Boes and Anna Hermann. *Kappa*, 2013 - 2018. `https://github.com/felixboes/kappa`.

[BH14] Felix J. Boes and Anna Hermann. *Moduli Spaces of Riemann Surfaces – Homology Computations and Homology Operations.* Rheinische Friedrich-Wilhelms-Universität Bonn, September 2014. Master's Thesis Mathematics, `http://www.math.uni-bonn.de/people/boes/masterarbeit_boes_hermann.pdf`.

[BCP97] Wieb Bosma, John Cannon, and Catherine Playoust. The Magma algebra system. I. The user language. *J. Symbolic Comput.*, 24(3-4):235–265, 1997. Computational algebra and number theory (London, 1993).

[BE88] B. H. Bowditch and D. B. A. Epstein. Natural triangulations associated to a surface. *Topology*, 27(1):91–117, 1988.

[Bö90a] Carl-Friedrich Bödigheimer. On the topology of moduli spaces of Riemann surfaces. Part I: Hilbert Uniformization. *Math. Gott. (Preprints of the SFB 170, Göttingen)*, 9, 1990.

[Bö90b] Carl-Friedrich Bödigheimer. On the topology of moduli spaces of Riemann surfaces. Part II: Homology Operations. *Mathematica Gottingensis*, 1990.

[Bö93a] Carl-Friedrich Bödigheimer. The harmonic compactification of the moduli space of Riemann surfaces. *Math. Gott. (Preprints of the SFB 170, Göttingen)*, 8, 1993.

[Bö93b] Carl-Friedrich Bödigheimer. Interval exchange spaces and moduli spaces. In *Mapping class groups and moduli spaces of Riemann surfaces (Göttingen, 1991/Seattle, WA, 1991)*, volume 150 of *Contemp. Math.*, pages 33–50. Amer. Math. Soc., Providence, RI, 1993.

[Bö06] Carl-Friedrich Bödigheimer. Configuration models for moduli spaces of Riemann surfaces with boundary. *Abhandlungen aus dem Mathematischen Seminar der Universität Hamburg*, 76:191–233, 2006.

[Bö07] Carl-Friedrich Bödigheimer. Hilbert uniformization of Riemann surfaces: I – short version. *preprint*, 2007. `http://www.math.uni-bonn.de/people/cfb/PUBLICATIONS/short-hilbert.pdf`.

[BB18a] Carl-Friedrich Bödigheimer and Felix J. Boes. Generators in the Homology of Moduli spaces. *in preparation*, 2018.

[BB18b] Carl-Friedrich Bödigheimer and Felix J. Boes. A Spectral Sequence for the Homology of the Moduli Spaces of Riemann Surfaces. *in preparation*, 2018.

[BT01] Carl-Friedrich Bödigheimer and Ulrike Tillmann. Stripping and splitting decorated mapping class groups. In *Cohomological methods in homotopy theory (Bellaterra, 1998)*, volume 196 of *Progr. Math.*, pages 47–57. Birkhäuser, Basel, 2001.

[CS99] Moira Chas and Dennis Sullivan. String topology. *preprint*, 1999, `arXiv:math/9911159`.

[Cha05] David Chataur. A bordism approach to string topology. *Int. Math. Res. Not.*, (46):2829–2875, 2005.

[CFP12] Thomas Church, Benson Farb, and Andrew Putman. The rational cohomology of the mapping class group vanishes in its virtual cohomological dimension. *Int. Math. Res. Not. IMRN*, (21):5025–5030, 2012.

[CLM76] Frederick R. Cohen, Thomas J. Lada, and J. Peter May. *The homology of iterated loop spaces*. Lecture Notes in Mathematics, Vol. 533. Springer-Verlag, Berlin-New York, 1976.

[CG04] Ralph L. Cohen and Véronique Godin. A polarized view of string topology. In *Topology, geometry and quantum field theory*, volume 308 of *London Math. Soc. Lecture Note Ser.*, pages 127–154. Cambridge Univ. Press, Cambridge, 2004.

[CHV06] Ralph L. Cohen, Kathryn Hess, and Alexander A. Voronov. *String topology and cyclic homology*. Advanced Courses in Mathematics. CRM Barcelona. Birkhäuser Verlag, Basel, 2006. Lectures from the Summer School held in Almería, September 16–20, 2003.

[CJ02] Ralph L. Cohen and John D. S. Jones. A homotopy theoretic realization of string topology. *Math. Ann.*, 324(4):773–798, 2002.

[CKS08] Ralph L. Cohen, John R. Klein, and Dennis Sullivan. The homotopy invariance of the string topology loop product and string bracket. *J. Topol.*, 1(2):391–408, 2008.

[Cos07a] Kevin Costello. A dual version of the ribbon graph decomposition of moduli space. *Geom. Topol.*, 11:1637–1652, 2007.

[Cos07b] Kevin Costello. Topological conformal field theories and Calabi-Yau categories. *Adv. Math.*, 210(1):165–214, 2007.

[DPR15] Gabriel Drummond-Cole, Kate Poirier, and Nathaniel Rounds. Chain-level string topology operations. *preprint*, 2015, `arXiv:1506.02596 [math.GT]`.

[Ega14a] Daniela Egas Santander. Comparing fat graph models of moduli space. *preprint*, 2014, `arXiv:1508.03433 [math.AT]`.

[Ega14b] Daniela Egas Santander. On the homology of Sullivan Diagrams. *preprint*, 2014.

[EK14] Daniela Egas Santander and Alexander P. M. Kupers. Comparing combinatorial models of moduli space and their compactifications. *preprint*, 2014, `arXiv: 1508.03433 [math.GT]`.

[Ehr97] Ralf Ehrenfried. *Die Homologie der Modulräume berandeter Riemannscher Flächen von kleinem Geschlecht*. Dissertation, Rheinische Friedrich-Wilhelms-Universität Bonn, 1997.

[Boost] Beman G. Dawes et al. *boost C++ libraries*, 1998 - 2018.

[FM12] Benson Farb and Dan Margalit. *A primer on mapping class groups*, volume 49 of *Princeton Mathematical Series*. Princeton University Press, Princeton, NJ, 2012.

[For98] Robin Forman. Morse theory for cell complexes. *Advances in mathematics*, 134(1):90–145, 1998.

[For81] Otto Forster. *Lectures on Riemann surfaces*, volume 81 of *Graduate Texts in Mathematics*. Springer-Verlag, New York-Berlin, 1981. Translated from the German by Bruce Gilligan.

[Fuk70] Dmitry B. Fuks. Cohomology of the braid group mod 2. *Funkcional. Anal. i Priložen.*, 4(2):62–73, 1970.

[Fé15] Yves Félix. Basic rational string topology. In *Free loop spaces in geometry and topology*, volume 24 of *IRMA Lect. Math. Theor. Phys.*, pages 223–242. Eur. Math. Soc., Züich, 2015.

[FT08] Yves Félix and Jean-Claude Thomas. Rational BV-algebra in string topology. *Bull. Soc. Math. France*, 136(2):311–327, 2008.

[Gal04] Søren Galatius. Mod p homology of the stable mapping class group. *Topology*, 43(5):1105–1132, 2004.

[Gal13] Søren Galatius. Lectures on the Madsen-Weiss theorem. In *Moduli spaces of Riemann surfaces*, volume 20 of *IAS/Park City Math. Ser.*, pages 139–167. Amer. Math. Soc., Providence, RI, 2013.

[GTMW] Søren Galatius, Ulrike Tillmann, Ib Madsen, and Michael Weiss. The homotopy type of the cobordism category. *Acta Math.*, 202(2):195–239, 2009.

[Get94] Ezra Getzler. Batalin-Vilkovisky algebras and two-dimensional topological field theories. *Comm. Math. Phys.*, 159(2):265–285, 1994.

[God04] Véronique Godin. *A category of bordered fat graphs and the mapping class group of a bordered surface*. ProQuest LLC, Ann Arbor, MI, 2004. Thesis (Ph.D.) – Stanford University.

[God07] Véronique Godin. The unstable integral homology of the mapping class groups of a surface with boundary. *Mathematische Annalen*, 337(1):15–60, 2007.

[GG08] Daciberg L. Gonçalves and John Guaschi. The classification and the conjugacy classes of the finite subgroups of the sphere braid groups. *Algebr. Geom. Topol.*, 8(2):757–785, 2008.

[GMP] Torbjörn Granlund et al. *GNU multiple precision arithmetic library*, 1991 - 2018. `https://gmplib.org/`.

[Han00] David Handel. Some homotopy properties of spaces of finite subsets of topological spaces. *Houston J. Math.*, 26(4):747–764, 2000.

[Har83] John Harer. The second homology group of the mapping class group of an orientable surface. *Invent. Math.*, 72(2):221–239, 1983.

[Har85] John L. Harer. Stability of the homology of the mapping class groups of orientable surfaces. *Math. Ann.*, 121:215–249, 1985.

[Har86] John L. Harer. The virtual cohomological dimension of the mapping class group of an orientable surface. *Invent. Math.*, 84(1):157–176, 1986.

[Har91] John L. Harer. The third homology group of the moduli space of curves. *Duke Math. J.*, 63(1):25–55, 1991.

[Hat11] Allan Hatcher. A short exposition of the Madsen–Weiss theorem. *preprint*, 2011, `arXiv:1103.5223 [math.GT]`.

[Heß12] Alexander Heß. *Factorable Monoids: Resolutions and Homology via Discrete Morse Theory*. Dissertation, Rheinische Friedrich-Wilhelms-Universität Bonn, 2012.

[Igu02] Kiyoshi Igusa. *Higher Franz-Reidemeister torsion*, volume 31 of *AMS/IP Studies in Advanced Mathematics*. American Mathematical Society, Providence, RI; International Press, Somerville, MA, 2002.

[Jon87] John D. S. Jones. Cyclic homology and equivariant homology. *Invent. Math.*, 87(2):403–423, 1987.

[KT08] Christian Kassel and Vladimir Turaev. *Braid groups*, volume 247 of *Graduate Texts in Mathematics*. Springer, New York, 2008. With the graphical assistance of Olivier Dodane.

[Kau07] Ralph M. Kaufmann. Moduli space actions on the Hochschild co-chains of a Frobenius algebra. I. Cell operads. *J. Noncommut. Geom.*, 1(3):333–384, 2007.

[Kau08a] Ralph M. Kaufmann. Moduli space actions on the Hochschild co-chains of a Frobenius algebra. II. Correlators. *J. Noncommut. Geom.*, 2(3):283–332, 2008.

[Kau08b] Ralph M. Kaufmann. A proof of a cyclic version of Deligne's conjecture via cacti. *Math. Res. Lett.*, 15(5):901–921, 2008.

[Kau10] Ralph M. Kaufmann. Open/closed string topology and moduli space actions via open/closed Hochschild actions. *SIGMA Symmetry Integrability Geom. Methods Appl.*, 6:Paper 036, 33, 2010.

[Kla13] Angela Klamt. Natural operations on the Hochschild complex of commutative Frobenius algebras via the complex of looped diagrams. *preprint*, 2013, `arXiv:1309.4997 [math.AT]`.

[Koc04] Joachim Kock. *Frobenius algebras and 2D topological quantum field theories*, volume 59 of *London Mathematical Society Student Texts*. Cambridge University Press, Cambridge, 2004.

[Kon92] Maxim Kontsevich. Intersection theory on the moduli space of curves and the matrix Airy function. *Comm. Math. Phys.*, 147(1):1–23, 1992.

[KS09] Maxim Kontsevich and Yan Soibelman. Notes on A_∞-algebras, A_∞-categories and non-commutative geometry. In *Homological mirror symmetry*, volume 757 of *Lecture Notes in Phys.*, pages 153–219. Springer, Berlin, 2009.

[KM00] Mustafa Korkmaz and John D. McCarthy. Surface mapping class groups are ultrahopfian. *Mathematical Proceedings of the Cambridge Philosophical Society*, 129(1):35–53, 2000.

[KS03] Mustafa Korkmaz and András I. Stipsicz. The second homology groups of mapping class groups of oriented surfaces. *Mathematical Proceedings of the Cambridge Philosophical Society*, 134(3):479–489, 2003.

[Koz08] Dmitry Kozlov. *Combinatorial algebraic topology*, volume 21 of *Algorithms and Computation in Mathematics*. Springer, Berlin, 2008.

[LS08] Pascal Lambrechts and Don Stanley. Poincaré duality and commutative differential graded algebras. *Ann. Sci. Éc. Norm. Supér. (4)*, 41(4):495–509, 2008.

[LW85] Ronnie Lee and Steven H. Weintraub. Cohomology of $\mathrm{Sp}_4(\mathbf{Z})$ and related groups and spaces. *Topology*, 24(4):391–410, 1985.

[Lod92] Jean-Louis Loday. *Cyclic homology*, volume 301 of *Grundlehren der Mathematischen Wissenschaften [Fundamental Principles of Mathematical Sciences]*. Springer-Verlag, Berlin, 1992. Appendix E by Maria O. Ronco.

[Loo95] Eduard Looijenga. Cellular decompositions of compactified moduli spaces of pointed curves. In *The moduli space of curves (Texel Island, 1994)*, volume 129 of *Progr. Math.*, pages 369–400. Birkhäuser Boston, Boston, MA, 1995.

[MW05] Ib Madsen and Michael Weiss. The stable mapping class group and stable homotopy theory. *European Congress of Mathematics, Eur. Math. Soc.*, pages 283–307, 2005.

[Meh11] Stefan Mehner. *Homologieberechnungen von Modulräumen Riemannscher Flächen durch diskrete Morse-Theorie*. Rheinische Friedrich-Wilhelms-Universität Bonn Bonn, December 2011. Diplomarbeit.

[Men09] Luc Menichi. Batalin-Vilkovisky algebra structures on Hochschild cohomology. *Bull. Soc. Math. France*, 137(2):277–295, 2009.

[Mum67] David Mumford. Abelian quotients of the Teichmüller modular group. *Journal d'Analyse Mathématique*, 18:227–244, 1967.

[Mur82] Kunio Murasugi. Seifert fibre spaces and braid groups. *Proc. London Math. Soc. (3)*, 44(1):71–84, 1982.

[Mü96] Meinhard Müller. *Orientierbarkeit des Raumes der Parallelschlitzgebiete*. Rheinische Friedrich-Wilhelms-Universität Bonn, 1996. Diplomarbeit.

[Pen87] R. C. Penner. The decorated Teichmüller space of punctured surfaces. *Comm. Math. Phys.*, 113(2):299–339, 1987.

[Pil13] Paweł Pilarczyk. *The Original CHomP Software*, 2013. `http://chomp.rutgers.edu/Projects/Computational_Homology/OriginalCHomP/software/`.

[PR11] Kate Poirier and Nathaniel Rounds. Compactified string topology. *preprint*, 2011, `arXiv:1111.3635v1 [math.GT]`.

[Pow78] Jerome Powell. Two theorems on the mapping class group of a surface. *Proceedings of the American Mathematical Society*, 68(3):347–350, 1978.

[RW16] Oscar Randal-Williams. Resolutions of moduli spaces and homological stability. *J. Eur. Math. Soc. (JEMS)*, 18(1):1–81, 2016.

[Sak12] Takuya Sakasai. Lagrangian mapping class groups from a group homological point of view. *Algebraic & Geometric Topology*, 12(1):267–291, 2012.

[ST08] Graeme Segal and Ulrike Tillmann. Mapping configuration spaces to moduli spaces. In *Groups of diffeomorphisms*, volume 52 of *Adv. Stud. Pure Math.*, pages 469–477. Math. Soc. Japan, Tokyo, 2008.

[ST07] Yongjin Song and Ulrike Tillmann. Braids, mapping class groups, and categorical delooping. *Math. Ann.*, 339(2):377–393, 2007.

[Str84] Kurt Strebel. *Quadratic differentials*, volume 5 of *Ergebnisse der Mathematik und ihrer Grenzgebiete (3) [Results in Mathematics and Related Areas (3)]*. Springer-Verlag, Berlin, 1984.

[Sul07] Dennis Sullivan. String topology background and present state. In *Current developments in mathematics, 2005*, pages 41–88. Int. Press, Somerville, MA, 2007.

[Tam09] Hirotaka Tamanoi. Stable string operations are trivial. *Int. Math. Res. Not. IMRN*, (24):4642–4685, 2009.

[Til97] Ulrike Tillmann. On the homotopy of the stable mapping class group. *Invent. Math.*, 130(2):257–275, 1997.

[Til16] Ulrike Tillmann. Homology stability for symmetric diffeomorphism and mapping class groups. *Math. Proc. Cambridge Philos. Soc.*, 160(1):121–139, 2016.

[Tom05] Orsola Tommasi. Rational cohomology of the moduli space of genus 4 curves. *Compos. Math.*, 141(2):359–384, 2005.

[Tom07] Orsola Tommasi. Rational cohomology of $\mathcal{M}_{3,2}$. *Compos. Math.*, 143(4):986–1002, 2007.

[Tra08] Thomas Tradler. The Batalin-Vilkovisky algebra on Hochschild cohomology induced by infinity inner products. *Ann. Inst. Fourier (Grenoble)*, 58(7):2351–2379, 2008.

[TZ06] Thomas Tradler and Mahmoud Zeinalian. On the cyclic Deligne conjecture. *J. Pure Appl. Algebra*, 204(2):280–299, 2006.

[Tsu59] Masatsugu Tsuji. *Potential theory in modern function theory.* Maruzen, 1959.

[Tuf02] Christopher Tuffley. Finite subset spaces of S^1. *Algebr. Geom. Topol.*, 2:1119–1145, 2002.

[Vai07] Dmitry Vaintrob. The string topology BV algebra, Hochschild cohomology and the Goldman bracket on surfaces. *preprint*, 2007, `arXiv:math/0702859v1`.

[Vis10] Balázs Visy. *Factorable Groups and their Homology.* Dissertation, Rheinische Friedrich-Wilhelms-Universität Bonn, November 2010.

[Vor05] Alexander A. Voronov. Notes on universal algebra. In *Graphs and patterns in mathematics and theoretical physics*, volume 73 of *Proc. Sympos. Pure Math.*, pages 81–103. Amer. Math. Soc., Providence, RI, 2005.

[Wah13] Nathalie Wahl. The Mumford conjecture, Madsen-Weiss and homological stability for mapping class groups of surfaces. In *Moduli spaces of Riemann surfaces*, volume 20 of *IAS/Park City Math. Ser.*, pages 109–138. Amer. Math. Soc., Providence, RI, 2013.

[Wah16] Nathalie Wahl. Universal operations in Hochschild homology. *J. Reine Angew. Math.*, 720:81–127, 2016.

[WW16] Nathalie Wahl and Craig Westerland. Hochschild homology of structured algebras. *Adv. Math.*, 288:240–307, 2016.

[Wan11] Rui Wang. *Homology Computations for Mapping Class Groups, in particular for* $\Gamma^0_{3,1}$. Rheinische Friedrich-Wilhelms-Universität Bonn, 2011. Dissertation.

[Wei95] Charles A. Weibel. *An Introduction to Homological Algebra.* Cambridge University Press, 10 1995.